The Application of Space-filling Curves to the Storage and Retrieval of Multi-dimensional Data

by
Jonathan Lawder

A thesis submitted in the fulfillment of the requirements
for the degree of
Doctor of Philosophy
in the
University of London

December 1999

Birkbeck College

Viva Voce : 30 March 2000
Professor D McGregor, Dr D A Cohen

ABSTRACT

Indexing of multi-dimensional data has been the focus of a considerable amount of research effort over many years but no generally agreed paradigm has emerged to compare with the impact of the B-Tree, for example, on the indexing of one-dimensional data. At the same time, the need for efficient methods is ever more important in an environment where databases become larger and more complex in their structures.

Mapping multi-dimensional data to one dimension, thus enabling one-dimensional access methods to be exploited, has been suggested in the literature but for the most part interest has been confined to the Z-order curve. The possibility of using other curves, such as the Hilbert and Gray-code curves, whose characteristics differ from those of the Z-order curve, has also been suggested.

In this thesis we design and implement a working file store which is underpinned by the principle of mapping multi-dimensional data to one of a variety of space-filling curves and their variants. Data is then indexed using a B+ Tree which remains compact, regardless of the volume and number of dimensions. The implementation has entailed developing algorithms for mapping data to one dimension and, most importantly, developing algorithms to facilitate the querying of data in a flexible way. We focus on the Hilbert curve but also consider other curves and propose new alternative algorithms for querying data mapped to the Z-order curve.

The current implementation accommodates data in up to sixteen dimensions but the approach is generic and not limited to this number. We report on preliminary testing of the implemetation, which provides very encouraging results. We also undertake a brief exploration of the application of space-filling curves to the indexing of spatial data.

This thesis is dedicated to my mother and father.

Četrdeset mi je godina, ružno doba: čovjek je još mlad da bi imao želja a već star da ih ostvaruje.

from *Derviš i smrt*
by *Meša Selimović*

This volume is a compact and abridged version of a thesis submitted in December 1999 in fulfilment of the requirements of the University of London for the degree of Doctor of Philosophy and amended following the Viva in March 2000. It differs from the copies held in the libraries of the University of London and Birkbeck College in formatting and in its omission of Appendices E and F.

CONTENTS

LIST OF FIGURES

LIST OF TABLES

LIST OF ALGORITHMS

ACKNOWLEDGEMENTS

I am grateful to my supervisor Professor Peter King for his advice, support, guidance, patience and good humour during my time as a student within the TriStarp Group and also for arranging funding which made my research possible. I would also like to thank Professor George Loizou for commenting on my work and for his encouragement. I am grateful to many colleagues and friends at Birkbeck. In particular, I thank Sylvie Jami for carefully reading and commenting on key chapters of the thesis, Andrew Watkins and the Systems Group for providing excellent computing facilities and Peter Newson for helping with LaTeX typesetting problems. Thanks also to Fefie Dotsika, Parviz Foroughian, Claude Gierl, Stephen Swift and Matt Smith, to name but a few, for contributing to a much appreciated supportive and convivial working environment, which is important for PhD research but easily overlooked, and to Mary Lynch for moral support. The work documented in this thesis was funded by the Engineering and Physical Sciences Research Council, by ICL and by a Keith Robinson Memorial Award, for which I record my thanks.

Chapter 1

INTRODUCTION

1.1 Background

A file of multi-dimensional data contains logical entities, each of which is defined by an ordered set of attributes, referred to as 'dimensions'. Moreover, these entities need to be organized and stored in some way so that sub-sets can be selectively and 'efficiently' retrieved according to values or ranges of values in one or more of any of their attributes.

A printed telephone directory is not an example of a multi-dimensional 'file of data' even though it contains entities with more than one attribute;

$$\langle\, name,\ address,\ telephone\ number \,\rangle.$$

This is because its purpose is to enable addresses and telephone numbers to be looked-up by name. No facility exists to enable questions like, "who lives at 21b Baker Street?", to be answered efficiently, ie within a comparable period of time to that required to answer questions of the type for which the directory was created. A binary search finds the address of a person whereas a serial search is required to find who lives at a particular address.

In order to transform a telephone directory into a multi-dimensional file, facilities must be provided to enable questions of the type exemplified above to be answered. This could be effected by making available a second copy of the file in which entities are ordered by the attribute *address* and a third copy in which entities are ordered by the attribute *telephone number*. This approach leads to a replication of data, requiring more storage. Furthermore, if a person changes their address, more than one entry must be updated. The problem grows as the number of attributes or dimensions increases.

The design of a multi-dimensional file organization method thus attempts to solve the conflicting problems of how to store data compactly while enabling it to be 'queried' flexibly and efficiently. This requires a strategy for partitioning the space containing data, or partitioning the data itself, and providing means to access it. Access to data is most commonly effected with the aid of one or more indexes. The telephone directory is effectively an index of *names* and the *name* attribute is called the 'primary key'. We can avoid replicating the directory by creating 'secondary' indexes on the *address* and *telephone number* attributes. An entry in the *address* index, for example, will list the people living at a particular address and entries will be ordered by *address* values.

Ideally, an index design should enable similar queries to be executed with similar efficiencies regardless of which attribute values are specified. For example, finding who lives in a particular street should be a task of similar complexity to that of finding the addresses of people sharing a particular name. This is not the case where data access is facilitated using a combination of primary keys and secondary indexes since data is ordered by primary key values. From the point of view of most or all other attribute values, records are ordered randomly.

A considerable volume of research has been carried out in the area of indexing multi-dimensional data over many years. Nevertheless, no paradigm appears to have emerged to

compare with the pre-eminence of the B-Tree [BM72] and its variants in the indexing of one-dimensional data. Indeed, the volume of previous and continuing research provokes the conclusion that the development of an optimum strategy for indexing multi-dimensional data very much remains a problem unsolved. This motivates the research described in this thesis. Relatively little work previously undertaken appears to have been embraced by commercially available implementations which, although they have been adapted, remain unchanged at the fundamental level.

The relational model, originating from the late 1960s and implemented using multiple one-dimensional indexes, continues to be the dominant choice in data storage applications. This applies even in such fields as 'Data-Mining', 'Intelligent Data Analysis' and 'Geographical Information Systems' (GIS) which are particularly oriented to application domains characterized by large volumes of high-dimensional data. Where querying patterns are predictable, present relational systems can be tuned, to some extent, but a lack of advance knowledge of how data will be accessed is not uncommon where data is analyzed with a view to extracting previously unknown patterns and interactions.

The dominance of relational systems is understandable given the resources and investment put into their development. Undoubtedly, the simplicity of the relational model has also contributed substantially to the success of these systems.

The relational implementations may have hitherto adapted to changing requirements for handling data but this does not ensure that they will be able to provide universal solutions in the future. Data generation and collection continues to grow at an ever accelerating rate along with aspirations for more sophisticated analysis and processing techniques and capabilities. Data which is being generated is also becoming increasingly high-dimensional in its nature.

The need for a file organization and retrieval method designed specifically to address the problems inherent in large volumes of multi-dimensional data will continue to grow. We believe that a successful solution must be not just effective in all respects but also simple. The design and implementation of such a solution, which addresses the partitioning and indexing of data, the organization of storage and the execution of queries, is the aim of the work described in this thesis.

1.2 Approach to Data Organization Developed in the Thesis

We approach the organization of multi-dimensional data by regarding the data as points lying on a curve passing through each point in a space. Such a curve is called a 'space-filling' curve where it passes through a space comprised of an infinite number of points.

The concept of a space-filling curve is originally attributed to Giuseppe Peano, who, in a paper published in 1890 [Pea90], expressed it in mathematical terms and represented the coordinates of points in space with a ternary radix. A translation in English of the original paper is given by Kennedy [Ken73]. The first graphical, or geometrical, representation of space-filling curves is attributed to the mathematician David Hilbert who described it in a paper published in 1891 [Hil91] and represented the coordinates of points-in-space with a binary radix.

We confine our interest to spaces containing finite numbers of points only and curves passing through points once and once only. Each point then lies a unique distance along the curve from its beginning and thus is placed in order along a one-dimensional line of distance, or sequence, values. Thus points in n-dimensional space are mapped to values in one dimension which may be stored in or indexed by a simple well known and well understood one-dimensional data structure. An important characteristic of space-filling

curves is that they are self-similar at all levels of detail. This is readily discernible from the figures which appear in chapters 3 and 4.

There are numerous examples of space-filling curves. Amongst others, but in particular, we utilize what has become known after Hilbert as the 'Hilbert curve'. Although Hilbert illustrated space-filling curves using a 2-dimensional example his curve is a concept and it may be expressed in an increasing variety of ways as the number of dimensions rises. In this thesis, we utilize a particular interpretation of the Hilbert curve and this interpretation is defined by the detail of the mapping algorithms we develop in chapter 4.

In common with other space-filling curves, the Hilbert curve has certain interesting properties whereby points which are close to each other in n-dimensional space are, in general, mapped to one-dimensional values which are also in proximity to each other. Where we confine our interest to spaces containing finite numbers of points, those points which are consecutive in their ordering are adjacent in space. Thus the mapping achieves a degree of clustering of data with similar values in all attributes or dimensions, which we consider desirable in the absence of prior knowledge of the pattern of queries which will be executed over a collection of data. We expect the clustering properties of the Hilbert curve to contribute significantly in making our indexing approach successful . An additional advantage of the Hilbert curve is that members of the domain and range in the mapping may readily be implemented in software since they are expressible in a binary radix.

The use of space-filling curves, including the Hilbert curve, in the manner described above is not itself a new idea but we found little practical work carried out on their application (see chapter 2), despite the assertion,

> Hilbert curves are used extensively as a basis for multi-dimensional indexing structures...

which appears in a paper by Jagadish [Jag97] studying the clustering properties of the curve in 2 dimensions. References are not cited in that paper to support the assertion nor have we found sufficient material in our search of the literature to justify it.

Initially, we made the conjecture that, simple though the concept may be, impediments to a practical implementation might account for the limited amount of previous work. During the course of our research we encountered a number of problems of a non-trivial nature which must be overcome in order to translate and develop the concept into a fully functioning file organization and retrieval method. The manner in which we address these problems is the principal subject and contribution of the work described in this thesis. Of particular importance is designing suitable strategies for the querying of data. Further details of this work and other work we have undertaken are given in section 1.5 of this chapter.

1.3 Problems with Existing Multi-dimensional Indexing Methods

The way in which one-dimensional data should be logically organized follows almost without thought since a unique natural order is inherent to it. The problem of indexing such data is thus principally refined to designing a suitable data structure to hold it which is compatible with computer hardware.

Additional problems arise in the indexing of multi-dimensional data, however, since it may be organized in more ways than one. This is reflected in the large number of proposals for organizing multi-dimensional data which have appeared in the literature over many years. More is said on this in chapter 2.

Most file organization methods partition data by dividing the space in which it is embedded into rectangles, or their equivalent in higher dimensions, and an index entry is created for each rectangle. When only a few rectangles are defined the index can be accommodated in memory and serially searched as updates and queries are performed. Once the number of such rectangles exceeds some threshold, they must be partitioned, initially, into 2 sub-sets, each of which is most commonly regarded as a node in a tree index structure. A problem arises, often immediately, in that rectangles enclosing a pair of sub-sets of smaller rectangles may overlap. Thus where data insertion is required, for example, it may be necessary to search more than one path in an index tree to locate the page on which to place the data. Avoiding or accommodating this has been the focus of much of the research into organizing multi-dimensional data.

The problem of overlapping rectangles can be avoided if all rectangles are parallel 'slices' of a space. Such an approach is unsatisfactory since it degrades to a one-dimensional partitioning of space. Yet this approach is effectively adopted where data is stored in a relational table and indexed by a 'primary key' corresponding to one of the dimensions of a space. Supplementary, ie 'secondary', one-dimensional indexes are used to access data according to values in other dimensions. Retrieving data in response to a query can require the intersection of several or all of these indexes.

Data organization methods specifically oriented towards multi-dimensional data, however, generally attempt to partition space into rectangles which approximate squares; for example, by way of successively dividing rectangles along dimensions chosen cyclically. This clusters data with similar values in all dimensions and facilitates a homogenous complexity in the retrieval of data from similarly proportioned query regions regardless of their spatial orientation.

We give below some examples of problems apparent in existing file organization methods but these are brief since comparative evaluations already abound in the literature. The subject is also dealt with in more detail in chapters 2 and 8.

The k-d-Tree [Ben75] partitions space into rectangles and is indexed by a tree which is unbalanced. Data or pointers to data are found at all levels of the tree. Deletion of a rectangle in the index can require a substantial amount of reorganization and the form of the index is sensitive to the order in which data is inserted.

The k-d-B-Tree [Rob81] resolves the problem of the unbalanced index of the k-d-Tree but additional problems are introduced. These include a potential requirement for substantial index reorganization on insertion of data, in addition to deletion, and an increased probability that pages with a low occupancy are allowed to remain.

The Grid File [NHS84] is characterized by an exponential directory growth rate, a need for periodic significant directory reorganization and the requirement for directory lists to be intersected in the execution of queries. Directory growth rate is ameliorated by the refinements of Hinrichs and Derakhshan [Hin85, Der89].

The R-Tree [Gut84] index is balanced and simple in comparison with many other methods and not subject to the same degree of reorganization on insertion and deletion of data. However, these benefits are gained at the expense of tolerating overlapping rectangles which degrade query performance. Overlap is reportedly minimized significantly in a recent variation proposed by Berchtold et al [BKK96] but this requires variable sized index nodes. In the pathological case, however, the index degrades to a linear array.

The BANG File [Fre87] tolerates overlapping rectangles but in a more controlled manner than in the R-Tree. It requires a complex, although balanced, index structure. This design has been the subject of a number of papers although none addresses algorithms for executing queries. We do not believe that this is because they are dealt with trivially.

1.4 The Major Contribution of this Thesis

The provision of effective facilities for executing 'partial-match' and range queries is an important and necessary feature of multi-dimensional data storage systems. To this end we developed a novel and successful technique for systems using the Hilbert curve. No technique applicable specifically to the Hilbert curve has been developed previously.

1.5 Review of the Work Undertaken

The work described in this thesis comprises the design and implementation of a fully-functioning persistent multi-dimensional point data store, underpinned by a radically different approach to indexing based on the concept of the space-filling curve which enables us to map multi-dimensional points to one-dimensional values.

Our software implementation enables us to demonstrate practically the correct functioning of the design of our data storage system, for a significantly high number of dimensions.

We focus in particular on the Hilbert curve but we also consider a number of others. We believe our work to be the first design and implementation of a data store which utilizes the Hilbert curve.

Carrying out our work entailed solving a number of non-trivial problems relating to query execution and mapping between one and n dimensions.

Our work has been carried out within the Triple Store Applications Research Project (TriStarp) [KDPS90] in the Department of Computer Science. A principal activity of this Project has been to develop functional programming languages which can update and query persistently held data conforming to a functional view of the binary relational data model. We provide our implementation with an interface enabling it to be integrated with higher-level software applications developed by other members of the Project so that it may be used as an alternative to the existing file store. The interface comprises a set of functions written in the 'C' computer programming language. TriStarp software currently requires a file store which functions in 3 or 4 dimensions. Additionally, our implementation can be applied more generally and currently supports the storage and retrieval of data in up to sixteen dimensions but can be easily be extended to accommodate data in higher dimensions.

We regard records of data held in a data store as being points lying on a space-filling curve, and call them *datum-points*. These *datum-points* are partitioned into logical units of storage in a file store, called *pages*, by conceptually cutting the curve into a set of consecutive sections. Thus a page corresponds to a single contiguous section of curve and it is notionally delimited by a pair of minimum and maximum sequence numbers of points on the curve. The length of a curve section depends on the density of data on it and the physical capacity of a page.

A mapping to a space-filling curve induces a logical ordering of pages, similar to the ordering of points. All of the points on any page map to lower one-dimensional values, which we call *derived-keys*, than do all of the points contained on all succeeding pages. In practice, the lowest *derived-key* corresponding to any *datum-point* placed on a logical page becomes the index entry, which we call the *page-key*, for the page, even if the *datum-point* is subsequently deleted from it. The first logical page is an exception in that it is indexed by the value of zero which corresponds to the first point on the curve.

Figure 1.1 provides an example of a Hilbert curve in 2 dimensions which has been partitioned into a number of pages, each of which holds a maximum of 4 *datum-points*.

In contrast to most alternative approaches for partitioning high-dimensional data, some of which are referred to above in section 1.3, our approach partitions data rather than the

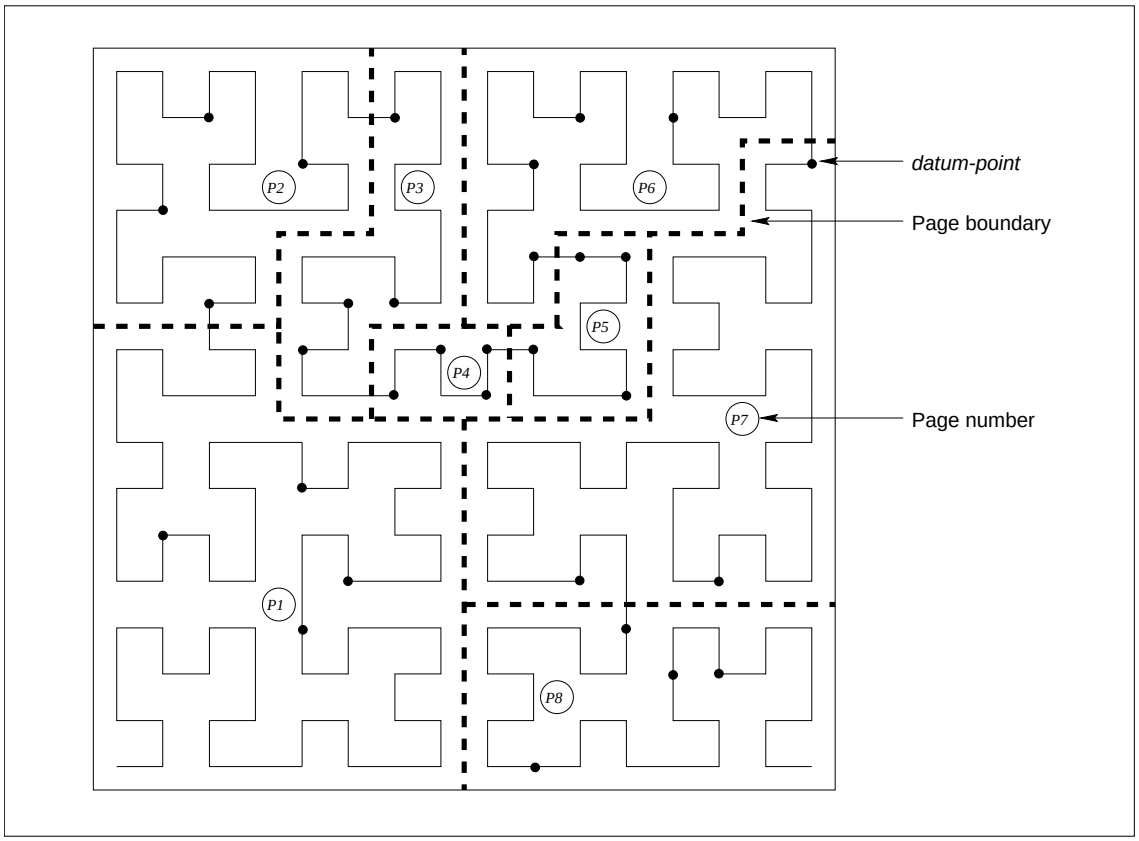

Fig. 1.1: Example Showing a Partitioning of Data Mapped to the Hilbert curve in 2 Dimensions

space within which it lies. Data oriented partitioning avoids overlap between partitions and, therefore, the problems associated with overlap.

Insertion of an item of data entails mapping its coordinates to a sequence number and placing it on the page which covers the section of curve on which it lies. Queries are executed by identifying and searching pages whose corresponding curve sections intersect with the set of curve sections which lie within a query region.

In addition to employing Hilbert curve mappings, we explore and develop the application of alternatives, focussing mainly on curves known as the 'Z-order' curve and the 'Gray-code' curve. Alternatives are studied since different algorithms for mapping and querying are available to them and because they cluster data differently and so variations of the file organization concept may be evaluated in comparison with each other. Unlike the Hilbert curve, these other curves, although also passing through every point in space, are 'discontinuous' in that some points which are consecutive in their ordering are not adjacent in space. This characteristic results in their not being space-filling curves in the limit according to the strict mathematical definition but this is no impediment to our utilization of them. We generally refer to all curves considered in this thesis as space-filling curves even if they are discontinuous.

The application of space-filling curves is only viable if suitable means exist for calculating the mapping between one and n dimensions. Calculations for the Z-order curve are trivial but this is not the case for the Hilbert curve. In this thesis we develop algorithms for generating state diagrams which enable calculation of mappings for the Hilbert curve to be carried out simply. Previous work of this nature has been confined to 2 and 3 dimensions. Insights gained during the development of our algorithms enable us to make useful improvements to an existing mapping technique which does not depend on state

diagrams and so is applicable in a higher number of dimensions.

We found no algorithms in the literature for executing queries on data mapped to the Hilbert curve. Our strategy for executing queries pivots on algorithms for calculating the index entries of successive pages which intersect with the query region, in a lazy manner.

The characteristic self-similarity of space-filling curves enables us to use a mapping to partition space hierarchically and thus conceptually express the curve as a tree, where members of a leaf node correspond to points and nodes correspond to sub-spaces. In consequence, querying entails tree traversal, descending the tree from root to leaf. Determining which child of a node to continue the search at each level of the tree is not trivial since the nodes are not all the same. The manner in which we solve this problem is detailed in chapter 6.

The development of these algorithms is facilitated by expressing space-filling curves as state diagrams but we extend the algorithms so that state diagrams are not required.

The technique can be applied to all of the curves we consider but, for the Z-order curve, we develop a radically different approach which relies on manipulating bit values within the coordinates of points and the one-dimensional sequence numbers corresponding to points.

Our algorithms facilitate execution of partial-match and range queries. We do not address more complex queries, such as joins, intersections and unions of sets of data. Typically these entail applying queries of the base forms to more than one data file and then filtering the retrieved data using set operations. As such, they are independent of the functionality of file store management and handled at a higher level in a Database Management System. They do not, therefore, fall within the scope of the work described in this thesis.

Having designed the algorithms required by the concept, it is implemented as working computer software. This entails addressing problems particular to the utilization of a mapping to a space-filling curve, not documented in the literature, in addition to solving more straightforward problems. A conflict arises in determining the most suitable format to store and order data facilitating both updates and query execution and this is discussed in chapter 7. To some extent similar or even more problematic conflicts arise in the design of other file organization methods but all too often they are not addressed in detail, for example in the PhD theses of Derakhshan [Der89] and Freeston [Fre97].

By mapping multi-dimensional data to one-dimensional values we are able to exploit a single, simple and *compact* B^+-Tree index to gain access to the data. Use of this data structure also enables us to process updates without the need for significant reorganization. Thus in contrast to other data storage systems described in the literature, our implementation is well-behaved in all respects.

We compare the design of our data storage system with those of two prominent existing systems; the Grid File [NHS84, Der89] and the BANG File [Fre87].

Application of the implementation to spatial data is discussed briefly.

Having implemented a working data storage system, we carry out some preliminary comparative performance tests using randomly generated data and queries. Tests are carried out for the different curves discussed in this thesis and we also compare different mapping techniques for the Hilbert curve. We are fortunate in having available an implementation of the Grid File [Der89] with which to compare the performance of our implementation. The results are recorded and discussed.

1.6 Structure of the Thesis

This thesis comprises 11 chapters. Chapter 2 reviews previous work relating to space-filling curves in data storage applications. Most previous research analyses the clustering

properties of space-filling curves and relatively little applies the concepts. That which does is mostly in the area of the indexing of spatial data. We also review previous work in the broader area of the indexing and retrieval of multi-dimensional data where this has not been dealt with in other reviews.

Chapter 3 describes the concept of space-filling curves in detail and documents how the concept is applied in a practical implementation.

Chapter 4 discusses and develops methods for performing mappings between multi-dimensional data and one-dimensional values. In particular we focus on the state diagram approach. The expression of mapping techniques as algorithms which can be implemented as computer software is given separately in chapter 5.

In some cases, particularly for the Z-order and Gray-code curves, it is difficult to isolate their definitions from the descriptions of techniques and algorithms for mapping. To some degree, chapter 3 addresses all these aspects for these curves.

Querying algorithms are described in chapter 6 for curves which can be represented by trees and detailed examples are given to illustrate how they function. Additionally, querying algorithms are given for data mapped to the Z-order curve which rely on manipulating bits in the coordinates and sequence numbers of points.

Chapter 7 describes the implementation of the concepts and addresses important practical considerations. The implementation is compared with the Grid File and the BANG File in chapter 8 and its application to spatial data is discussed in chapter 9.

We describe and present the results of some performance tests in chapter 10 where we also discuss the issues relating to testing.

Finally in chapter 11 we present our conclusions and suggest a number of areas in which further research remains to be carried out.

A number of appendices appear at the end of the thesis.

Appendix A tabulates symbols used in the equations and algorithms given throughout the thesis.

Appendix B relates to the Hilbert curve and contains examples of state diagram generator tables and state diagrams (both in tabular and graphical form) discussed in chapter 4. We discuss in this thesis a technique by Butz [But71] for calculating the coordinates of a point from a one-dimensional value in the range of a mapping to the Hilbert curve and so we reproduce it for reference in this appendix. We also show how the technique is used in the inverse mapping, which is not discussed by Butz.

Appendix C relates to our variation of a curve described by Moore [Moo00] and discussed in chapter 4. It contains examples of state diagram generator tables.

Appendix D relates to the Gray-code curves described in chapter 3. We give details of how state diagram generator tables can be produced for these curves and provide a number of examples of the tables.

Source code, in the 'C' programming language, for generating state diagrams is listed in appendix E. Source code for the file store implementation, including the index and querying facilities, is listed in appendix F.

A number of terms are defined in this thesis, either within the text or as formal definitions, to express various concepts succinctly. At the end of this thesis, we provide an index of terms which notes on which pages their definitions appear.

In a number of places in this thesis, we refer to individual bit positions within binary numbers. We generally refer to the left-most bit, ie the most significant bit, as occupying bit position '1', except where stated otherwise.

Chapter 2

PREVIOUS WORK

This thesis is principally concerned with the application of space-filling curves, and related curves sharing some of the characteristics of space-filling curves, to the storage and retrieval of multi-dimensional point data. In this chapter our review of previous work is divided into three categories:

1. Methods of mapping between multi-dimensional data, viewed as points lying on a space-filling curve, and one-dimensional values, regarded as distances of points on a line from its origin.

2. The application of space-filling curves to multi-dimensional storage structures.

3. Other approaches to the storage and retrieval of multi-dimensional data.

Relatively little previous work has been carried out on the first two of these categories but a considerable amount of work has been carried out on storage structures over a period exceeding thirty years. Furthermore, a significant amount of reviewing and comparison of these storage structures has also already been undertaken.

To provide a review of multi-dimensional access methods which is comprehensive would require a prohibitive amount of time and is likely to add little knowledge which is not already available. Our approach, therefore, is to focus mainly on a representative sample of access methods which are either particularly prominent in the literature or relatively recent. Furthermore, given that our work is oriented to practical application, we pay particular attention to aspects of other approaches which impact on their implementation but which are all too often overlooked, both in the reviews and in the original works.

2.1 Mapping to Space-filling Curves

2.1.1 The Hilbert Curve

In his paper of 1891 [Hil91], Hilbert illustrates the concept of a space-filling curve in 2-dimensions and uses a binary radix to represent the coordinates of points. We describe what has become known as the 'Hilbert curve' in detail in chapter 3 and confine the present discussion to previous work relating to algorithmic expression of the concept.

A number of techniques have been described in the literature for generating the co-ordinates of points in the sequence that the Hilbert curve passes through them. These have mostly been confined to the 2-dimensional case and are, therefore, of little use in our application which addresses indexing in higher dimensions.

Recursive procedures which map one-dimensional values to 2-dimensional points sequentially for the purpose of drawing the curve but which neither provide mappings for arbitrary points nor provide inverse mappings are given by Wirth [Wir76], Goldschlager [Gol81], Cole [Col83] and Witten and Wyvill [WW83]. Table, or state diagram, driven versions are given by Griffiths [Gri85, Gri86].

An iterative table driven version which does enable the mapping of arbitrary one-dimensional values to 2-dimensional points is given by Fisher [Fis86]. A table driven version which additionally facilitates the inverse mapping, from arbitrary 2-dimensional points to one-dimensional values, is given by Cole [Col86, Col87].

Bially [Bia67, Bia69], who was motivated by the problem of bandwidth reduction in the transmission of data, describes a technique for constructing state diagrams which encapsulate space-filling curves. The technique entails following a set of rules for producing a *state diagram generator table* from which the state diagram itself is derived.

Bially's technique is general purpose and makes no specific reference to the Hilbert curve or any other, except that some examples are given for illustrative purposes. The technique initially requires the selection of the number of dimensions in space through which the space-filling curve passes and the radix to be used for the representation of coordinates of points and corresponding one-dimensional values. The particular form of the curve which results depends on the choices made in the application of the rules.

These choices allow for flexibility in the application of the technique but also require the generator table to be constructed manually, when the number of dimensions exceeds 2. In higher dimensions, certain choices result in conflict and, even where they do not, may fail to produce a valid generator table. Thus Bially acknowledges that a process of 'trial and error' is required in order to successfully apply the technique. Furthermore, as the number of dimensions increases, so also does the complexity of the task of constructing generator tables manually.

The adaptation of Bially's technique to enable state diagrams for the Hilbert curve to be generated automatically is a significant contribution of this thesis and is of particular importance to our application of space-filling curves. We therefore leave a detailed description of Bially's work to chapter 4 as a preliminary to supplementing and specializing his rules to suit our purpose.

Whereas state diagrams are useful in the implementation of mapping algorithms, their application is limited by their space complexity. This grows exponentially as the number of dimensions in space increases, both in terms of the number of states in a diagram and in terms of the size of individual states. Butz [But68, But69, But71] overcomes this limitation by describing how to calculate mappings from one-dimensional values to points on the Hilbert curve in any number of dimensions. Butz' algorithm manifests the same computational complexity as that which utilizes state diagrams but its complexity includes a higher constant element.

We reproduce the algorithm given in 1971 by Butz [But71] in appendix B since we make many references to it later in this thesis and also make improvements to it by reducing the constant element of its computational complexity. Butz does not give an algorithm for the inverse mapping, from coordinates of points to one-dimensional values. We therefore provide an algorithm to facilitate the inverse mapping, derived from the original, in the same appendix.

Quinqueton and Berthod [QB81] describe a recursive algorithm which uses the Hilbert curve to order a set of points in n dimensions for image processing applications.

A mathematical formula for mapping from one-dimensional values to 2-dimensional points is defined by Sagan [Sag94], who also gives a BASIC program which implements it for the fourth order Hilbert curve but which does not produce correct results. A different formula would be required for each number of dimensions through which the Hilbert curve passes.

Kamata et al [KKN95] apply the Hilbert curve to the analysis of images. They refer to a technique for sequentially mapping one-dimensional values to coordinates of n-dimensional points which appears in Japanese in an earlier publication by the same authors. Where arbitrary mappings are required they utilize the method described by Butz.

Liu and Schrack [LS96] provide formulae for mapping from coordinates of 2-dimensional points to one-dimensional values and the inverse which they found in experimentation to be significantly more computationally efficient than the algorithms given by Fisher in [Fis86].

The Hilbert curve is sometimes referred to in the literature as the 'Peano' curve, for example in [QB81].

2.1.2 The Z-order Curve

Z-order mapping is attributed to Morton [Mor66] who used the concept as a linear index for 2-dimensional spatial data. The mapping from the coordinates of a point to a one-dimensional value is effected trivially by interleaving bits taken from each coordinate in a cyclical manner. The inverse follows automatically by reversing this operation. Bit-interleaving may be performed in a number of different ways and this is discussed further in section 3.7.1 of chapter 3.

The simplicity of the mapping and the way in which it achieves some degree of proximity amongst one-dimensional values corresponding to points which are close to each other in space has resulted in it being used in a number of applications. Some of these are referred to below in section 2.2.

The term 'Z-ordering' appears to have been first used by Orenstein and Merrett in [OM84].

The Z-order curve is also sometimes referred to in the literature as the 'Peano' curve, for example in [FR91].

2.1.3 The Gray-code Curve

The 'Gray-code sequence' is a sequence of binary numbers in which two successive numbers differ in value in one bit position only. This sequence is originally attributed to Gray [Gra53] who applied it to the electronic transmission of data. Members of the sequence are referred to as 'Gray-codes'.

The Gray-code sequence does not describe a space-filling curve. The concept is, however, exploited to enable the definition of a curve by Faloutsos [Fal86, Fal88]. The Gray-code curve offers a compromise between the complexity of mapping algorithms required for the Hilbert curve and the discontinuity of the Z-order curve.

The manner in which Gray-code sequences are generated is described in more detail in section 3.7.2 in chapter 3. Calculation of mappings between arbitrary Gray-codes and their sequence numbers and the inverse operation is described by Reingold et al [RND77] and we provide more detail of this in section 5.5 in chapter 5.

2.2 The Application of Space-filling Curves to Indexing Multi-dimensional Data

Previous work viewing multi-dimensional data as points lying on a space-filling curve can be divided broadly into two categories as follows:

1. Analysis of the clustering properties of space-filling curves.
2. The application of space-filling curves in practical implementations.

2.2.1 Clustering Properties of Space-filling Curves

A study of the clustering properties of space-filling curves falls outside of the scope of this thesis but we provide a brief review of previous work in this area, since the results motivate our interest in the Hilbert curve in particular.

The earliest work of which we are aware is that of Faloutsos and Roseman [FR89a] who propose the application of mapping multi-dimensional data to the Hilbert curve in an indexing application. Some experiments are reported in 2, 3 and 4 dimensions. In these, the number of contiguous curve sections which pass through hyper-cubes placed in all possible locations in a space containing finite numbers of points, are counted. The experiments are repeated for different sized hyper-cubes. Comparisons are made with the Z-order curve. Between approximately 10% and 50% more Z-order curve sections than Hilbert curve sections are found to pass through the hyper-cubes. This implies that more pages of data are likely to require searching in the execution of a query over data mapped to the Z-order curve compared with data mapped to the Hilbert curve.

Jagadish [Jag90] compares the performance of partial match and range queries executed over Hilbert, Gray-code, Z-order, Snake and Scan curve mappings in 2 dimensions, by both analysis and simulation experiments. Performance is measured by counting the numbers of contiguous curve lengths 'retrieved'. In the experiments, curves passing through 256^2 points are divided into simulated 'pages' of data and so a retrieved curve length may contain points which do not lie within the query regions. In summary, the conclusion which emerges is that the curves can broadly be ranked in terms of diminishing performance in the order that we list them above.

Jagadish [Jag97] continues this analysis for the Hilbert curve in 2 dimensions, focussing on calculating closed-form expressions for the average number of contiguous curve sections which intersect with square range queries containing 4 points. Such ranges are found to intersect with 2 curve sections, on average.

Faloutsos and Rong [FR91] propose the application of the Hilbert curve in the indexing of spatial data. Their paper includes a study of the number of contiguous curve sections retrieved during the execution of range queries over straight line segments mapped to 2-dimensional curves. The Hilbert and Z-order curves are compared. This study finds that, on average, nearly twice as many Z-order curve sections intersect with queries as Hilbert curve sections. It implies that where a mapping to the Hilbert curve is utilized, fewer pages are 'touched', ie searched, during query execution.

Simulation experiments are also carried out by Kumar [Kum94] for the Hilbert, Gray-code, Z-order and 'nu-ordering' curves passing through 512^2 points in 2 dimensions. The last of these curves is a variation on the Gray-code curve and proposed by Kumar. As with Jagadish [Jag90], coordinate space is divided into simulated 'pages' and the numbers of pages touched by rectangular range queries are counted. A larger range of query size is used in the experimentations. In contrast to the experiments carried out by Jagadish, in Kumar's experiments the superior performance of the Hilbert curve is more pronounced and the difference between the Z-order and Gray-code curves is less pronounced. The performance of Kumar's 'nu-ordering' is closer to that of the Hilbert curve than the others.

Moon et al [MJFS99] carry out an analysis for the Hilbert curve, providing closed-form expressions for the numbers of clusters, or contiguous curve sections, retrieved in the execution of range queries of arbitrary shape and size. The analysis is not confined to 2 dimensions and queries are not confined to hyper-rectangular form. The correctness of the analysis is demonstrated by experiments in 2 and 3 dimensions in which queries are simulated.

The implications for clustering of data mapped to the Gray-code curve are studied by Faloutsos analytically [Fal86, Fal88]. In these two papers, the numbers of consecutive curve sections which intersect with partial match and range queries are calculated and found to be up to 50% less on average than where mappings to the Z-order curve are utilized. These findings, however appear to be contradicted by the simulation experiments of Kumar [Kum94].

2.2.2 The Utilization of Space-filling Curves

2.2.2.1 The Hilbert Curve

A significant amount of interest in the Hilbert curve is expressed in the literature, as evidenced by the work reviewed in section 2.2.1 above. Nevertheless, we have not found details of any practical implementation which applies the Hilbert curve to the indexing and retrieval of multi-dimensional data. Most previous work in the area is confined to spatial data and is conceptual or theoretical in nature. Furthermore, most previous work has been confined to space in only two and three dimensions.

The Proposed Use of the Hilbert Curve

The application of the Hilbert curve is proposed in outline for the indexing of point data by Faloutsos and Rong [FR89a] and the indexing of spatial data by Faloutsos and Roseman [FR91] but practical considerations and, most importantly, strategies for executing queries are not addressed.

An extended version of the first of these papers [FR89b], proposes the use of Bially's state diagram generator table, rather than state diagrams, in calculating mappings between one and n dimensions. An example of a generator table is given in 4 dimensions. It appears that a process of trial and error has been used in applying Bially's rules to create the table. Entries in one of the columns, referred to in chapter 4 as column X_2, lack the symmetry which is characteristic of the Hilbert curve.

In the second paper [FR91] the proposal for indexing spatial data maps n-dimensional hyper-rectangles to $2n$-dimensional points which are, in turn, mapped to one-dimensional values in the domain of a mapping to points on the Hilbert curve. We pursue this notion further in chapter 9.

The Hilbert R-Tree

The Hilbert R-Tree [KF94] is a variation of Guttman's R-Tree [Gut84]. The R-Tree was designed to index hyper-rectangular spatial objects, or minimum bounding boxes (MBBs) containing spatial objects, in a 'balanced' tree data structure. All paths from the root to a leaf in a balanced tree are of equal length. A non-leaf R-Tree node contains a set of MBBs, each of which encloses a node at the next lower level in the tree. Since spatial objects may overlap, the nodes of an R-Tree must of necessity be permitted to overlap (unless spatial objects are divided, as in the R^+-Tree [SRF87]). Where the concept is applied to point data, MBBs at the leaf level do not overlap but they may overlap in non-leaf nodes. An example illustrating the concept is given in Figure 2.1.

A problem arises in the original design in that there are many ways of partitioning a set of spatial objects into sub-sets. Partitioning is significantly influenced by the order in which updates are carried out and a considerable amount of overlap between nodes can arise. This degrades the efficiency of the search process in the execution of queries since a search for an object may require descent of the tree to more than one leaf and the accessing of more than one page of data.

The Hilbert R-Tree orders leaf nodes so that the centre points of hyper-rectangles within any node map to lower one-dimensional values than those of the successor node. The MBBs enclosing nodes may overlap as in the original R-Tree. The execution of queries is performed in a similar manner as in the original R-Tree and so the impact of the Hilbert curve is primarily in the partitioning of data. In [KF94], a significant improvement in query processing efficiency is reported over the original design and over an earlier improved design called the R^*-Tree [BKSS90].

In essence, the Hilbert R-Tree 'borrows' from the concept of the Hilbert curve in representing and ordering objects which are then placed within an R-Tree.

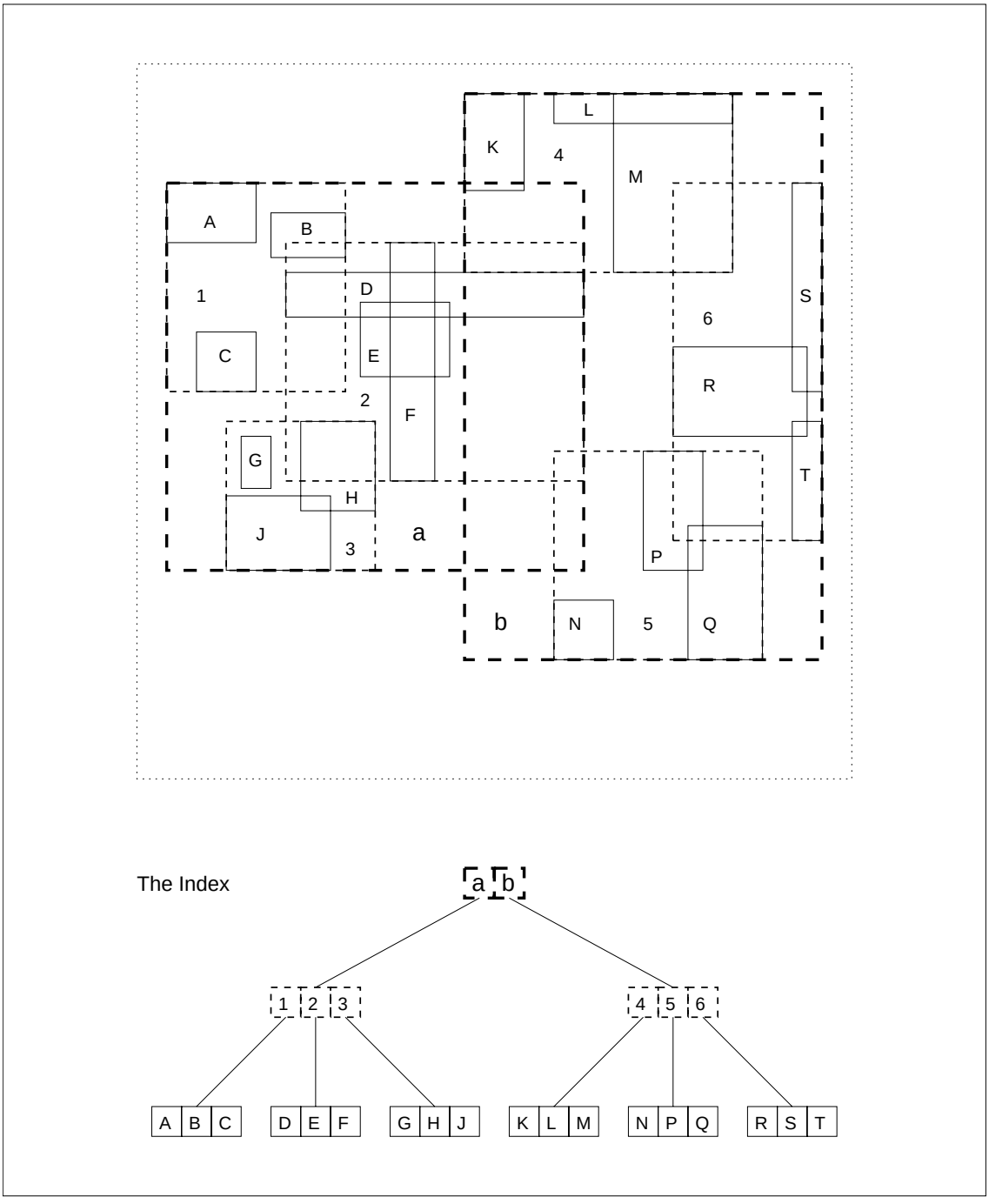

Fig. 2.1: Example Partitioning and Index in the R-Tree in 2 Dimensions

2.2.2.2 The Z-order Curve

The concept of Z-ordering is most commonly applied in the literature to the indexing of spatial objects and to the indexing of sub-spaces containing points. In this section we review a number of prominent examples which make use of Z-ordering.

The Quad Tree

The Quad Tree is a well known and long established data structure which hierarchically partitions space but it is not a file organization method. Quad Trees are discussed in considerable depth by Samet [Sam90a, Sam90b], where extensive bibliographies appear. The Quad Tree partitions 2-dimensional space by dividing it into 4 squares, then dividing each of these into 4 and continuing in a similar manner until the desired level of granularity (ie minimum size of sub-square) is arrived at. The concept may be extended into higher dimensions. The relationship with Z-ordering is that the latter may be used conveniently to identify and order the sub-squares. Z-ordering allows a number to be ascribed to a square which is a prefix of all of the numbers applied to sub-squares within it.

Whereas Quad Trees may be applied to point data applications, they are more commonly applied to spatial data and also to the digital representation of images. We illustrate the latter with a simple example in Figure 2.2, which also shows that the Quad Tree is neither a binary tree nor balanced. Not only do Quad Trees enable a digital representation of an image but they also facilitate a *compact* representation. In this context, the smallest sub-square within a space is known as a 'pixel'.

We leave a description of how the numbers are ascribed to sub-squares of varying size to section 3.7.1 in chapter 3 where we describe the Z-order curve in more detail. An insight may be gained rapidly by reference to Figure 3.11 in that chapter.

The PROBE Project

Orenstein describes a spatial data storage application [OM84, Ore86, Ore89a, Ore89b, Ore90, Ore91], called the 'PROBE Project' in which an object is decomposed into a set of variable sized sub-squares using the Quad Tree approach. The members of a set are located in space using the Z-ordering technique and, additionally, all share a common identifier. A B^+-Tree is used for storage purposes.

The main contribution of the work lies in the development of algorithms for performing spatial queries such as finding pairs of overlapping objects or identifying which objects overlap or are contained within a region of space. Much of the work is oriented to 2-dimensional space, although the concepts can be generalized into higher dimensions.

The BANG File

The BANG File of Freeston [Fre87], is a method for partitioning space containing point data. It does not map points lying on a space-filling curve to one-dimensional values but uses the concept of Z-ordering to identify and order regions. The identifier of a region is a variable length prefix of the one-dimensional values corresponding to all of the points contained within it and considered as lying on a Z-order curve. The hierarchical nature of Z-ordering explained in chapter 3, enables the definition of regions which lie, ie are nested, within larger regions. The index used to store region identifiers is a variation of the B-Tree (see section 2.5).

Much subsequent work addresses the problem of index design for the BANG File and extends the original concept to accommodate spatial objects [Fre89a, Fre89b, Fre92, Fre93, Fre95a, Fre95b, Fre97]. We leave a more detailed discussion of this file organization method to chapter 8 where practical issues relating to implementation are dealt with.

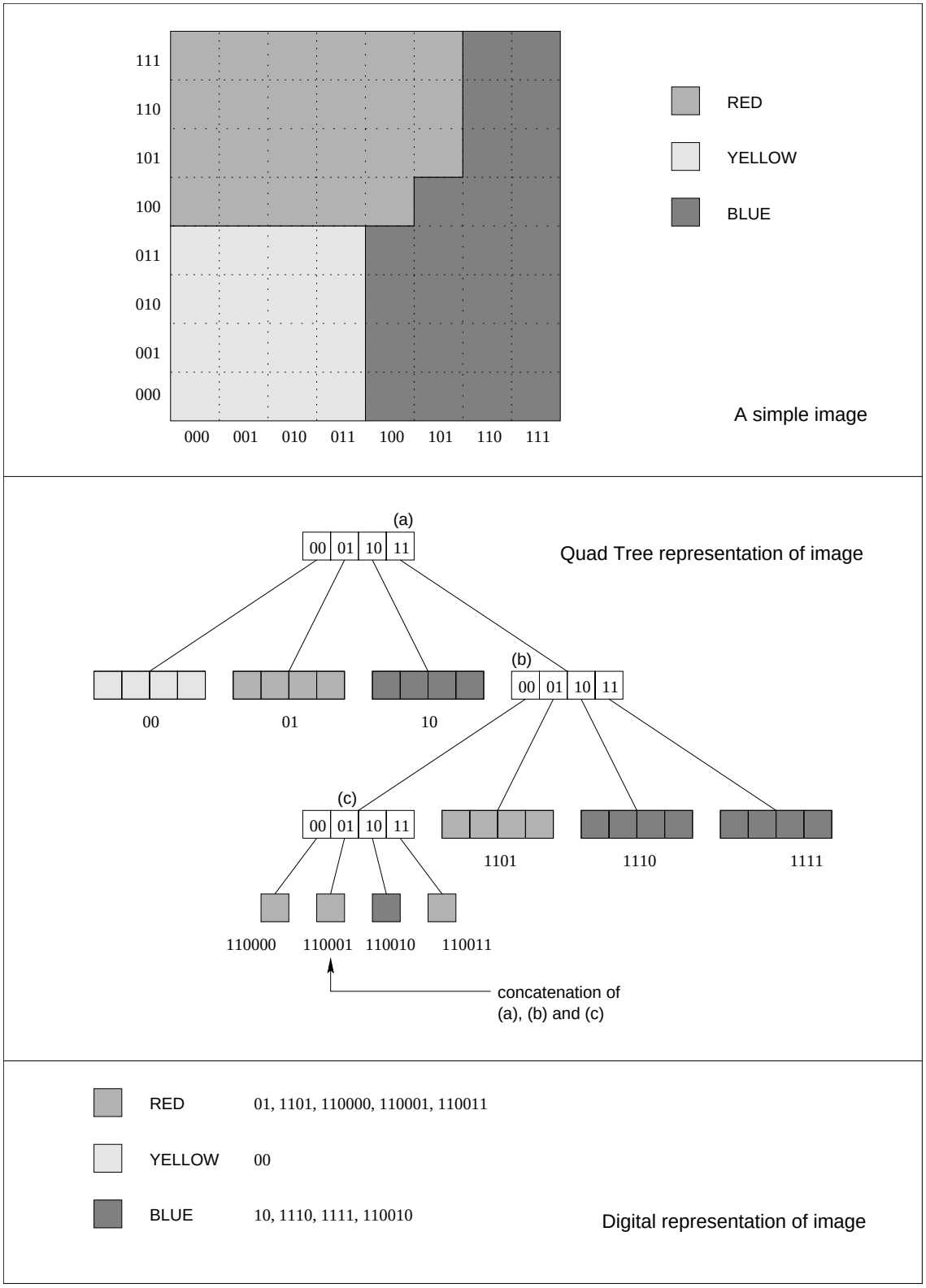

Fig. 2.2: The Application of the Quad Tree to an Image

The Nested Interpolation Based Grid File of Ouksel and Mayer [OM91, OM92] adopts a similar partitioning strategy to the BANG File but differs in its index design.

Oracle

Oracle Corporation describe a set of functions and procedures comprising the 'Oracle8 Spatial Cartridge' [Ora97]. This is designed to enhance their Relational Database Management System so that it supports the storage, retrieval and analysis of spatial data more efficiently.

Spatial objects appear to be represented and indexed in the manner of the PROBE Project, although reference is not made to this work. An object is represented by a list of variable length one-dimensional values corresponding to sub-squares within a Quad Tree data structure. Thus the Z-order curve is used to decompose objects whose shapes are complex into sets of rectangles and / or squares which are then stored in relational tables.

Generic Query Processing

A recent review of previous work by Gaede and Günther [GG98] on multi-dimensional data file organization methods refers to an algorithm for performing range queries on point data mapped to space-filling curves by Tropf and Herzog [TH81]. This algorithm is specifically oriented towards the Z-order curve and is quite different from our own for that curve, given in chapter 6.

2.2.2.3 The Gray-code Curve

In common with the Hilbert curve, we see in section 2.2.1 that considerable interest has been shown in the Gray-code curve but we are not aware of any practical implementations which utilizes this curve.

We referred to two papers by Faloutsos [Fal86, Fal88] which specifically relate to the Gray-code curve. In these, it is suggested that mappings to the Gray-code curve may be applied to Nievergelt's Grid File [NHS84] and to Orenstein's work [OM84]. Faloutsos leaves these applications of Gray-codes as a subject for further research.

2.3 Other Multi-dimensional Storage Structures

In this section, we consider previous work on multi-dimensional storage structures other than those which make use of the concept of a space-filling curve.

We noted earlier in this chapter that a considerable number of methods for the storage and retrieval of multi-dimensional have been proposed in the literature and that much previous work has been undertaken in reviewing these methods.

Probably the most comprehensive review of previous work is that given by Gaede and Günther [GG98]. This review addresses file organization methods for both point and spatial data and includes a review of comparative studies and an extensive bibliography. In Figure 2.3, we reproduce Figure 1 from this paper which illustrates the taxonomy of data organization methods and gives an indication of the volume of previous work.

As the authors of this review acknowledge, classification of storage structures is difficult since many are hybrids. They divide point file organization methods into three broad categories as follows:

1. Multi-dimensional hashing.
2. Hierarchical file organization methods.
3. Space-filling curves.

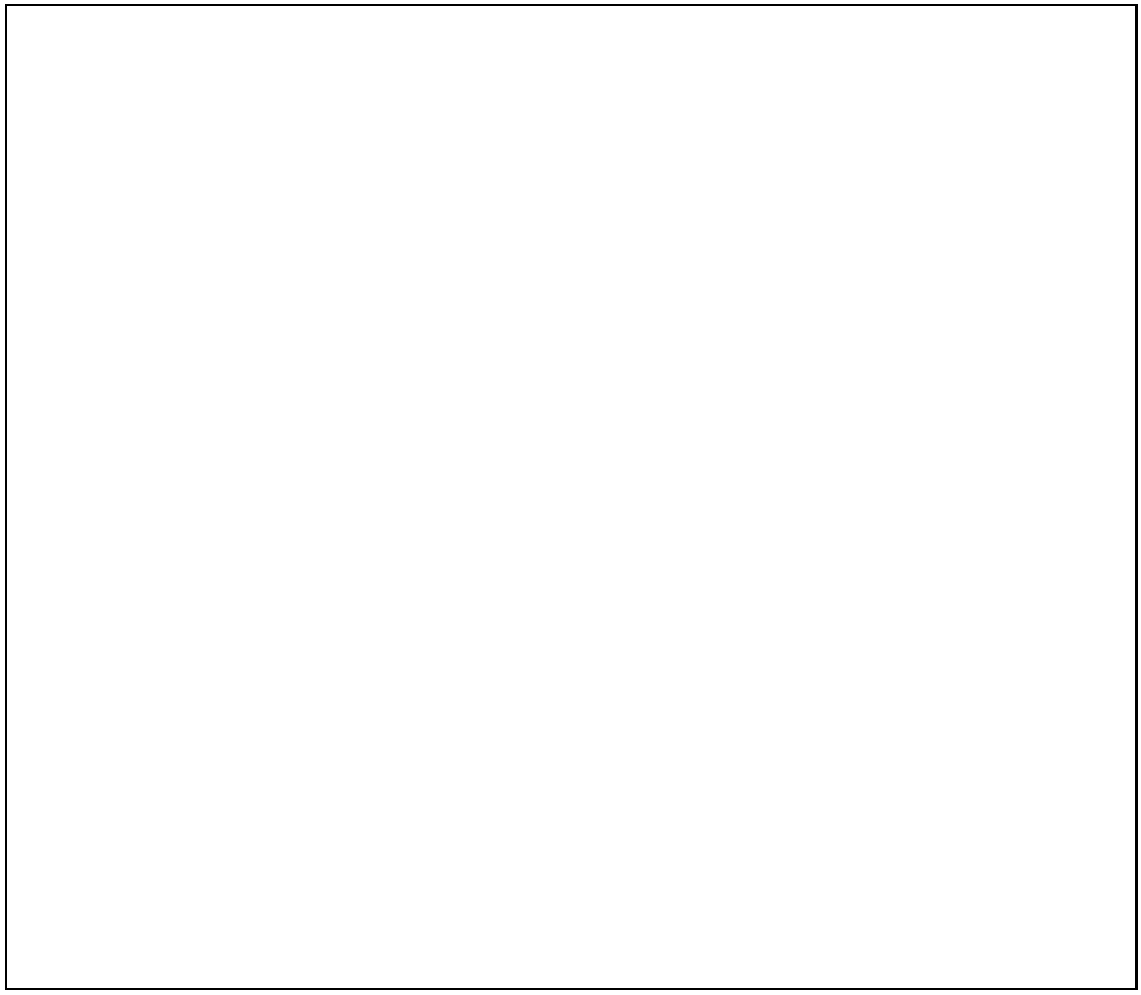

Fig. 2.3: Taxonomy of Data Organization Methods from [GG98]

Most prominent amongst the first of these categories is the Grid File of Nievergelt et al [NHS84] and its variants including the Two-Level Grid File [Hin85] and the Twin Grid File [HSW88]. We found the Grid File to be the most commonly cited multi-dimensional file organization method in the literature. We leave a more detailed description of this approach to chapter 8 where we discuss it in the context of our own design and implementation underpinned by space-filling curves. An implementation of the Grid File using an index strategy which addresses problems left open in the original paper is given by Derakhshan [Der89].

The hierarchical methods for point data generally partition space and place disjoint sub-spaces in a tree structure such that sub-spaces within any node are enclosed by a sub-space in its parent node. With the exception of the k-d-Tree of Bentley [Ben75] and its variants, including the k-d-B-Tree of Robinson [Rob81], which are well documented elsewhere, we found Freeston's BANG File to be the most frequently cited in the literature. Given the association between the BANG File and Z-ordering noted in section 2.2.2.2, we also discuss this file organization method in more detail in chapter 8.

Other than the applications of space-filling curves noted above in section 2.2.2, no implementations of file organization methods using space-filling curves are referred to by Gaede and Günther [GG98] and neither have any been identified by ourselves during the course of our literature search.

More detailed reviews of some of the earlier multi-dimensional file organization methods, including the k-d-Tree and k-d-B-Tree, are given by Derakhshan [Der89], Ooi [Ooi90] and Freeston [Fre97].

2.3.1 Recent Methods

An area of focus for very recent work has been the organization and retrieval of spatial data although this work can often be readily applied to point data. We provide a summary of methods not already discussed in surveys. Such methods include the the SS-Tree of White and Jain [WJ96], the SR-Tree of Katayama and Satoh [KS97], the X-Tree of Berchtold et al [BKK96] and the Pyramid-Technique of Berchtold et al [BBK98].

The first three of these are developments of the R-Tree [Gut84], described in section 2.2.2.1, and its enhancement as the R*-Tree [BKSS90].

The SS-Tree

The SS-Tree is described as a 'similarity' indexing method oriented to the storage of multi-dimensional data in a manner which supports 'similarity queries'. Such queries may be of the forms, "find objects similar to a reference", "find pairs of objects which are similar" and "find a representative sample of objects", in addition to conventional query forms. Data is transformed into 'feature vectors', which take account of the varying significances of values in different dimensions. The input of a domain expert is required for this purpose. Space containing feature vectors is then partitioned into spheres which theoretically contain the k-nearest neighbours of their centre points. We say 'theoretically' since, in practice, the spheres may overlap in the way that the rectangles of the R-Tree do. White and Jain [WJ96] report an improvement in performance over that of the R-Tree.

The SR-Tree

The SR-Tree is similar to the SS-Tree except that feature space is partitioned into regions defined by the intersection of spheres and rectangles (where spheres are not wholly contained within the rectangles). The benefit of this approach is that partitions overlap to a lesser extent than in the SS-Tree. The authors report an improvement in performance over that of the SS-Tree.

The X-Tree

The X-Tree addresses the problem of overlapping regions manifest in the R-Tree. This is achieved by allowing nodes in a tree to be of variable rather than fixed size.

If the rectangles in an overfull node cannot be partitioned into 2 roughly equal sized sub-sets whose minimum bounding boxes overlap within the limits defined in some threshold then an 'overlap-free' split is sought. This entails consulting a data structure which records the history of previous splits. At least one overlap-free split can always be found for a node but if it results in one of the new nodes being populated with fewer rectangles than defined in some threshold, then the original node is not split but allowed to become enlarged instead. Enlarged nodes are called 'supernodes'. Where spatial data rather than point data is stored, the term 'overlap-free' is substituted by 'overlap-minimal'.

The X-Tree is thus a hybrid between a linear array index and an R-Tree index. It appears that the design attempts to coerce the unbalanced k-d-Tree index, with fixed sized nodes, into a balanced tree.

Whereas spatial objects may overlap, this is clearly not the case with point data. It is debatable whether data organization methods which permit overlapping regions in the partitioning of point data do so because they are specializations of methods primarily designed for spatial data or because there is some inherent advantage in tolerating overlap. Nevertheless, the performance benefits of the X-Tree reported in [BKK96] are particularly impressive.

The Pyramid-Technique

The Pyramid-Technique appears to be a significant departure from most other multi-dimensional data organization methods described in the literature. Space is partitioned in a 2-stage process. In the first stage, space is divided into pyramids all of whose apexes lie at the centre of the space. In the second stage, each pyramid is divided into slices, the bases of which are all hyper-planes parallel to the base of the pyramid. The authors use the analogy of concentric layers of an onion. Each slice of a pyramid corresponds to a page of the data file.

Multi-dimensional points are transformed into one-dimensional values by a mapping which is not bijective, thus more than one point may map to the same value, which necessitates the storage of both the coordinates of points and their one-dimensional values. A one-dimensional value designates which pyramid a point lies in and its height above its base. Thus the one-dimensional value is the addition of the integer pyramid number and the real height. The concept is illustrated in 2 dimensions if Figure 2.4.

The paper describes a query processing algorithm but we do not describe it here since the authors acknowledge that it is a "complex operation".

The technique can be adapted to skewed data distributions by moving the apex of all of the pyramids into the centre of a data cluster, creating asymmetrical pyramids. Data sets, however, may contain more than one cluster and the locations of clusters may be dynamic. A dynamic pyramid apex location does not, however, appear to be practicable.

The manner in which pyramids are divided into slices appears to suggest that partitioning may degrade locally such that all points on a page share similar values in one dimension but potentially very diverse values in all others.

Notwithstanding our reservations, the evaluation included in the paper concludes that the Pyramid-Technique out-performs the X-Tree and Hilbert R-Tree, particularly in higher than 12 dimensions.

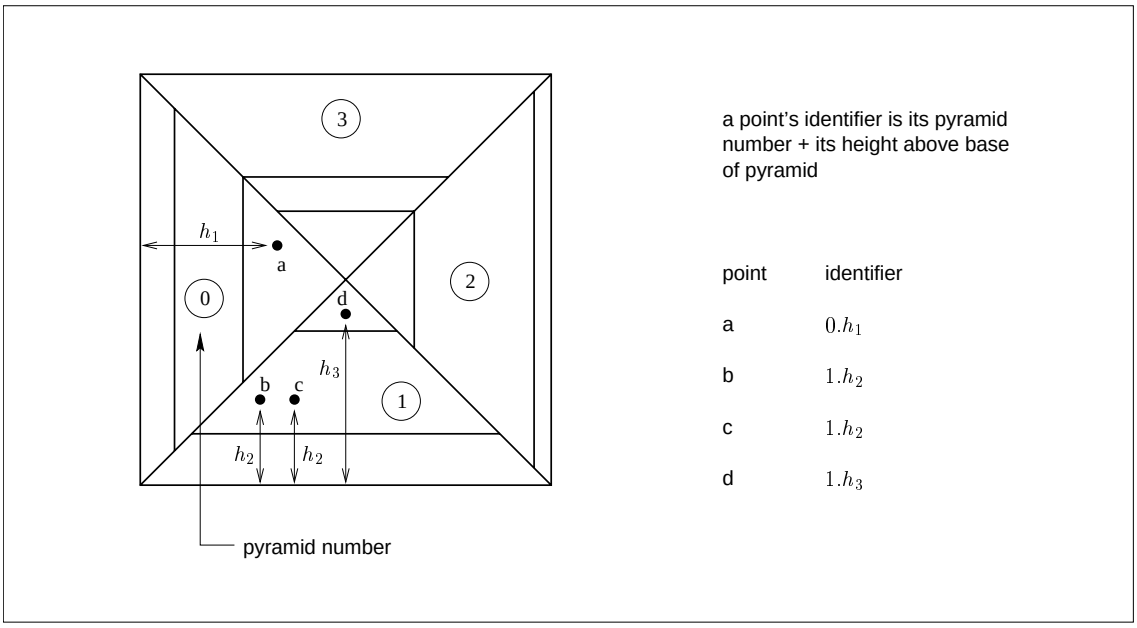

Fig. 2.4: Partitioning within the Pyramid-Technique

2.4 Current Commercially Available Software

There can be little doubt that both commercial and academic multi-dimensional data storage applications most commonly utilize commercially produced implementations of the relational data model [Cod70]. More specifically, this commercially available software generally implements the indexing of the relational model using a combination of 'primary keys' and 'secondary indexes'.

Multi-dimensional 'records' of data are conceptually stored as rows in a table. Rows are ordered by values in one dimension, ie column or 'field', or by a particular combination of dimensions. The dimension(s) used in the ordering is known as the 'primary key'. Where a significant amount of querying would benefit from access via attributes other than the primary key or where querying patterns are diverse then supplementary indexes, called 'secondary indexes', can be created to improve performance.

Since data is effectively clustered according to primary key values, queries which require the retrieval of a set of records having a narrow range of primary key values are processed efficiently but others are not. Records which have a large range of primary key values but narrow ranges of values in other columns are effectively placed randomly in a table. Thus they potentially require significantly more page accesses to retrieve them in comparison with file organization methods specifically designed for the flexible querying of multi-dimensional data. Furthermore, the intersection of several secondary indexes may be required in order to locate the records.

Utilization of primary keys and secondary indexes is not in itself an inherent characteristic of the relational model. Indeed, records can be ordered in a table by regarding them as being points on a space-filling curve and mapping them to points on a line. Nevertheless, this concept was not well-known at the time when commercial implementations of the relational model were designed. Furthermore, early database applications and expectations of them were not as sophisticated and as unbounded by practical hardware considerations as they are currently.

While commercial implementations of the relational model can provide a practical and general purpose solution, they are not necessarily optimized for large data sets within high-dimensional space and where flexibility in the way queries are composed is required.

In the author's experience, a large number of secondary indexes can require more storage than the underlying data itself. Even where multiple indexes exist, querying generally entails a significant amount of set intersection and projection which are computationally expensive operations.

Arguments for the use of currently available commercial software for the storage of multi-dimensional and spatial data are given in a 'White Paper' published by Oracle [Ora97].

The growth in volume and complexity of data sets and aspirations for data processing and analysis have motivated research into alternative methods to the use of primary keys and secondary indexes in the organization of data, which are more suited to it.

2.5 B-Trees

The purpose of mapping multi-dimensional data to points on the line is, in part, to enable an implementation to exploit existing simple, well known and well behaved one-dimensional storage structures.

The B-Tree, and its variants, are generally accepted as the paradigm in organizing one-dimensional data. We utilize the B^+-Tree in our implementation described in chapter 7 and, therefore, conclude this chapter with a brief reference to work relating to B-Trees.

The B-Tree was introduced by Bayer and McCreight in 1972 [BM72]. The main characteristic of the B-Tree is that it is balanced, ie all leaves are held at the same level. Nodes are of fixed size and a node's occupancy is guaranteed not to fall below 50%. The height of the tree varies as data is inserted and deleted. The original B-Tree stores data within nodes at all levels along with pointers to child nodes, thus a traversal may not always require descent to the leaf level.

The B^+-Tree differs from the original in that all data resides at the leaf level. In Comer's 'The Ubiquitous B-Tree' [Com79], which reviews the subject, the B^+-Tree is attributed to Knuth [Knu73], as is the B^*-Tree which differs in that a lower bound of 66% is achieved for node occupancy.

Surprisingly, despite the ubiquity of the B-Tree, Jannink [Jan95] notes that the literature offers little in terms of algorithms for deletion and so addresses this problem in his paper; which has proved useful for our implementation.

Chapter 3

SPACE-FILLING AND RELATED CURVES AND THEIR APPLICATION

3.1 Introduction

Space-filling curves pass through every point in a space. In this chapter, we explain how they do this, beginning by defining them and then by showing how they are constructed. For the most part, we focus on the Hilbert curve since, later on, we identify it as the most suitable space-filling curve for our application. We often refer to the Hilbert curve in 2 dimensions as an example, since it expresses the concept of space-filling curves in a simple manner and can be generalized to higher dimensions.

Our interest in space-filling curves arises from a correspondence between points in cartesian product space and records of data, composed of a fixed number of attributes, which may exist in a data store. A record, defined in chapter 1 as a *datum-point*, with n attributes can then be seen as a point defined by n coordinates in n-dimensional space.

This correspondence, in conjunction with the concept of a space-filling curve, which passes through every point in space in a particular sequence, presents us with the possibility of mapping such data to points on a line. Thus multi-dimensional data is ordered and may be referenced by one-dimensional sequence numbers, defined in chapter 1 as *derived-keys*. This enables *datum-points* to be indexed using simple, well known and well behaved one-dimensional index structures such as the B-tree [BM72] or one of its variants.

This approach to indexing restricts us to considering space-filling curves which are described by bijective functions, ie where there is a one-one correspondence between points on the line and points in space. There must exist a *derived-key* which unambiguously corresponds to each and every potential *datum-point*.

With the implementation of our indexing application in mind, we then focus on the binary representation of *derived-keys* and *datum-points* lying on 'approximations' of space-filling curves, which pass through a finite number of points only. We show how an approximation may be represented as a tree of finite depth as this will prove useful in chapter 6 where we present algorithms for performing queries on data. Some examples of approximations of 2-dimensional Hilbert curves are given in Figure 3.1. The terms *order* and *approximation* are defined below in section 3.4.1.

Having considered space-filling curves, we examine a number of other curves which do not conform to the definition of space-filling curves but share some of their characteristics. Certain drawbacks are associated with these curves but they are considered as alternatives to space-filling curves. This is because they enable our application to be implemented more efficiently, both in terms of performing mappings between one and multi-dimensional space and in terms of executing queries. We identify two curves in particular, known as the Z-order curve and the Gray-code curve, which together with the Hilbert curve are the focii of interest in later chapters.

In the concluding section of this chapter, we apply our understanding of space-filling and related curves and their approximations to a practical indexing application and show

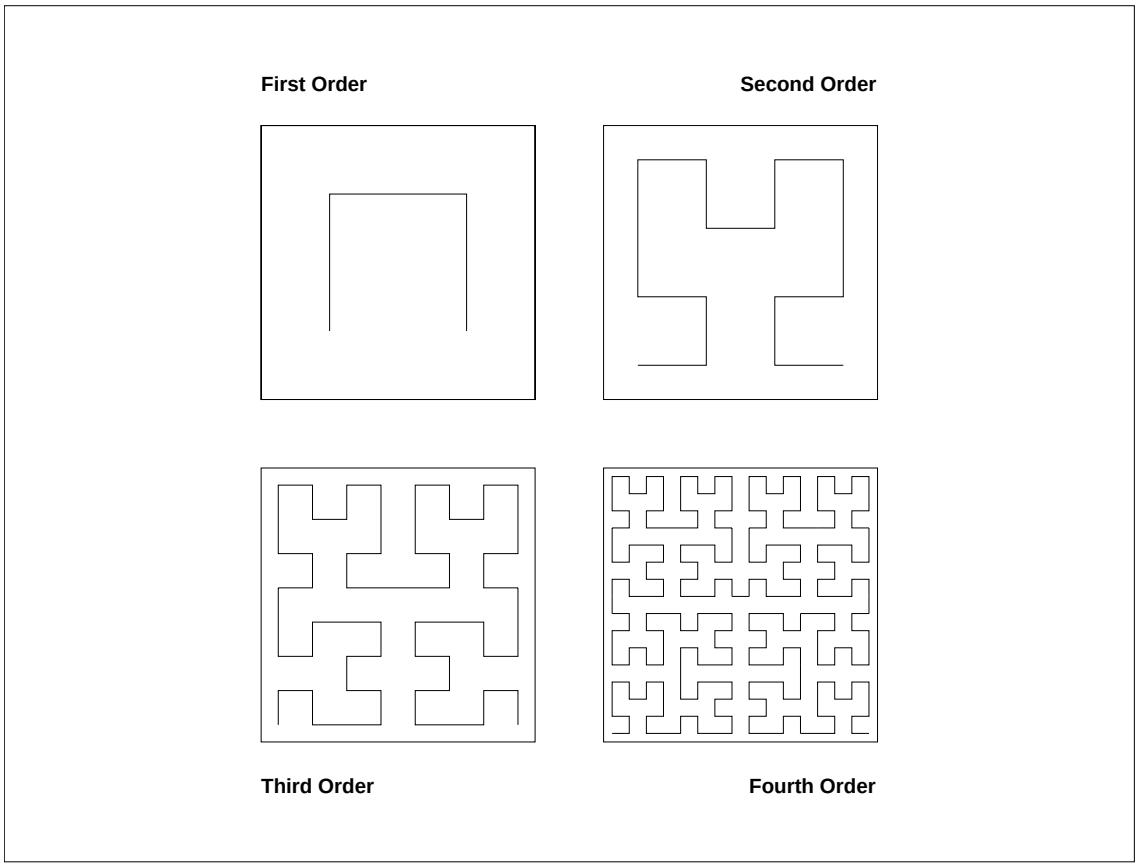

Fig. 3.1: Approximations of the Hilbert Curve in 2 Dimensions

how they may be utilized.

3.2 The Origin of Space-filling Curves

The concept of a *space-filling curve* emerged in the 19-th Century and is originally attributed to Peano [Pea90] who expressed it in mathematical terms and represented the coordinates of points in space with a ternary radix.

The first graphical, or geometrical, representation of the space-filling curve is attributed to Hilbert [Hil91]. He illustrates the concept in 2-dimensional space and uses a binary radix to represent the coordinates of points in space. We describe what has become known as the *Hilbert curve* in more detail in section 3.4.

3.3 The Definition of a Space-filling Curve

A *curve* can be defined as the image of the unit interval [0, 1] under a continuous function. A *space-filling* curve is then the image of a particular type of function which is surjective and whose range is the unit square $[0,1]^2$, cube $[0,1]^3$ or hyper-cube $[0,1]^n$, where n denotes the number of dimensions in a space. The limit of the function is a mapping from an interval to its cartesian product. As such, the curve passes through every point in a space of some finite number of dimensions.

A detailed study of space-filling curves from a mathematical perspective is given in [Sag94], from which we draw the following formal definition:

> Given a closed unit interval I and an n-dimensional Euclidean space E^n, if a continuous function $f : I \rightarrow E^n$ has an image with positive Jordan content then the image is a space-filling curve.

Space-filling curves constitute a sub-set of what are commonly known as fractals, although a fractal is not necessarily space-filling or even a curve. The term *fractal* was introduced by Mandelbrot [Man82] and the subject is discussed in depth by Peitgen et al [PJS92].

Whereas functions which describe space-filling curves are surjective, they need not also be injective, ie they may visit the same point in space more than once. Examples include Peano's 'C(w)' curve described by Moore [Moo00], the 'Dragon' curve [WW83] and Sierpinski's curve [Sag94]. As noted in the introduction to this chapter, however, we confine our interest to space-filling curves which are described by bijective functions.

3.4 The Construction of Hilbert Space-filling Curves

3.4.1 The Hilbert Curve in 2 Dimensions

In his paper published in 1891, Hilbert illustrated the concept of a space-filling curve in 2 dimensions by giving a method for the stepwise construction of an infinite sequence of finite curves, each of which is defined by a linear ordering of the sub-spaces resulting from the construction process. Hilbert then showed that this process defines in the limit a curve passing through all points in the space, this curve being everywhere continuous and nowhere differentiable [Sag94]; it is now known as the Hilbert curve.

Before considering Hilbert's construction process, we define two closely related terms often used in this thesis.

Definition 3.4.1: *order of curve : the* order *of a curve designates the number of steps, or iterations, for which the construction process has been carried out.*

Definition 3.4.2: *approximation : a Hilbert curve of some finite* order *is said to be an* approximation *of a Hilbert space-filling curve. It does not pass through every point in space but it passes through all of the centre points of a finite number of equal-sized sub-squares, the union of which comprises the whole of the unit square.*

We now describe the first two steps in Hilbert's construction process before defining higher order curves generally. This section is then concluded by comments and observations relevant to the application of space-filling curves.

The Construction Process

Step 1: Both the one-dimensional interval $[0, 1]$ and the square $[0, 1]^2$ are initially divided into 4 congruent quarters. Each sub-interval is then mapped to a different sub-square in such a way that sub-squares mapped to from adjacent sub-intervals share a common edge.

The sub-squares are thus ordered. This is expressed graphically (see Figure 3.2) by drawing a line, made up of straight segments, passing through their centre points in the sequence in which they are mapped to from successive sub-intervals of the line. The line passing through the centre points of the sub-squares is referred to as a *first order* Hilbert curve.

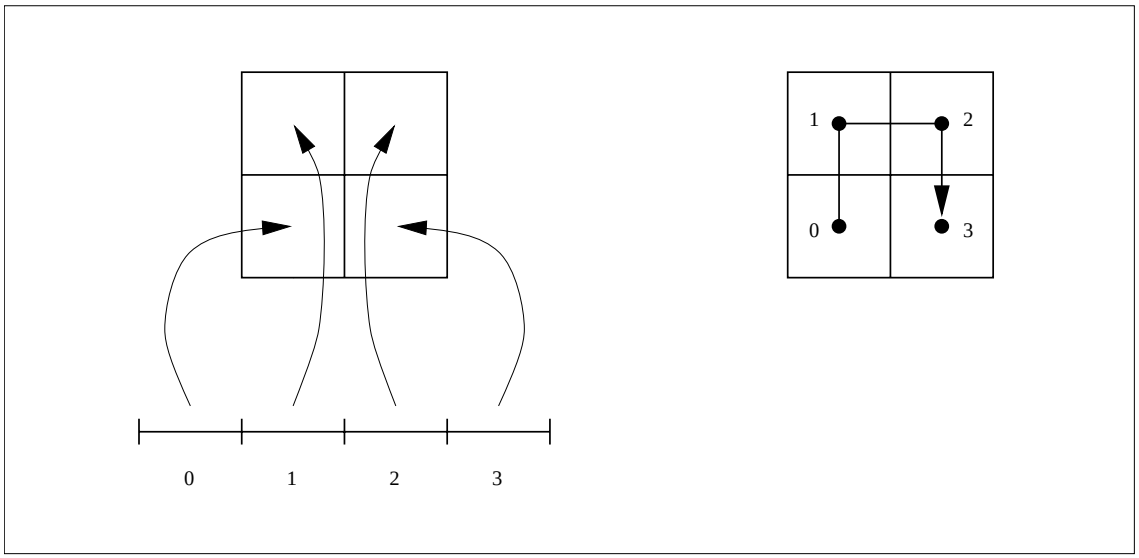

Fig. 3.2: First Order Hilbert Curve: Mapping between Sub-squares and Sub-intervals in 2 Dimensions

Step 2: The process of division of intervals and squares is repeated for each of the four pairs of sub-intervals and sub-squares produced in the first step. This results in 4 groups of 4 equal-sized sub-intervals and sub-squares. Since the sub-squares from which the groups are derived are ordered, the groups themselves are also ordered.

Within each group, a mapping is established between sub-intervals and sub-squares and a first order curve is drawn in a similar manner to that already described in the first step. The particular order in which sub-squares are mapped to from sub-intervals within a group is chosen such that the last sub-square shares a common edge with the first sub-square of the successor group. This may result in a first order curve within the group having a different orientation to and/or being a reflection of the first order curve drawn in the first step.

This procedure transforms a *first order* curve into a *second order* curve, shown in Figure 3.3 where we move to a binary radix in expressing coordinates and sequence numbers.

Higher Order Approximations: A curve of order k, where $k > 1$, is conceptually constructed by *replacing* each point on a curve of order $(k-1)$ by a scaled-down curve of order 1. These first order curves are automatically ordered according to their corresponding points on the curve of order $(k-1)$. They are then suitably rotated and/or reflected so that they can then be connected to each other in such a way that the last point on one curve is adjacent to the first point of its successor. The distance between any such pair of points is the same as the distance between any other pair of points on the resulting curve of order k. The process is equivalent to replacing every point on a curve of order 1 by a curve of order $(k-1)$.

Figure 3.4 shows the third and fourth order curves generated in this manner.

Comments and Observations

It is a consequence of the characteristic whereby line segments in the curve always join squares sharing a common edge that the curve obtained in the limit is continuous.

The recursive, or hierarchical, way in which space is partitioned tends to result in points located within a particular sub-square, being placed closer to each other within the linear ordering than they are to points which lie within any other sub-square of the same

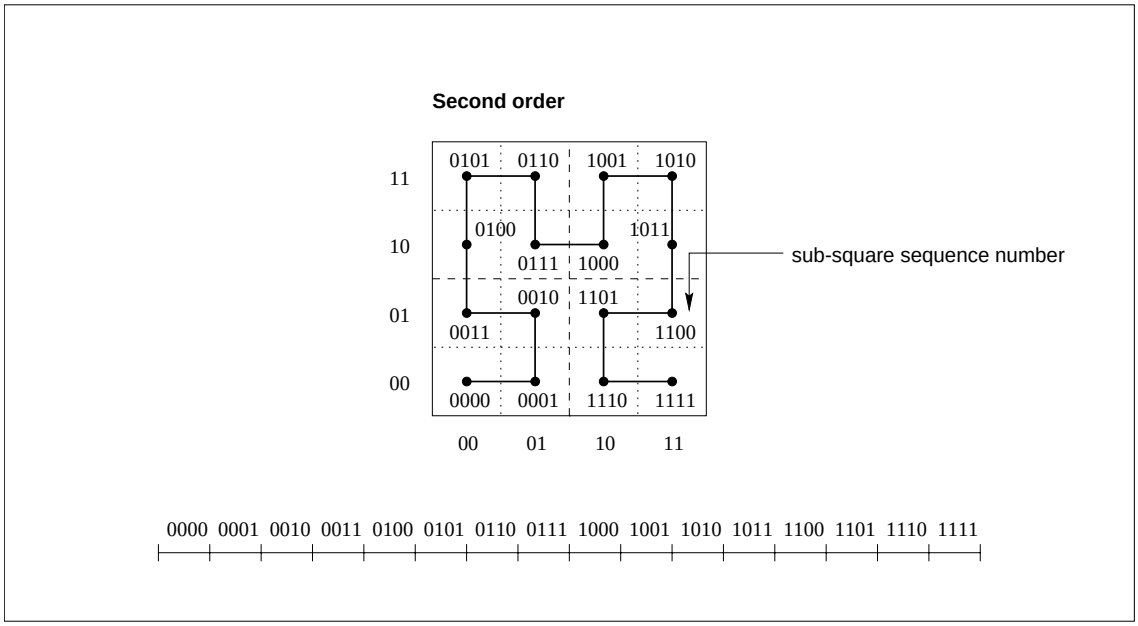

Fig. 3.3: Second Order Hilbert Curve in 2 Dimensions

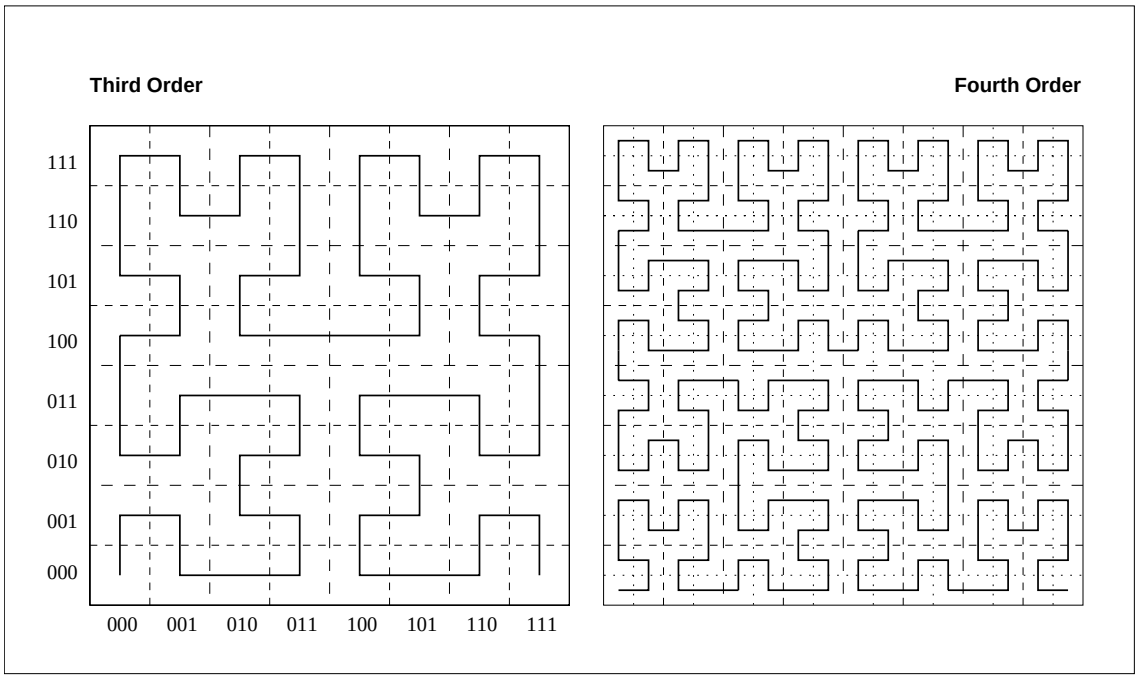

Fig. 3.4: Third and Fourth Order Hilbert Curves in 2 Dimensions

size. As noted in chapter 1, we expect this to be a useful characteristic in our application which should restrict the numbers of pages of data which need to be searched in the course of a typical query.

The mapping produced in step 1 and illustrated in Figure 3.2, ie the choice of ordering of sub-squares, is arbitrarily made from a finite number of available alternatives. Different choices made in this step simply result in different but topologically equivalent orientations of the curve.

We note from Figure 3.3 that the second order curve comprises 4 ordered and connected first order curves. The first and last have different orientations to the curve produced in the first step while the middle two have the same orientation. Furthermore, it can be seen from Figure 3.4 that each of the middle two first order curves within the second order curve of figure 3.3 transforms to curves of the same form and orientation (as the second order curve within the third order curve). The relevance of these observations becomes apparent when we discuss practical methods of performing mappings in chapter 4.

In this way we can see that these finite curves are typified by a characteristic of self-similarity under magnification. This provides us with an insight into how we can express algorithmically such curves of some arbitrary order. Developing this notion is the principal subject of chapter 4.

3.4.2 The Hilbert Curve in Higher Dimensions

The concept of space-filling curves as described by Hilbert can be extended into higher-dimensional space. For example, in 3 dimensions, we begin by dividing a cube into 8 sub-cubes and order them so that sub-cubes which are mapped to from adjacent sub-intervals share a common face. Three examples of first order curves which result from such a mapping are shown in Figure 3.5. We note from the third of these examples that a mapping need not describe a symmetrical curve. A stepwise process of division of sub-intervals and sub-cubes then proceeds in a similar manner to that described in the previous section.

Hilbert curves in higher-dimensional space differ importantly from the 2-dimensional curve, however, in that once an arbitrary first order curve has been drawn, there is a greater choice in ways of transforming it into a second order curve. For example, in 3 dimensions, two of a number of possible alternative ways of transforming the first two points of the curve shown in Figure 3.5(a) are illustrated in Figure 3.6. It is also possible to draw valid first order curves which cannot be transformed into valid second order curves, whereby the adjacency property of successive points is maintained. An example of such a first order curve is given in Figure 3.7.

The existence of alternatives complicates the problem of expressing the Hilbert curve algorithmically. As noted in chapter 1, we utilize a particular definition of the Hilbert curve in our practical application. This definition results from the detail of how we calculate mappings as described in chapter 4. For the time being, however, we note that the existence of alternatives serves to illustrate that the Hilbert curve is a concept rather than a specific phenomenon. Research into alternative Hilbert curves has been undertaken by Alber and Niedermeier who give a mathematical formalism allowing combinatorial study of the Hilbert curve in higher dimensions in [AN98].

3.5 Binary Representation of the Hilbert Curve

In this section we show how to express the correspondence between the one-dimensional sub-intervals and the 2-dimensional sub-squares in binary for approximations of the Hilbert

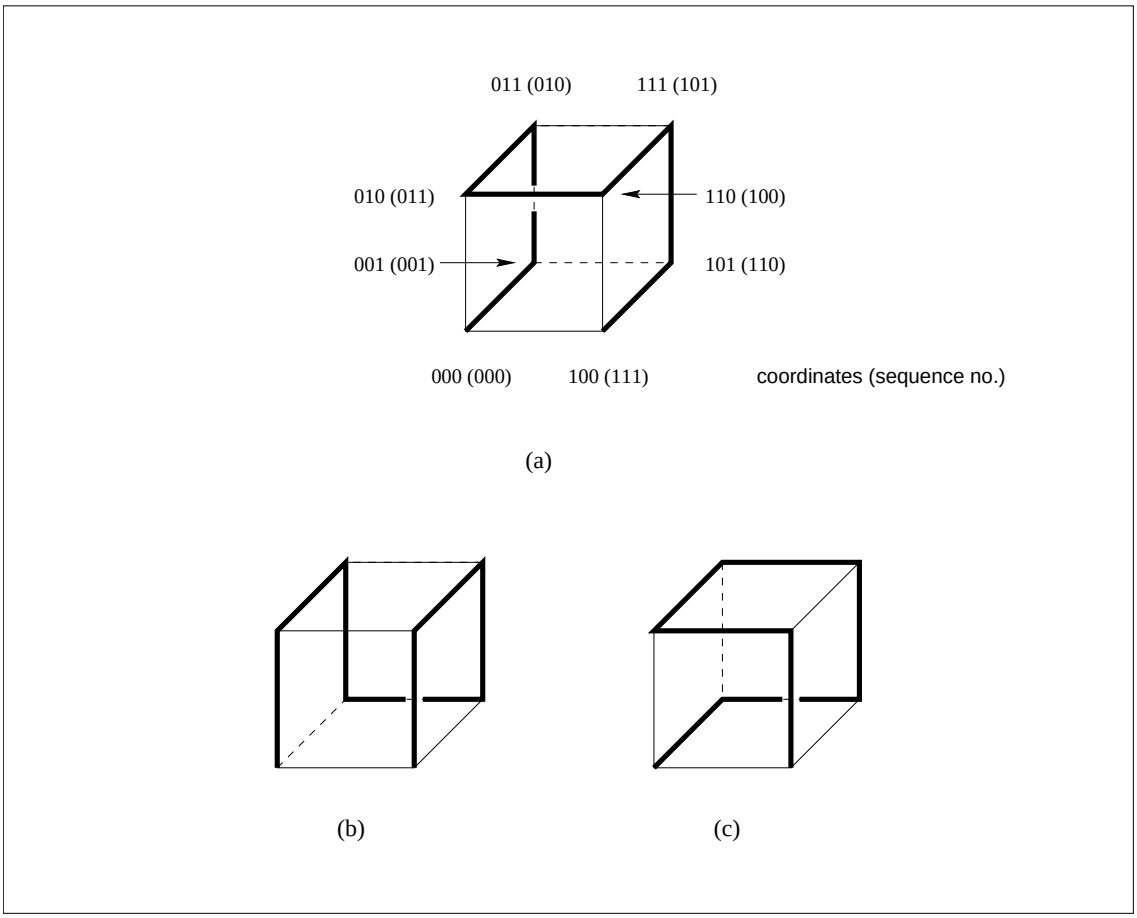

Fig. 3.5: Hilbert First Order Curves in 3 Dimensions

curve. These correspondences are used in the Tree Representation of the Hilbert curve which we discuss later in section 3.6 and more generally in our implementation.

For the first order Hilbert curve shown in Figure 3.2, we note that dividing the square into 4 results from a division of the intervals which define each axis into 2 equal sized sub-intervals. These sub-intervals are placed in sequence and each can be represented by a single digit integer sequence number expressed in binary, ie by 0 or 1. These sequence numbers can now be used to give coordinates to the sub-squares, namely $\langle\ 0,0\ \rangle$, $\langle\ 0,1\ \rangle$, $\langle\ 1,1\ \rangle$ and $\langle\ 1,0\ \rangle$.

The number of sub-intervals into which the line is divided is also 4. These sub-intervals are also in sequence and can be numbered in binary; 00, 01, 10 and 11.

This numeric identification of sub-squares and sub-intervals is shown in Figure 3.8(a).

In the second step of the Hilbert curve construction process, the number of sub-intervals of each axis is doubled and so an additional binary digit is required to represent their values. The number of intervals in the line increases four-fold, and thus an additional 2 binary digits are required to represent the sequence numbers.

Since a group of 4 sub-squares produced in the second step is nested within a sub-square of the first step, the coordinates representing the latter become prefixes of the coordinates representing the former. For example, the sub-square produced in the first step and represented by coordinates $\langle\ 1,0\ \rangle$ is divided into sub-squares represented by coordinates $\langle 10,00\rangle$, $\langle 10,01\rangle$, $\langle 11,00\rangle$ and $\langle 11,01\rangle$. Similarly, since the sequence number of the sub-square represented, for example, by coordinates $\langle 1,0\rangle$ is 11, the sequence numbers of the 4 sub-squares it divides into are all prefixed by 11. This is shown in Figure 3.8(b).

In higher dimensional space, we use the following definitions of terms;

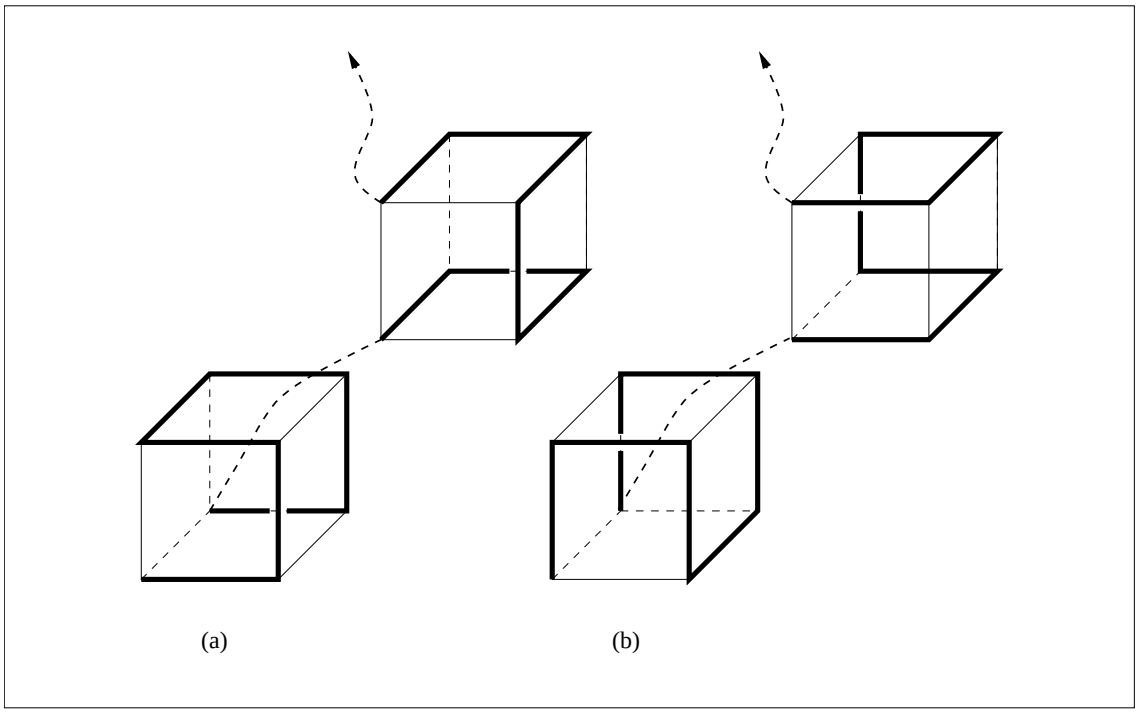

Fig. 3.6: Connecting 3-Dimensional First Order Hilbert Curves

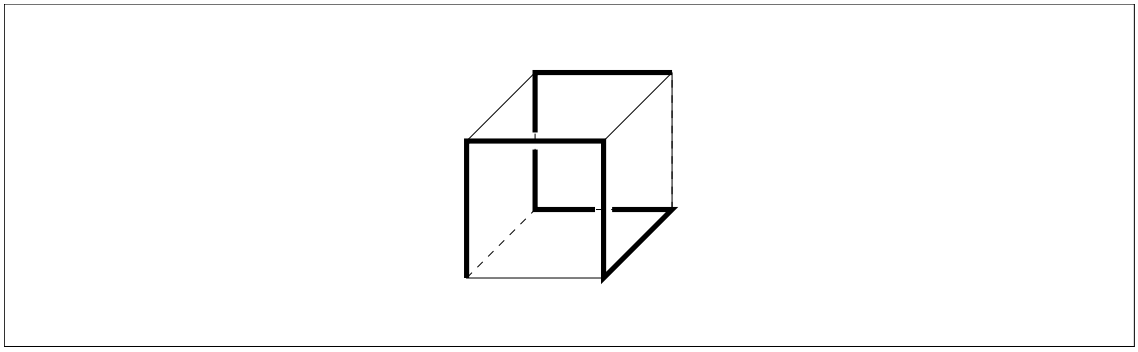

Fig. 3.7: An 'Unsuitable' 3-Dimensional First Order Curve

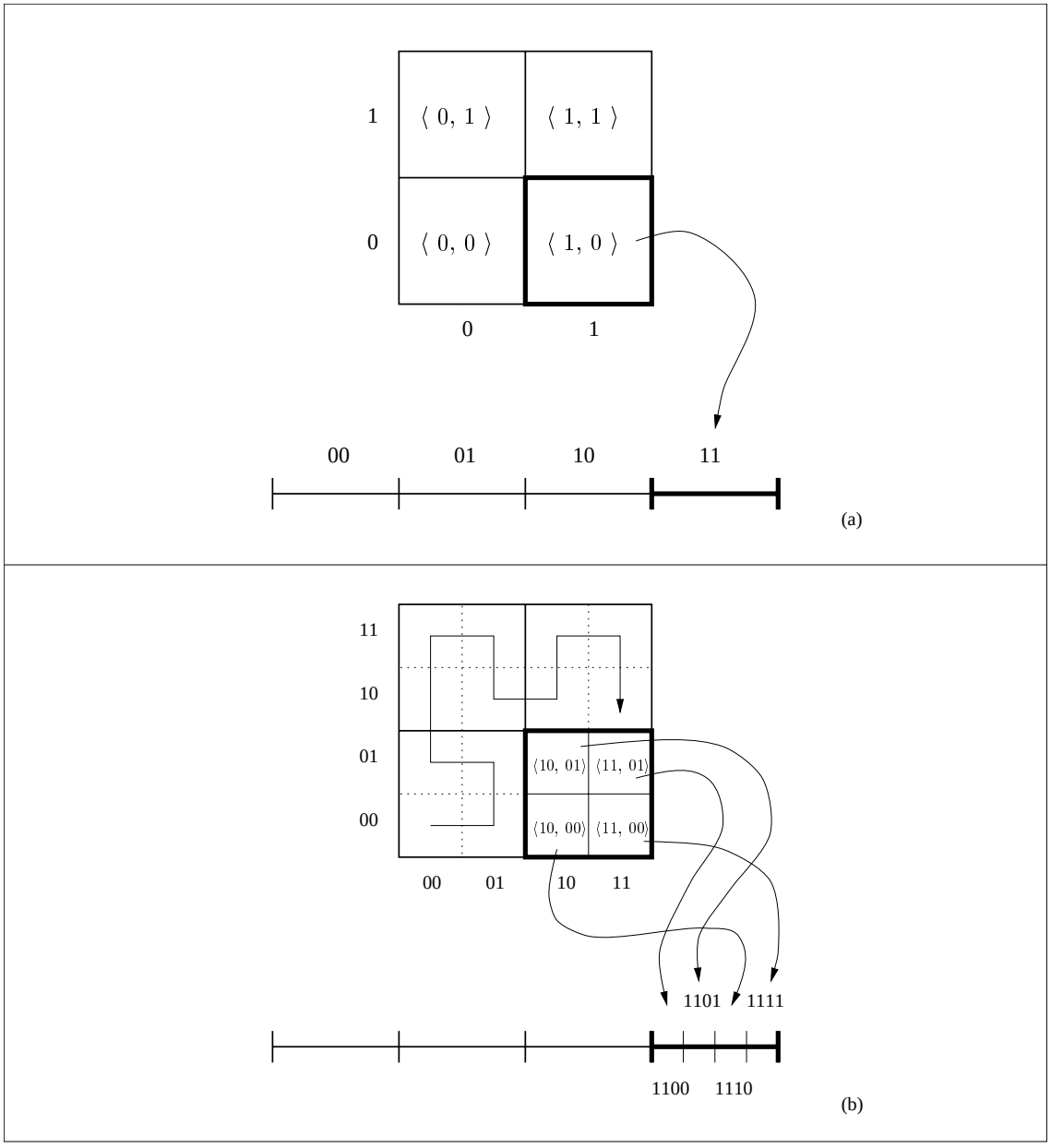

Fig. 3.8: Second Order Hilbert Curve: Mapping between Coordinates and Sub-interval Sequence Numbers in 2 Dimensions

Definition 3.5.1: *hyper-cube : The equivalent in n-dimensional space of a square in 2-dimensional space or a cube in 3-dimensional space, where* $n > 3$.

Definition 3.5.2: *hyper-rectangle : The equivalent in n-dimensional space of a rectangle in 2-dimensional space, where* $n > 2$.

Generally, in n dimensions we note that a first order Hilbert curve passes through 2^n hyper-cubes and that with each increment in the order of a curve, the granularity of the coordinate space for the centre points of these is increased by a magnitude of 2^n. Thus the number of points on a curve of order k is given by

$$2^{kn} \tag{3.1}$$

and so their maximum one-dimensional sequence number requires kn binary digits to represent it, if the first is 0 and not 1.

We saw that a coordinate of a point on a first order curve is expressed by a single binary digit. An additional digit is required to represent distinct coordinate values with each increment in the order of the curve since the number of distinct values increases by a magnitude of 2. Thus the number of digits required to represent coordinate values of a point on a curve of order k is k.

It therefore follows that the number of digits required to represent the sequence number corresponding to a point equals the number of digits required to represent the n coordinates of the point.

3.6 A Tree Representation of Space-filling Curves

As a result of the recursive fashion in which a space-filling curve is constructed, a mapping to a space-filling curve can be expressed as a tree structure. Not only does this provide an insight into how mappings are performed but, more importantly, a tree-like conceptual view greatly aids the development of algorithms which are used to facilitate the execution of queries. This becomes apparent in chapter 6 where our querying algorithms are described.

The height of a tree for a space-filling curve is infinite but, for an approximation, it is finite and equal to the order of the curve. In this section, we confine our interest to approximations of curves but the concepts discussed are applicable generally.

We use the example of the 2-dimensional Hilbert curve in describing the construction of the tree but, again, the process is applicable to other curves and to higher dimensions. We make use of the following term in this section and frequently throughout the remainder of this thesis:

Definition 3.6.1: *n-point : a set of one-bit coordinates of a point lying on a first order curve concatenated into a single n-bit value. These points represent the centre points of sub-squares into which space is partitioned.*

Note that a *derived-key* corresponds to each *n-point* in the same way that a *derived-key* corresponds to each point on a curve of any finite order. The *derived-key* of an *n-point* is an n-bit value.

We begin by placing a first order curve at the root of the tree. If we express the coordinates of points lying on a first order curve as *n-points* then the mapping from one-dimensional sub-interval sequence numbers to coordinates shown in Figure 3.8(a) results in a root node comprising the set of ordered pairs: $\langle 00, 00 \rangle$, $\langle 01, 01 \rangle$, $\langle 10, 11 \rangle$ and $\langle 11, 10 \rangle$. In this notation, the first value of each pair is the derived-key of a sub-interval in the domain of the mapping and the second value is the *n-point* representation of a point lying at the centre of a sub-square.

In the transformation to a second order curve each of these ordered pairs becomes the parent of a node similar to the root and also comprising of a set of ordered pairs and so the height of the tree increases to 2. Note that two of the child nodes express a first order mapping which is the same as that of their parent (root) and two of them express mappings which are different. The fact that some nodes are the same as others is exploited in chapter 4 where we discuss state diagrams. A state diagram of finite size can replace a tree of any height. An example of a tree whose height is 3 is given in Figure 3.9. Tree levels 1 and 2 in this Figure correspond to the mapping shown in Figure 3.8(b). The state diagram which encapsulates this tree is given in Figure 4.1 in chapter 4.

The process of growing the tree can then be continued for each node at the lowest current level as the order of the curve increments. We note that the fanout of the tree equals the number of points on a first order curve.

The set of ordered pairs in all of the leaves corresponds to the finite set of points through which the curve passes while non-leaf nodes correspond to sub-squares which contain a sub-set of points at the leaf level.

Having constructed the tree, we can determine the Hilbert *derived-key*, D, of any point, P, by traversing the tree from root to leaf in the manner described informally in Algorithm 3.6.1. We leave a more formal expression of the algorithm to chapter 5.

Given a *derived-key*, we can determine the coordinates of the point to which it corresponds in a similar manner. If a mapping is required from the coordinates of a point to its *derived-key* then the process is more readily facilitated if the ordered pairs in the nodes are sorted by *n-point* values rather than by sub-square sequence numbers. Figure 3.9 is thus more suited for determining to which point a given *derived-key*, or sequence number, corresponds.

Algorithm 3.6.1 Finding the *derived-key* of a Point by Traversing the Tree Representation of the Hilbert Curve

```
1:  current_level ⇐ 1
2:  current_node ⇐ root
3:  D ⇐ the empty bit-string
4:  repeat
5:     p ⇐ one bit in position current_level taken from each coordinate in P, concatenated
       into an n-point
6:     d ⇐ the n-bit derived-key taken from current_node corresponding to p
7:     append d to D
8:     if current_level < leaf level then
9:        current_node ⇐ node pointed to by the ordered pair ⟨ p, d ⟩ within current_node
10:    end if
11:    current_level ⇐ current_level +1
12: until current_level > leaf level
```

3.7 Alternatives to Space-filling Curves

We saw in the introduction to this chapter that the existence of a function which maps integers to points in a one-to-one manner, such as a mapping to the Hilbert curve, is essential to our application. In this section we consider alternative mappings which share this characteristic but do not technically describe space-filling curves. Generally, this is because they are discontinuous, although we note in the introductory chapter that we also apply the term 'space-filling' curve to discontinuous curves. A discontinuity occurs when a pair of points which are not adjacent in space are consecutive in their ordering.

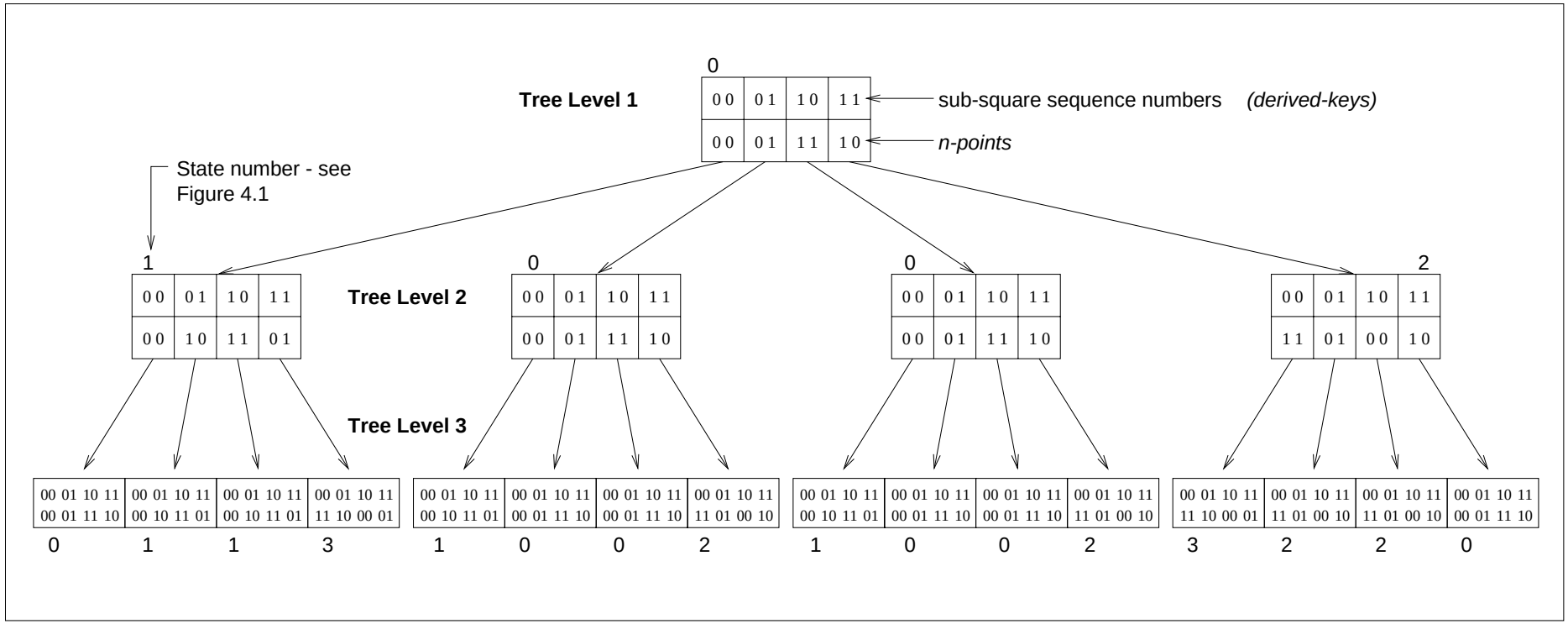

Fig. 3.9: The Tree Representation of the Third Order Hilbert Curve in 2 Dimensions

With the exception of the 'Scan' and 'Snake' curves, those discussed in this section are constructed in a similar manner to that described for the Hilbert curve in section 3.4 above. Thus sections 3.5 and 3.6 above relating to binary and tree representations also apply to discontinuous curves. An important distinction, however, is that during the recursive process of division of space, the requirement that each consecutively ordered pair of sub-squares share a common edge is relaxed for discontinuous curves.

We note that the distance between consecutive points separated by a discontinuity is variable and, as the magnitude of a discontinuity increases, the frequency with which it occurs decreases. This is apparent from the illustrations of the Z-order and Gray-code curves given later in this section and arises from the recursive way in which space is divided.

Although discontinuities exist in some curves, a general proximity between points which are close in space can be maintained in their one-dimensional ordering.

The reasons for considering alternatives to 'true' space-filling curves are twofold. Firstly, as we shall see in chapters 4 to 6, different algorithms for calculating mappings and executing queries may be employed where non-space-filling curves are utilized. Some of these algorithms prove to be more efficient than those required by the Hilbert curve. Secondly, data is clustered differently when non-space-filling curves are utilized. We therefore have an opportunity to compare the results of implementations with different combinations of algorithms and data clustering properties. In part, such comparisons explore the conjecture that clustering arising from the application of the Hilbert curve is beneficial.

3.7.1 The Z-order Curve

The Z-order curve is first attributed to Morton [Mor66]. It has been the subject of considerable interest and has found application in may areas of research. Notable examples of the application of Z-ordering include Quad Trees [Sam90a], the PROBE Project [OM88] and the BANG file [Fre87].

Our interest arises from the particular simplicity with which Z-order mappings are performed and because the curve appears to provide a compromise between the clustering properties of the Hilbert curve and some other non-space-filling curves described below, namely the Scan and Snake curves.

Examples of first to fourth order curves in 2 dimensions are shown in Figure 3.10 which clearly illustrates self-similarity as the curve transforms from one order to the next. We note that a discontinuity exists between each pair of points. This is a characteristic which holds regardless of the number of dimensions in a space. We note that some of the discontinuities arise from the fact that the sub-squares within every square are always given the same orientation or ordering.

The inverse of the mapping to the Z-order curve is carried out by a process which is often referred to as *bit-interleaving* in the literature. An example showing the calculation of the *derived-key* of a point lying on a 2-dimensional third order curve is given in Figure 3.11. I a space containing a finite number of points, a point corresponds to a sub-square within the space. Where coordinates are expressed in binary notation, as in the example, a bit is taken from each coordinate in turn, in a cyclical manner, and these bits are concatenated into a single value. For example, if all of the bits of the coordinates of a 2-dimensional point, P, lying on a curve of order k, are given as:

$$P = \langle\, x_1 x_2 x_3 \ldots x_k,\ y_1 y_2 y_3 \ldots y_k \,\rangle \tag{3.2}$$

where x_1 and x_k are the most and least significant bits respectively in a coordinate value in dimension x, then the Z-order *derived-key*, Z, which results from bit-interleaving is:

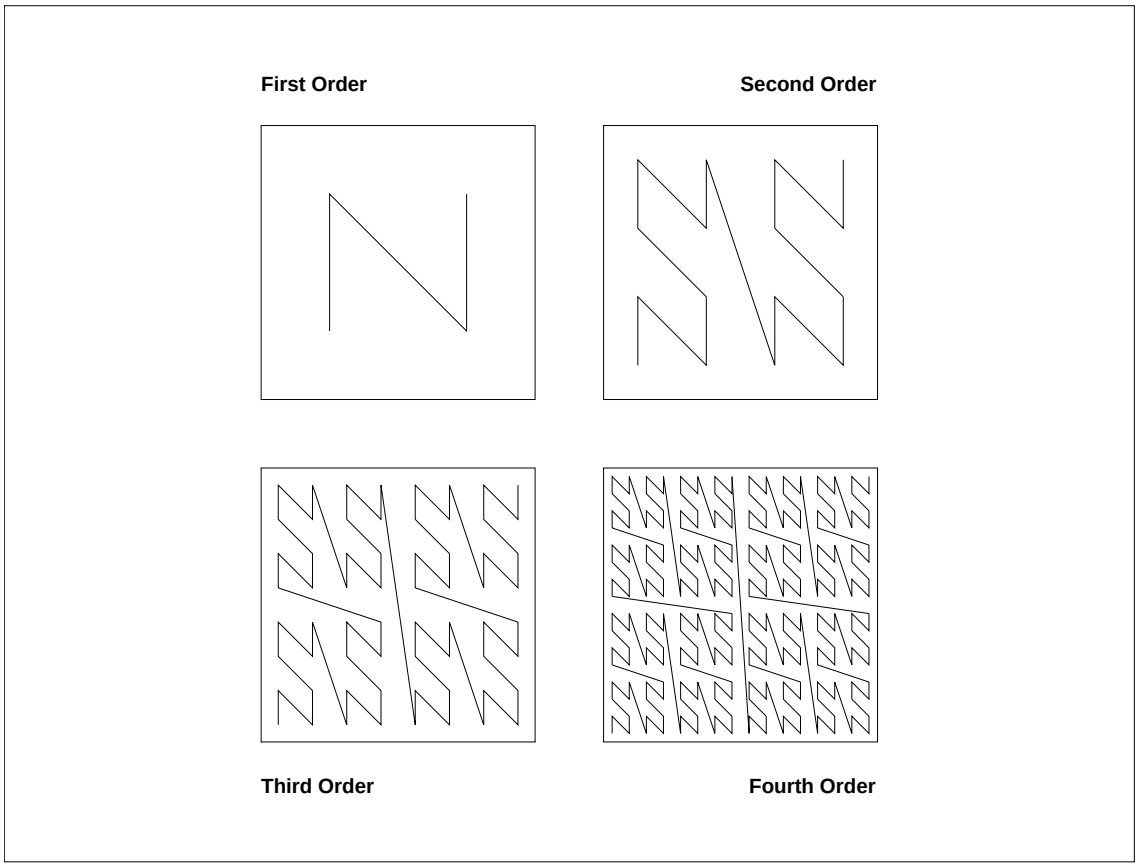

Fig. 3.10: Approximations of the Z-order Curve in 2 Dimensions

$$Z = x_1 y_1 x_2 y_2 x_3 y_3 \ldots x_k y_k \tag{3.3}$$

Figure 3.10 illustrates the curve arising from this process of bit-interleaving.

Generally, in n dimensions, the coordinates of P can be expressed as:

$$P = \langle\, p_1,\ p_2, \ldots,\ p_n \,\rangle \tag{3.4}$$

where each p_i is a coordinate in dimension i and i is in the range $[\,1 \ldots n\,]$. Each p_i is composed of k bits and so the coordinates of P can also be expressed as:

$$P = \langle\, p_{1_1} p_{1_2} \ldots p_{1_k},\ p_{2_1} p_{2_2} \ldots p_{2_k},\ \ldots,\ p_{n_1} p_{n_2} \ldots p_{n_k} \,\rangle \tag{3.5}$$

where p_{i_j} is a single bit and j is in the range $[\,1 \ldots k\,]$. Thus p_{i_1} is the most significant bit of the coordinate in dimension i and p_{i_k} is the least significant bit in the same coordinate.

The Z-order *derived-key* of P can be derived from (3.5) by bit-interleaving as:

$$Z = p_{1_1} p_{2_1} \ldots p_{n_1} p_{1_2} p_{2_2} \ldots p_{n_2} \ldots p_{1_k} p_{2_k} \ldots p_{n_k} \tag{3.6}$$

This *derived-key* comprises k sequences of n bits. If p_{i_j} is a bit, then all of the bits within any one of these k sequences have the same value for j. The n most significant bits may then be expressed more succinctly as z_1, the next n bits as z_2, and so on until the n least significant bits are expressed as z_k.

The Z-order *derived-key* of P can be expressed succinctly as:

$$Z = z_1 z_2 \ldots z_k \tag{3.7}$$

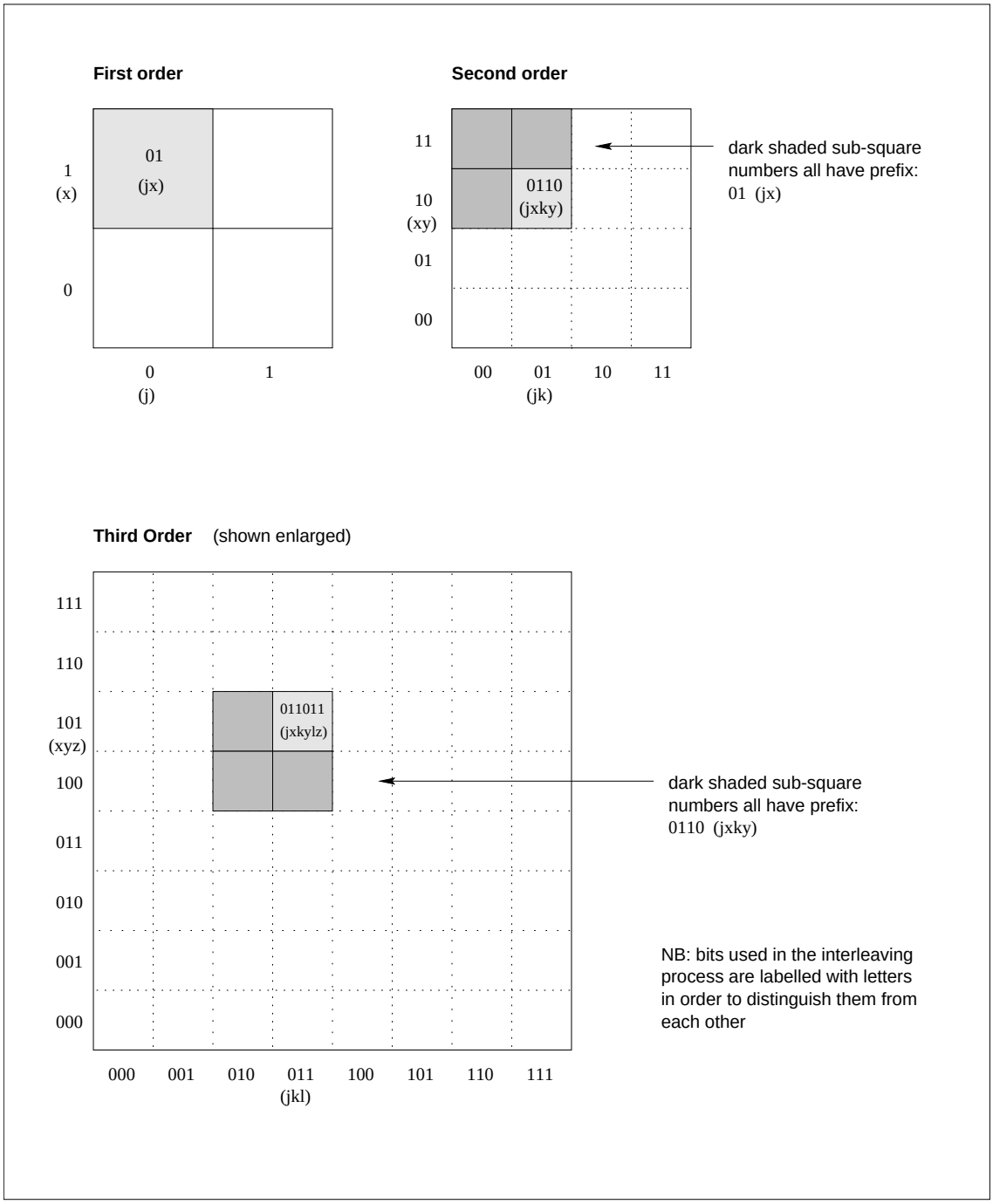

Fig. 3.11: Calculation of the Z-order *derived-key* of a Point

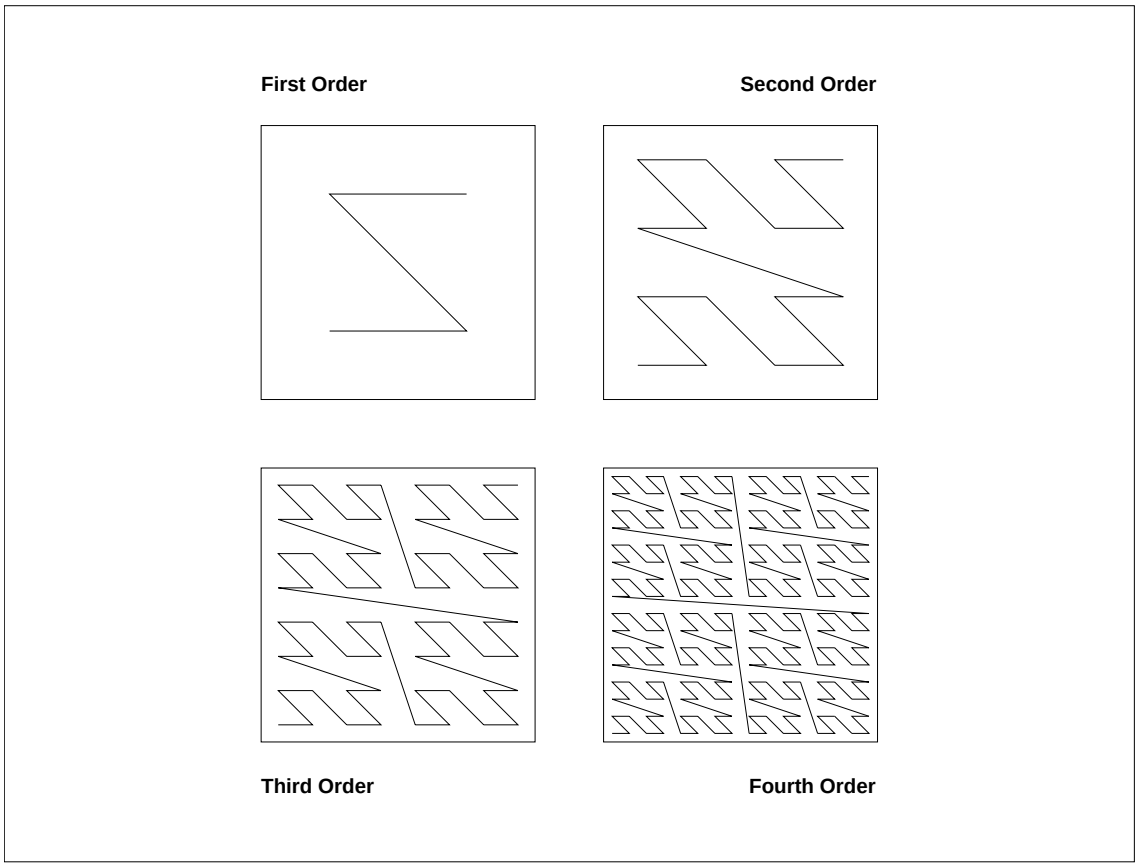

Fig. 3.12: Alternative Approximations of the Z-order Curve in 2 Dimensions

where each z_i is in the range $[0 \ldots 2^n - 1]$ or, more generally, $[0 \ldots r^n - 1]$.

In a similar way in which the concept of 'approximations' is applied to the Hilbert curve, we see that z_1 is a first order approximation of Z, $z_1 z_2$ is a second order approximation, and so on. Similarly, z_i locates a hyper-cube in coordinate space, or a node in a tree representation, containing P within a hyper-cube defined by z_{i-1}.

Continuing with the 2-dimensional example, bits may be taken from the coordinates in a different order to produce, for example, a *derived-key* of:

$$Z = y_1 x_1 y_2 x_2 y_3 x_3 \ldots y_k x_k \tag{3.8}$$

The first to fourth order curves which result from this ordering are shown in Figure 3.12. The corresponding n-dimensional Z-order *derived-key* of point P, given above in (3.5), is expressed as:

$$Z = p_{n_1} p_{(n-1)_1} \cdots p_{1_1} p_{n_2} p_{(n-1)_2} \cdots p_{1_2} \cdots p_{n_k} p_{(n-1)_k} \cdots p_{1_k} \tag{3.9}$$

In general, when we refer to the 'Z-order' curve in this thesis, *derived-keys* are defined by (3.6) rather than by (3.9), but where we wish to distinguish between the two variations specifically, we refer to them as the Z^A-order curve and Z^B-order curve respectively.

Another variation still interleaves groups of bits rather than individual bits, producing, for example, a *derived-key* of:

$$Z = x_1 x_2 y_1 y_2 x_3 x_4 y_3 y_4 \ldots x_{k-1} x_k y_{k-1} y_k \tag{3.10}$$

This implies that the concept applies equally to coordinates which are expressed in any radix, in which case, $x_{i-1} x_i$, where i is even, is the binary representation of a digit in

expressed in a radix of 4, ie in the range $[0 \ldots 3]$.

It follows from the way that a mapping to the Hilbert curve proceeds by dividing space into sub-squares, rather than sub-rectangles, that the coordinate domains in all dimensions are of equal size. The process of bit interleaving, however, offers a greater degree of flexibility. In a 2-dimensional approximation, for example, if the x coordinate domain requires m bits to represent any value and the y coordinate domain requires k bits and $m = 2k$, interleaving may proceed in the following manner:

$$Z = x_1 x_2 y_1 x_3 x_4 y_2 x_5 x_6 y_3 \ldots x_{m-1} x_m y_k \tag{3.11}$$

This allows *derived-keys* to be stored more compactly, in $m+k$ bits rather than in $2m$ bits as would be required for the Hilbert curve.

The process of bit-interleaving results, importantly, in a direct relationship between the values of bits (or digits) in particular positions within particular coordinates and the values of bits (or digits) in particular positions within *derived-keys*, and vice-versa. Furthermore, the value of any bit within a *derived-key* is independent of the value of any higher bit. These characteristics are not true of the Hilbert curve. They are exploited in chapter 6 where alternative querying algorithms to those developed for the Hilbert curve are given for the Z-order curve. These Z-order curve algorithms provide the advantage of a lower computational complexity.

3.7.2 The Gray-code Curve

The Gray-code Sequence

The Gray-code sequence is a sequence of binary numbers in which any two successive numbers differ in value in one bit position only. This sequence is originally attributed to Gray [Gra53] who applied it to the electronic transmission of data. The sequence does not describe a space-filling curve but the concept has been explored in the context of indexing multi-dimensional data and used in the design of a discontinuous curve by Faloutsos [Fal86, Fal88].

The sequence is generated iteratively in the following way:

1. The sequence is initialized as $[0, 1]$.
2. This sequence is then reflected to produce $[0, 1, 1, 0]$. Members of the lower half of the sequence are all prefixed with a bit of value 0 and members of the upper half are prefixed with a bit of value 1, producing the sequence $[00, 01, 11, 10]$.
3. The previous step is repeated to produce successively longer sequences, doubling in size with each iteration. The number of bits required to represent a member of the sequence increases by one with each iteration.

The sequence produced after n iterations contains 2^n distinct members, called *Gray-codes* and each comprised of n bits, in the range $[0 \ldots 2^n - 1]$. Thus the Gray-code sequence is an ordering of the integers.

The first sixteen members of the Gray-code sequence are listed in Figure 3.13. Methods of calculating the Gray-code of an arbitrary number and, inversely, the sequence number, ie *derived-key*, of an arbitrary Gray-code are given in section 5.5 of chapter 5.

Faloutsos' Application of the Gray-code Sequence

The curve proposed by Faloutsos and which exploits the concept of the Gray-code sequence is less discontinuous than the Z-order curve. It has become known in the literature as the 'Gray-code' curve. In this thesis, we refer to the Gray-code curve described by

Sequence no.	Gray-code
0000	0000
0001	0001
0010	0011
0011	0010
0100	0110
0101	0111
0110	0101
0111	0100
1000	1100
1001	1101
1010	1111
1011	1110
1100	1010
1101	1011
1110	1001
1111	1000

Fig. 3.13: The Sequence of Gray-codes of Length 4

Faloutsos as the 'Gray-code^F' curve in order to distinguish it from variations described later in this section. In the remainder of this thesis, we use the term 'Gray-code curve' only where the distinction between the variations is not relevant or to refer to a category of curves.

We saw that the Z-order curve contains a discontinuity between each pair of points. In contrast, the Gray-code^F curve contains a discontinuity between each sequence of 2^n points, this being the number of points on a first order curve. Furthermore, whereas a pair of points on the Z-order curve separated by a discontinuity differ in coordinate values in between 2 and n dimensions, a similar pair on the Gray-code^F curve differ in one dimension only, regardless of n. Most simulation and analytical studies described in section 2.2.1 in chapter 2 suggest that applications using Gray-code^F curves should outperform those using Z-order curves when processing queries. This is attributed to the 'superior' clustering properties of the former arising from the nature of its discontinuity.

The manner in which mappings are calculated is more complex than is the case with the Z-order curve but more straightforward in comparison with the Hilbert curve, at least conceptually. This becomes apparent in chapters 4 and 5 which focus on mapping algorithms, particularly for the Hilbert curve.

The Gray-code^F curve in 2 dimensions is illustrated in Figure 3.14 and the second order curve in 3 dimensions is illustrated in Figure 3.15. First order Gray-code^F curves are similar to first order Hilbert curves.

A mapping from a point, P, to its Gray-code^F curve *derived-key* is carried out in the following manner:

1. Each coordinate of P is substituted by its Gray-code.

2. The bits of the n Gray-codes produced in the previous step are interleaved in the manner described for the Z-order curve. This creates a single value, G, which is regarded as being a Gray-code.

3. The sequence number of the Gray-code G is calculated (using Algorithm 5.5.1 given in chapter 5). This is the Gray-code^F curve *derived-key* of P.[1]

[1] This step appears to have been erroneously omitted in the description of the Gray-code curve on page 109 of [Sam90b].

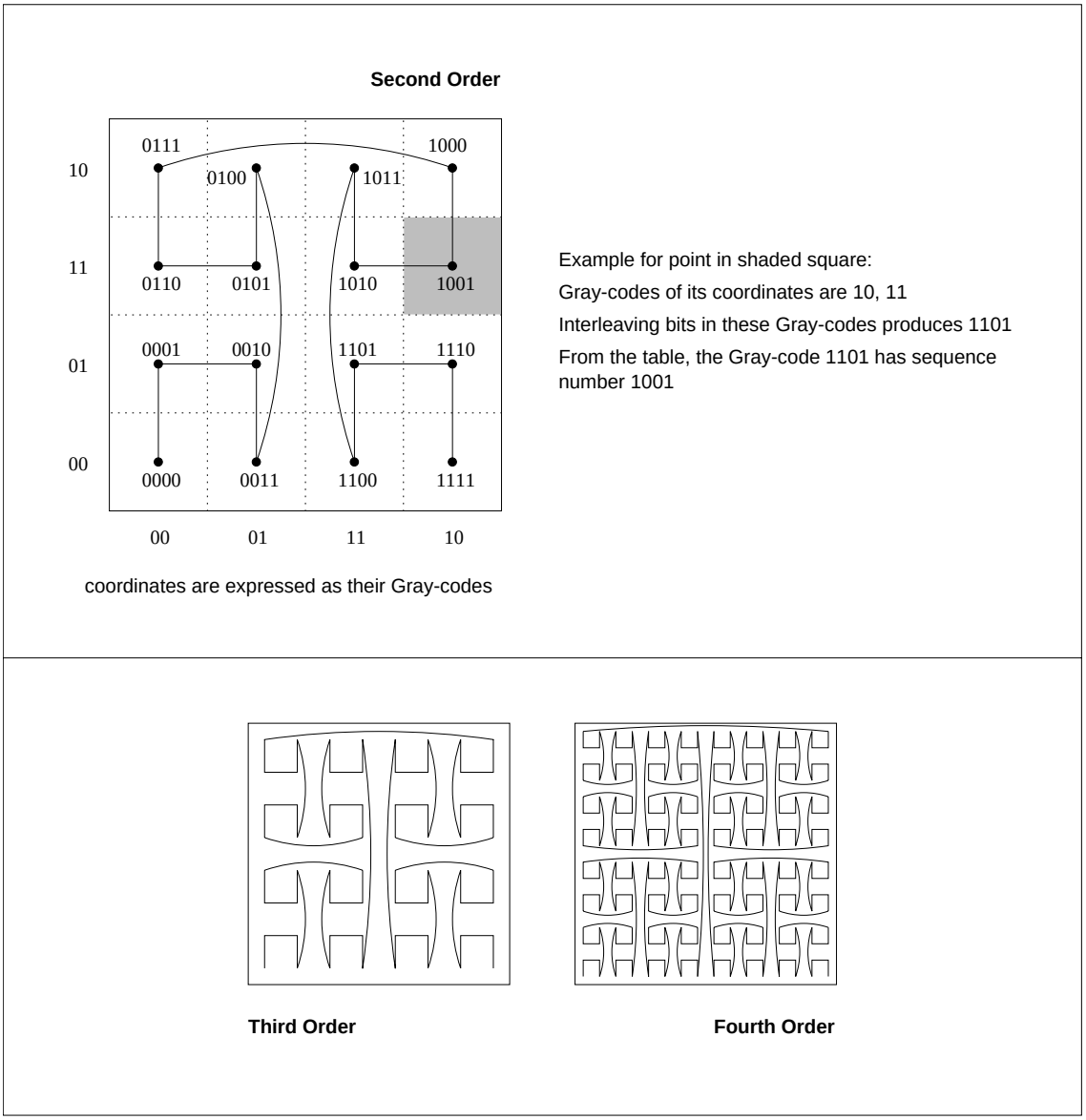

Fig. 3.14: The Gray-code^F Curve in 2 Dimensions (after Faloutsos)

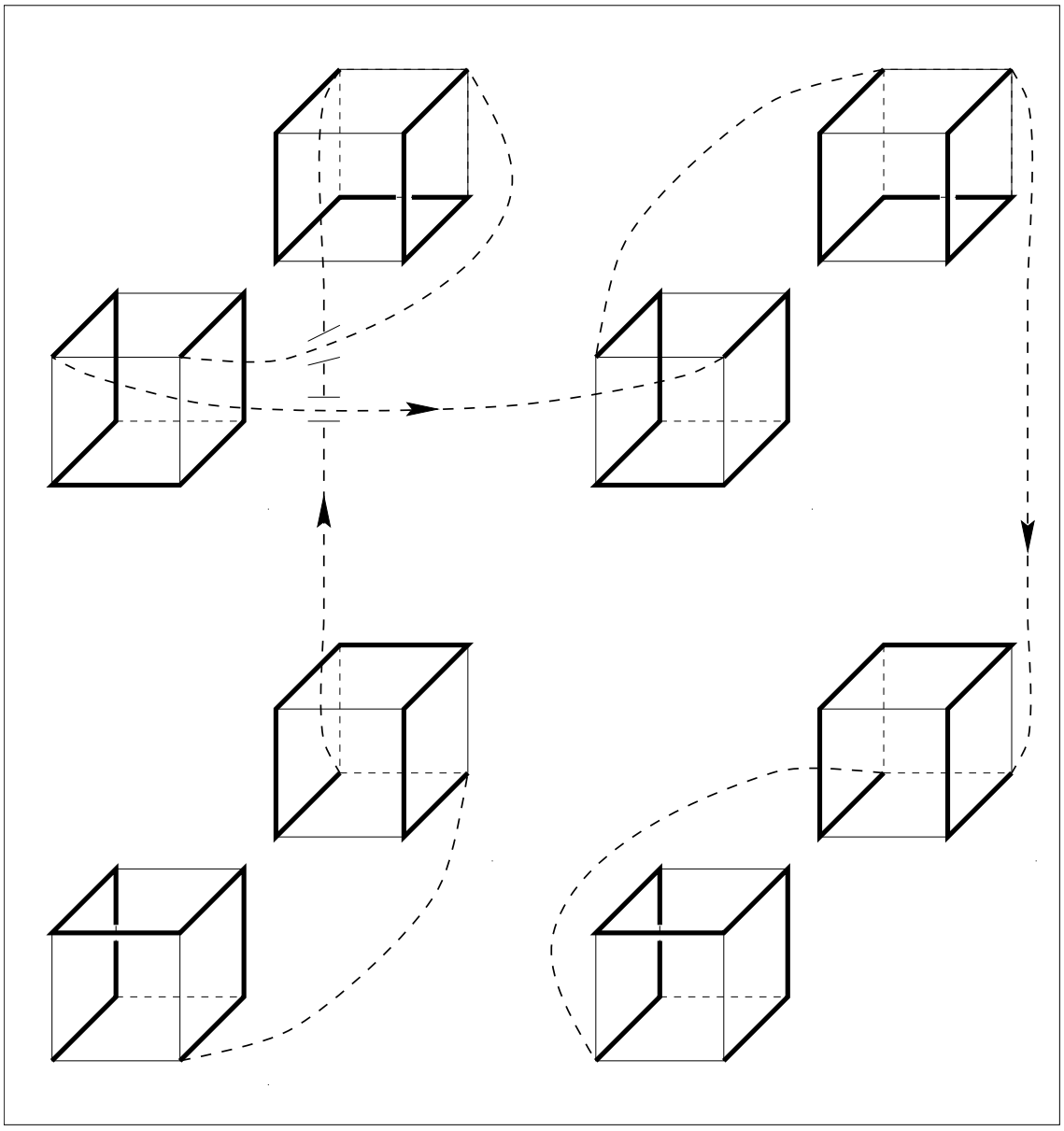

Fig. 3.15: The Gray-code^F Curve in 3 Dimensions (after Faloutsos)

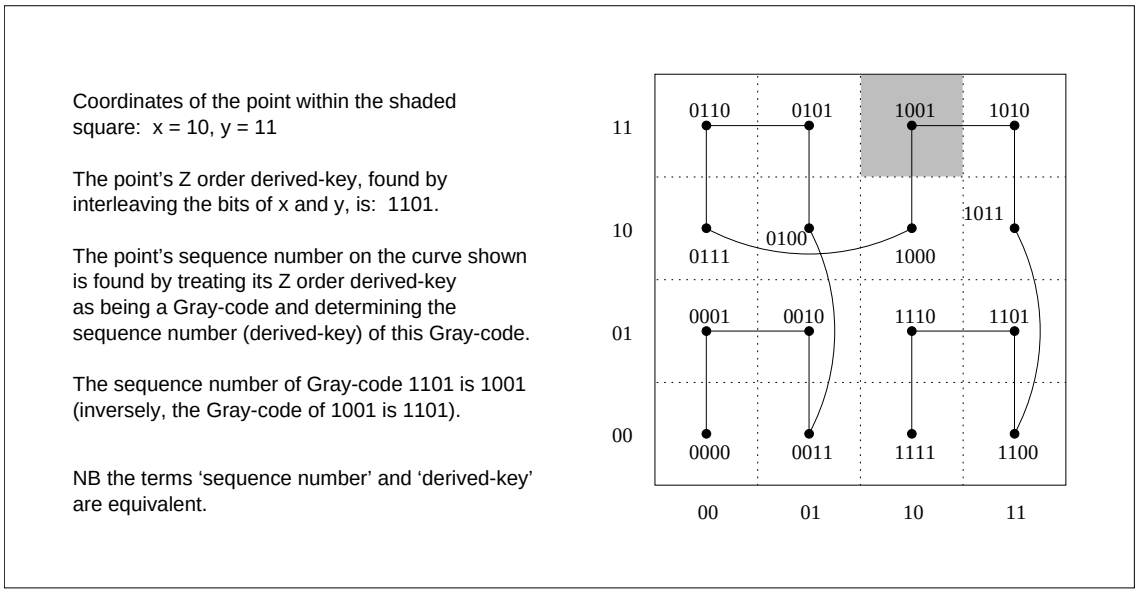

Fig. 3.16: The Gray-code^A Curve in 2 Dimensions

The inverse mapping, from a Gray-code^F curve *derived-key* to its corresponding point, P, is carried out in a similar manner as follows:

1. G is assigned the Gray-code of the Gray-code^F *derived-key*.
2. The coordinates of P are initially determined from G by a process which is the reverse of bit-interleaving.
3. Each of the coordinates of P are transformed into their Gray-code sequence numbers (using Algorithm 5.5.1).

The complexities of the mappings in both directions are equivalent and this becomes apparent in chapter 5.

Alternative Applications of the Gray-code Sequence

We are able to make use of the Gray-code sequence to produce variations on the curve proposed by Faloutsos. We briefly consider two of these as they offer some improvement in the efficiency of mapping between points and *derived-keys* and the first variation appears to provide closer clustering of points.

The first variation, which we call the Gray-code^A curve, differs from the Gray-code^F curve in that step 1 is omitted in the mapping from points to their *derived-keys*. Thus the Gray-code^A curve *derived-key* of a point is calculated as the Gray-code sequence number of the Z-order *derived-key* of the point. Similarly, step 3 in the Gray-code^F curve mapping from *derived-keys* to points is omitted for the Gray-code^A curve.

We see in chapter 5 that the mapping from sequence numbers to their Gray-codes is less complex than the inverse. Thus for the Gray-code^A curve, the mapping from one dimension to n dimensions is less complex than the inverse.

The characteristics of this curve are similar to those of the Gray-code^F curve except that any 2 successive points separated by a discontinuity are closer together in space. This is apparent from a comparison of the illustrations given for the 2 curves. Second order Gray-code^A curves in 2 and 3 dimensions are shown in Figures 3.16 and 3.17.

The second variation, which we call the Gray-code^B curve, is similar to the Gray-code^A curve, except that in one curve, Gray-code mapping calculations are always carried out

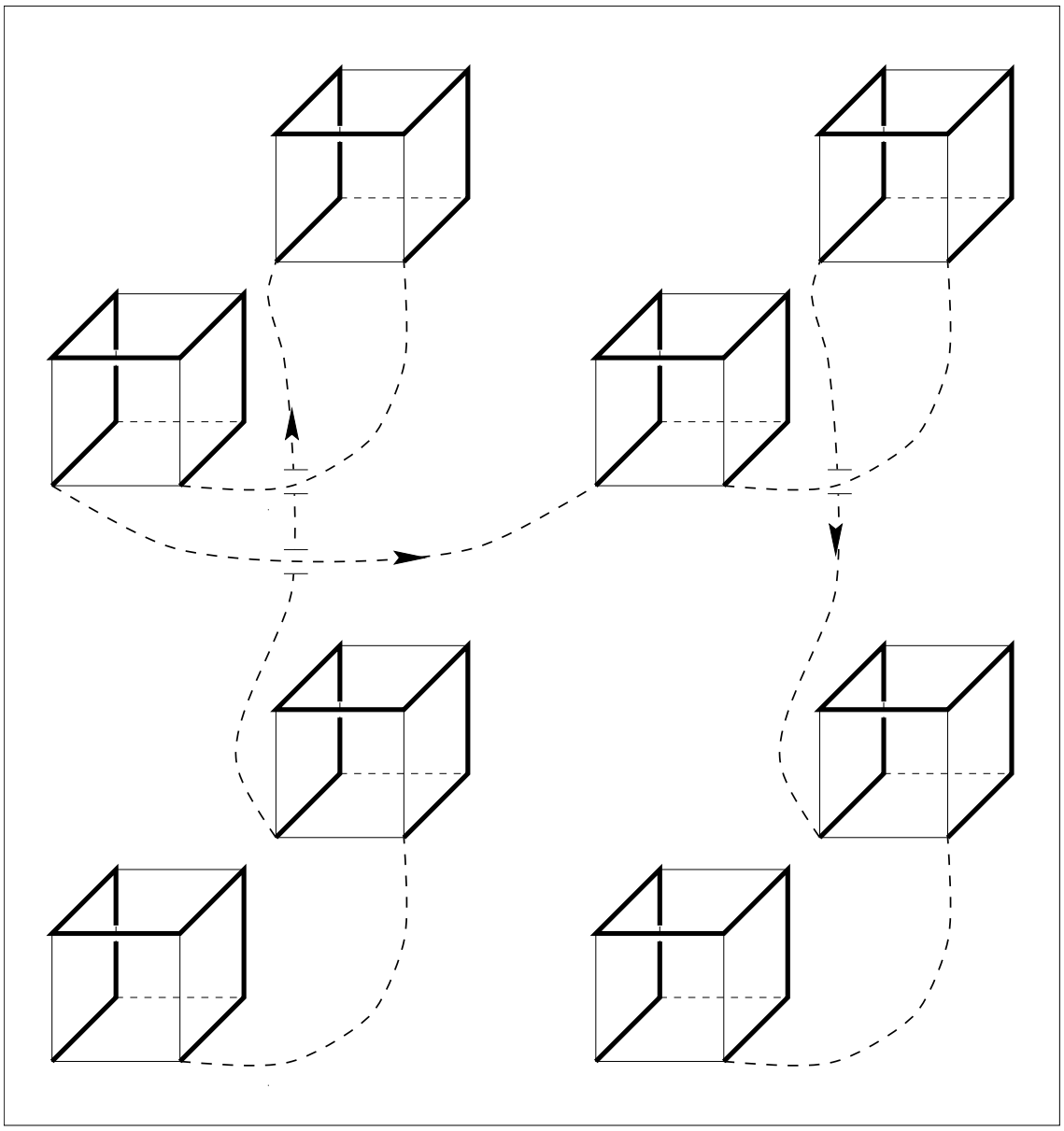

Fig. 3.17: The Gray-code^A Curve in 3 Dimensions

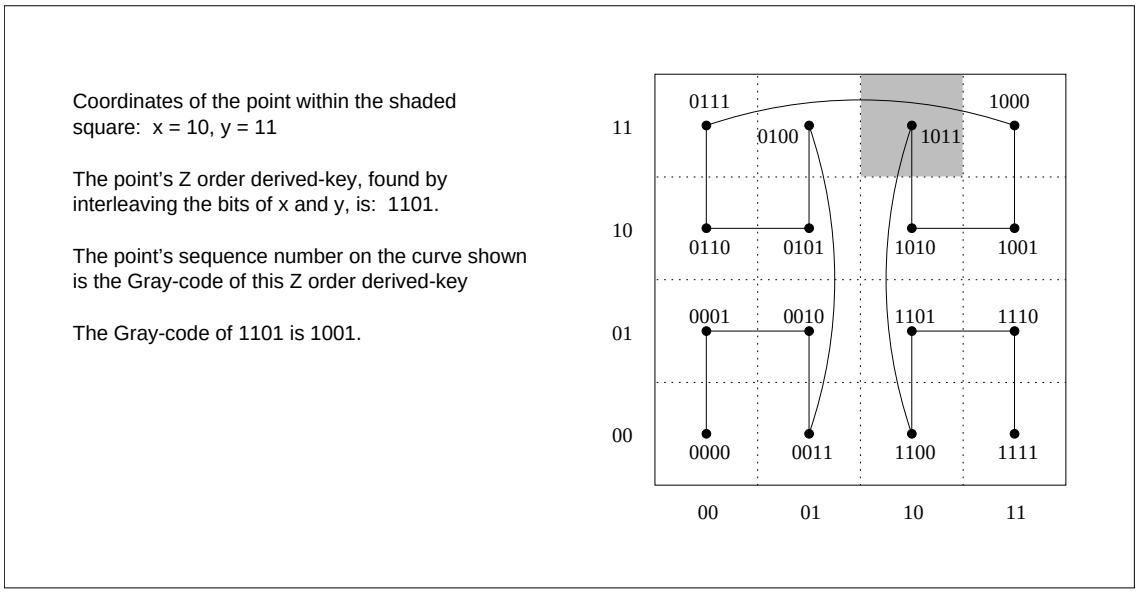

Fig. 3.18: The Gray-code^B Curve in 2 Dimensions

in the opposite direction to those carried out in the other. Thus the Gray-code^B curve *derived-key* of a point is calculated as the Gray-code of the Z-order *derived-key* of the point. Similarly, the coordinates of the point corresponding to a Gray-code^B curve *derived-key*, B, are found by calculating the Gray-code sequence number of B and then performing the reverse of the Z-order bit-interleaving process on the result.

Similar to those of the Gray-code^A curve, the mapping algorithms for the Gray-code^B curve are less complex than those of the Gray-code^F curve. In contrast to the Gray-code^A curve, mapping from a point to its *derived-key* is less complex than the inverse.

The Gray-code^B curve manifests a discontinuity between each group of 4 points regardless of the number of dimensions. The 2-dimensional curve appears the same as the Gray-code^F curve but, as described above the mapping is carried out differently. An example is given in Figure 3.18. The 3-dimensional curve, shown in Figure 3.19, is quite different and contains discontinuities in which successive points differ in coordinate values in more than one dimension.

The relevance of the distinction between the Gray-code^A and Gray-code^B curves, in part, lies in the fact that their mappings are of different complexities, in opposite directions. Updates make frequent use of mappings from points to *derived-keys* whereas our querying algorithms rely primarily on mappings from *derived-keys* to points. Thus the Gray-code^A should handle queries more efficiently and the Gray-code^B should handle updates more efficiently.

3.7.3 The Scan and Snake Curves

Probably the simplest way of mapping between points in n dimensions and points on a line is to express coordinates as fixed length integers and then to concatenate all of the coordinates of a point to produce a single value. This is commonly known as the *Scan* curve and we illustrate the 2 dimensional case in Figure 3.20. As with bit-interleaving, the order in which coordinates are concatenated is flexible. Whatever ordering is chosen, a discontinuous curve results.

A variant of the *Scan* curve is the *Snake* curve, also shown in Figure 3.20, in which adjacent pairs of parallel lines in n-dimensional space are joined together alternately by their beginnings or ends. This avoids the discontinuities present in the scan curve.

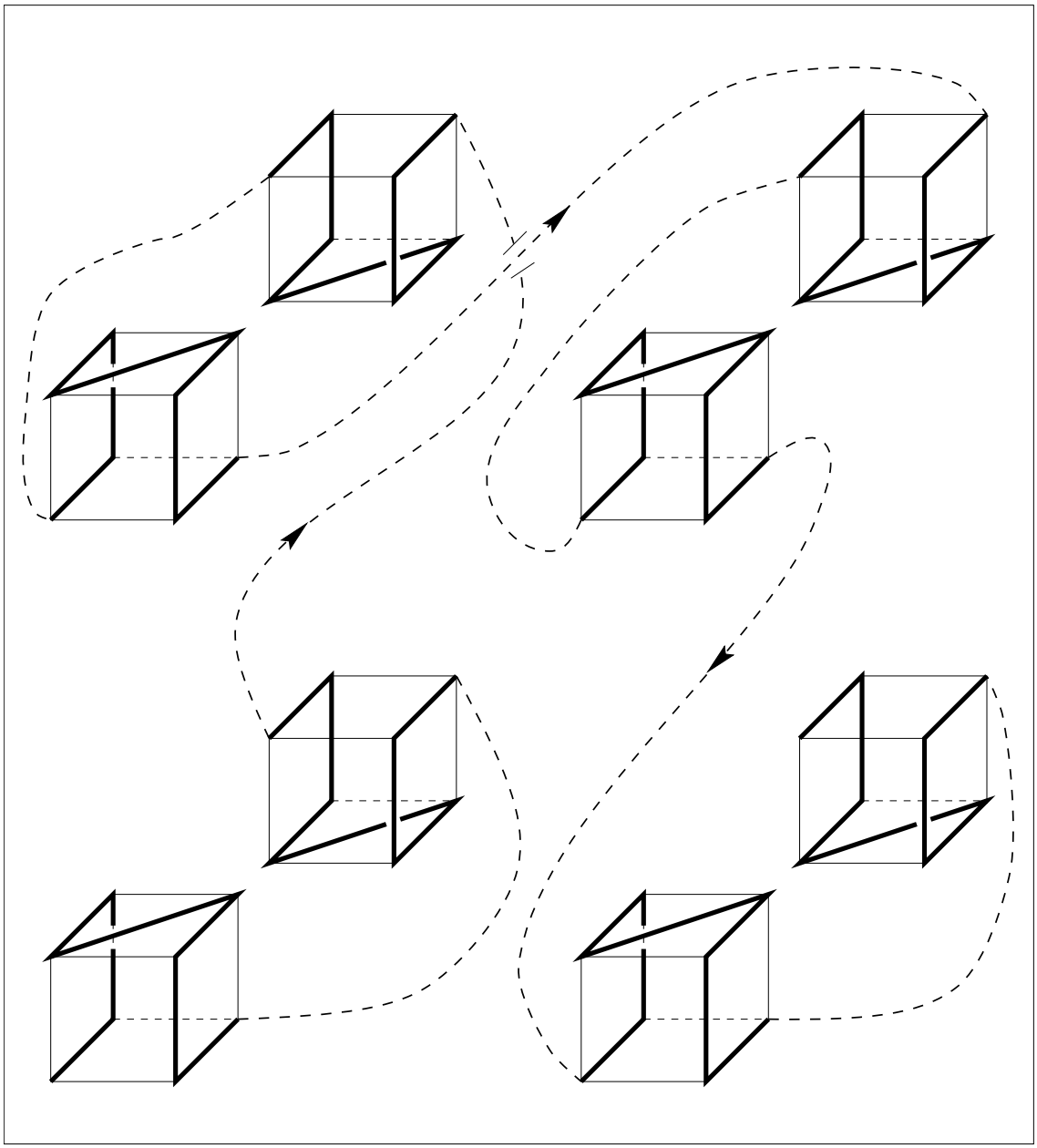

Fig. 3.19: The Gray-code^B Curve in 3 Dimensions

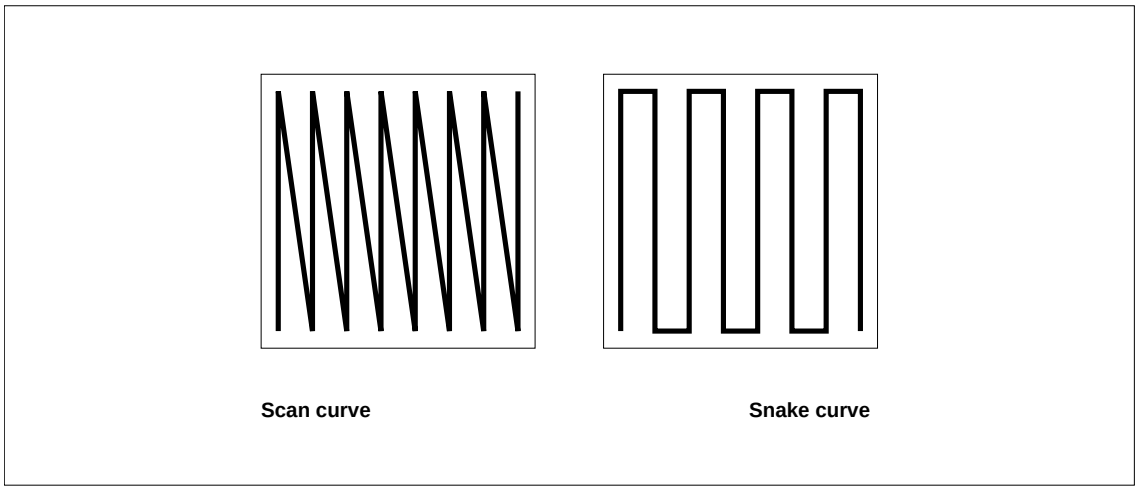

Fig. 3.20: The 2-dimensional 'Scan' and 'Snake' Curves in 2 Dimensions

Unlike curves described previously, the Scan and Snake curves can only be defined as approximations. They are not defined by recursively partitioning space and so the tree representation described in section 3.6 does not apply.

Scan and Snake curve concepts are commonly applied to the serial processing or transmission of 2-dimensional images but the Scan curve is often also used as the the basis for ordering the rows within relational tables. Rows are ordered by values in the first column and where they have the same value, they are ordered by values in the second column, and so on. Thus the Scan curve establishes a hierarchy of preference amongst the different dimensions in space in terms of the clustering of data.

Returning to the 3-dimensional example of the telephone directory used in the introductory chapter, values in the 'dimensions' called *name*, *address* and *telephone number* determine successively lower bits in a row's *derived-key*. 'Points' (people) with the same value in their *name* 'coordinates' will be clustered closer together in their ordering than points with the same value in their *address* coordinates. A similar but more pronounced relationship exists between points with the same value in their *address* coordinates and points with the same value in their *telephone number* coordinates, which are effectively placed in random locations within a telephone directory.

The clustering properties of the Scan and Snake curves are discussed further, for example, by Jagadish [Jag90].

We do not consider either of these curves further in this thesis since the 'uneven' preference given to different dimensions is likely to make their value application-specific rather than general purpose.

3.7.4 Other Curves

We noted in the description of the Z-order curve above that the ordering of sub-squares within every square is always the same. This concept could be applied to any ordering of sub-squares, including that of the first order Hilbert curve. Examples are shown for first to fourth order curves in Figure 3.21. A study of this curve is not made in this thesis and is left as a topic for further research.

Asano et al [ARR$^+$95] present an interesting curve in 2 dimensions which combines some of the characteristics of the Hilbert curve and the Z-order curve. No algorithm for performing mappings is given in the paper. Due to the complexity of this curve, we consider it doubtful whether the concept could be practicably implemented in higher dimensions, particulary from the point of view of querying.

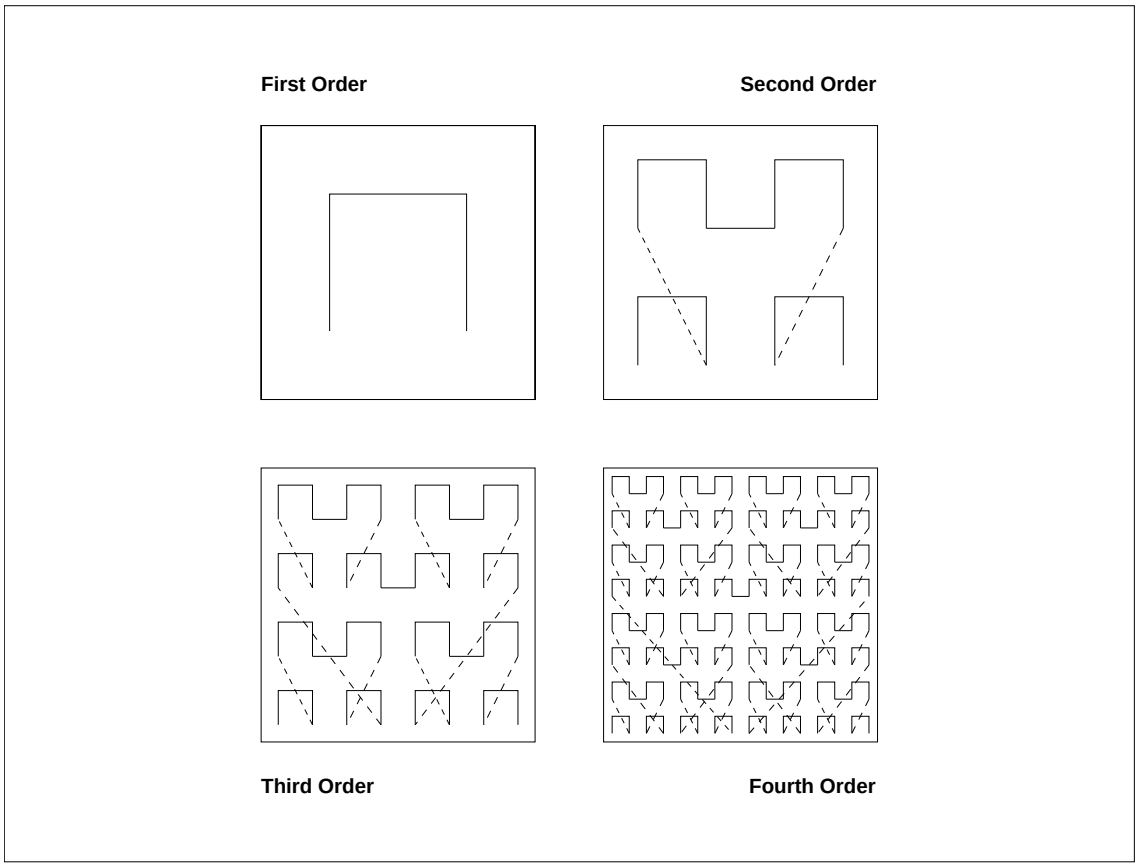

Fig. 3.21: Approximations of a Single-State Curve in 2 Dimensions

3.8 The Application of Space-filling Curves

We conclude this chapter by summarizing how we make use of space-filling curves in our data storage application.

3.8.1 Use of Approximations of Space-filling Curves

In our application we are concerned with data domains which are finite in size, ie which correspond to finite sets of points. Thus a mapping between one-dimensional *derived-keys* and points can be effected using an approximation of a space-filling curve. The *derived-keys* are then implemented as integers and the attributes of a (multi-dimensional) *datum-point*, corresponding to the coordinates of a point may also be mapped to integers.

In our implementation, we choose to store attribute values of *datum-points* as 32 bit integers since the range of values which 32 bits can accommodate is sufficient for most applications. This implies utilization of approximations of curves of order $k = 32$. We saw in section 3.5 that *derived-keys* require a number of bits equal to the sum of the the bits in all of the attributes, ie coordinates.

3.8.2 The Choice of Curve

In the introductory chapter we declared that our interest in space-filling curves arises, in part, from their anticipated ability to maintain any proximity of data existing in space in its storage in a file. In this chapter, we have seen how the recursive division of space should contribute to this, even where some measure of discontinuity exists in a mapping.

From our study of the space-filling and related curves presented in this chapter we conclude that the Hilbert, Z-order and Gray-code curves appear to provide suitable means of mapping between one and n dimensions.

Although the Hilbert and Peano curves share characteristics which are relevant to our application, the Hilbert curve is a logical choice in terms of a practical implementation. This follows from the binary representation of integers in computer hardware. We recall that Hilbert *derived-keys* are calculated from the coordinates of points by examining one bit from each coordinate in each of k steps, where k is the order of the curve or the height of its tree representation. The same observation applies to the Z-order and Gray-code curves.

The application of the Peano curve would imply that the digits of *derived-keys* and the coordinates of *datum-points* are expressed in a radix of 3. Clearly, digits of this type cannot be accommodated in computer hardware with the same economy of storage as binary integers.

Nevertheless, use of curves in which each axis of the square is partitioned into a number of sub-intervals equal to certain radices other than 2 in each step is feasible. For example, if a radix of 4 is used, a 2-dimensional first order curve could be drawn which appears the same as the second order Hilbert curve shown in Figure 3.1. If coordinates are still represented as binary integers, then calculation of *derived-keys* would entail examination of 2 bits of each coordinate at each step of the mapping process instead of one.

3.8.3 Partitioning of Data

A set of multi-dimensional data can be partitioned by dividing a corresponding space-filling curve into consecutive sections. Each section can then correspond to a fixed-sized page of physical storage and can be of variable length. These curve lengths are determined by a combination of the number of *datum-points* which lie on the sections and the storage capacity of a page.

This approach enables a page to be located by placing an ordered pair into the index of a data store. An ordered pair is composed of the lowest (or highest) *derived-key* of a point lying on its corresponding section of curve (defined as the *page-key* in chapter 1) and the address of the page.

The implementation of our indexing application is discussed in detail in chapter 7 but we note here that we choose to index a page by a *page-key* which is equal to or less than the lowest *derived-key* of any *datum-point* placed on it. In general, the *page-key* is a *derived-key* of a *datum-point*. The first logical page in a data store is an exception in that its *page-key* is always zero, corresponding to the first point on the curve. Furthermore, if the *datum-point* whose *derived-key* is the *page-key* is deleted from a page, we do not update that page's *page-key*, in which case it will no longer correspond to a *datum-point*. The reason for this approach is to minimize updates to the index.

Figure 3.22 builds on the example given in Figure 1.1 in chapter 1 showing a Hilbert curve in 2 dimensions which has been partitioned into a number of pages, each of which holds a maximum of 4 *datum-points*. The *page-key* of each page is identified. The ordered pairs which are placed within the index are listed.

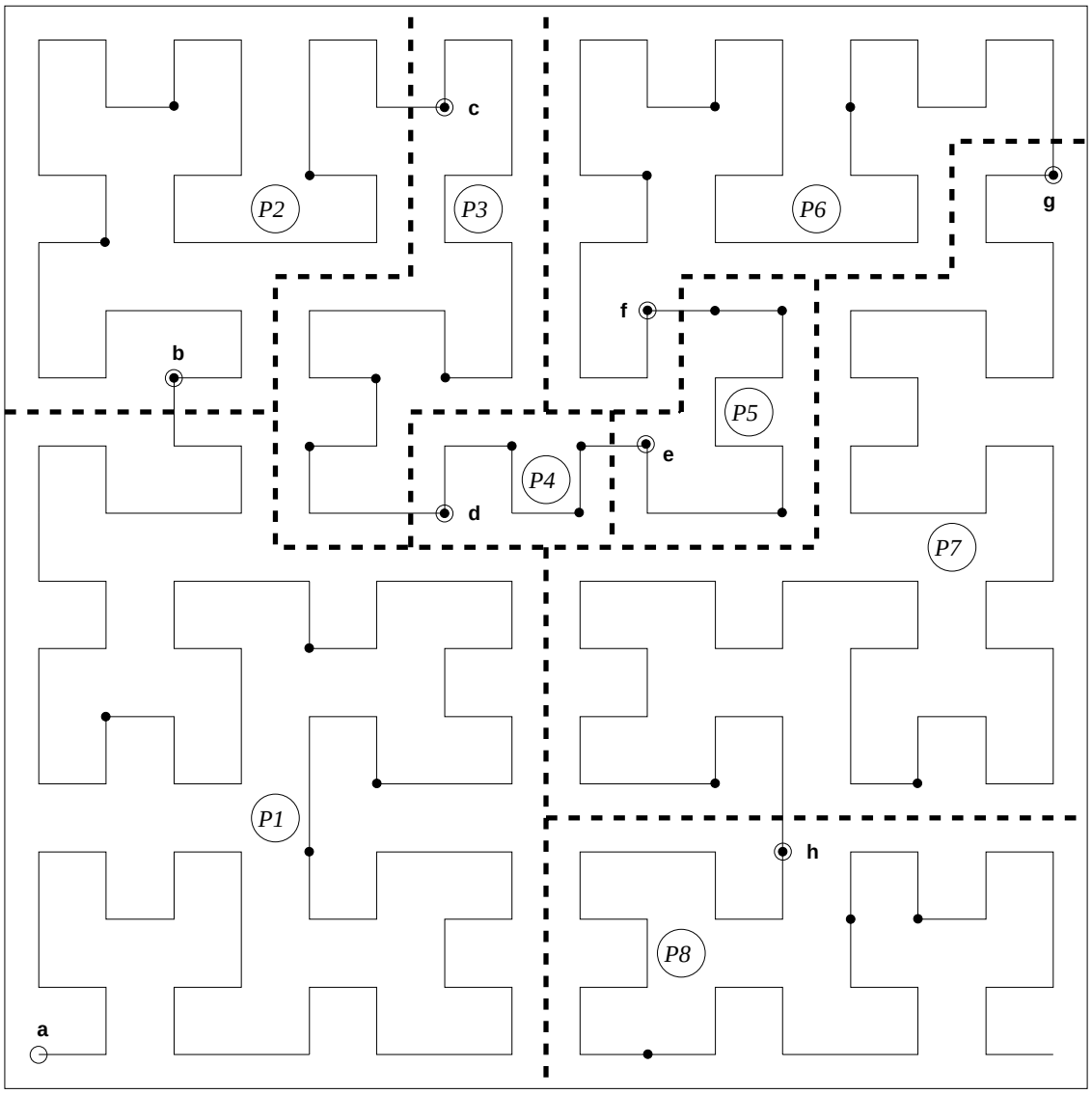

Key to symbols

P3 Page number

Page boundary

Datum-point

Point whose derived-key is a Page-key

Index entries

derived-key	Page number	Label used in Figure
0	*P1*	**a**
72	*P2*	**b**
103	*P3*	**c**
124	*P4*	**d**
130	*P5*	**e**
140	*P6*	**f**
172	*P7*	**g**
224	*P8*	**h**

Fig. 3.22: Example Showing a Partitioning of Data Mapped to the Hilbert Curve in 2 Dimensions

Chapter 4

TECHNIQUES FOR MAPPING TO AND FROM SPACE-FILLING CURVES

4.1 Introduction

In chapter 3, we identify three curves on which we mainly focus our interest in our application. These are the Hilbert curve, the Z-order curve and the Gray-code curve. More accurately, these names relate to families of curves since we have seen that they may be defined in more ways than one. The last two of these types of curve are not space-filling curves according to the strict definition, since they are not continuous. Implementing mappings for them is relatively straightforward but this is not the case with the Hilbert curve. In this chapter, for the most part we concentrate on mapping techniques for the Hilbert curve and on the use of state diagrams in particular. State diagrams are also applied to a discontinuous variation of the Hilbert curve and to the variations of the Gray-code curve.

To implement the mappings, we require a technique which will enable us to produce an algorithm which, given a set of coordinates defining a point as input, will produce the sequence number for the point on the line as output. We also require an algorithm to perform the inverse of this operation. In chapter 1 we defined sequence numbers or ordinal positions as *derived-keys*.

In chapter 2 we discussed previous work relating to the implementation of mappings for the Hilbert and other curves and referred to a general purpose technique for constructing state diagrams for space-filling curves described by Bially [Bia67, Bia69].

Bially's technique is not oriented towards any curve in particular and allows any radix to be used in the representation of coordinates of points and their *derived-keys*. It comprises a set of rules for producing a *state diagram generator table* from which a state diagram is derived. These rules are not complete for curves which pass through more than 2 dimensions and choices must be made in following them. Thus the tables must be populated manually with data and, in order for them to be completed successfully, this generally requires a process of 'trial and error', particularly in higher dimensions.

State diagrams can be used as a tool by a mapping algorithm. We discuss the state diagram approach in depth and introduce new additional rules enabling it to be applied specifically to the Hilbert curve in any number of dimensions automatically. We leave a description of an algorithm which uses the state diagram to perform the mapping from the coordinates of a multi-dimensional point to its *derived-key* and the inverse mapping to chapter 5.

Insights gained in specializing the state diagram generation technique enable us to introduce a new method for calculating Hilbert curve mappings, in section 4.5. This new method does not prove to be more effective than an existing method given by Butz [But71] but does help us later, in section 5.3 of chapter 5, to improve improve Butz' method.

We noted in section 3.4.2 of chapter 3 that the Hilbert curve is a concept and can be expressed in different ways. Alber and Niedermeier [AN98] show that the number of different ways increases with the number of dimensions, n. Our rules for generating state

diagrams and our algorithm for calculating mappings enable us to perform a particular mapping for each value of n. We believe that these mappings describe valid Hilbert curves and have satisfied ourselves empirically that they produce correct results. They constitute our definitions of the Hilbert curves used throughout this thesis. However, we leave a formal proof of the correctness of our techniques as a matter for future work.

4.2 Summary of Alternative Mapping Techniques for the Hilbert Curve

In this section, we identify three alternative techniques for performing Hilbert curve mappings. These are to store the tree representation of the curve described in chapter 3 and traverse it in the manner described in section 3.6, to represent the tree more compactly as a state diagram and traverse this instead and to calculate the coordinates of points from *derived-keys* and vice versa. We also provide a discussion on these three options.

Traversing the Tree Representation of the Hilbert Curve

It is not a practical option to base the mapping implementation on storing the tree representation of a curve in memory and traversing it from root to leaf since the number of nodes to be accommodated would be excessive. The number of nodes which exist in a tree is given by

$$\sum_{j=1}^{k} \frac{2^{jn}}{m} \tag{4.1}$$

where n is the number of dimensions, m is the number of children of a node (equal to 2^n) and k is the height of the tree. This can be re-stated as

$$\frac{2^{nk} - 1}{2^n - 1} \tag{4.2}$$

As noted in chapter 3, the height of a tree is equivalent to the order of a curve. The size of the tree thus grows exponentially with its height and the number of dimensions.

The Application of State Diagrams

There is, however, a finite number of distinct node types, ie orientations of first order curve, which exist in a tree and this number is independent of the height of a tree. This is apparent from Figure 3.9 showing the tree representation of the Hilbert curve and from the graphical representations given in Figures 3.3 and 3.4, for example. Thus it is possible to represent the tree as a state diagram in which each node type corresponds to a state. Once the height of the tree exceeds a relatively low threshold, there are more nodes than states. A state diagram thus enables us to express the tree in a compacted form, since the states are not replicated in the diagram.

The size of a state diagram is determined by the number of dimensions, by the form of the first order approximation of the curve and by the detail of the way that a first order approximation transforms into a second order approximation. We find that in a useful number of cases it is practicable to store the state diagram in memory.

We gain an insight into the number of states required in a state diagram for the Hilbert curve by examining the 3-dimensional example and recalling that different first order curves, which are equivalent to states, are self similar in form. Figures 3.5 and 3.6 in chapter 3 show that a first order curve traverses the 8 points lying at the corners of a cube and that the first and last points are adjacent, ie they lie on the same edge. Although we see in these figures that there is more than one *route* from one particular corner to an

adjacent one, there is no reason why more than one of the alternatives should be utilized in a tree or a state diagram. Thus an upper limit on the total number of different states required is prescribed by the number of edges of a cube, ie 12. The same logic applies to the square in 2 dimensions and to hyper-cubes in higher than 3 dimensions.

The number of edges in a hyper-cube with 2^n vertices is given by

$$n\,2^{n-1} \tag{4.3}$$

since each vertex is connected to n others (we divide $n\,2^n$ by 2 otherwise edges are counted twice). This equation yields a smaller solution than equation (4.2) where the order of the curve, k, is above a relatively low threshold and certainly where we have chosen a value of 32 for k as indicated in section 3.8.1 of chapter 3. We note, however, that like equation (4.2), equation (4.3) is also exponential.

We saw in chapter 3 that a space-filling curve is self-similar at every level of granularity and that first order curves are its building blocks. A state diagram can therefore be viewed as a catalogue of the different variations of first order curves which make up a curve and which encapsulates the relationships between them.

There are a number of benefits arising from encapsulating a space-filling curve in a state diagram. Firstly, since it tabulates calculations which are performed once for all time and which can conveniently be *looked-up*, we are able to implement a mapping in a more efficient manner from a time-complexity point of view, as we shall see later. These calculations are non-trivial and would otherwise need to be carried out repeatedly.

We also find that the same algorithms and even specific computer programs written for the purpose of performing mappings and querying in a database application which uses a particular state diagram can be applied to any other state diagram using the same radix. Such table driven software allows us to quickly explore the characteristics of variations to the Hilbert curve, including discontinuous variations such as the Gray-code curve.

Furthermore, conceptualizing a curve as a state diagram aids an understanding of how the mapping takes place. In turn, this aids the process of developing algorithms for performing queries in a database application, whether or not a state diagram is ultimately used.

Calculation of Mappings to the Hilbert Curve

The third option for performing mappings is to calculate them. The benefit of the use of calculation is that, since little memory is required, it is possible to perform mappings in higher dimensions than is practicable where state diagrams are stored. The disadvantage of the method is that it is more time consuming to perform, at least with computer hardware which is currently available. (Our research has been carried out using a SUN Ultra II Workstation, running under the Unix operating system, SunOS 5.7, and implemented in the ANSI 'C' programming language).

4.3 State Diagrams

In this section we describe the manner in which state diagrams for space-filling curves are generated. We begin by showing how this can be done manually before summarizing the procedure described by Bially.

We extend Bially's method by presenting additional rules which enable the automated generation of state diagrams for the Hilbert curve in particular. We then apply the concept of state diagram generator tables to discontinuous curves, which we consider as alternatives to the Hilbert curve for use in our application. Having described procedures for producing generator tables, we describe how they are used to construct the state diagrams themselves. This section concludes with comments on state diagram growth rates.

4.3.1 Generating State Diagrams by Hand

State diagrams can only be constructed, or drawn, manually, within a reasonable amount of time, for curves which pass through 2 or 3-dimensional space. In this section we describe an algorithm for doing this.

Each distinct state within a state diagram is identified by a unique state number. Where values are expressed in a radix of r, a state comprises a set of r^n triples, $\langle\, y,\ x_1,\ tm \,\rangle$, one triple for each of the points on a first order curve. y values are sequence numbers, ie *derived-keys*, of points, x_1 values are coordinates of points, expressed as *n-points*, as defined in chapter 3, and tm values are *next-state* numbers. y and x_1 values are in the range $[\,0 \ldots r^n - 1\,]$. The terms y, x_1 and tm are equivalent to the terms Y, X_1 and $\overline{T(Y)}$ used in Bially's paper which is discussed in the next section. The main distinction is that Bially's $\overline{T(Y)}$ is a 'transformation matrix' which defines a state rather than a number which identifies a state. The semantics of the transformation matrix are explained on page 61 in section 4.3.2.

An algorithm for drawing a state diagram begins by arbitrarily drawing an initial first order curve, ie state. It then draws the first order curves, ie the *next-states* , which replace points lying on it when it transforms into a second order curve. Finally, the previous step is repeated recursively for each newly encountered form of *next-state* and the process is complete when no more new states emerge. One of a number of possible procedures which can be used to construct a state diagram manually is given informally in more detail as Algorithm 4.3.1.

Where state diagrams are required for curves passing through higher than 3 dimensional space, we need to be able to automate the process or at least the major part of it. Addressing this problem is the subject of the next two subsections of this chapter.

4.3.2 Bially's Algorithm for Creating a State Diagram Generator Table

Bially's method for creating state diagrams is carried out in 2 stages. The first stage entails following a set of rules which results in the production of a *state diagram generator table*. This table principally describes how a particular first order curve transforms into a second order curve. The table is then used as a tool for creating the state diagram itself.

In this section we summarize Bially's generic rules for populating state diagram generator tables manually. Since Bially gives little detail on the significances of the various entries in the table, we provide a brief explanation of their semantics in order to develop the understanding which underlies our work described in section 4.3.3. This work comprises the formulation of additional rules which enable tables to be produced automatically and specifically for the Hilbert curve in any number of dimensions.

We leave an explanation of how the state diagram itself is derived from the table until section 4.3.6. This process is independent of whatever curve the generator table relates to.

Examples of state diagram generator tables for the Hilbert curve in 2 and 3 dimensions are given in Tables 4.1 and 4.2. A graphical representation of the state diagram for the Hilbert curve in 2 dimensions which is derived from the first of these tables is given in Figure 4.1. Graphical representations in the style adopted in Bially's paper for 2 and 3 dimensions are given in Figures B.1 and B.2 in appendix B. Table 4.3 shows the generator table for the Hilbert curve in 4 dimensions. In Table B.1 in appendix B, a generator table for the Hilbert curve in 5 dimensions is given.

These examples are produced by following our extended procedure described in section 4.3.3 but they are given in this section as an aid to understanding the present discussion.

Since the examples relate to the Hilbert curve, the table entries are expressed in a

Algorithm 4.3.1 A Procedure for Drawing a State Diagram Manually

1: Initialize the *current-state* as state 0.

2: Instantiate the first state in the diagram by drawing a first order curve of some arbitrary orientation. The first and last points should lie on the 'surface' of the hyper-cube which encloses all of the points. Points, x_1, on this curve are given sequence numbers, y, in the range $[\ 0, \ldots, r^n - 1\ ]$. Thus the y and x_1 values of the triples for state 0 are recorded.

3: Transform the first order curve of the *current-state* into a second order curve by 'replacing' each point on it with a first order curve of the same form as that defined in step 2, choosing orientations in the following manner:

(a) Draw first order curves to replace the first and last points such that the first point of the first curve and the last point of the last curve are positioned in relation to each other in a similar way as are the first and last points on the *current-state*.

(b) Draw first order curves to replace points with sequence numbers, y, in the range $[\ 1 \ldots r^n - 2\ ]$. Their orientations are chosen such that when the curves for points y and $y+1$ are positioned in space relative to each other in the same way that points y and $y+1$ are positioned, the last point of the curve replacing y is adjacent to the first point of the curve replacing $y+1$.

4: Label each of the first order curves drawn in step 3 with state numbers, tm. Curves which are the same as each other are always given the same state number and curves which are different from each other are always given different state numbers.

5: For each triple defining the *current-state*, record the tm value identified in step 4 which corresponds to its x_1 (or y) value.

6: Instantiate a new state for each distinct first order curve identified in step 4, provided that it has not been instantiated previously, and label it with the number, tm, given in step 4. Record the y and x_1 values of its triples. These are determined by the curves drawn in step 3.

7: For each new state instantiated in step 6, set the *current-state* to that state and recursively repeat steps 3 to 6, terminating the process when no new states are instantiated in step 6.

Y	X_1	X_2	δY	$T(Y)$	
00	00	00	01	0	1
		01		1	0
01	01	00	10	1	0
		10		0	1
10	11	00	10	1	0
		10		0	1
11	10	11	01	0	-1
		10		-1	0

Tab. 4.1: State Diagram Generator Table for the Hilbert Curve in 2 Dimensions

Y	X_1	X_2	δY	$\overline{T(Y)}$
000	000	000	001	0 0 1
		001		1 0 0
				0 1 0
001	001	000	010	0 1 0
		010		0 0 1
				1 0 0
010	011	000	010	0 1 0
		010		0 0 1
				1 0 0
011	010	011	100	1 0 0
		111		0 -1 0
				0 0 -1
100	110	011	100	1 0 0
		111		0 -1 0
				0 0 -1
101	111	110	010	0 -1 0
		100		0 0 1
				-1 0 0
110	101	110	010	0 -1 0
		100		0 0 1
				-1 0 0
111	100	101	001	0 0 -1
		100		-1 0 0
				0 1 0

Tab. 4.2: State Diagram Generator Table for the Hilbert Curve in 3 Dimensions

Y	X_1	X_2	δY	$\overline{T(Y)}$
0000	0000	0000	0001	0 0 0 1
		0001		1 0 0 0
				0 1 0 0
				0 0 1 0
0001	0001	0000	0010	0 0 1 0
		0010		0 0 0 1
				1 0 0 0
				0 1 0 0
0010	0011	0000	0010	0 0 1 0
		0010		0 0 0 1
				1 0 0 0
				0 1 0 0
0011	0010	0011	0100	0 1 0 0
		0111		0 0 -1 0
				0 0 0 -1
				1 0 0 0
0100	0110	0011	0100	0 1 0 0
		0111		0 0 -1 0
				0 0 0 -1
				1 0 0 0
0101	0111	0110	0010	0 0 -1 0
		0100		0 0 0 1
				1 0 0 0
				0 -1 0 0
0110	0101	0110	0010	0 0 -1 0
		0100		0 0 0 1
				1 0 0 0
				0 -1 0 0
0111	0100	0101	1000	1 0 0 0
		1101		0 -1 0 0
				0 0 1 0
				0 0 0 -1
Top half of table				

Y	X_1	X_2	δY	$\overline{T(Y)}$
1000	1100	0101	1000	1 0 0 0
		1101		0 -1 0 0
				0 0 1 0
				0 0 0 -1
1001	1101	1100	0010	0 0 1 0
		1110		0 0 0 1
				-1 0 0 0
				0 -1 0 0
1010	1111	1100	0010	0 0 1 0
		1110		0 0 0 1
				-1 0 0 0
				0 -1 0 0
1011	1110	1111	0100	0 -1 0 0
		1011		0 0 -1 0
				0 0 0 -1
				-1 0 0 0
1100	1010	1111	0100	0 -1 0 0
		1011		0 0 -1 0
				0 0 0 -1
				-1 0 0 0
1101	1011	1010	0010	0 0 -1 0
		1000		0 0 0 1
				-1 0 0 0
				0 1 0 0
1110	1001	1010	0010	0 0 -1 0
		1000		0 0 0 1
				-1 0 0 0
				0 1 0 0
1111	1000	1001	0001	0 0 0 -1
		1000		-1 0 0 0
				0 1 0 0
				0 0 1 0
Bottom half of table				

Tab. 4.3: State Diagram Generator Table for the Hilbert Curve in 4 Dimensions

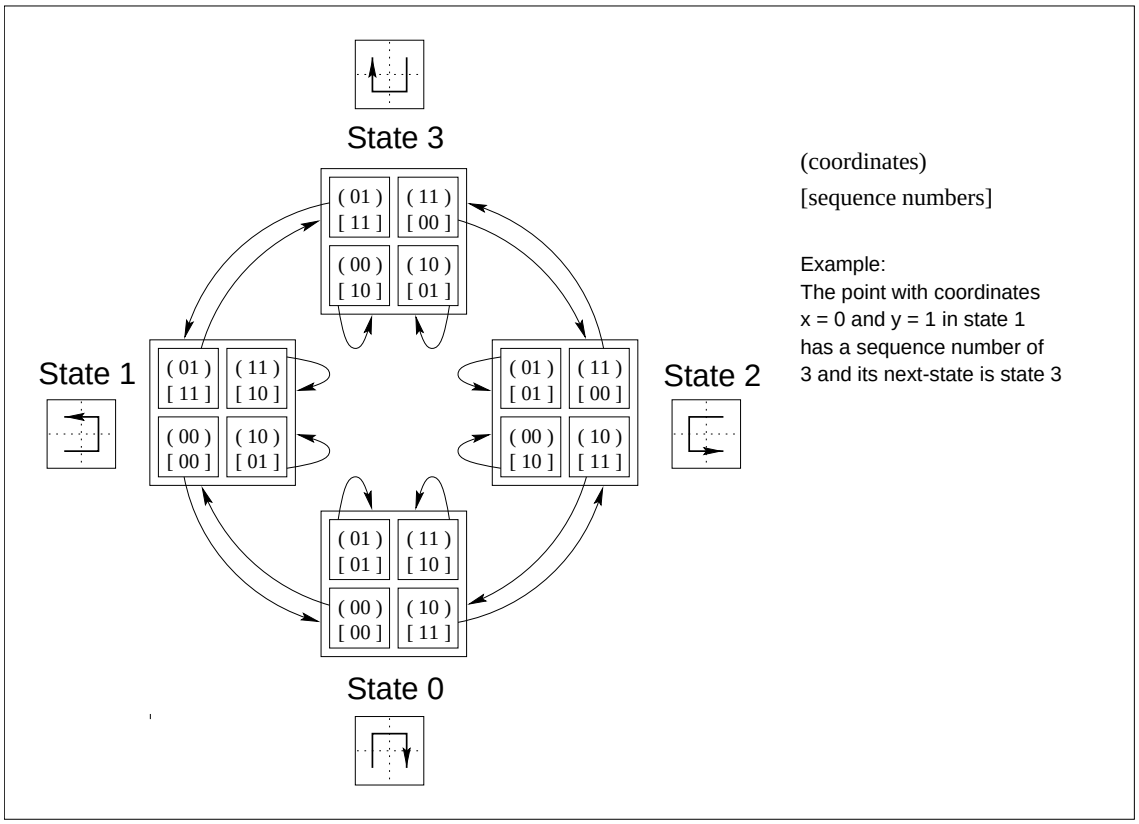

Fig. 4.1: A State Diagram for the Hilbert Curve in 2 Dimensions

binary radix. Bially does not, however, confine his interest to spaces where the coordinates of points are expressed in any particular radix and so he does not apply his technique to any curve in particular. For example, Bially illustrates the application of his technique with a generator table for the Peano curve in 2 dimensions (Fig. 2 in [Bia69]) which is expressed in a ternary radix and the Hilbert curve in 3 dimensions (Fig. 3 in [Bia69]) which is expressed in a binary radix. We note that the latter is a different definition of the curve to that we produce in Figure B.2 in appendix B.

A generator table is comprised of a fixed number of rows and columns. Each row corresponds to a point lying on a first order curve, thus there are r^n rows in total, where r denotes the radix used for representing coordinate values. The rows are ordered according to the sequence numbers of the points on the curve and together they define the first order curve which corresponds to the first state in the diagram.

The table also encapsulates how a transformation of a first order curve to a second order curve is effected. We recall from chapter 3 that conceptually this is done by *replacing* each point on the first order curve with another first order curve of some particular orientation, possibly the same as the original. In the context of a state diagram, these replacement curves are called *next-states*. These *next-states* are defined, in part, by *transformation matrices*, which are described in more detail below.

The table is populated by following rules which determine the relationships between various entries within the generator table. These enable the table to be populated manually but following the rules can be problematic since choices sometimes need to be made between options which equally satisfy them. Bially does not provide algorithms which enable the table to be populated in a routine manner, in part because every variation effectively results in the description of a different curve. He notes that some apparently suitable choices may prevent the process from being completed and, therefore, a certain

amount of 'trial and error' may be required.

The columns in the generator table are headed with the terms Y, X_1, X_2, δY and $\overline{T(Y)}$, the meanings of which are given below. It is in the rules for populating columns X_1, X_2 and $\overline{T(Y)}$ in particular where ambiguities lie.

SUMMARY OF THE RULES

In the remainder of this section, we summarize Bially's rules, providing a commentary on their significances. We distinguish the rules from the commentary by setting the rules in a different typeface from that generally used in this thesis and by indenting them.

Column Y

> Each row contains a number taken from the integer range $[0, \ldots, r^n - 1]$. No number is used twice. The numbers are arranged in ascending order. Each number contains n digits, where n is the number of dimensions. Each digit is taken from the range $[0, \ldots, r - 1]$.

Column Y holds all of the members of the domain of a mapping from one dimension to points in n-dimensional space for a first order curve. Each value is a distance from the start of a curve, ie the *derived-key*, of a point on the curve.

Column X_1

> Contains the same numbers used in column Y but re-ordered such that pairs of adjacent entries differ in one digit only and the difference between different digits is 1. The first entry is 0 and the last entry contains only the digits 0 and $(r - 1)$. The number of digits of $(r - 1)$ in value is assigned to a variable H for later reference. Numbers which require less than n digits are padded on the left with zeros.

Similar to column Y, column X_1 holds all of the members of the range of a mapping. Each member is a point lying on a first order curve, expressed as a set of single digit coordinates concatenated into a single value, ie an *n-point* as defined in chapter 3. The *derived-key*, or distance of a point from the first point on the curve, is the corresponding column Y value in the same row. It is because points which are of unit distance apart on the curve are also adjacent in space that a pair of *n-points* in adjacent rows in the table differ by unit value in one coordinate, ie digit, only.

A value of 0 for the first entry in column X_1 is equivalent to starting the curve at the origin of space. This in not, however, necessary. We could, for example, construct a table for the Hilbert curve as shown in Tables 4.1, 4.2 and 4.3 but with the sequence of column X_1 values reversed from top to bottom in the table. The specification of the last entry implies that the curve ends at a (different) point on the surface of a hyper-cube described by a first order curve. This follows automatically where a radix of 2 is used. If a first order curve did not begin and end at points on the surface of the hyper-cube, then it would not be possible to transform it to a continuous second order curve.

Taken together, columns Y and X_1 completely describe a mapping to a particular first order curve or state. This state is numbered state S_0.

Column X_2

1. Each row contains a pair of entries.
2. The first entry in the first row equals the first entry in column X_1.
3. The second entry in the last row equals the last entry in column X_1.
4. All other entries are numbers comprising the digits 0 and/or $(r-1)$ only. (This follows automatically where $r = 2$).
5. Two entries in the same row differ in H digits. (See rule for Column X_1 for definition of H).
6. Any two adjacent entries which are in different rows differ in 1 digit only - the same digit in which their corresponding entries in column X_1 differ, but in the opposite sense.

A pair of entries in column X_2 are *n-points* which lie at the start and end of a first order curve. This curve *replaces* the *n-point* in the same row's column X_1 entry when the curve specified by columns Y and X_1, ie state S_0, transforms into a second order curve. Thus a pair of column X_2 entries partially specify a first order curve, ie the *next-state* for the row's column X_1 *n-point* which has a particular order in state S_0, determined by the row's column Y entry. If the column X_2 entries are not the same as the first and last column X_1 entries then they partially specify a different state to state S_0.

Sub-rules 2 and 3 are broadly equivalent to step 3a of Algorithm 4.3.1 given above in section 4.3.1. The rule for column X_1 results in each coordinate of the first and last points in state S_0 having minimum or maximum first order curve domain values. (This follows automatically where $r = 2$). Sub-rules 2 and 3 for column X_2 therefore imply that corresponding coordinates of corresponding points on the second order curve to which the first order curve transforms also have minimum or maximum second order curve domain values. For example, the coordinates of the last point on the second order curve are found by interleaving the digits of the last *n-point* in the last row in column X_1 with the second column X_2 *n-point* in the same row. This produces a $2n$-digit number in which each pair of digits is a coordinate value.

Sub-rules 4 and 5 indicate that the first and last points of a first order curve replacing a point in state S_0 relate to each other in a similar way as the first and last points in state S_0. The digit values ensure that first and last points lie on the surface of a hyper-cube described by a first order curve. The relationship between a pair of column X_2 values ensure that they correspond to points which are the same distance apart in space as the first and last column X_1 *n-points*.

Sub-rule 6 is equivalent to step 3b in Algorithm 4.3.1 and so ensures that the second order curve to which state S_0 transforms is continuous. Thus if the point in row i transforms to a first order curve whose *last* point is j and the point in row $i+1$ transforms to a first order curve whose *first* point is k, then j and k (which are points on a second order curve) must be adjacent to each other.

The set of n 2-digit coordinates placing point j on a second order curve is found by interleaving the digits of the column X_1 value in row i with the same row's second column X_2 value. The set of n 2-digit coordinates placing point k are found by interleaving the digits of the column X_1 value in row $i+1$ with the same row's first column X_2 value. Thus points j and k differ, by unit value, in one and only one coordinate which is the same coordinate in which the column X_1 entries in row i and $i+1$ differ.

Column δY

> Each row contains a number such that each digit is the magnitude of the difference between the corresponding digits in the same row's 2 entries in column X_2. The number will contain H digits with value $(r-1)$ and $(n-H)$ digits with the value 0.

This column was implied only in Bially's paper. The δY values are used in determining the permutation matrices in the last column of the table. The entry in column δY for any row indicates in which dimension(s) the start and end points of the first order curve at the second order level have different coordinate values. A corresponding value for the entries in the first and last rows in column X_1 would be equal to the last entry in column X_1, since the first entry contains zero-valued digits only.

Column $\overline{T(Y)}$

1. Initialize each row's transformation matrix as a permutation matrix defined such that when the matrix is applied to its row's δY value, it produces a value equal to the last entry in column X_1.
2. Adapt the permutation matrix in the following manner: if the i-th digit of the first of its row's pair of X_2 entries is non-zero then the non-zero element of the i-th column within the matrix is set to -1.

A transformation matrix encapsulates how a first order curve differs from the first order curve which is defined by columns Y and X_1 and which we call state S_0. In the context of the generator table, it encapsulates how a first order curve whose first and last point's coordinates (expressed as *n-points*) are given as a pair of entries in column X_2 differs from state S_0. Thus the matrices imply the *next-state* for each point in state S_0, ie each point in column X_1.

The transformation matrix for state S_0 itself is equal to the identity matrix which, if applied to points in column X_1, induces no changes.

Generally, a transformation matrix implies some state S_i, $S_i \neq S_0$, by enabling any point P_i in state S_i to be transformed into the equivalent point P_0 in state S_0 which has the same distance from the beginning of the curve in state S_0 as does point P_i in state S_i. The distance, ie sequence number, of point P_i from the start of the curve in state S_i is then determined by looking up the column Y value for point P_0 in state S_0.

It follows that applying a row's matrix to its first entry in column X_2 should transform it to the first entry in column X_1 and applying it to its second entry should transform it to the last entry in column X_1.

In general, more than one transformation matrix satisfying the rules given above can be constructed for any row and different choices may ultimately result in state diagrams which contain a different number of states for the same curve.

Concluding Remarks

In general, a state diagram will contain many more states than are encapsulated in the table. The characteristics of all other states can be determined, however, from the information contained in it.

An algorithm allowing all states required to produce a state diagram which utilizes the generator table is given in section 4.3.6.

We do not describe here how a matrix is used to transform a point or another matrix but address this also in section 4.3.6.

The rules summarized in the previous section do not guarantee that a state diagram can be successfully generated and nor do they guarantee that a state diagram containing the minimum possible number of states can be generated. This is discussed further in Bially's PhD thesis [Bia67].

4.3.3 State Diagram Generator Table for the Hilbert Curve

In the context of Bially's state diagram generation technique, the Hilbert curve is the special case of a space-filling curve for which coordinates and *derived-keys* are expressed using a binary radix.

In this section, we present specialized algorithms which extend Bially's rules for populating columns X_1, X_2 and $\overline{T(Y)}$ of the generator table. These are used in conjunction with the rules for columns Y and δY described above. Together, they enable a generator table for an *arbitrary variant* of the Hilbert curve to be constructed for any number of dimensions.

The precise form of the arbitrary variant is dictated by the detail of our rules. For example, the rules for columns Y and X_1 determine the orientation and direction of traversal of the first order approximation of the curve. The rules for each of columns X_1, X_2 and $\overline{T(Y)}$ may be modified to produce alternative variants of the curve and we discuss this further in section 4.3.4.

In Figure 4.2 we give an example of the second order 3-dimensional Hilbert curve implied by the generator table given in Table 4.2 which was constructed in accordance with the rules described in this section.

Once implemented, the rules enable the table to be constructed automatically. This is desirable since populating the tables manually becomes increasingly time consuming as the number of dimensions in a space rises.

The task of developing algorithms for the generator table is facilitated by identifying and ensuring that we preserve in higher dimensions two characteristics of the 2-dimensional Hilbert curve.

The first of these is a symmetry about a line which is the normal to one of the axes. The corollary of this is that all of the points lying on one half of the curve have the value of zero for their coordinates in one dimension and all of the others have the value of one for their coordinates in the same dimension. In higher than 2 dimensions, curves need not be symmetrical, as illustrated in Figure 3.5(c) in chapter 3, but we confine our interest to those which are since they are more readily described in a state diagram generator table.

The second characteristic is that the first and last points of a first order approximation are adjacent. In higher than 2 dimensions it is possible to construct first order curves which do not have this characteristic, as illustrated in Figure 3.7 in chapter 3. In 3 dimensions at least we are unable to utilize them to produce higher order curves which are continuous.

In the remainder of this section we set out our rules for populating the generator table for the Hilbert curve. In doing so, we provide a commentary on their significances. We use the term *bit* where the term *digit* was used in the summary of Bially's rules in the previous section, since the Hilbert curve is represented using a binary radix.

Column Y

```
As described in section 4.3.2.
```

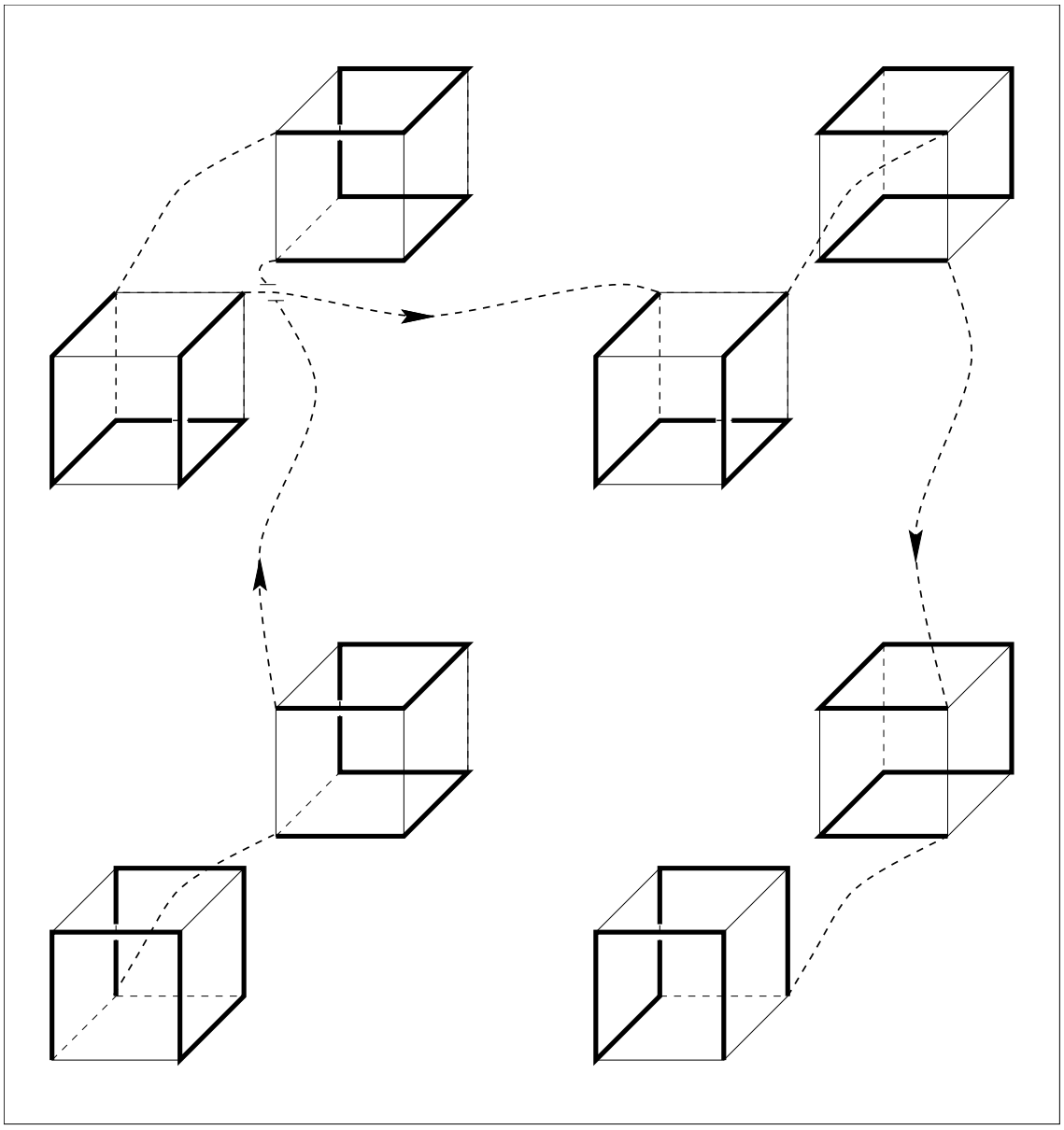

Fig. 4.2: Second Order 3-dimensional Hilbert Curve Implied by our State Diagram Generator Table in Table 4.2

Column X_1

Column X_1 expresses the ordering of points on a first order curve. The characteristics identified above together with those required by Bially's generic rules are conveniently found to be shared by the *Gray-code* sequence of numbers described in chapter 3. Thus the rule for column X_1 may be stated as follows:

> `Calculate each column` X_1 `entry as` $Y \oplus Y/2$`, as described in [RND77]`[1]`.`

A member of a Gray-code sequence of order n can be considered as the set of co-ordinates of a point on a first order curve in n dimensions where the coordinates have been concatenated into a single value, ie expressed as an *n-point*. A complete sequence of Gray-codes of order n is then equivalent to the set of points on a first order curve ordered such that adjacent points in the sequence are adjacent in space; that is, they differ in one coordinate (or bit in an *n-point*) only.

Populating column X_1 with the Gray-code sequence thus ensures that the first entry has the value of zero in all bits and that the last entry has the value of one in one bit only. The Gray-code sequence dictates that this is the top bit. We label this bit position P for reference later on. Use of the Gray-code sequence results in the first and last entries being adjacent points in space and the value of the variable H, defined by Bially in his rule for column X_1 , becomes one. The symmetry of the Hilbert curve is also achieved since the first half of the values have a zero in bit position P and the second half have a value of one and, in other bits, the values in row i equal the values in row $2^n - 1 - i$. Bit position P indicates the axis in n-dimensional space which the start and end of the curve of any order lie on.

The use of Gray-codes was suggested by Faloutsos [FR89b] without explanation.

Column X_2

In populating column X_2, one method of specializing Bially's rules for the Hilbert curve proceeds as follows:

In the first row, the first entry is set to 0 and the second is set to equal the X_1 value found in the second row.

For each row, from the second to the last in the first half of the table, we copy the second entry from the previous row into the first entry in the current row and adjust it according to Bially's sub-rule 6 for column X_2. We then copy the first entry from the current row into the second entry of the current row and again adjust the second entry according to sub-rule 6.

As with column X_1, all of the entries, taken individually, in the second half of the table are a reflection of those in the first half, except in the bit in position P. All of the entries in the first half will have bits in position P set to 0 except for the last entry where it will equal 1 and all of the entries in the second half will have bits in position P set to 1 except for the first entry where it will equal 0.

In 2 and 3 dimensions, the above procedure enables the column to be populated automatically. A problem occurs in higher dimensions, however, in that sometimes a pair of entries in the same row may have the same value.

This problem needs to be resolved by changing the value of one of the bits in the second entry. This change must result in no entry in the column being equal to its corresponding entry in column X_1 (except for the first and last entries which must equal their X_1 values). Any bit may be chosen arbitrarily, provided it is not the bit in position P or the bit whose value is determined by Bially's sub-rule 6 for column X_2.

[1] Refer to appendix A for a key to symbols.

A pattern emerges from an examination of the column X_2 entries produced in the above manner for 2 and 3-dimensional curves which can be expressed as an algorithm enabling the column to be automatically generated in higher dimensions. The algorithm is similar to that which generates the Gray-code sequence. We call its output the *X2Gray-code* sequence and its construction can be illustrated with the following examples:

Order 1: $[0, 1, 0, 1]$[2]
Order 2: $[00, 01, 00, 10, 00, 10, 11, 10]$
Order 3: $[000, 001, 000, 010, 000, 010, 011, 111, 011, 111, 110, 100, 110, 100, 101, 100]$

Our rules which generate the sequences is given as follows:

1. Initialize a sequence of order 1 as: $[0, 1, 0, 1]$. Individual members of this sequence are identified by labels as follows: $[a, b, c, d]$.
2. The order 2 sequence is derived from the order 1 sequence in a number of steps as follows:
   (a) Initialize the sequence as the order 1 sequence followed by the reverse of the order 1 sequence thus: $[a, b, c, d, d, c, b, a]$.
   (b) Replace the fourth value with the third value and the fifth value with the sixth value thus: $[a, b, c, c, c, c, b, a]$.
   (c) Prefix members of the first half of the sequence with a bit of value zero and the members of the second half with a bit of value one thus: $[0a, 0b, 0c, 0c, 1c, 1c, 1b, 1a]$.
   (d) Invert the values of the top bits of the fourth and fifth members of the sequence thus: $[0a, 0b, 0c, 1c, 0c, 1c, 1b, 1a]$. This produces the following sequence of binary numbers: $[00, 01, 00, 10, 00, 10, 11, 10]$. This is the sequence of order 2.
3. Generally, given a sequence of order j as: $[a_0,\ a_1, \ldots, a_{2^{j+1}-2},\ a_{2^{j+1}-1}]$, where each a_i is a binary value, the sequence of order $j+1$ is defined as: $[0a_0,\ 0a_1, \ldots, 0a_{2^{j+1}-2},\ 1a_{2^{j+1}-2},\ 0a_{2^{j+1}-2},\ 1a_{2^{j+1}-2}, \ldots, 1a_{2^{j+1}-1}]$.

Thus the sequence of entries for rows in column X_2 for a curve in n dimensions can be populated with an *X2Gray-code* sequence of order n. Each pair of values corresponds to the first and last coordinates of points on a first order curve to which a point taken from column X_1 transforms to at the second order level.

[2] NB: usage of the term *order* here is distinct from usage in the context of *order of curve*

Alternatively, the algorithm can be stated more simply in the following terms, where we derive a column X_2 sequence for a curve of n dimensions from the sequence for $n-1$ dimensions, initializing the sequence for 1 dimension as [0, 1, 0, 1].

1. Initialize the sequence for Order n equal to the sequence for order $n-1$.
2. Set the value of the last member of the sequence (for order $n-1$) equal to the value of the penultimate member.
3. Prefix the last member of the sequence with a bit of value 1 and all other members each with a bit of value 0.
4. Double the size of the sequence by reflecting it such that the last member equals the first and so on.
5. Invert the values of the most significant bits of all of the members in the second half of the sequence.

In experiments, the application of both of the above procedures has enabled us to produce correct results but a proof of correctness for them needs to be formulated.

Column δY

As described in section 4.3.2.

For the Hilbert curve, any row's δY value contains only one bit set to one and all other bits set to zero. (This is consistent with the variable H referred to above having a value of one). The bit which is set to one denotes the axis on which lie the first and last points of the first order curve, partially encapsulated by entries in column X_2, to which a point in column X_1 transforms to at the second order level.

A single non-zero digit within a δY value implies that a pair of column X_2 entries lie on the same edge of a hyper-cube described by the line connecting the points lying on a first order curve. This is consistent with the observation made in section 4.2 above where we consider the number of different types of node which can exist in the tree representation of the Hilbert curve.

Column $\overline{T(Y)}$

The transformation matrices for the Hilbert curve may be calculated in a more straightforward manner than that described in the generic procedure. This arises from column δY values containing a single non-zero bit only. We label the bit positions in δY: $1, 2, 3, \ldots, n$, where bit position 1 corresponds to the most significant bit and bit position n corresponds to the least significant bit.

For each row:

1. Initialize the matrix to the identity matrix.
2. Create a permutation matrix by interchanging the first row of the matrix with the j-th row, where j designates the position of the single non-zero bit in the row's δY value.
3. Determine the signs of the non-zero elements of the permutation matrix in accordance with Bially's rule given in the previous section, thus creating a transformation matrix.

It follows from these rules that if a column δY value is $10\ldots0$, then the permutation matrix produced in step 3 is the identity matrix.

We discuss state diagram growth rates, as the number of dimensions in a space increases, below in section 4.3.7. Equations (4.7) and (4.8) given in that section express lower and upper bounds on the number of states which result from application of the generator table. We note here, however, that the rules given above result in the production of valid state diagrams containing a number of states equal to the upper bound. Clearly, it is desirable if state diagrams are as compact as possible since they occupy memory.

We are able to achieve the lower bound on state diagram size by modifying our method of setting up the permutation matrices in sub-rules 1 and 2. In doing this, it is convenient to represent each row in a matrix as an n-bit value, ie where all of a row's column entries are concatenated into a single value. Thus the sub-rules are replaced by the following:

1. `Set the first row of a matrix equal to its corresponding column` δY `value.`
2. `For each row, numbered` $2\ldots n$`, in the matrix, set row` i `equal to the value in row` $i-1$`, circular right-shifted one bit position.`

In the remainder of this thesis, we adopt this approach for the definition of transformation matrices where we use state diagrams.

4.3.4 Variations to State Diagram Generator Tables for the Hilbert Curve

We note in chapter 3 that the Hilbert curve is a concept which may be expressed in different ways. We also recall that our rules for the Hilbert curve state diagram generator table enable the production of a state diagram for an arbitrary variant of the curve. In this section, we briefly discuss some of the ways in which our rules may be altered in order to produce different variations.

In presenting our rules for column X_1 in the previous section, we labelled the top bit position P. The values in the rows in the top half of the table all have the value zero in this position and those in the bottom half all have the value one in this position. Having constructed the table in the manner described, we can define an alternative orientation of the curve as a whole. This is done by interchanging the values of the bit in position P with the value of the bit in some other position j in all entries in all columns except in column Y.

We noted in section 4.3.2 that our state diagram given in Figure B.2 in appendix B for the 3-dimensional Hilbert curve differs from that given in Fig. 3 of [Bia69]. Clearly, this implies that Bially populated column X_2 of the generator table in a different manner to that adopted by ourselves.

We saw in the previous section that there are alternative ways of initializing the permutation matrices during the process of defining transformation matrices. The second alternative may be simply varied by performing circular left-shift operations instead of circular right-shift operations in defining the individual rows of the matrices.

In concluding this section, we note that the number of possible variations of the Hilbert curve increases as the number of dimensions rises and many variants can be encapsulated by state diagram generator tables. Some of these will result in state diagrams which contain a larger number of states than others.

In the context of an implementation of an indexing application, one form of the Hilbert curve is likely to be as suitable as any other, except that it is desirable to choose one where the state diagram is as compact as possible.

4.3.5 State Diagram Generator Tables for Discontinuous Curves

Our motivation for carrying out research into the Hilbert curve arises, in part, from an assumption that it is desirable to base our application on a continuous curve. The results of preliminary tests carried out and reported on in chapter 10 appear to support this assumption.

State diagram sizes are discussed in more detail in section 4.3.7 below but for the time being it is sufficient to note that their growth rate for continuous curves is exponential in the number of dimensions. According to equation (4.7) in that section, state diagrams for the Hilbert curve contain at least $n\,2^{n-1}$ states.

According to Bially's equations (4.4) and (4.5), a lower minimum requirement of 2^{n-1} states applies for space-filling curves in which the difference between *all* pairs of coordinates of the first and last points of a first order curve equals their radix minus one. When this occurs, the variable H, defined in Bially's rule for column X_1, given in section 4.3.2, equals the number of dimensions, ie n. Nevertheless, this still represents an exponential growth rate. Furthermore, in experiments in 2 and 3 dimensions, we are only able to draw continuous curves, where H equals n, if coordinates are expressed in an odd numbered radix. Thus Peano's curve can be represented by a state diagram with only 2^{n-1} states but Hilbert's cannot.

Given the exponential growth rates of state diagrams for continuous curves we are motivated in this section to consider utilization of discontinuous curves as a compromise for application in higher dimensions. A number of discontinuous curves may be expressed more compactly with fewer states than continuous curves such as those of Hilbert and Peano.

4.3.5.1 The Z-order Curve

The Z-order curve [Mor66] can be represented by a state diagram which contains a single state only. Every point on a curve of order k transforms to the same first order curve at order $k+1$. This is apparent from Figures 3.10 and 3.12 in chapter 3. Nevertheless, the simplicity with which mappings to the Z-order curve are performed renders the application of state diagrams superfluous. Indeed, the mapping between coordinates, expressed as *n-points*, in the Z-order curve's single state and sequence numbers is encapsulated by the identity function.

We recall from chapter 3, however, that the Z-order curve manifests a considerable number of discontinuities. Pairs of points are adjacent, ie unit distance apart, but the second point of any pair is never adjacent to the first point of the successor pair. Thus the number of discontinuities within an approximation is given by $(2^{nk}/2) - 1$ or $2^{nk-1} - 1$.

The magnitude of discontinuities needs to be considered in conjunction with their frequency when assessing the relative merits of different discontinuous curves. Although discontinuities occur frequently in the Z-order curve, most are small in magnitude and therefore should have little adverse effect on clustering. Nevertheless, the frequency of discontinuities motivates us to consider alternative less discontinuous curves.

4.3.5.2 Moore's Curve

The curve which we describe in this section is our discontinuous variation of Moore's continuous variation of the Hilbert curve [Moo00, Sag94]. Although Moore's curve requires the same number of states as the Hilbert curve, our variation requires fewer. Compared with the single state curves the discontinuities found in our variation are fewer in number and more localized in their extent. We illustrate first to fourth order approximations of

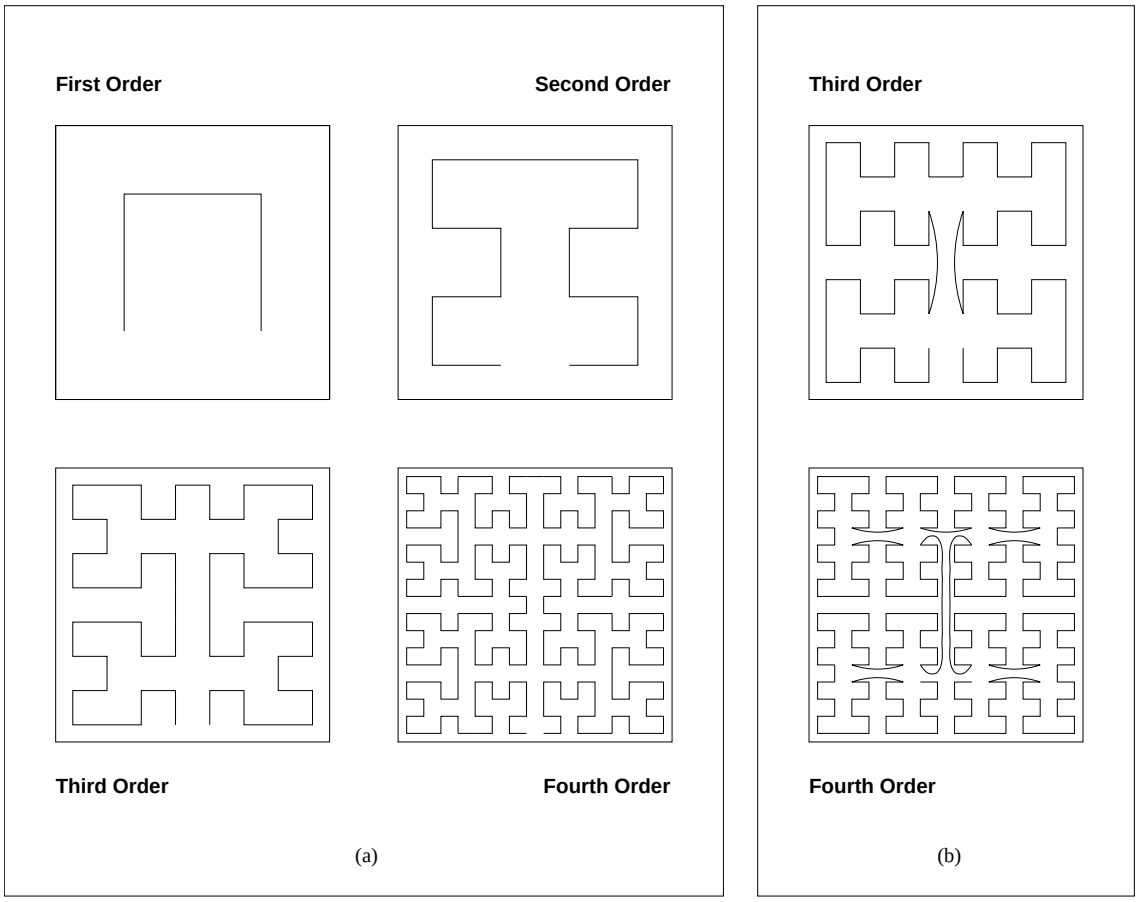

Fig. 4.3: Approximations of Moore's Curve in 2 Dimensions and our Variations at the Third and Fourth Orders

Moore's curve in 2 dimensions in Figure 4.3(a). Discontinuities are introduced in our variation in curves of orders 3 and above and this is shown in Figure 4.3(b).

In 2 dimensions, Moore's first order curve has the same form as Hilbert's but the transformation to a second order curve entails a different set of rotations and reflections. The transformation to any higher order k, where $k > 2$, entails *replacing* each first order *curve* within the *curve of order* k with Hilbert's curve of order 2, suitably rotated and/or reflected, rather than replacing each *point* with a *first order curve*. The result is a continuous curve but it is not self-similar at every level as the form of the second order curve is not reproduced in any other order.

Our variation on this curve, replaces every first order curve within a curve of order k, where $k > 2$, with the curve of order 2. The resulting curve is not continuous in orders greater than 2 but it is self-similar.

An interesting feature of the curve is that in orders higher than 2, the start and end points do not lie on any surface of the space through which it traverses.

The procedure for creating the state diagram generator table is the same as for the Hilbert curve except in columns X_2 and $\overline{T(Y)}$. Examples of generator tables for 2 – 4 dimensions are given in Tables C.1, C.2 and Table C.3 in Appendix C.

Column X_2

As with the Hilbert curve, after manually populating column X_2 in 2 and 3 dimensions, we are able to identify a pattern which can be expressed as an algorithm, again similar to that for the Gray-code sequence. We call this the *MX2Gray-code* sequence. The pattern

is illustrated with the following examples:

Order 1: [0, 1, 0, 1][3]
Order 2: [10, 11, 10, 11, 01, 00, 01, 00]
Order 3: [110, 111, 110, 111, 101, 100, 101, 100, 000, 001, 000, 001, 011, 010, 011, 010]

Our rules which generate the sequences for order n are given as follows:

1. Append a reflection of the sequence for order $n-1$ to the sequence for order $n-1$, thus doubling its size.
2. Prefix each member of the first half of the enlarged sequence with a bit of value one.
3. Prefix each member of the second half of the enlarged sequence with a bit of value zero.

Thus the sequence of entries for rows in column X_2 for a curve in n dimensions can be populated with an *MX2Gray-code* sequence of order n. Each pair of values corresponds to the first and last coordinates of points on a first order curve to which a point taken from column X_1 transforms to at the second order level.

Column $\overline{T(Y)}$

The permutation matrices used in column $\overline{T(Y)}$ are set up by exchanging the first row of the identity matrix with one (or no) other, in the manner initially considered for the Hilbert curve.

We recall that this approach fails to produce state diagrams for the Hilbert curve which are as compact as possible and that we resolve this by modifying our rules, employing circular-shifting. In the case of our variation to Moore's curve, the comparative effect of these two methods of defining the matrices, in terms of state diagram size, is the reverse of that which obtains for the Hilbert curve.

4.3.5.3 The Gray-code Curves

We identify three of a number of possible curves which use Gray-codes in section 3.7.2 of chapter 3 and they are referred to as Gray-code^F, Gray-code^A and Gray-code^B.

We saw in chapter 3 that Gray-code curve mappings rely on mappings between Gray-codes and their sequence numbers. These are relatively simple and are described in chapter 5. Alternatively, Bially's state diagram approach can be adapted and applied to performing mappings to the various Gray-code curves. A detailed description of how this is done is given in appendix D.

4.3.6 Production of State Diagrams from Generator Tables

The information contained within the generator table is sufficient to enable all and only the states required in a state diagram to be calculated and for the relationships between those states to be determined.

The method by which a state diagram generator table is used to produce a state diagram is not detailed in Bially's paper [Bia69] although it is addressed from a mathematical perspective in his PhD thesis [Bia67]. In this section we present an algorithm for generation of the state diagram in terms which more readily enable it to be implemented as a

[3] NB: usage of the term *order* here is distinct from usage in the context of *order of curve*

computer program. The method is independent of the particular curve which is encapsulated by the table. The number of states contained in the resulting state diagram depends on the detail of the curve as set out in the generator table and not on the way the table is manipulated.

The generator table is used to produce a temporary list of all of the states which together define a state diagram. Once created, not all of the information within it is needed in the final state diagram. The list is therefore traversed to extract relevant information only.

We follow the algorithm with details and examples of how calculations which use transformation matrices are carried out. This section is concluded with an example showing how part of a state diagram for the Hilbert curve in 2 dimensions is constructed.

The Algorithm

The first state placed in the temporary list is the state encapsulated by the generator table itself; by the mapping defined by columns Y and X_1 and by the *next-states* for each point as defined by transformation matrices in column $\overline{T(Y)}$.

There is no relationship between consecutive states within the list of states. They are simply placed in it in the order that they are encountered in the calculation process.

A member of the temporary list defines a state and is a record containing the following information:

1. A state number, u, identifying the state.

2. A set of r^n triples, one for each point on a first order curve. Each triple is of the form: $\langle\, Y_u^i,\ X1_u^i,\ tm_u^i \,\rangle$. Y_u^i is a sequence number, in the range $[0, \ldots, r^n - 1]$, of a point in state number u. $X1_u^i$ is the *n-point* representation of the coordinates of the point, in the same range. tm_u^i is the number of the *next-state*, ie first order curve, to which the point transforms to in a second order curve. Each distinct tm_u^i number corresponds to a transformation matrix, examples of which are found in column $\overline{T(Y)}$ of the generator table, defining a distinct state.

3. A Transformation Matrix. This encapsulates how this state differs from the first state in the list. When the matrix is applied to a point, it is transformed into the equivalent point in the first state in the list which has the same sequence number as the point in this state.

4. A pointer to the next member in the list.

The procedure for building the temporary list of states is given in Algorithm 4.3.2.

In effect, this algorithm constructs a tree representation of a space-filling curve in a depth-first manner. As new nodes are defined, they are appended to a list. No node is added if a node of the same type already exists in the tree (ie, list) and so the tree is not balanced.

A state diagram, derived from the temporary list of states, can be implemented as an array of states with one element for each state in the list. A state is identified by its number, which can be implied by its position within the array of states, and defined by its list of triples. Each list of triples can also be stored as an array. The elements of these arrays may be expressed compactly as pairs since one of the attributes, Y_u^i or $X1_u^i$, of a triple can be implied by its position in the array, depending on how the triples are sorted.

Thus two state diagrams can be produced from the state list. One is required for performing a mapping from one dimension to n dimensions. The triples within it are sorted by Y_u^i values, which may be implied. An example for the 2-dimensional Hilbert curve is given in Table B.2 in appendix B. The other is required for performing a mapping

Algorithm 4.3.2 Algorithm to Create a List of States

{Using the generator table, initialize the first member, ie state, of the list}
1: current_state $\Leftarrow 0$
2: next_state_num $\Leftarrow 1$
3: **for all** i such that $0 \leq i < r^n$ **do**
4: $Y_0^i \Leftarrow i$
5: $X1_0^i \Leftarrow X_1$ value from row i of the generator table
6: **end for**
{The tm_0^i attributes of the triples are initially undefined}
7: current_state transformation matrix $\Leftarrow$ the identity matrix
{Initialize the tm_0^i attributes, ie *next-state* numbers, of the triples in state 0}
8: **for all** i such that $0 \leq i < r^n$ **do**
9: **if** no state exists in the state list whose transformation matrix equals that found in row i of the generator table **then**
10: append a new state to the list
11: new state's number $\Leftarrow$ next_state_num
12: next_state_num $\Leftarrow$ next_state_num + 1
13: new state's transformation matrix $\Leftarrow$ matrix from row i of the generator table
14: $tm_0^i \Leftarrow$ new state's number
15: **else**
16: $tm_0^i \Leftarrow$ the number of the state found in the list
17: **end if**
18: **end for**
{State 0 is now fully defined. A new state has been added to the list for each distinct transformation matrix, other than the identity matrix, found in column $\overline{T(Y)}$ of the generator table}
{Initialize the attributes of the triples in all of the states remaining in the list, appending any new states required in the process}
19: **for all** states, u, in the list (excluding state 0) **do**
20: **for all** i such that $0 \leq i < r^n$ **do**
21: $Y_u^i \Leftarrow i$
22: **end for**
23: **for all** i such that $0 \leq i < r^n$ **do**
24: $j \Leftarrow i *$ the transformation matrix for state u
25: $p \Leftarrow$ the row in state 0 such that $X1_0^p = j$
26: $X1_u^p <= i$
{ie assign i to the $X1$ value in row p of the current state u}
27: $TM \Leftarrow$ (transformation matrix corresponding to tm_0^p) $*$ (transformation matrix corresponding to state u)
{NB TM is a transformation matrix defining a state, not a state number}
28: **if** no state exists in the state list whose transformation matrix equals TM **then**
29: Add a new state to the list
30: State Number of the new state $\Leftarrow$ next unused number
31: Transformation matrix of the new state $\Leftarrow$ TM
32: **end if**
33: $tm_u^p \Leftarrow$ the State Number of the state whose transformation matrix equals TM
34: **end for**
35: **end for**

from n dimensions to one dimension. The triples are sorted by $X1_u^i$ values, which may be implied. An example for the 2-dimensional Hilbert curve is given in Table B.3. Both of these examples are produced from the generator table given in Table 4.1 and define the state diagram illustrated in Figure 4.1.

Similarly, Tables B.4 and B.5 in the appendix correspond to the 3-dimensional Hilbert curve and are derived from the generator table given in Table 4.2 and define the state diagram illustrated in Figure B.2. Tables B.6 and B.7 correspond to the 4-dimensional Hilbert curve and are derived from the generator table given in Table 4.3.

Transformation Matrix Operations

Two different transformation matrix calculations are employed in Algorithm 4.3.2; in line numbers 24 and 27. We conclude this section with a description of how these calculations are performed.

In our description, matrix rows are numbered in the range $[1, \ldots, n]$ from top to bottom and columns are numbered in the same range from left to right. A state is referred to as 'S_u', where 'u' is the state number. State S_0 is the state which is encapsulated by the generator table itself.

We define P_u^e as the column Y value corresponding to the column X_1 value equal to e, in state S_u. e is expressed as a binary number and u is expressed as a decimal number. Determining the value of P_u^e is achieved with the aid of the calculation performed in line 24 of Algorithm 4.3.2. e is multiplied by the transformation matrix for state S_u in order to determine the equivalent column X_1 value, f, in state S_0 which maps to the same column Y value. Thus $P_u^e = P_0^f$.

The multiplication is carried out in the following manner, using a temporary variable V which is an n-bit vector:

1. V is initialized such that column i contains a non-zero value if the non-zero value in the same column in the transformation matrix for state S_u is negative, for all $1 \leq i \leq n$. Thus V encapsulates the signs of the non-zero elements of the matrix for state S_u.

2. f is initialized as $e \ \oplus \ V$.

3. For each row i in the matrix for S_u, if a non-zero value exists in column j of row i and a non-zero value exists in the same column in f, then the non-zero value in column j of f is moved to column i in f.

4. P_u^e is assigned the value of P_0^f, found by looking up the column Y value corresponding to the column X_1 of f in the generator table.

The order in which the above operations is performed is significant.

Having found the column Y value for e, we need also determine its *next-state*. This is achieved with the aid of the calculation performed in line 27 of Algorithm 4.3.2. The *next-state* transformation matrix (A) for e is defined as the *next-state* transformation matrix for f in state S_0 (B) multiplied by the transformation matrix for state S_u (C). More succinctly, $A \Leftarrow B * C$.

The multiplication is carried out by examining each row of matrix B in turn:

1. If in row i of matrix B, a non-zero bit exists in column j, then row i of matrix A takes the value of row j of matrix C.

2. If the signs of the non-zero values in row i of matrix B and row j of matrix C are different, ie one is positive and one is negative, then the sign of the non-zero value in row i of matrix A becomes negative, otherwise it becomes positive.

The matrix multiplication is not commutative.

Figure 4.4 gives an example of the transformation matrix calculations described in this section when applied to the 3-dimensional Hilbert curve defined in Table 4.2 and illustrated in Figure B.2. The example shows how the column X_1 value of '010' in state number '11' (decimal) maps to the column Y value of '111' and that it's *next-state* is state number '2'. This is consistent with Figure B.2.

An Example

Figure 4.5 illustrates part of the process of constructing a list of states for the Hilbert curve in 2 dimensions.

4.3.7 State Diagram Growth Rate

Having described and developed the state diagram approach to mapping between one dimension and n dimensions for a number of space-filling curves, in this section we compare them from the point of view of state diagram size.

4.3.7.1 The Hilbert Curve

Bially observed that it is possible to limit the number of states in a state diagram for a *continuous* space-filling curve to the smaller of those given by

$$\frac{n\,!}{(n-H)\,!}\,2^{n-\frac{1}{2}(1-(-1)^H)} \tag{4.4}$$

and

$$\frac{n\,!}{H\,!}\,2^{n-\frac{1}{2}(1-(-1)^H)} \tag{4.5}$$

An upper limit on the number of states required is given by

$$n\,!\,2^{n-\frac{1}{2}(1-(-1)^H)} \tag{4.6}$$

In the case of the Hilbert curve, where $H = 1$, we can replace equation (4.4) with

$$n\,2^{n-1} \tag{4.7}$$

and replace equations (4.5) and (4.6) with

$$n\,!\,2^{n-1} \tag{4.8}$$

We note that equation (4.7) is the same as equation (4.3) from section 4.2 above, which gives the number of edges in a hyper-cube.

The number of states produced by our technique for the Hilbert curve, described in section 4.3.3, conforms with (4.7) or (4.8), depending on how the transformation matrices are initialized. Were we to interchange the first row of an identity matrix with one other, the latter would apply. Where the first row of a matrix is initialized to its row's column δY value and successive rows are determined by circular shifting, the former applies.

In accordance with equation (4.7), the rate at which the number of states in a diagram increases is exponential in the number of dimensions. This limits the number of dimensions in which mappings may be performed with the aid of state diagrams in the implementation of our indexing application. The rate of increase in the size of an individual state is also exponential in the number of dimensions. The size of a state is proportional to the number of points on a first order curve.

Table 4.4 contains a summary of the number of states required for the Hilbert curve, and others discussed in this chapter, as the number of dimensions varies. Considering the

Example for: state $u = 11$ (decimal)
$e = 010$ (binary)
(e is a column X_1 value)

Matrix for state **11** (decimal) is shown in the state diagram of Figure B.2 in appendix B. This matrix is referred to as 'matrix C' below.

Find the column Y value, P_u^e, for e

Step 1: $V \Leftarrow 011$ (since 1's in last 2 columns of matrix C are negative)

Step 2: $f \Leftarrow 010 \oplus 011$ (ie $f \Leftarrow e \oplus V$, therefore, $f = 001$)

Step 3: The **1** in column 3 of row 1 in matrix C causes the **1** in column 3 of f to move to column 1.

Thus $f \Leftarrow 100$

Other rows in matrix C have no effect since 1's in their columns all correspond to 0's in the same columns in f.

Step 4: From generator table (Table 4.2 – encapsulating state **0**), $P_0^f = 111$

Therefore, $P_u^e \Leftarrow 111$

Find the ***next-state*** for e

next-state for f ($= 100$) in state **0** is state **4** (matrix B) – from generator table.

Step 1: apply matrix B to matrix C to create matrix A

0	0	-1	(1)
-1	0	0	(2)
0	1	0	(3)

B

$*$

0	0	-1	(4)
1	0	0	(5)
0	-1	0	(6)

C

$\rightarrow$

0	-1	0	(7)
0	0	-1	(8)
1	0	0	(9)

A

(1) causes (6) to move to (7),
(2) causes (4) to move to (8),
(3) causes (5) to move to (9).

Step 2: adjust signs of non-zero elements in matrix A

signs in (1) and (6) are both negative, therefore sign in (7) becomes positive,
signs in (2) and (4) are both negative, therefore sign in (8) becomes positive,
signs in (3) and (5) are both positive, therefore sign in (9) becomes positive.

Thus matrix $A \Leftarrow$

0	1	0
0	0	1
1	0	0

From the state diagram in Figure B.2, matrix A corresponds to state **2**

Therefore, ***next-state*** for $e \Leftarrow$ state **2**.

Fig. 4.4: Example Showing Calculations Carried Out Using Transformation Matrices

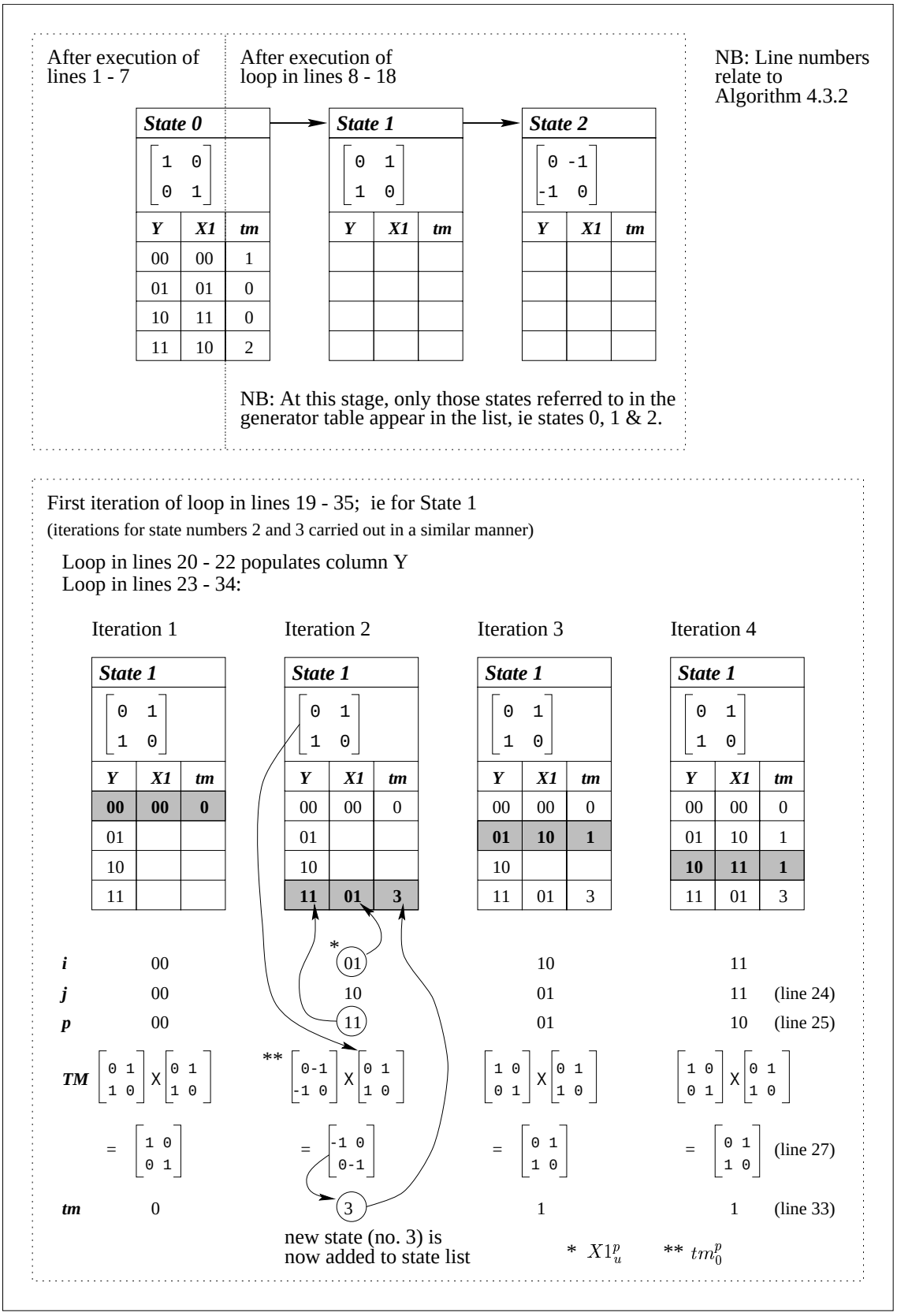

Fig. 4.5: An Example of the State Diagram Generation Process

No. of dims	Hilbert		Moore		Gray-code^F		Gray-code^{A,B}	
	No. of states	size (kB)	No. of states	size (kB)	No. of states	size (kB)	No. of states	size (kB)
3	12	0.1875	8	0.125	4	0.0625	2	0.03125
4	32	1	16	0.5	8	0.25	2	0.0625
5	80	5	32	2	16	1	2	0.125
6	192	24	64	8	32	4	2	0.25
7	448	168	128	32	64	16	2	0.5
8	1024	768	256	128	128	64	2	1
9	2304	4608	512	1024	256	384	2	3
10	5120	20480	1024	4096	512	2048	2	6
11	11264	90112	2048	16384	1024	8192	2	12
12	24576	393216	4096	65536	2048	32768	2	24
13	53248	1703936	8192	262144	4096	131072	2	48
14	114688	11010048	16384	1048576	8192	524288	2	96
15	245760	47185920	32768	4194304	16384	2097152	2	192
16	524288	201326592	65536	16777216	32768	8388608	2	384

Tab. 4.4: State Diagram Generator Table Growth Rates and Memory Requirements

growth rates of both state diagrams and individual states the table also summarizes the amount of memory required to store state diagrams. It appears that a practical upper limit of 8 or 9 dimensions applies to the Hilbert curve. It appears that above 8 or 9 dimensions state diagram storage requirements for the Hilbert curve become prohibitive. The stepped horizontal line in the table notionally indicates the numbers of dimensions for different curves beyond which it becomes impracticable to store state diagrams in memory, given current hardware constraints.

When evaluating the cost of utilizing state diagrams, factors other than their sizes need also to be taken into account.

As the size of a state diagram increases with the increase in the value of n, so also does the time taken to load the diagram into memory. However an application using a state diagram needs only to load it once each time it is executed.

From a practical view, it is also advantageous to maintain two copies of the state diagram in memory since some operations entail mapping from one dimension to n dimensions while others entail the inverse. Clearly this doubles the memory requirements listed in Table 4.4.

4.3.7.2 Discontinuous Curves

We noted in the previous section that the size of a state grows exponentially with an increase in the number of dimensions and so the size of a state diagram grows exponentially regardless of the number of states in it. Nevertheless, curves whose state diagrams contain fewer states than others may be of practical use in a higher number of dimensions.

By following the procedure for constructing state diagram generator tables for our variation of Moore's curve, described in section 4.3.5.2, the state diagram growth rate is found to be 2^n. This is exponential and little better than that for the Hilbert curve. In practical terms, Moore's curve can only be used in a space defined at most by one more dimension than that which can be traversed by the Hilbert curve.

All of the state diagrams produced from the generator tables for the Gray-code^A and

Gray-code^B curves contain 2 states, regardless of the number of dimensions. The size of a state diagram is clearly dominated by the size of a single state and this allows us to utilize these variations of the Gray-code curve in up to about 20 dimensions, for which diagrams require approximately 10 Mega-bytes of storage.

In contrast, state diagrams for the Gray-code^F curve grow exponentially, containing 2^{n-1} states. Thus state diagrams for this curve can be accommodated for up to about 11 dimensions.

4.4 Mapping to the Hilbert Curve Using the State Diagram Generator Table

State diagrams facilitate mappings between one and n dimensions by avoiding the need to perform calculations but their growth rate imposes a limit on the size of n. Mappings in higher-dimensional space must either be performed by calculation alone or by a process in which there is a compromise between the amount of calculation required and the amount of storage required by data structures.

When Faloutsos suggests the application of Bially's state diagram generation method to the Hilbert curve in [FR89b] he envisages storing the generator table in main memory and using this data structure for the calculation of Hilbert *derived-keys* rather than using it as a means of producing a state diagram. In this section, we explore and develop this notion.

The generator table essentially encapsulates the transformation of a particular first order curve to a second order curve only, but it permits all other transformations occurring in a higher order curve to be inferred. Its rate of growth with the increase in the number of dimensions is, therefore, the same as that of a single state rather than that of a state diagram. Thus in higher than 2 dimensions, a generator table occupies considerably less memory than a state diagram and so it is practicable to store generator tables in a higher number of dimensions than it is to store state diagrams. Utilization of generator tables does, however, require some calculations to be performed during the mapping process.

In using a generator table to construct a state diagram, as described in section 4.3.6, we effectively perform mappings for a number of points. Since our interest is in identifying different states, mappings terminate at some finite order once we encounter a state which has already been encountered before, either for the point in question or for some other point processed previously. It follows that, for any point, we can perform a mapping for some constant order of curve, whether or not we encounter new states at each step of the calculation. Clearly, this can be achieved with no more information than is held in the generator table.

If the generator table is required for the purpose of performing mappings, it may be stored compactly since not all of the data held in it is needed once it has been constructed. The required information comprises the mapping between sequence numbers and coordinates of points on a first order curve, which are encapsulated by columns Y and X_1, and the *next-state* transformation matrices within each row of the table.

A transformation matrix may also be stored compactly since the rules for column $\overline{T(Y)}$ given in sections 4.3.2 and 4.3.3 show that it can be derived from just two values. These are the first entry in column X_2, which determines the signs of the non-zero elements within it, and the column δY value, which determines which two rows in an identity matrix need be interchanged. We noted in the commentary on our rules for populating column $\overline{T(Y)}$ for the Hilbert curve in section 4.3.3 that this method of defining a transformation matrix does not yield an optimally compact state diagram but, since we do not store it, this is of no concern.

The table can be stored as an array of rows. Thus either the point sequence numbers (column Y) can be implied by the array element number or the rows can be sorted in column X_1 order and the coordinates of points (column X_1) can be implied. The choice depends on whether the structure is required for performing a mapping from one to n dimensions or from n dimensions to one. Generator tables for the Hilbert curve require a little less memory than state diagrams for the Gray-code^A curve, indicated above in Table 4.4.

In chapter 5, we present algorithms which perform mappings using a state diagram and also show how they are adapted where a state diagram generator table is stored instead.

4.5 Mapping to the Hilbert Curve by Calculation

Although the growth rate of state diagram generator tables is lower than that of state diagrams, it is still exponential in the number of dimensions and so mapping techniques which rely on their storage are limited in practical applications to little more than 20 dimensions.

We noted in section 2.1.1 of chapter 2, however, that a method of mapping from Hilbert *derived-keys* to n-dimensional points is described by Butz [But71] which does not require the storage of data structures. The procedure effectively descends the tree representation of the Hilbert curve iteratively from the first order level to some finite order k and simply requires the storage of the results of some of the calculations carried out in the previous iteration.

In this section, we extend the technique described in section 4.4 to provide an alternative to Butz' method which also does not require the storage of a data structure. We have already seen that it is possible to perform Hilbert curve mappings if just 3 values for each point on a first order curve are stored. These are either of the values in columns Y or X_1, depending on the required direction of the mapping, the first column X_2 value and the column δY value. Instead of storing these values they can be calculated with little difficulty on demand.

We noted in section 4.3.3 that a column X_1 value can be defined as the Gray-code of its corresponding column Y value. The inverse, or *derived-key*, of a Gray-code is found calculated in accordance with Algorithm 5.5.1 given in chapter 5 and can be effected in up to n steps.

With regard to column X_2 values, an examination of state diagram generator tables constructed in the manner described in section 4.3.3 for 2 to 8 dimensions enables relationships between column Y values and the first entries in column X_2 to be identified. For any row containing an odd column Y value, the corresponding first entry in column X_2 is the same as the Gray-code of the preceding row's (even) column Y entry, ie the column X_1 entry of the preceding row. A similar relationship exists for rows with even column Y values since any such row shares the same first column X_2 with its preceeding row. The first row in the generator table is a special case where its first X_2 entry equals $00\ldots00$.

With regard to column δY values, the tables also show that for any row containing an odd column Y value an EXCLUSIVE-OR operation on the Gray-code of the column Y value and the Gray-code of its (even) successor results in the row's δY value. Similarly, for rows containing even column Y values we find δY by performing an EXCLUSIVE-OR operation on the Gray-code of the column Y value and the Gray-code of its (odd) predecessor. The first and last rows of the generator table are special cases where their δY entries both equal $00\ldots01$.

It is important to note that the above observations apply specifically where generator tables have been constructed in the manner described in section 4.3.3. They would not necessarily apply, for example, where generator tables are constructed in the manner

implied by Fig. 3 in [Bia69].

We leave a comparison of the mapping technique described in this section with that of Butz to chapter 5.

Chapter 5

ALGORITHMS FOR MAPPING TO AND FROM SPACE-FILLING CURVES

In the previous chapter, we identified a number of techniques for performing a mapping between one dimension and n dimensions for the Hilbert curve and we identified and developed tools to assist in this process. One of these tools, the state diagram, can also be readily applied to other space-filling curves.

In this chapter, we focus on the practical implementation of Hilbert curve mapping algorithms. We also summarize mapping algorithms for curves other than the Hilbert curve although these are already well known. We consider the complexities of the various algorithms and determine which are the most suitable for use in our application.

5.1 Algorithm for Hilbert Curve Mapping using a State Diagram

In chapter 4, we note that a state diagram expresses the tree representation of the Hilbert curve introduced in chapter 3 in a compacted form. In this section, we develop Algorithm 3.6.1 from section 3.6, which informally describes how the tree is descended to find the sequence number, or *derived-key*, of a point. In doing so, we utilize state diagrams and apply them to curves of any finite order and passing through any number of dimensions.

We recall that a 'state' represents a mapping between points on a first order curve and the sequence in which they are ordered. A point on a first order curve comprises a set of n single bit coordinate values, which we concatenate into an n-bit value, defined in chapter 3 as an *n-point*. The *derived-key* of an *n-point* is also an n-bit value.

Once state diagrams have been constructed, finding the *derived-key* of a point and finding the coordinates of a point corresponding to a particular *derived-key* are straightforward iterative processes.

The coordinates of an n-dimensional point, P, lying on a curve of order k were expressed in (3.5) on page 36 and repeated here as:

$$P = \langle\ p_{1_1} p_{1_2} \dots p_{1_k},\ p_{2_1} p_{2_2} \dots p_{2_k},\ \dots,\ p_{n_1} p_{n_2} \dots p_{n_k}\ \rangle \tag{5.1}$$

where, if i is in the range $[\,1 \dots n\,]$ then each vector p_i is one of n coordinates (in dimension i) and composed of k bits; thus p_{i_j} is a single bit.

The Hilbert *derived-key*, HK, of point P is expressed as:

$$HK = h_{1_1} h_{1_2} \dots h_{1_n} h_{2_1} h_{2_2} \dots h_{2_n} \dots h_{k_1} h_{k_2} \dots h_{k_n} \tag{5.2}$$

where, if j is in the range $[\,1 \dots k\,]$ then each vector h_j is one of k sequences and composed of n bits; thus h_{j_i} is a single bit. Each h_j corresponds to a *derived-key*, or column Y value, within a state in the state diagram and is a value in the range $[\,0 \dots 2^n - 1\,]$ or, more generally, $[\,0 \dots r^n - 1\,]$. During the iterative mapping process, the state of which h_j is a

member is called the *current-state*. Initially, when $j = 1$, the *current-state* is state number 0. In subsequent iterations, the *current-state* is updated to become the '*next-state* for h_j within the *current-state*' and it is read from the state diagram. Given any two values a and b, h_a and h_b may or may not be members of the same state, regardless of their values.

In contrast to the Z-order curve described in section 3.7.1 and later in this chapter in section 5.4, there is no direct relationship between any pair of bits in P and in HK. Instead, h_j is determined by the position of the sequence of n bits taken from P:

$$p_{1_j} p_{2_j} \cdots p_{n_j} \tag{5.3}$$

in the ordering of such sequences within the *current-state*. Thus in determining HK from P we examine successive sequences of the form given in (5.3) for all values of j. We refer to a sequence of this form as z_j and note that it corresponds to a column X_1 value in the generator table or within a state in the state diagram. We recall from (3.7) on page 36 that the sequence $z_1 z_2 \ldots z_k$ represents the Z-order *derived-key* of P. Thus a mapping from P to HK entails, amongst other things, calculating the Z-order *derived-key* of P.

We recall from section 3.7.1 that z_j locates a hyper-cube in coordinate space within z_{j-1}. Thus in the first iteration of a mapping from P to HK, z_1 identifies a hyper-cube containing P within the whole space. The *current-state*, S_c, is initially state number 0 and so from the state diagram, h_1 is found to be the *derived-key* corresponding to z_1 in state 0. The *current-state* is then updated from the state diagram to become the *next-state*, S_c, for the $\langle z_1, h_1 \rangle$ pair in state 0.

In the second iteration, z_2 then locates a hyper-cube containing P within z_1. From the state diagram, h_2 is found to be the *derived-key* corresponding to z_2 in state S_c. The *current-state* is then updated from the state diagram to become the *next-state* for the $\langle z_2, h_2 \rangle$ pair in state S_c.

The algorithm then continues in a similar manner until h_k is identified from state S_c as the *derived-key* corresponding to z_k. Thus n bits of HK are identified in each iteration, from 1 bit taken from each coordinate in P, beginning with the most significant bits. This algorithm effectively describes a descent from the root to a member of a leaf in the tree representation of the Hilbert curve.

The algorithm described here is expressed in Algorithm 5.1.1. It utilizes state diagrams in which $\langle z_i, h_i \rangle$ pairs are ordered by z_i (column X_1) values. Examples for the Hilbert curve in 2, 3 and 4 dimensions are given in Tables B.3, B.5 and B.7 respectively, in appendix B.

Algorithm 5.1.1 Finding the Hilbert *derived-key* of a Point using the State Diagram

1: $P \Leftarrow \langle p_{1_1} p_{1_2} \ldots p_{1_k}, p_{2_1} p_{2_2} \ldots p_{2_k}, \ldots, p_{n_1} p_{n_2} \ldots p_{n_k} \rangle$
   {the coordinates of point for which the Hilbert *derived-key* is required}
2: $S_c \Leftarrow 0$ {*current-state*}
3: $HK \Leftarrow 0$ {the *derived-key*}
4: $i \Leftarrow 1$
5: **while** $i \leq$ *order-of-curve* **do**
6: $\quad z_i \Leftarrow p_{1_i} p_{2_i} \ldots p_{n_i}$
7: $\quad h_i \Leftarrow$ the *derived-key* in state S_c corresponding to z_i
8: $\quad S_c \Leftarrow$ the *next-state* corresponding to h_i in state S_c
9: $\quad HK \Leftarrow HK \ll n$ bits
10: $\quad HK \Leftarrow HK + h_i$
11: $\quad i \Leftarrow i + 1$
12: **end while**
13: **return** HK

The inverse mapping, from Hilbert *derived-keys* to the coordinates of a point, is performed in a similar manner and is given in Algorithm 5.1.2. Modification of this last algorithm to avoid calling the function to map a Z-order *derived-key* to the coordinates of a point as a post-processing operation is trivial but has no bearing on the complexity of the algorithm. The algorithm utilizes state diagrams in which $\langle z_i, h_i \rangle$ pairs are ordered by h_i (column Y) values. Examples for the Hilbert curve in 2, 3 and 4 dimensions are given in Tables B.2, B.4 and B.6 respectively, in appendix B.

Algorithm 5.1.2 Finding the Coordinates of a Point from its Hilbert *derived-key* using the State Diagram

1: $HK \Leftarrow h_{1_1} h_{1_2} \ldots h_{1_n} h_{2_1} h_{2_2} \ldots h_{2_n} \ldots h_{k_1} h_{k_2} \ldots h_{k_n}$
{the Hilbert *derived-key* for which the coordinates of point are required}
2: $S_c \Leftarrow 0$ {*current-state*}
3: $P \Leftarrow 0$ {the coordinates of the point mapped to by HK}
4: $Z \Leftarrow 0$ {the Z-order *derived-key* of P}
5: $i \Leftarrow 1$
6: **while** $i \leq$ *order-of-curve* **do**
7: $h_i \Leftarrow h_{i_1} h_{i_2} \ldots h_{i_n}$
8: $z_i \Leftarrow$ the *n-point* in state S_c corresponding to h_i
9: $S_c \Leftarrow$ the *next-state* corresponding to z_i in state S_c
10: $Z \Leftarrow Z \ll n$ bits
11: $Z \Leftarrow Z + z_i$
12: $i \Leftarrow i + 1$
13: **end while**
14: $P \Leftarrow z\_to\_p(Z)$ {a function which returns the mapping from a Z-order *derived-key* to the coordinates of a point}
15: **return** P

5.2 Algorithm for Hilbert Curve Mapping using a State Diagram Generator Table

In section 4.4 of chapter 4, we consider performing Hilbert curve mappings with the aid of the state diagram generator table stored in memory rather than the state diagram itself. Since the generator table is more compact, this approach enables mappings to be performed in a higher number of dimensions before memory requirements become prohibitive. In this section we show how our mapping algorithms which utilize a state diagram presented above require minor modification only to achieve this objective.

We recall that where a mapping is required from points to *derived-keys*, the table is sorted by column X_1 values, which are implied, and column Y values are stored. For the inverse mapping, the table is sorted by column Y values, which are implied, and column X_1 values are stored. In both cases, the *next-state* matrices (column $\overline{T(Y)}$) are also stored. We saw that a *next-state* matrix can be encapsulated compactly by two values. One is the column δY value within a row in the table. In this section, this is regarded as specifying how the matrix differs from the identity matrix by interchanging the first row in the latter with one other (although, in section 4.3.3 of chapter 4, we saw an alternative interpretation which we exploit in the production of state diagrams since the resulting diagrams contain fewer states). The other is the first of a pair of column X_2 values within a row in the table, which specifies the signs of the non-zero elements within a *next-state* matrix.

Where state diagrams are utilized, the *current-state*, S_c, is effectively a pointer to a

state within the state diagram, thus it can be expressed compactly as an integer. Where the generator table is utilized instead, however, the *current-state* matrix must be stored in detail. In the first iteration of the algorithm, the *current-state* matrix equates to the identity matrix. In subsequent iterations, the next *current-state* matrix is calculated by multiplying the *current-state* matrix by a matrix taken from column $\overline{T(Y)}$ of the generator table. Successive multiplications may cause the *current-state* matrix to differ from the identity matrix in a more complex manner than the interchanging of the first row of the latter by one other.

Thus S_c is a data structure comprising an n-bit value for each row of the matrix. Each bit corresponds to a column within a row. An additional value within the structure encapsulates the signs of the non-zero bits within each row. An example of a matrix and the way in which it is stored in S_c is:

Conceptual View					Implementation: Matrix Rows				Signs			
0	0	1	0	→	0	0	1	0	1	0	0	1
-1	0	0	0	→	1	0	0	0				
0	0	0	-1	→	0	0	0	1				
0	1	0	0	→	0	1	0	0				

From the foregoing, Algorithm 5.1.1 may be restated as Algorithm 5.2.1 where state diagram generator tables are stored in place of state diagrams. The generator table is ordered by column X_1 values which are implied. In the context of state diagram generator tables, the variables h_i and z_i correspond to column Y and column X_1 values respectively.

Algorithm 5.2.1 Finding the Hilbert *derived-key* of a Point using the State Diagram Generator Table

1: $P \Leftarrow \langle p_{1_1}p_{1_2}\ldots p_{1_k}, p_{2_1}p_{2_2}\ldots p_{2_k}, \ldots, p_{n_1}p_{n_2}\ldots p_{n_k} \rangle$
{the coordinates of point for which the Hilbert *derived-key* is required}
2: $S_c \Leftarrow$ the identity matrix {*current-state*: the matrix sign value contains zeros in all bits}
3: $HK \Leftarrow 0$ {the *derived-key*}
4: $i \Leftarrow 1$
5: **while** $i \leq$ *order-of-curve* **do**
6: $z_i \Leftarrow p_{1_i}p_{2_i}\ldots p_{n_i}$
7: $z_i \Leftarrow z_i * S_c$
8: $h_i \Leftarrow$ the column Y value in row z_i of the generator table
9: $S_c \Leftarrow$ the *next-state* in row z_i of the generator table $* S_c$
10: $HK \Leftarrow HK \ll n$ bits
11: $HK \Leftarrow HK + h_i$
12: $i \Leftarrow i + 1$
13: **end while**
14: **return** HK

Algorithm 5.2.1 differs from Algorithm 5.1.1 in that line #7 is inserted in the former and lines #7 and #8 in the latter are replaced by lines #8 and #9 in the former.

Line #7 in Algorithm 5.2.1 transforms a z_i value in the *current-state* into its equivalent in state 0 which maps to the same h_i value. This is in accordance with the calculation process given on page 73. This first entails an EXCLUSIVE-OR operation on z_i with the variable encapsulating the sign of the *current-state* matrix. The individual bits in the

result are then permuted according to the characteristics of the *current-state* matrix, in up to n steps.

The matrix multiplication carried out in line #9 in Algorithm 5.2.1 is carried out in accordance with the calculation process given in chapter 4 on page 73. Determining the rows of the new *current-state* matrix is trivial since any *next-state* matrix is an identity matrix with one row interchanged with the first. Thus the *current-state* matrix is modified by interchanging two of its rows. The signs of the non-zero elements of the *current-state* matrix are updated in n steps, one for each bit.

The inverse mapping, from *derived-keys* to the coordinates of points, differs from Algorithm 5.2.1 in a similar way as Algorithm 5.1.2 differs from Algorithm 5.1.1. The main difference is in the way z_i is computed from h_i. This is carried out as follows:

1. z_i is read from column X_1 in row h_i of the generator table.
2. Columns, ie bits, in z_i are permuted as follows: for each row j in S_c, if a non-zero exists in column k of row j and a non-zero exists in column j of z_i, then the non-zero in column j of z_i is moved to column k in z_i.
3. z_i takes the value of the exclusive-or of itself and the variable encapsulating the signs of the non-zero elements in S_c.

The order and detail of the calculation process given here is different from that given on page 73 since here we mapping from *derived-keys* to the coordinates of points rather than the inverse.

5.3 Algorithm for Hilbert Curve Mapping using Calculation

In chapter 4 we saw that the definition of the Hilbert curve we use regards column X_1 values as Gray-codes of column Y values and so given either one of these values, the other may be calculated readily. We saw that their corresponding *next-state* matrices can also be calculated. Thus the algorithms given in the previous section can be developed with little difficulty in order to avoid not only the storage of state diagrams but also the storage of generator tables. This approach removes practical restrictions on the number of dimensions in which mappings may be performed. We say more about the complexity of the mapping algorithms later in this chapter but note here that such developments appear to offer no real improvement over the algorithms given by Butz [But71]. They are not, therefore, pursued further.

Nevertheless, we find that in developing our algorithms, we are provided with insights which enable modification of Butz' algorithm for mapping from *derived-keys* to points and thereby improve its efficiency, although its complexity remains unchanged.

In this section we describe, using his notation, the modifications we make to specific operations within Butz' algorithm. Since an understanding of this algorithm is required in order to place these modifications in context, we reproduce Butz' algorithm, taken from his paper of 1971 [But71] in appendix B. The algorithm for mapping from *derived-keys* to points appears in Table B.8 and the example, taken from the same paper, showing how mapping takes place, is reproduced in Table B.9.

Calculation of σ^i: Butz' variable ρ^i corresponds to a column Y value, ie *derived-key*, from the generator table, according to its definition taken from the paper and noted in appendix B. The variable σ^i is derived directly from the value of ρ^i. We make the conjecture that a σ^i value corresponds to a column X_1 value and, analysis of the definition

of the former confirms that it is the Gray-code of ρ^i. Thus σ^i may be defined in a single operation rather than in n steps as indicated in Butz' paper[1]:

$$\sigma^i \Leftarrow \rho^i \oplus (\rho^i/2) \tag{5.4}$$

Calculation of τ^i: In describing how the value of the variable τ^i is determined, Butz notes that the result is always of 'even parity', by which is meant that it contains an even number of non-zero bits. We observe from the state diagram generator tables, in all numbers of dimensions for which they have been constructed, that this characteristic is shared, specifically and only, by the first of a pair of column X_2 values appearing in any row. This leads to the conjecture that there is a correspondence between these two values and this is supported by the results of experiments. Thus we are able to calculate values for τ^i simply, in accordance with the method for calculating the first of a pair of column X_2 entries and described in section 4.5 of chapter 4. This is detailed in Algorithm 5.3.1.

Algorithm 5.3.1 Simplified Calculation of τ^i in Butz' Algorithm

```
1: if ρ^i < 3 then
2:    τ^i ⇐ 0
3: else
4:    if ρ^i % 2 then
5:       τ^i ⇐ (ρ^i − 1) ⊕ ((ρ^i − 1)/2)
6:    else
7:       τ^i ⇐ (ρ^i − 2) ⊕ ((ρ^i − 2)/2)
8:    end if
9: end if
```

The calculations for other variables in Butz' algorithm are performed in our implementation in accordance with Table B.8.

We noted in section 4.3.4 of chapter 4 that the second order 3-dimensional Hilbert curve implied by our state diagram generator table in Table 4.2 differs in detail from the curve implied by Fig. 3 in Bially's paper [Bia69]. We note here that our implementation of Butz' algorithm produces the same curve as that shown in our Table 4.2.

To conclude this section, we note that while Butz provides an algorithm for mapping from Hilbert *derived-keys* to the coordinates of points, he does not detail the inverse of the procedure. We therefore provide the solution to this problem, using a similar notation to that adopted by Butz, in Table B.10 in appendix B, since this mapping is required, for example, in updating our file store.

5.4 Algorithms for the Z-order Curve

Algorithms for mapping from points to Z-order *derived-keys* and the inverse are trivial and follow automatically from the definition of a Z-order *derived-key* given in section 3.7.1 of chapter 3. In that chapter, (3.5) defines a point and (3.6) defines a Z-order *derived-key* by way of interleaving successively lower bits taken from each of the coordinates of a point in turn. An alternative order in which bits are taken from a point is given in (3.9) in the same chapter along with some other possible variations.

The two interpretations of Z-order *derived-keys* are topologically equivalent but we see in chapter 7 that the choice of ordering of coordinates in bit-interleaving has subtle implications for querying in a practical implementation.

[1] Refer to appendix A for a key to symbols.

Given a point P lying on a Z-order curve of order 32 and with coordinates

$$\langle\, x_1x_2x_3x_4,\ y_1y_2y_3y_4,\ z_1z_2z_3z_4 \,\rangle$$

where each x_i, y_i and z_i is a byte:

if $x_1 = 6$	=	0			0			0			0			0			1			1			0			
then																										
$Z\_MAP[6]$	=	0	0	0	0	0	0	0	0	0	0	0	0	0	0	0	1	0	0	1	0	0	0	0	0	
if $y_1 = 145$	=	1			0			0			1			0			0			0			1			
then																										
$Z\_MAP[145]$	=	1	0	0	0	0	0	0	0	0	1	0	0	0	0	0	0	0	0	0	0	0	1	0	0	
if $z_1 = 203$	=	1			1			0			0			1			0			1			1			
then																										
$Z\_MAP[203]$	=	1	0	0	1	0	0	0	0	0	0	0	0	1	0	0	0	0	0	1	0	0	1	0	0	

if Z is the *derived-key* of P
then
the 24, ie $8n$, most significant bits of Z are calculated as:

$$Z\_MAP[6] + (Z\_MAP[145] \gg 1) + (Z\_MAP[203] \gg 2)$$

ie:

	0	0	0	0	0	0	0	0	0	0	0	0	0	0	0	1	0	0	1	0	0	0	0	0	
		1	0	0	0	0	0	0	0	0	1	0	0	0	0	0	0	0	0	0	0	0	1	0	
+			1	0	0	1	0	0	0	0	0	0	0	0	0	1	0	0	0	0	0	1	0	0	1	
=	0	1	1	0	0	1	0	0	0	0	1	0	0	0	1	1	0	0	1	0	1	0	1	1		

The 48 least significant bits of Z are calculated in a similar manner, 24 bits at a time, and appended to the 24 most significant bits

Fig. 5.1: Example Showing Optimized Calculation of a Z-order *derived-key*

Complexity of mapping algorithms is discussed in more detail in section 5.6 below but we note here that bit-interleaving implies a complexity which is proportional to the number of bits in a Z-order *derived-key*. This is determined by the number of dimensions, n, in a space multiplied by the order of the curve, k, which passes through it.

We recall from section 3.8.1 of chapter 3 that our implementation stores a point on a curve of order 32 in an array of 32 bit integers where each coordinate is held in an element of the array. A *derived-key* is also held in an array of the same size and so the bit values within a *derived-key* are divided between the array elements.

If a suitable data structure of modest size is held in main memory then, for some values of n, it is possible to implement the mapping more efficiently by processing more than one bit of each coordinate of a point simultaneously.

This data structure is an array of integers, which we call Z_MAP. Where n is in the range $[\,2, \ldots, 8\,]$, Z_MAP enables us to interleave 8 bits from each coordinate simultaneously. For values of n in this range, Z_MAP contains 256 elements, indexed in the range $[\,0, \ldots, 255\,]$. If j is a byte of 8 bits, $j_1j_2 \ldots j_8$, then the binary value of $Z\_MAP[j]$ is $j_10 \ldots 0j_20 \ldots 0 \ldots j_80 \ldots 0$. The number of zero-valued bits placed between bits j_i and j_{i+1} equals $n - 1$. Thus the number of significant bits in the value of each element of Z_MAP is $8n$. Where $n > 4$, an implementation requires the availability of 64 bit integers.

The application of Z_MAP is illustrated by an example in 3 dimensions in Figure 5.1.

More generally, in n dimensions, the value of Z is given by:

$$\sum_{\substack{b=1,\\ step\ B}}^{k-B} \left(\sum_{d=1}^{n} Z\_MAP[P_{db}P_{d(b+1)} \ldots P_{d(b+B-1)}] \gg (d-1) \right) \ll n(k-b-B-1) \qquad (5.5)$$

where k is the order of the curve (number of bits in a coordinate value), B is the number of bits of a coordinate which are processed simultaneously – always a factor of k, P_d is the coordinate of point P in dimension d and P_{db} is the value of the bit in position b in coordinate P_d.

Where the upper limit on integer size supported by a program compiler is 64 bits, the above approach can also be applied where n is in the range $[9, \ldots, 16]$. The number of bits from each coordinate of a point which can be interleaved simultaneously is, however, restricted to 4. For this range of values of n, the array Z_MAP contains 16 elements instead of 256.

Where 128 bit integers are supported, 16 bits of the coordinates of points may be interleaved simultaneously, for n in the range $[2, \ldots, 8]$, and 8 bits simultaneously for n in the range $[9, \ldots, 16]$. Z_MAP requires up to 1 Megabyte and 4 Kilobytes of main memory where n equals the upper limits of these two ranges respectively.

In the case of the mapping from Z-order *derived-keys* to points, a similar approach is less straightforward. An array element within the implementation of a *derived-key* will, in general, not contain the same number of bits corresponding to all of the coordinates of a point. In 3 dimensions, for example, the array element containing the 32 most significant bits of a *derived-key* holds 11 bits corresponding to the x and y coordinates of a point and 10 bits corresponding to the z coordinate. The second element contains 11 bits corresponding to the x and z coordinates and 10 bits corresponding to the y coordinate. The element containing the 32 least significant bits holds 11 bits corresponding to the y and z coordinates and 10 bits corresponding to the x coordinate. Nevertheless, in our application, greater use is made of mapping from points to *derived-keys* than the inverse.

5.5 Algorithms for the Gray-code Curve

We saw in section 4.3.5.3 of chapter 4 that it is possible to express the Gray-code curves described in section 3.7.2 of chapter 3 as state diagrams. Where this is done, the mapping algorithms described for the Hilbert curve above in section 5.1, and indeed the computer code which implements them, can be applied to these curves.

Alternatively, mappings from *derived-keys* to points and the inverse may be calculated. Such calculations entail a combination of Z-order bit-interleaving (or the inverse) and calculation of Gray-codes (or the sequence numbers of Gray-codes), as outlined in section 3.7.2 of chapter 3.

Methods of calculating mappings between Gray-codes and their sequence numbers, or *derived-keys*, are defined by Reingold et al [RND77]. A Gray-code is calculated simply from its *derived-key* as[2]:

$$Gray\_code \Leftarrow derived\text{-}key \oplus (derived\text{-}key/2) \qquad (5.6)$$

[2] Refer to appendix A for a key to symbols.

Calculation of the *derived-key* of a Gray-code is more complex. Each bit in position d_i of the *derived-key* is set to 1 if the sum of the bits in bit position g_i and above in the Gray-code is odd, otherwise it is set to 0. Thus:

$$d_j \Leftarrow \left[\sum_{i=1}^{j} g_i\right] \% \, 2, \qquad 0 < j \leq t \tag{5.7}$$

where t is the number of bits in a Gray-code, the most significant bit occupies bit position 1 and the least significant bit occupies bit position t. This equation implies a computational complexity which is proportional to the number of bits in a Gray-code multiplied by half of the number of bits, ie $O(t^2)$. A more efficient implementation, with a computational complexity of $O(t)$, is given in Algorithm 5.5.1.

Algorithm 5.5.1 Finding the *derived-key* of a Gray-code

```
    {d is the derived-key of Graycode g}
1:  d ⇐ 0
2:  while g > 0 do
3:      d ⇐ d ⊕ g
4:      g ⇐ g/2
5:  end while
```

5.6 Complexity of the Mapping Techniques

The complexity of all of the algorithms for mapping between one dimension and points on a space-filling curve described in this chapter can be seen to be $O(kn)$, where k is the order of the curve and n is the number of dimensions.

This is inherent to the problem and arises from the way in which a curve is drawn following repeated sub-division of space. The number of iterations in this process equals the chosen order of curve. Within each iteration, 1 bit is processed from each of n coordinates, in either direction of the mapping, effectively performing a mapping to or from the Z-order curve. Except in the case of the Z-order curve, other operations of constant complexity are carried out in addition. Thus the amount of work required is directly proportional to the number of bits which represent a *derived-key*.

The differences between the mapping algorithms, therefore, lie in the detail of their implementations and the effect this has on the constant elements of their complexities.

The Hilbert Curve

We have considered 4 alternative methods for performing Hilbert curve mappings in this chapter. These are: to utilize state diagrams stored in memory, to utilize state diagram generator tables stored in memory, to extend the latter to avoid the storage of data structures and to implement the algorithm given by Butz.

The difference between the efficiency of the Hilbert curve mapping algorithms depends on the number of iterations of complexity $O(n)$ which are carried out within each iteration of the outer loop of complexity $O(k)$. Where a state diagram is employed, we require one such inner loop only, as in line #6 of Algorithm 5.1.1. In Algorithm 5.2.1, employing a state diagram generator table, a further 2 inner loops are introduced as a result of the matrix operations in lines #7 and #9.

If we develop this algorithm to dispense with the generator table, we see from section 4.5 of chapter 4 that an additional inner loop is required to determine the (n-bit)

Hilbert *derived-key* of a point on a first order curve since this entails calculating the co-ordinates of a point which corresponds to a Gray-code. This was expressed previously as calculating a column X_1 value from a column Y value in Bially's table. Other data is required in order to define the *next-state* matrix corresponding to a point within the *current-state*, namely Bially's column $X2$ and δY values, but we saw that these can be found by simple EXCLUSIVE-OR operations. In short, our method of performing mappings by calculation requires a total of 3 inner loops of complexity $O(n)$ within the outer loop of $O(k)$.

An examination of Butz' algorithm in Table B.8 of appendix B for mapping from one dimension to n dimension shows that a total of 4 inner loops of complexity $O(n)$ are required, in the calculations of J_i, σ^i, τ^i and α^i. Our improvements detailed above in section 5.3 enables this to be reduced to only 2 by simplifying the calculations of σ^i and τ^i.

The Z-order Curve

A complexity of $O(kn)$ is particulary clear in the case of the Z-order curve. Where it can be exploited, the optimized method of mapping to the Z-order curve described in the previous section simply divides the running time of the algorithm by a constant and so does not alter its complexity.

The Gray-code Curve

Where Gray-code mappings are performed utilizing state diagrams, their complexities are identical to those which apply where Hilbert curve mapping utilizes state diagrams.

A Z-order curve mapping is required as a pre-processing or post-processing operation in any Gray-code curve mapping, as with the Hilbert curve. In addition, a mapping to Gray-codes requires a simple EXCLUSIVE-OR operation while the inverse requires execution of Algorithm 5.5.1 which has a complexity of $O(kn)$.

5.7 Conclusions

The results of experiments in which running time is measured where multi-dimensional data is mapped to one dimension during the process of inserting data into a data store are presented in chapter 10 for comparative purposes. It appears that a useful performance benefit can be enjoyed by employing state diagrams where it is practicable to accommodate them and that our implementation of Butz' calculated method should otherwise be used, given the current-state of technology in terms of speed of memory access compared with speed of performing calculations within computer hardware.

Chapter 6

ALGORITHMS FOR QUERYING DATA MAPPED TO SPACE-FILLING CURVES

6.1 Introduction

A decision to store data clearly implies that there may be a requirement to retrieve it. Where stored data is indexed there is also an implication of a demand for it to be recalled in some particular order or, more commonly, that only a sub-set of it which meets specific criteria is of interest at any particular time. The description of the criteria which data to be retrieved must match is the specification of what is referred to as a *query*.

When a query is executed then the data store must be searched in order to identify data which constitute matches. The purpose of indexing is to organize the data in order to minimize the proportion of the total which must be examined so that the process can be performed as efficiently as possible.

It follows that a multi-dimensional indexing strategy must include effective facilities to query data stores and this is the subject of this chapter. In particular, we concern ourselves with algorithms for identifying which pages may contain matches to a query. A query can be viewed as a region contained within the data-space or the domain of our application. Pages of data can be viewed similarly and so the problem we address can be restated as determining which pages intersect with the query.

In this chapter, we describe the forms of query which we address in our application and present the strategy we use for the execution of a query. We then detail our algorithms which enable us to identify pages to be searched. This is done firstly where we use the Hilbert curve, both with and without the aid of state diagrams, and secondly where we use the Z-order curve. We then address the complexities of the algorithms and finish with concluding remarks.

6.2 Types of Query

A *query region* or *query range* is a hyper-rectangular space contained within a data space. When a query is executed, the outcome is the retrieval of one or more or all of those *datum-points* which exist within the range, depending on how exhaustive the search is required to be.

A range or *range query* is defined by a pair of fully specified sets of coordinates representing a pair of points. One point is the *lower bound* of the range and the other is the *upper bound*. No coordinate value within the lower bound can be larger than its corresponding value in the upper bound.

If the lower bound coordinates are expressed as $\langle L_1, L_2, \ldots, L_n \rangle$ and the upper bound coordinates are expressed as $\langle U_1, U_2, \ldots, U_n \rangle$, where each L_i and U_i are coordinate values in dimension i, then a range can be expressed as a set of intervals as

$$\langle [L_1, \ldots, U_1], [L_2, \ldots, U_2], \ldots, [L_n, \ldots, U_n] \rangle$$

in which an interval $[\ L_i, \ldots, U_i\ ]$ defines the extent of the range in dimension i.

Datum-points which have values for all of their coordinates which lie within the corresponding intervals which define the range *match* the query.

A *partial match* query can be viewed as a special type of range query where an interval which specifies the range in at least one but not all dimensions is a point, ie L_i equals U_i, and where in all other dimensions the intervals span their entire domains.

The motivation for giving special consideration to this type of query is twofold. Firstly, some applications, such as the functional programming language FDL [KP88, Pou89], are implemented without any requirement to perform range queries which are not partial match queries. Secondly, some optimizations to our querying algorithms may be made for the execution of partial match queries, especially where a mapping to the Z-order curve is utilized.

The complete set of possible partial match queries in three dimensions, for example, may be expressed as

$$\langle\ x,\ y,\ ?\ \rangle,\ \langle\ x,\ ?,\ z\ \rangle,\ \langle\ ?,\ y,\ z\ \rangle,\ \langle\ x,\ ?,\ ?\ \rangle,\ \langle\ ?,\ y,\ ?\ \rangle \text{ and } \langle\ ?,\ ?,\ z\ \rangle.$$

In this notation, we say that x, y and z are intervals in which the lower and upper bounds are equal to each other and that they are *specified*. A '?' denotes the range

$$[\ \textit{minimum coordinate value}, \ldots, \textit{maximum coordinate value}\ ]$$

and we say that the interval is *unspecified*. A matching *datum-point* may contain any value in a dimension whose interval is unspecified.

An *exact match* query is another special type of range query in which all of the intervals for the coordinates each contains a single value and so it simply specifies a point. In contrast to other forms of query, at most one *datum-point* is retrieved. Such queries are dealt with trivially and do not require us to adopt the procedures described in this chapter. We simply map the query point to a *derived-key*, retrieve the page which will contain the query point if it is a *datum-point* and determine whether or not it is a *datum-point*.

In the remainder of this chapter, when we use the term *range query* we generally refer to queries which are not *partial match* queries.

6.3 Querying Data Mapped to Space-filling Curves

In this section we outline our strategy for executing queries and illustrate it with an example which employs the Hilbert curve. The method is, however, quite general and can be used for any curve which exhibits the properties which are required in our application as discussed in chapter 3.

Where multi-dimensional data is mapped to a space-filling curve, a page always represents a section of curve, ie a contiguous set of points, and will contain the *datum-points* which lie on that section. A query region, which is a hyper-rectangle, will always overlap one or more sections of the curve with intervening lengths which join them lying outside of the region. In other words, the curve may enter, leave and re-enter the query region a number of times.

These curve sections within the query region define a set of points and in turn this set defines a set of *derived-keys*. We reduce this set of *derived-keys* in a step by step process, at each step removing a sub-set, the values in which are lower than those remaining; at the same time any *datum-points* corresponding to the removed sub-set are retrieved. The original set is thus progressively reduced to the empty set when the query process is complete.

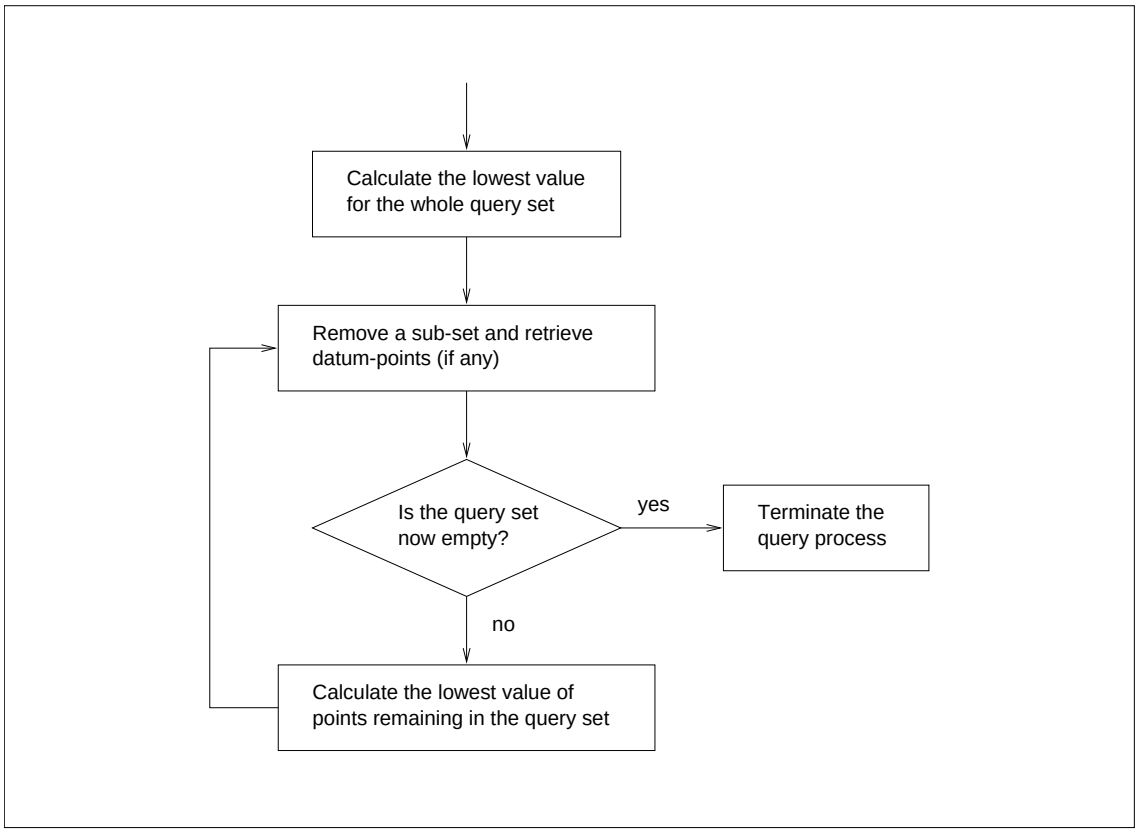

Fig. 6.1: The Query Process — in Broad Outline

We control this process with a parameter which is the lowest of those values remaining in the set. The parameter is initially calculated and set at the lowest value for the whole set of points in the query region. After the removal of a sub-set we calculate the new lowest value. We leave an explanation of how we determine this new lowest value to later on in this chapter when we describe our implementation in more detail. Once the query set has been reduced to the empty set it is no longer possible to calculate a new lowest value.

In broad outline, our algorithm thus proceeds as shown in Figure 6.1.

In our implementation, we refer to the controlling parameter, ie the lowest value remaining, as the *next-match*. Calculation of the *next-match* is performed by a function, *calculate_next_match*, and the same function is also used initially to determine the lowest possible, ie first, *next-match* to the query. Note that a *next-match* may or may not be the *derived-key* of a *datum-point*. At each step of the query process, we retrieve the page of data from the data store which will contain this *datum-point*, if it exists, and we search this page for all *datum-points* which lie within the query. All matching *datum-points* found are then retrieved.

A retrieved page corresponds to a set of contiguous points on the curve. This set of points contains the lowest sub-set of points, or possibly all of the remaining points, within the query set. The upper bound of the set of points corresponding to a page, if it is not the last logical page in the data store, is the *page-key* of the successor page minus one. If the page is the last logical page then the upper bound is the *derived-key* of the last point on the curve.

In the first call to the *calculate_next_match* function, before any sub-set has been removed, we calculate the first *next-match* as being a value which is equal to or minimally greater than the *page-key* of the first logical page in the data store. In subsequent steps,

after a page has been searched, the query process is complete if that page is the last logical page in the data store. Otherwise we attempt to calculate a new *next-match* and, if one exists, it is equal to or minimally greater than the successor page's *page-key*. An inability to determine a new *next-match* signifies that the query set is now empty and that the query process is complete.

Definition 6.3.1: *current-page-key : the* page-key *for which we wish to find the* next-match*, ie the* next-match *is equal to or minimally greater than the* current-page-key*. The* current-page-key *is assigned a new* page-key *value prior to each call to the* calculate_next_match *function. Each new value is greater than the previous value, if any, assigned to the* current-page-key*.*

We can now express our querying algorithm in more detail, as shown in Figure 6.2 on page 96.

In Figure 6.3, on page 97, we extend the example given in Figure 3.22 to show a range query in 2-dimensional space, through which passes a fourth order Hilbert curve and where the capacity of a page is four *datum-points*. Execution of the query proceeds in the following manner:

{ initialization }

1. The query region is defined by specifying its lower and upper bounds as coordinates. These are points **F** and **P**, respectively, in Figure 6.3.

2. The *current-page-key* is initialized to the *page-key* of page $P1$, ie to 0.

   { first iteration of the loop within the querying algorithm }

3. The *calculate_next_match* function is called and determines the lowest match to the query, which is the *derived-key* of point **B**.

4. The index is searched and the *derived-key* of point **B** is found to lie between the *page-keys* of pages $P3$ and $P4$ which are the *derived-keys* of points **A** and **G** respectively. Hence if the lowest match is a *datum-point* it will be found on page $P3$ and so pages $P1$ and $P2$ are excluded from the space to be searched.

5. Page $P3$ is now searched and *datum-points* **C**, **D** and **E** are found which lie within the query range and are retrieved.

6. The *current-page-key* is set to the *page-key* of the page following the one just searched, this being $P4$. Its *page-key* is the *derived-key* of point **G**.

   { second iteration of the loop within the querying algorithm }

7. The *calculate_next_match* function is called and determines the *next-match* to the *current-page-key* to be the *derived-key* of point **G**, ie the *current-page-key* is its own *next-match*.

8. The index is searched and the *derived-key* of point **G** is found to be the *page-key* of page $P4$. Hence if the *next-match* is a *datum-point* it will be found on page $P4$.

9. Page $P4$ is now searched and *datum-points* **G**, **H**, **J** and **K** are found which lie within the query range and are retrieved.

10. The *current-page-key* is set to the *page-key* of the page following the one just searched, this being $P5$. Its *page-key* is the *derived-key* of point **L**.

    { third iteration of the loop within the querying algorithm }

11. The *calculate_next_match* function is called and determines the *next-match* to the *current-page-key* to be the *derived-key* of point **N**.

12. The index is searched and the *derived-key* of point **N** is found to lie between the *page-keys* of pages $P6$ and $P7$ which are the *derived-keys* of points **M** and **Q** respectively. Hence if the *next-match* is a *datum-point* it will be found on page $P6$ and so page $P5$ is excluded from the space to be searched.

13. Page $P6$ is now searched and no *datum-points* are found which lie within the query range.

14. The *current-page-key* is set to the *page-key* of the page following the one just searched, this being $P7$. Its *page-key* is the *derived-key* of point **Q**.

    { fourth iteration of the loop within the querying algorithm }

15. The *calculate_next_match* function is called and determines that there is no higher *next-match* to the *current-page-key*. The query process therefore terminates.

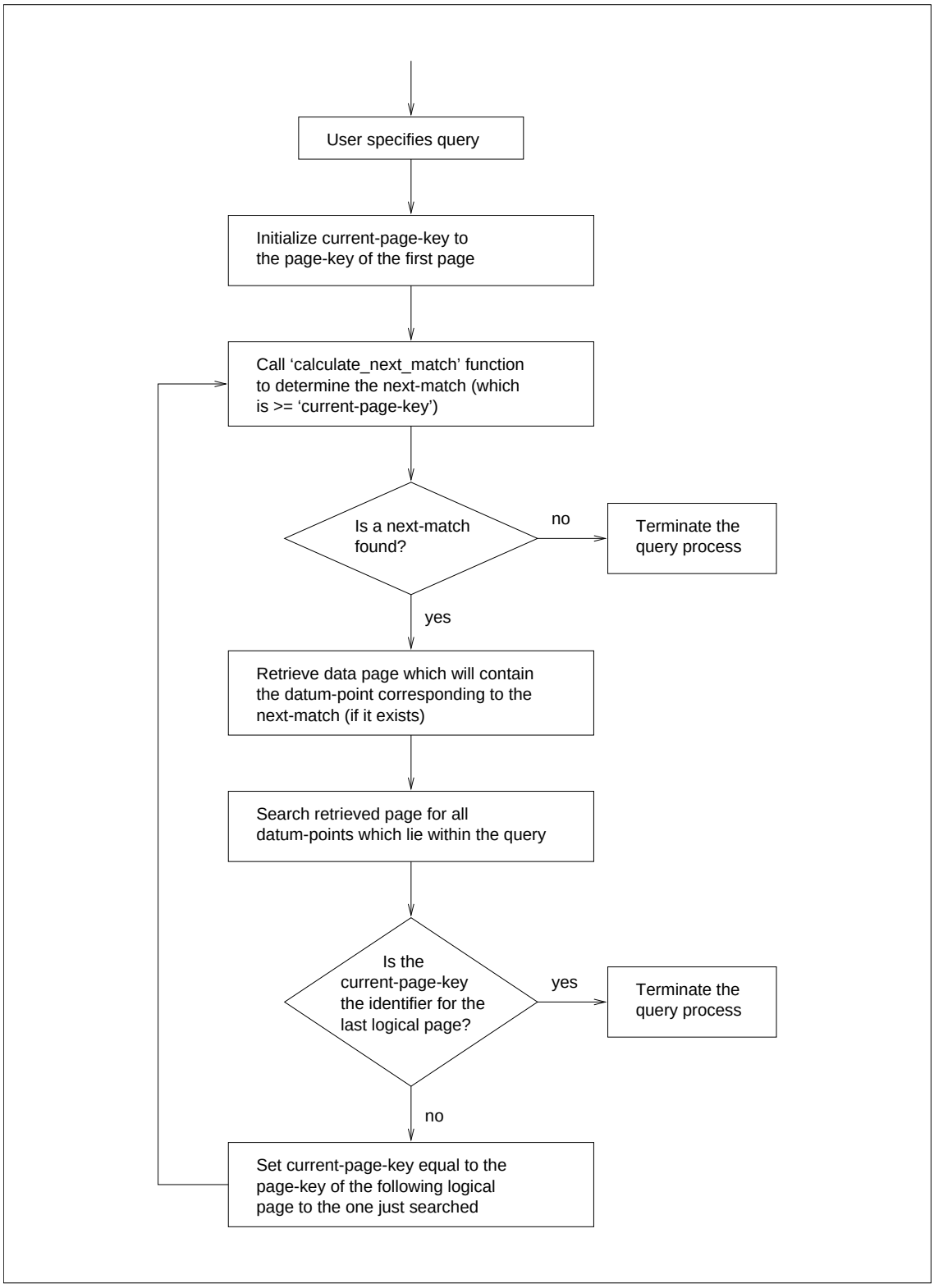

Fig. 6.2: An Algorithm for the Query Process

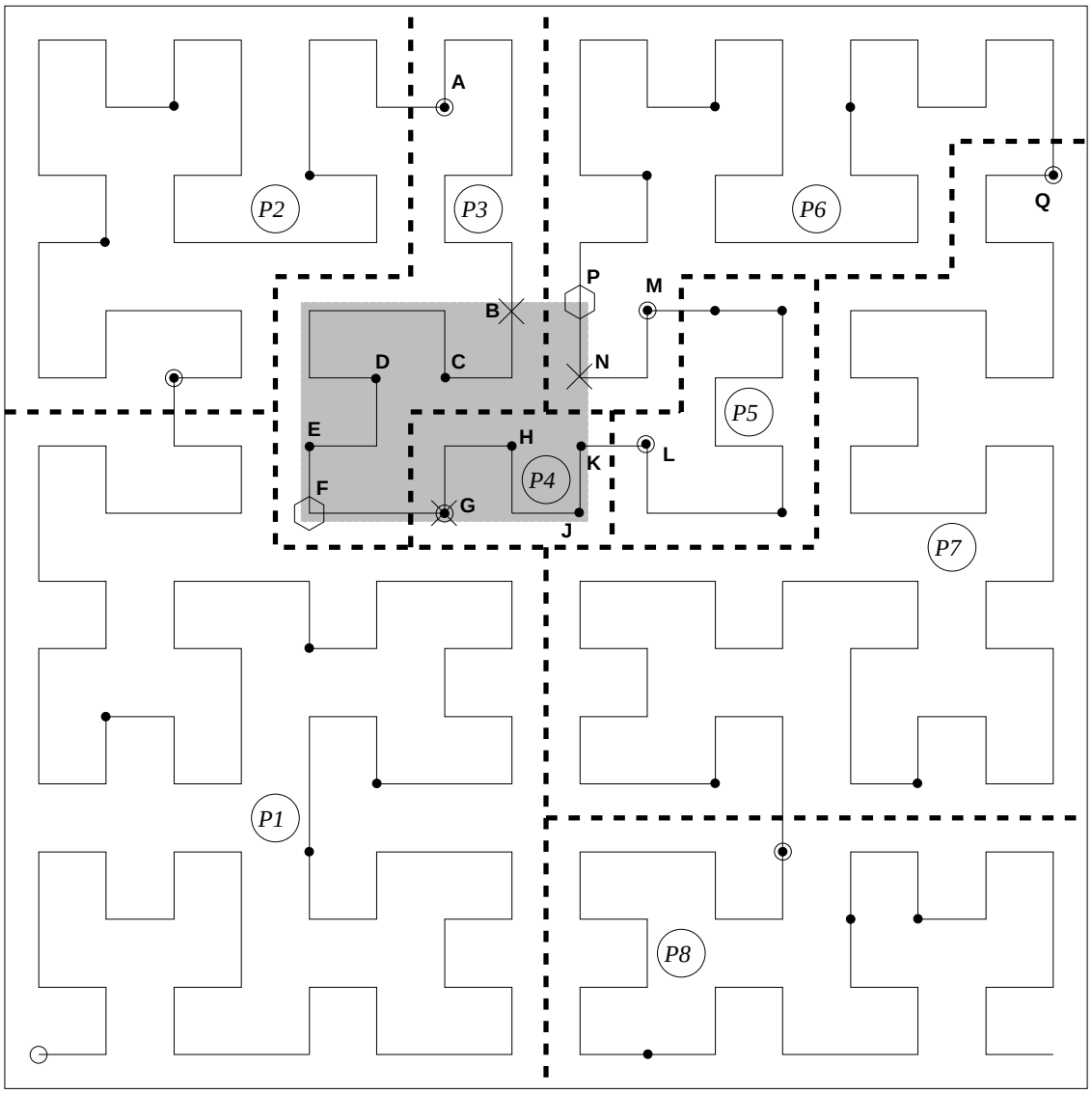

Fig. 6.3: Example of a Range Query on Points Mapped to the Hilbert Curve in 2 Dimensions

Developing algorithms and implementing them as functions to calculate the *next-match* is one of the most important contributions of our work. These *calculate_next_match* functions take as parameters the definition of the query, the *current-page-key* to which the *next-match* is required and a variable passed by reference into which the result is placed. The functions return a value *true* or *false* depending on whether a *next-match* is successfully found. In the execution of a query, the *calculate_next_match* function is always called at least twice unless the first page searched is the last logical page within the data store. The first call will always return the value *true*, having calculated the lowest possible match to a query. When the function returns the value *false* this signifies the completion of the query process.

For convenience, we make use of a number of terms which we define as follows:

Definition 6.3.2: *next-match-point : the point whose* derived-key *is the* next-match.

Definition 6.3.3: *page-key-point : the point whose* derived-key *is the* page-key.

Definition 6.3.4: *current-page-key-point : the point whose* derived-key *is the* current-page-key.

In the following two sections of this chapter, we describe methods of determining the *next-match* which is equal to or minimally greater than an arbitrary *derived-key*. We saw in our example above, however, that in our application these arbitrary *derived-keys* are always *page-keys* and that the *page-key* which is of interest at any time is defined as the *current-page-key*. Section 6.4 relates to the Hilbert curve and section 6.5 relates to the Z-order curve.

In our descriptions, we generally assume that a *current-page-key* is not the *derived-key* of a point which lies within a query region, and so is its own *next-match*, but note that the algorithms make no distinction between *current-page-keys* which relate to points within or outside of a query region.

6.4 The Hilbert Curve

In this section we focus on the Hilbert curve and detail our algorithms for calculating *next-match* values when using this curve. The algorithms can also be applied to the Gray-code curve where state diagrams are utilized.

Before describing our algorithms for the Hilbert curve, we present two examples showing how *next-matches* are calculated in the execution of a range query in 2 dimensions, building on the example of section 6.3. We utilize the state diagram of Figure 4.1 given in chapter 4.

We then describe the algorithms in detail, beginning with range queries. We present the algorithm which utilizes state diagrams and show how it can be developed for use in higher dimensions where the storage of state diagrams is not practicable. Finally, we adapt the algorithm to apply it specifically to partial match queries.

6.4.1 Introductory Examples

The examples illustrate how our search for a *next-match* is equivalent to finding the appropriate path in the descent of the tree representation of the Hilbert curve, discussed in chapter 3, from root to leaf. With each iteration of the process, we effectively search a node of the tree at a particular level in order to determine which of its children to visit during the next iteration.

The first example, given in Figure 6.4 on pages 100–102, shows how we calculate the lowest *derived-key* or first *next-match* for a set of points within the query region using an iterative process. This calculates the *next-match* to be the *derived-key* of point **B** in the example given in Figure 6.3. This example shows that sometimes it is not necessary to search nodes at all of the lower levels of the tree and thereby descent to a leaf can be accelerated.

The second example, given in Figure 6.5 on pages 103–108, shows how we calculate the *next-match* which is greater than the *derived-key* of a point lying outside of the query region and where the latter is greater than the previously calculated *next-match*. This shows how we produce the *derived-key* of point **N** when the *current-page-key* is known to be the *derived-key* of point **L** in the example given in Figure 6.3. This example shows how a search for a *next-match* can require a number of iterations which is greater than the height of the tree. This occurs when an initially chosen search path fails to lead to a *next-match* and back-tracking is required to a higher and previously visited level of the tree prior to a second descent along an alternative path.

In Figure 6.6 we show the tree representation of the Hilbert curve and the path taken through it in the execution of the second example.

The following definitions are used within the examples and our description of the querying algorithm:

Definition 6.4.1: *current-search-space : a space which is a hyper-cube in form and in which we pursue a* next-match *in a particular iteration of the querying process. In the first iteration, the* current-search-space *is the whole space and in subsequent iterations it is a sub-space which is* $1/2^n$ *of the previous iteration's* current-search-space.

Definition 6.4.2: *current-query-region : a hyper-rectangular space which is a sub-space of both the query region and the* current-search-space *in which we pursue a* next-match *in a particular iteration of the querying process. In the first iteration, the* current-query-region *is the originally specified query region and in subsequent steps it is the intersection of the* current-search-space *and the* current-query-region *of the previous iteration.*

Definition 6.4.3: *quadrant : a hyper-cubic sub-space of a* current-search-space*, all of whose dimensions are half of those of the* current-search-space*, regardless of the number of dimensions in space. All quadrants within a* current-search-space *are disjoint.*

Definition 6.4.4: *current-quadrant : the* quadrant *within the* current-search-space *to which the latter is restricted at the end of an iteration of the querying algorithm.*

As each level of the tree is visited, we examine n bits of the *current-page-key* and the *next-match* grows by n bits starting with the most significant bits at the root level. During back-tracking, the least significant known n bits of the *next-match* are removed for each level of ascension and they are subsequently recalculated once we find we are able to resume our descent.

6.4.2 Querying Algorithms

In this section we describe in detail our algorithms which we implement in the *calculate_next_match* function used in the query execution process presented above in section 6.3 to find the *next-match* which is equal to or greater than the *current-page-key*.

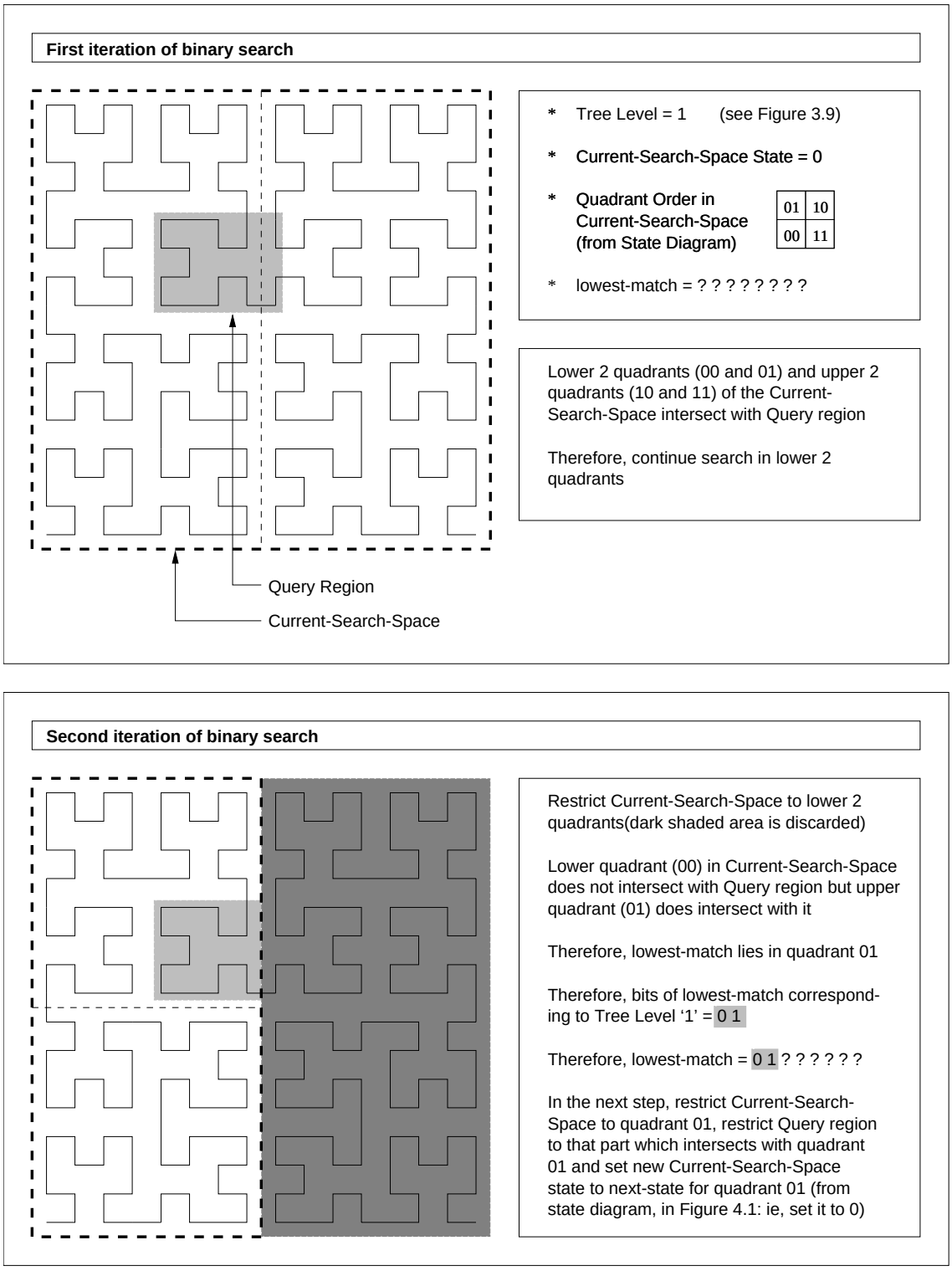

(a) Step 1 (of 3)

Fig. 6.4: Finding the *next-match* to a Range Query: Example 1

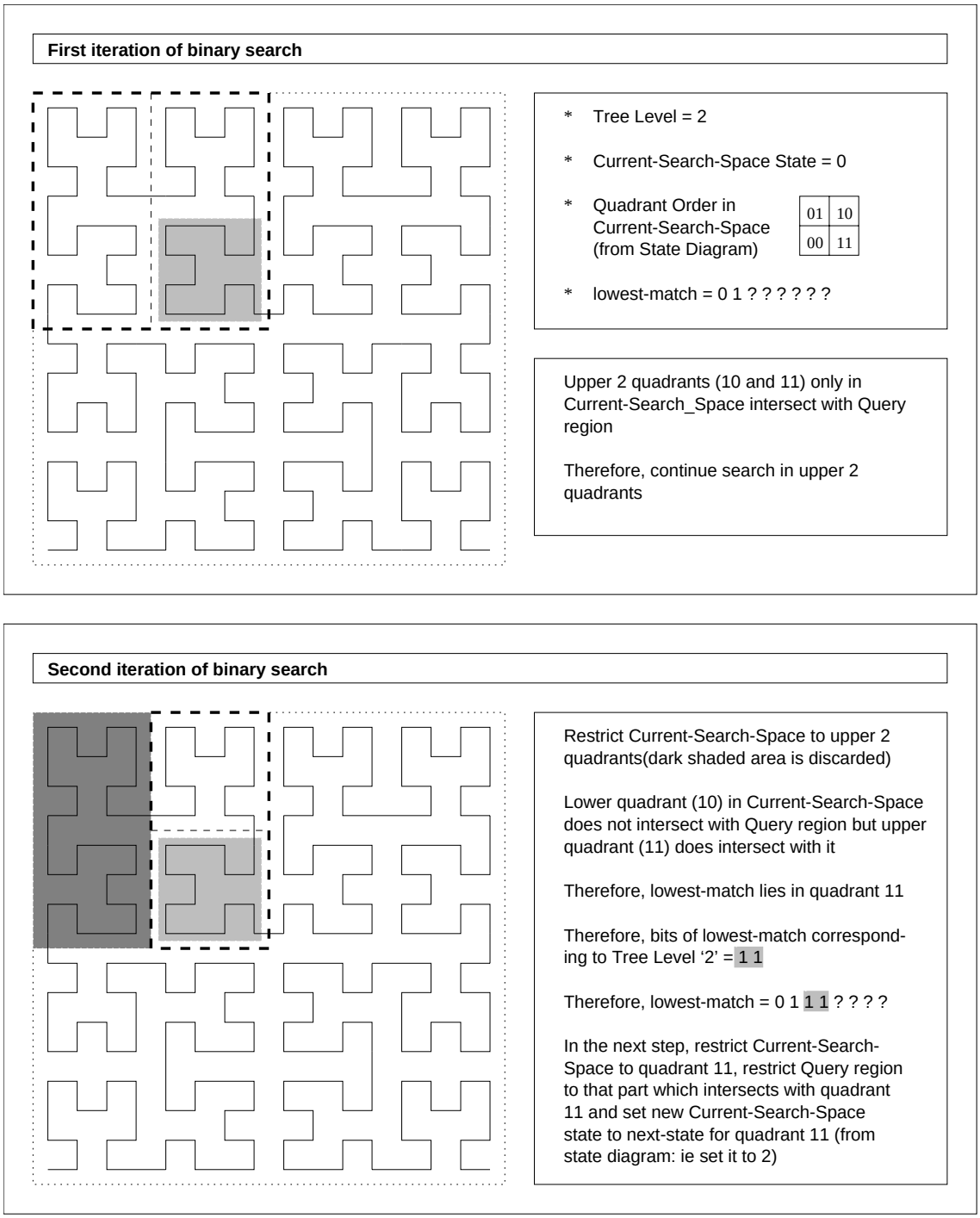

(b) Step 2 (of 3)

Fig. 6.4: Finding the *next-match* to a Range Query: Example 1 (cont'd)

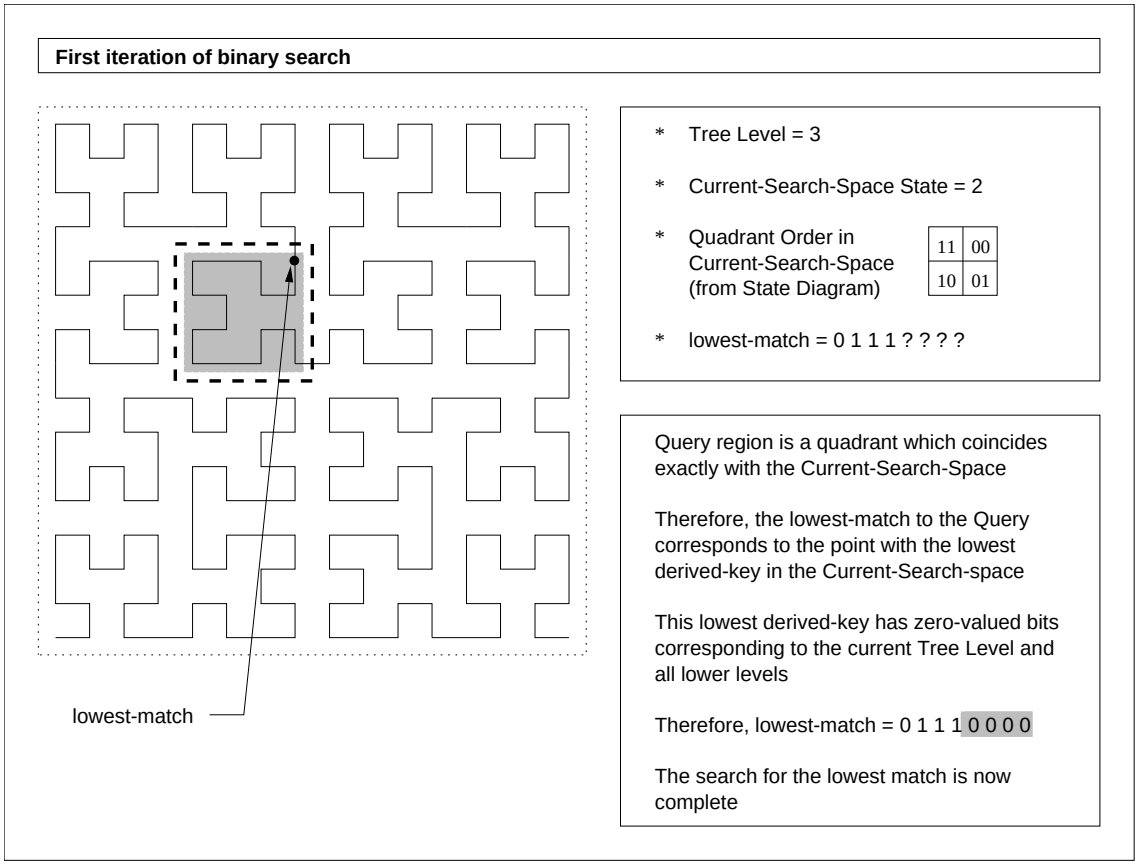

(c) Step 3 (of 3)

Fig. 6.4: Finding the *next-match* to a Range Query: Example 1 (cont'd)

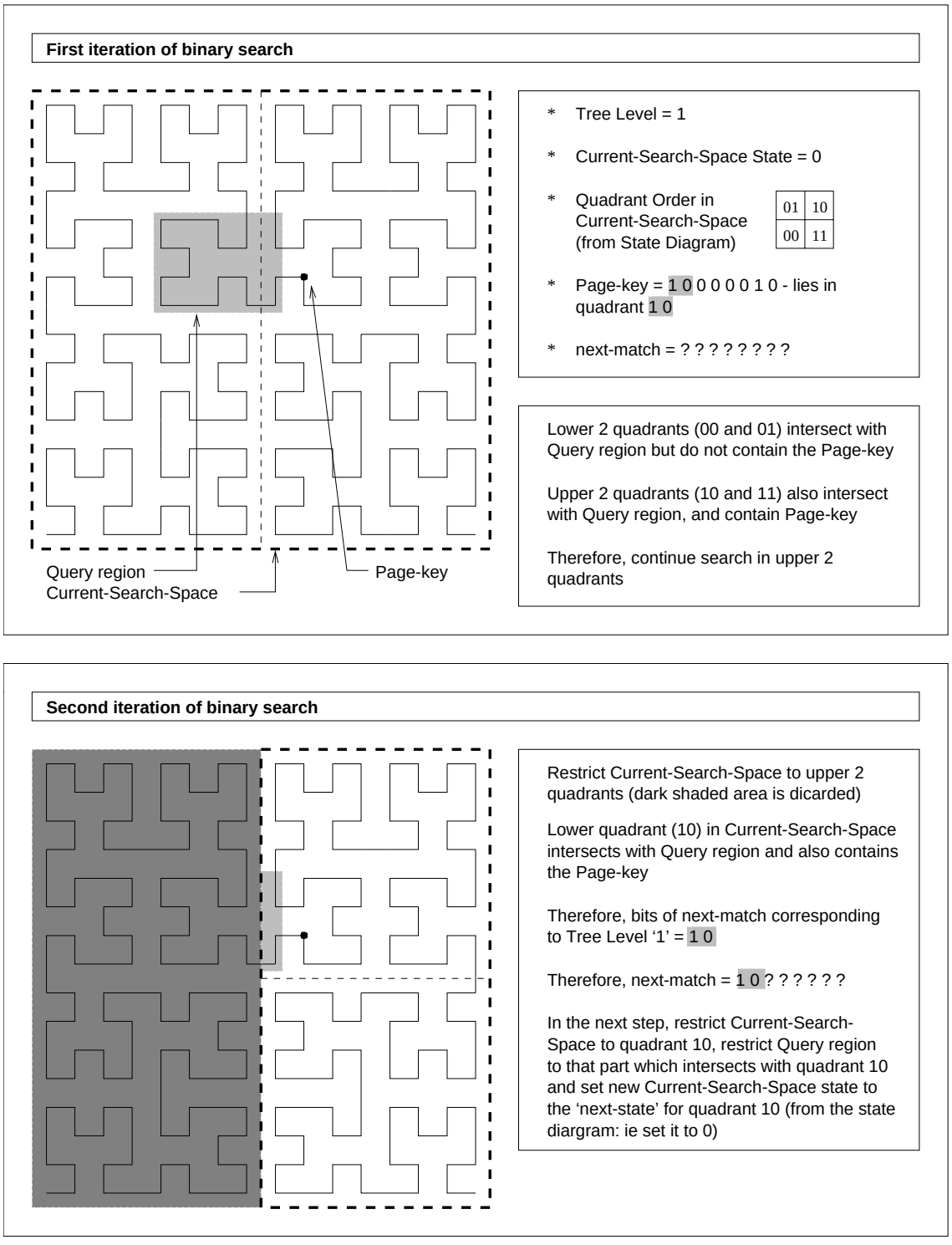

(a) Step 1 (of 6)

Fig. 6.5: Finding the *next-match* to a Range Query: Example 2

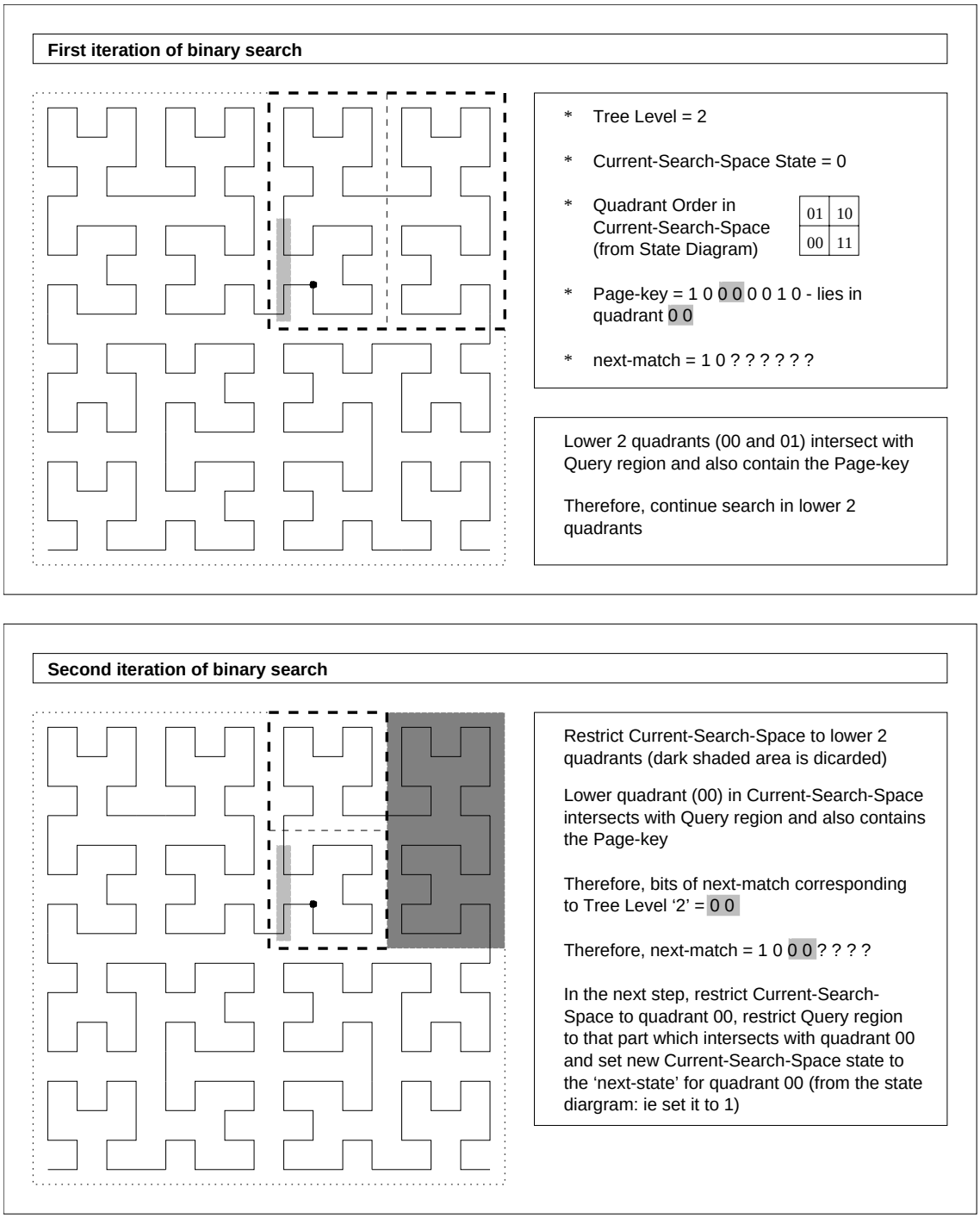

(b) Step 2 (of 6)

Fig. 6.5: Finding the *next-match* to a Range Query: Example 2 (cont'd)

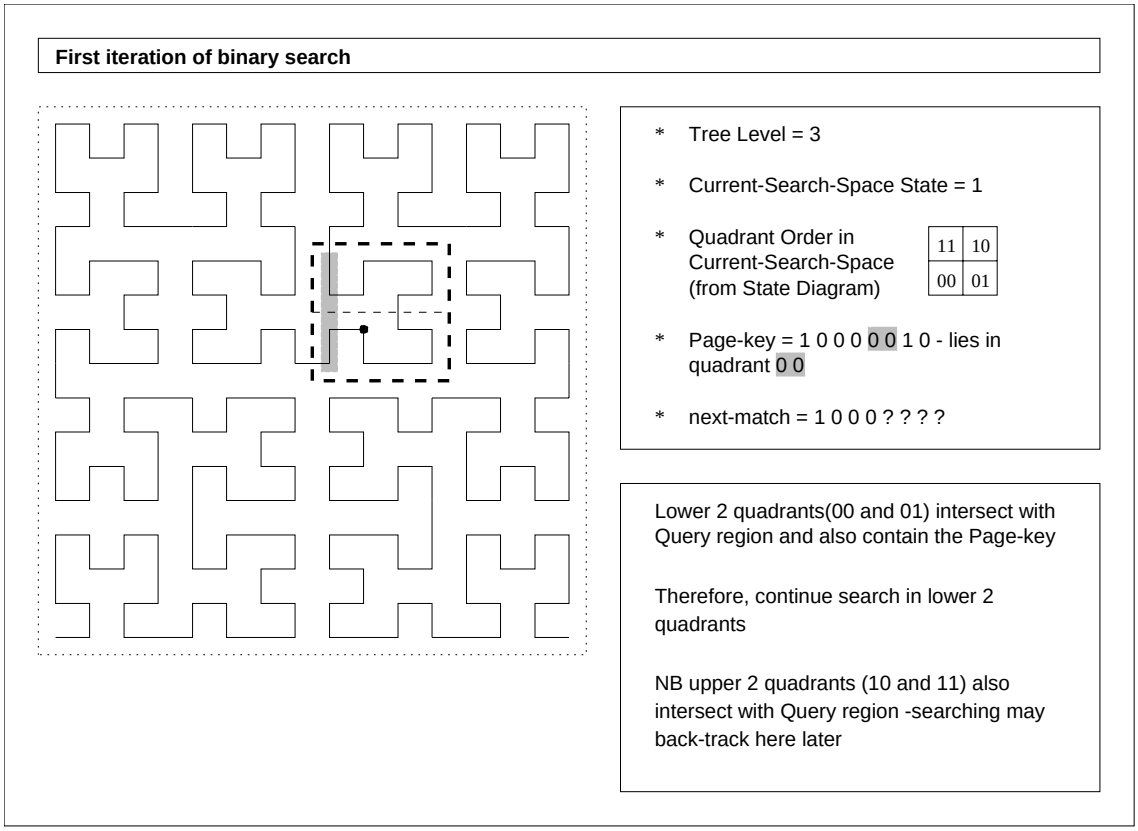

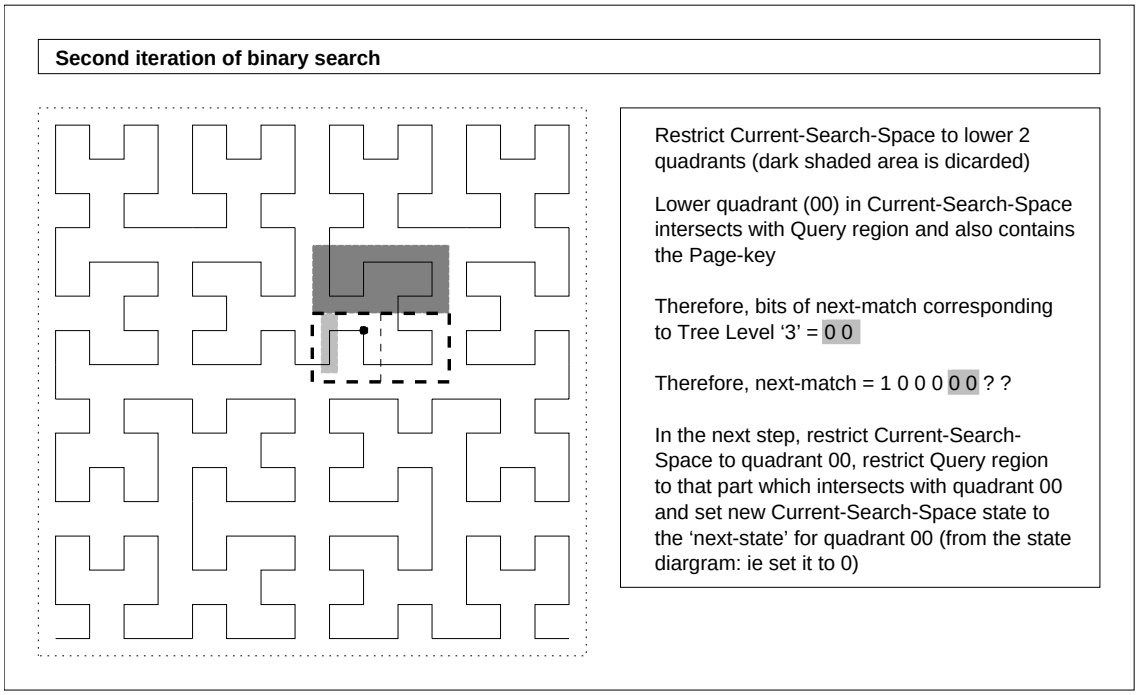

(c) Step 3 (of 6)

Fig. 6.5: Finding the *next-match* to a Range Query: Example 2 (cont'd)

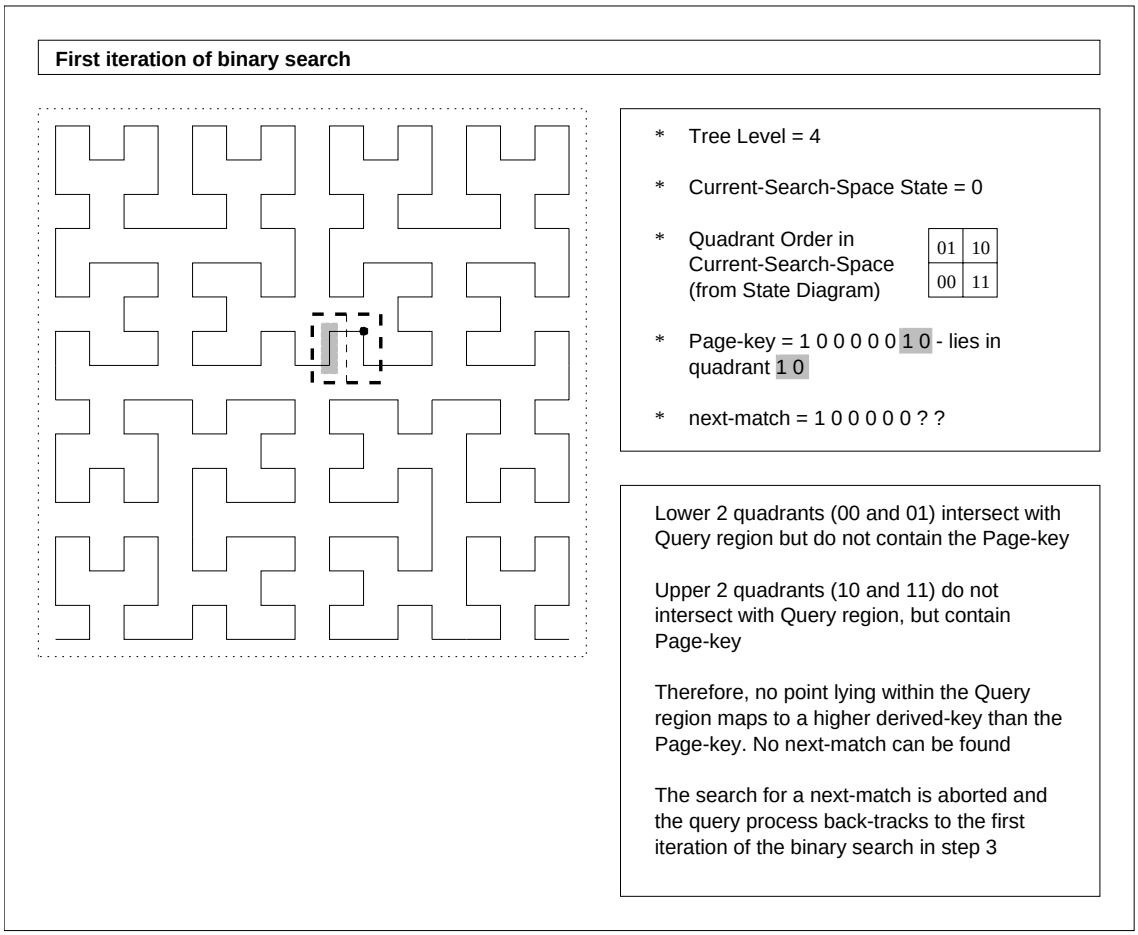

(d) Step 4 (of 6)

Fig. 6.5: Finding the *next-match* to a Range Query: Example 2 (cont'd)

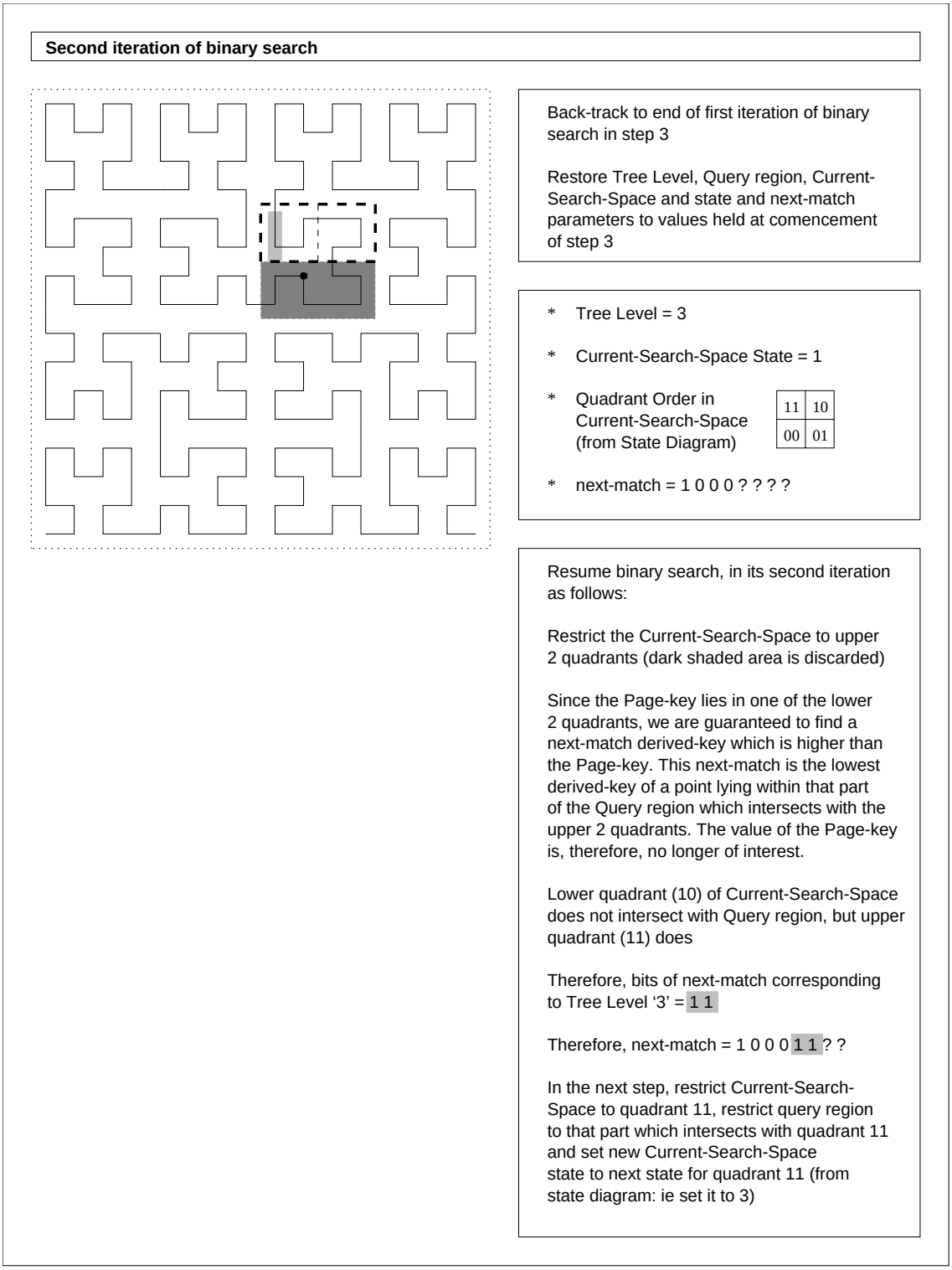

(e) Step 5 (of 6)

Fig. 6.5: Finding the *next-match* to a Range Query: Example 2 (cont'd)

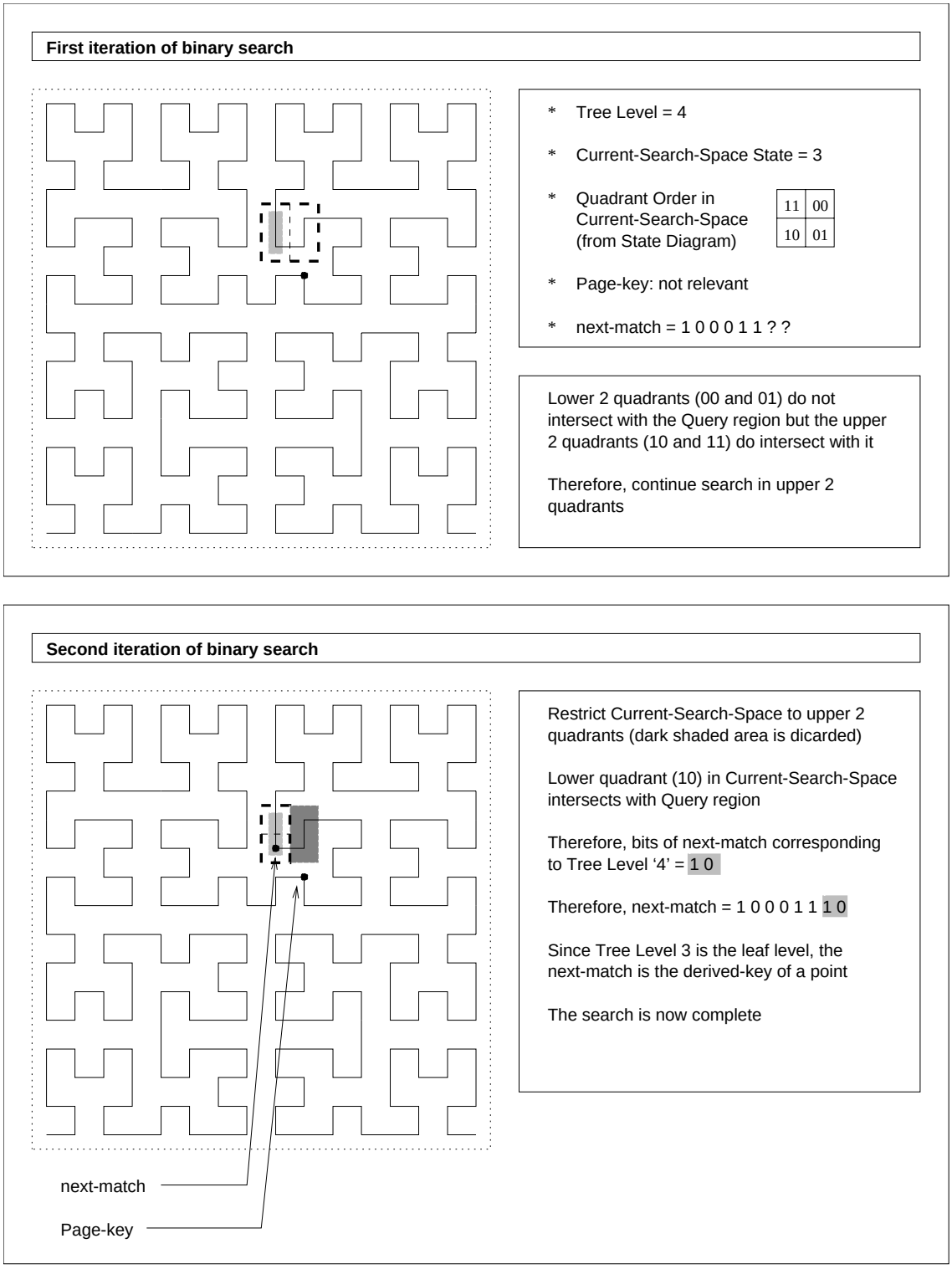

(f) Step 6 (of 6)

Fig. 6.5: Finding the *next-match* to a Range Query: Example 2 (cont'd)

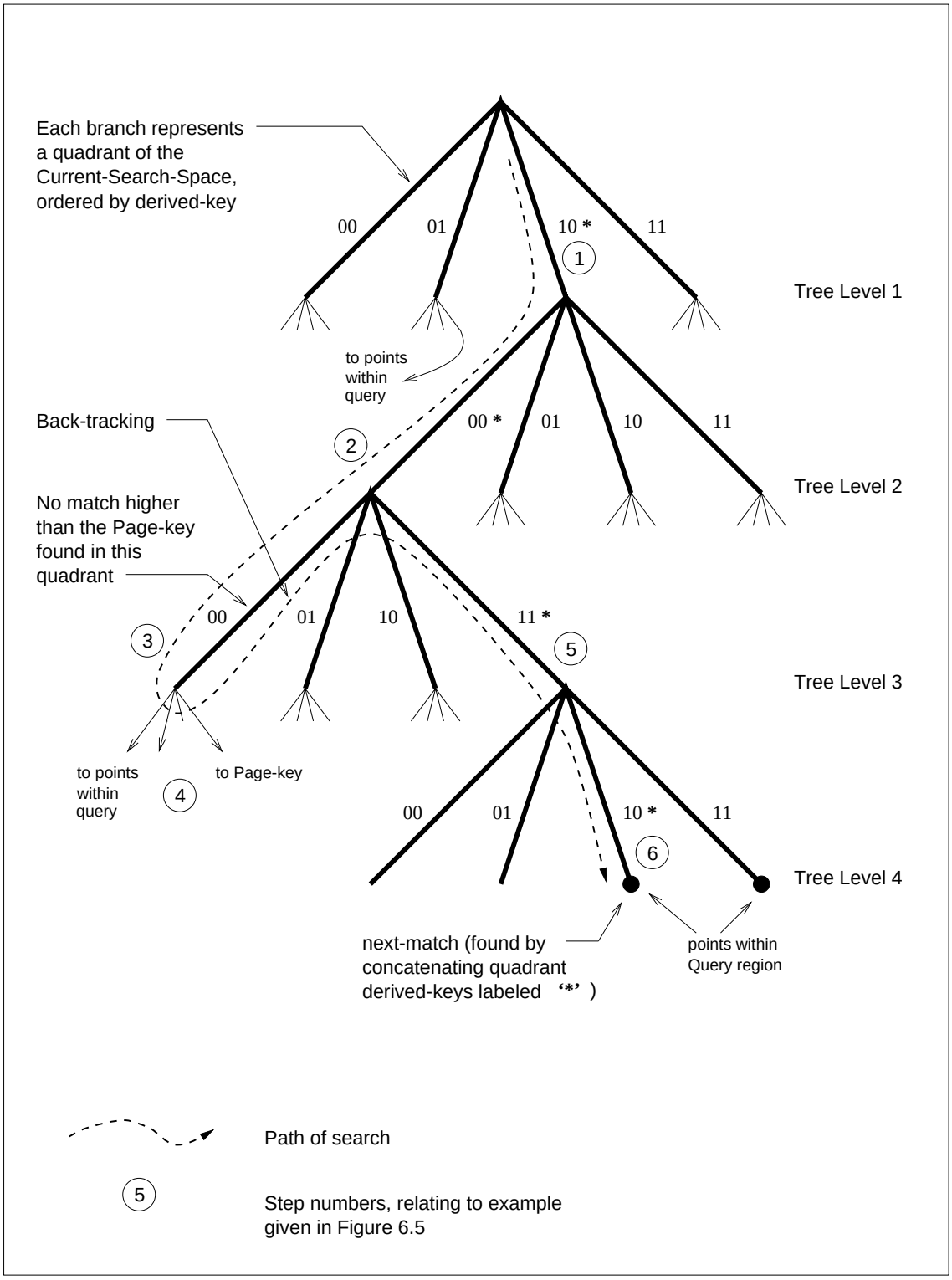

Fig. 6.6: Example: How the Tree Representation of the Hilbert Curve is Traversed in finding a *next-match*

6.4.2.1 Range Queries

6.4.2.1.1 Overview of the Algorithm

Our approach to finding a *next-match* utilizes an iterative process of partitioning of the *current-search-space*, which is initially the whole data-space. At the end of each iteration we restrict the area of space in which we search to one of the 2^n sub-spaces created by drawing n planes which bisect the *current-search-space* and to each of which one of the axes is the normal.

As seen in the examples, this approach allows us to view the data-space as a hierarchy of sub-spaces, each of which contains 2^n quadrants and this hierarchy is equivalent to the tree representation of the Hilbert curve introduced in chapter 3. The set of quadrants within a sub-space is equivalent to a node in the tree. Our search for a *next-match* is then equivalent to descending a tree from the root to a member of a leaf. Thus with each successive iteration of the algorithm, we descend the tree by one level.

During each iteration we determine the *current-quadrant* within the *current-search-space* which is the parent of the node in which to continue the search in the next iteration. This is not straightforward where a mapping to the Hilbert curve is utilized since quadrants in space may be ordered differently in different nodes. We recall that where we utilize state diagrams, a unique ordering of quadrants by their Hilbert curve *derived-keys* within a node is referred to as a *state* in a state diagram.

Once identified, a *current-quadrant* within the *current-search-space* is a quadrant which intersects with the *current-query-region* and either contains the *current-page-key-point* or, if the latter does not lie within it, contains points whose *derived-keys* are minimally greater than the *current-page-key*. In preparation for the next iteration, in addition to restricting the *current-search-space* to that part which intersects with the *current-quadrant*, we also restrict the *current-query-region* in a similar manner.

On completion of each iteration, n bits of the value of the *next-match* are, at least tentatively, identified and appended to any previously identified bits in it. These n bits are precisely the *derived-key* of the *current-quadrant*.

If, during any iteration of the algorithm, the *current-query-region* is found to coincide with the *current-search-space*, then the search can be completed immediately, without it being necessary to continue searching nodes at successively lower levels within the tree. When such a coincidence occurs, either the *current-page-key-point* also lies within the query region or else it does not. If it does lie within the query region then the *current-page-key* is itself a match and, therefore, the *next-match* to the query. Otherwise, the *next-match* is the lowest *derived-key* of any point within the *current-query-region*. The third iteration of Example 1 from section 6.4.1 given in Figure 6.4(c) illustrates the case where the *current-query-region* and *current-search-space* coincide. This enables unresolved bit values within the *next-match* to be immediately set to zero, since the *current-page-key-point* does not lie within the *current-search-space*. Thus a coincidence of the *current-query-region* and the *current-search-space* can enable the *next-match* to be determined in a number of iterations less than the height of the tree, or order of the curve.

If nodes are searched at all levels down to and including the leaf level of the tree and a *current-quadrant* is found then it contains a single point whose *derived-key* is the *next-match*.

In order to identify the *current-quadrant* which maps to the lowest suitable *derived-key* in which to restrict our search, we utilize a representation of nodes in which quadrants are ordered by their *derived-keys*. Our search of a node then takes the form of an iterative binary search of the *derived-keys* of the quadrants within a node. In each iteration of this search, what remains of the *current-search-space* (initially a whole node) is divided into two halves, each of which contains one or more quadrants. In the next iteration (of the binary search), the search is restricted to one or the other of these halves, thus one half

is discarded. The *derived-keys* of the quadrants in one half are all lower than those of the other. We call these the *lower* and *upper* halves. These terms do not relate to the locations in space of the quadrants but to their *derived-keys*.

We recall, however, that the *current-query-region* is expressed as the coordinates of the lower and upper bound points. The *derived-keys* of these points tell us little about which quadrants intersect with the region. Thus, given a set or sub-set of ordered *derived-keys* representing quadrants within a node, we need a method for determining whether the *current-query-region* intersects with the lower half or the upper half or both. This is given in Algorithm 6.4.3 and in the description of the detail of its implementation, in the next section.

Sometimes, where the *current-query-region* intersects with a sub-set of quadrants containing the *current-page-key-point*, a search for a *next-match* ultimately fails at a lower level in the tree. This occurs when no *current-quadrant* can be found in which to continue the search, as is exemplified by the fourth iteration of Example 2 from section 6.4.1 given in Figure 6.5(d).

In such cases, it will be possible to back-track and continue the search in another sub-set of quadrants if a sub-set was previously found to intersect with the *current-query-region* and it contains quadrants mapping to higher *derived-keys* than the *current-page-key*. Any such sub-set of quadrants will correspond to a search-space which is larger than the *current-search-space*. This sub-set will not correspond to the whole of a node within the tree, as was the case in Figure 6.5(e) in Example 2. As our binary searches of nodes progress, we therefore identify and record details of sub-spaces to which we can back-track, if necessary. Every such sub-space which is found is smaller than any other found previously and thus it renders them obsolete.

Back-tracking to a higher level in the tree requires the removal of n lower order bits from the, as yet incomplete, *next-match*. n bits are removed for each level of ascension.

In the absence of any sub-space having been identified to which the search may return, a requirement to back-track implies that no *next-match* to the query exists and, therefore, that the query process is complete. Conversely, an opportunity to back-track implies that a *next-match* is guaranteed to exist, whether or not this opportunity is subsequently required.

Generally, we note that while the search for a *next-match* continues, it is always tentative either until after back-tracking has taken place, if it is required, or until the *current-query-region* is found to coincide with the *current-search-space*.

If and once back-tracking to some sub-space does takes place, the search may proceed in a more straightforward manner and without regard to the value of the *current-page-key* since it will always be satisfied by the lowest *derived-key* of any point within that part of the query region which intersects with the sub-space. It is no longer necessary to identify further sub-spaces to which back-tracking may return since this process is only required at most once in any search. This is exemplified in the fifth and sixth iterations of the example given in Figures 6.5(e) and 6.5(f).

We implement the algorithm described in this section by examining the values of one bit from each coordinate of both the lower and upper bounds of the range and n bits from the *current-page-key* at each level of the tree, ie during each iteration of the algorithm, starting with the most significant bits.

We make use of the notion that if we define a point A by taking the top bit from each of the coordinates of a point B, then A approximates the position in a space of B. Alternatively, if a space is divided into quadrants then A specifies in which of these that B lies. Let us label this quadrant $quad_A$. In a similar fashion, we see that we can define a point C by taking the second from top bit from each of the coordinates of point B and it approximates the position of B within $quad_A$. This process can be repeated to a

depth equal to the number of bits which are used to represent a coordinate value. These concepts, related to points, are readily applied to ranges since they are specified by 2 points.

We recall the definition of an *n-point* from section 3.6 of chapter 3 and note that in the present context an *n-point* is a set of one-bit coordinates, which locate a quadrant within a *current-search-space*, concatenated into a single n-bit value. A mapping to a first order curve is established by ordering the *n-points* and ascribing them with their sequence numbers.

6.4.2.1.2 Algorithms which Utilize State Diagrams

In this section, we present our algorithm for the Hilbert curve which is implemented as the *calculate_next_match* function and which uses the state diagrams described in chapter 4. We follow with a commentary on how the main operations performed within it are implemented.

The algorithm contains two loops. The first is executed until one of three possible conditions arises:

1. the *current-page-key* is found to be its own *next-match*.
2. the *current-page-key* is found not to be its own *next-match* but that a *next-match* does exist.
3. it is found that a *next-match* does not exist.

The first condition arises when we find that the *current-page-key-point* lies within a *current-search-space* which is coincident with the *current-query-region*. This signifies completion of the search for a *next-match*.

The second condition arises when it is found that the *current-page-key-point* does not lie within the query region but that the latter intersects with a part of the search space whose points map to higher *derived-keys* than the *current-page-key*. This will always occur once back-tracking takes place, for example, in step 5 of the example given in Figure 6.5(e), but may also occur when it is not required.

The third condition arises when it is found that the *current-page-key-point* lies within a quadrant whose *derived-key* is greater than that of any which intersects with a *current-query-region* and that no sub-space has previously been identified to which back-tracking may return. Both the search for a *next-match* and the execution of the query now terminate, since the *current-page-key* is greater than the highest matching *derived-key*.

During execution of the first loop, successively lower sets of n bits of the *next-match* are calculated, but only tentatively, as explained in the previous section. Sub-spaces to which back-tracking may return if required are also identified during its execution.

When the second condition arises, control is passed to the second loop which behaves in a similar but simpler manner than the first loop. Its purpose is to find the lowest *derived-key* of any point within the *current-query-region* and, therefore, the value of the *current-page-key* is no longer of interest. Iteration of the second loop may terminate early without it being necessary to search nodes at all levels down to the leaf level of the tree if the *current-query-region* is coincident with the *current-search-space*.

Once the second loop has been entered, no requirement to back-track will ever arise.

The total number of iterations of both loops cannot exceed twice the order of the curve used in the mapping, and depends on whether back-tracking and/or a search of nodes at all levels down to the leaf level of the tree is required.

Binary searches of nodes or states are performed in both loops.

We break the algorithm into three parts. The first is an overview, given in Algorithm 6.4.1 on page 114. It does not include the detail of the second loop referred to above

but indicates where control is passed to it. Neither does it include the detail of the binary search of quadrants within a node. The second details the operation of the second loop and is given in Algorithm 6.4.2. The third, Algorithm 6.4.3, provides the detail of the binary search of a node containing the quadrants which make up the *current-search-space*.

We conclude this section with a commentary on the main operations performed in the algorithm, given in the order of their execution.

Step 1: (Algorithm 6.4.1, Line #8: Algorithm 6.4.2, Line #6) By visualizing space as a hierarchy, ie a tree, we locate a point within a particular quadrant of the root node by examining the top bit of each of its coordinates. Similarly, the *k-th* bits of the coordinates determine the quadrant at the *k-th* level of the tree in which the point lies. Thus at each iteration of the statement step 1 of the algorithm, we *extract* the *k-th* bits of the coordinates of the lower and upper bound points of the *current-query-region*. For both points we concatenate these n one-bit values into *n-points* for use in other steps. We refer to these values below as Q_{lower} and Q_{upper}.

Step 2: (Algorithm 6.4.1, Line #9) A similar operation is performed by the statement in step 2 except that in each iteration we extract n bits of the *current-page-key*, starting with the most significant bits when the *current-tree-level* is 1, corresponding to the root. These n bits are the *derived-key* of the quadrant within the *current-search-space* containing the *current-page-key-point*. We note that this step is not required in Algorithm 6.4.2.

Step 3: (Algorithm 6.4.1, Line #10: Algorithm 6.4.3) During each iteration of the binary search, we reduce the number of quadrants within the *current-search-space*, in which we pursue the *next-match*, by half. The quadrants are ordered under the mapping and so their *derived-keys*, in the range $[0, \ldots, 2^n - 1]$, are known by implication. Their coordinates are not known but may be found from the state diagram in which they are stored as *n-points*.

We determine whether the query intersects with the half of the sub-set of quadrants of current interest whose *derived-keys* are the lowest in the manner described below and illustrated by example in Figure 6.7.

If the *derived-keys* of a sub-set of quadrants are in the range

$$[\ lowest, \ldots, max\text{-}lower,\ \ min\text{-}higher, \ldots, highest\ ]$$

then all of the quadrants whose *derived-keys* are in the lower sub-range

$$[\ lowest, \ldots, max\text{-}lower\ ]$$

have the same value, 0 or 1, in their coordinates in one particular dimension, i. Similarly, all of the quadrants whose *derived-keys* are in the higher sub-range

$$[\ min\text{-}higher, \ldots, highest\ ]$$

have the opposite coordinate value, 1 or 0, in the same dimension, i. This characteristic does not apply in any other dimension.

We recall that quadrants whose *derived-keys* are consecutive are adjacent in space. Thus an *n-point* which contains a single non-zero bit corresponding to the dimension, i, which divides this range into two is evaluated by

$$partitioning\_dimension \Leftarrow \text{d\_to\_c}\,(max\text{-}lower) \oplus \text{d\_to\_c}\,(min\text{-}higher)^{1} \qquad (6.1)$$

[1] Refer to appendix A for a key to symbols.

Algorithm 6.4.1 Finding a Range Query *next-match* using State Diagrams

1: *current-search-space* $\Leftarrow$ the whole space
2: *current-query-region* $\Leftarrow$ the whole specified query region
3: *next-match* $\Leftarrow 0$
4: *current-state* $\Leftarrow$ state 0
5: *page-key* $\Leftarrow$ the *current-page-key* of the query process
6: *current-tree-level* $\Leftarrow$ the root of the tree, ie level 1
7: **while** the *current-tree-level* is higher than or equal to the leaf level **do**
8: find in which quadrants of the *current-search-space* the lower and upper bounds of the *current-query-region* lie
9: $H \Leftarrow n$ bits taken from the *page-key* corresponding to the *current-tree-level*
{this is effectively the *derived-key* of the quadrant of the *current-search-space* in which the *page-key-point* lies}
10: perform a binary search, given in Algorithm 6.4.3, of the *derived-keys* of the quadrants within the *current-search-space* to find, if it exists, the *current-quadrant*, which intersects with the *current-query-region* and whose *derived-key* is a minimum (which must be $\geq H$)
{Note that if back-tracking takes place during the binary search, the values of *current-query-region*, *next-match*, *current-state* and *current-tree-level* are restored to values held in previous iterations of the loop in this algorithm.}
11: **if** the binary search failed to identify a *current-quadrant* **then**
12: return FALSE {the query execution is now complete}
13: **end if**
14: **if** *current-tree-level* $\neq$ the leaf level **then**
15: *current-query-region* $\Leftarrow$ *current-query-region* $\cap$ *current-quadrant*
16: *current-search-space* $\Leftarrow$ *current-quadrant*
17: **end if**
18: **if** $H =$ the *derived-key* of the *current-quadrant* **and** *current-query-region* $=$ *current-quadrant* **then**
19: *next-match* $\Leftarrow$ *page-key*
20: return TRUE
{The *page-key* lies within the originally specified query and is its own *next-match*. The *next-match* has therefore been identified}
21: **end if**
22: *next-match* $\Leftarrow$ *next-match* + ((the *derived-key* of the *current-quadrant*) $\ll$ (n(tree-height $-$ *current-tree-level*)))
{append the *derived-key* of the *current-quadrant* to the *next-match*}
23: *current-state* $\Leftarrow$ the *next-state* corresponding to the *derived-key* of the *current-quadrant* in the state diagram for the *current-state*
24: *current-tree-level* $\Leftarrow$ *current-tree-level* $+1$
25: **if** $H <$ the *derived-key* of the *current-quadrant* **then**
26: break out of the loop and go to the second loop, given in Algorithm 6.4.2
27: **else**
28: continue with the next iteration of the current loop
29: **end if**
30: **end while**
31: execute second loop, given in Algorithm 6.4.2

Algorithm 6.4.2 Second Loop Referred to in Algorithm 6.4.1

{On entry to this loop, the *current-query-region* has been restricted to a quadrant in which the *derived-keys* of all of the points contained within it are greater than the *page-key* and so a *next-match* exists. All that remains to be done is to identify the lowest of these *derived-keys*. The bit values within the *next-match* which correspond to higher levels in the tree than the *current-tree-level* have already been placed in it during successive executions of the statement on line 22 above}

1: **while** the *current-tree-level* is higher than or equal to the leaf level **do**
2: **if** the *current-query-region* = *current-quadrant* **then**
3: all bit values within the *next-match* which correspond to the *current-tree-level* and all lower levels $\Leftarrow 0$
4: return TRUE
{The *next-match* has been identified}
5: **end if**
6: find in which quadrants of the *current-search-space* the lower and upper bounds of the *current-query-region* lie
7: perform a binary search of the *derived-keys* of the quadrants within the *current-search-space* to determine the *current-quadrant* which intersects with the *current-query-region* and whose *derived-key* is a minimum.
{this operation is simpler than the binary search performed in Algorithm 6.4.3 since we need not have any regard to the value of the *page-key* nor concern ourselves with identifying sub-spaces to back up}
8: **if** *current-tree-level* $\neq$ the leaf level **then**
9: *current-query-region* $\Leftarrow$ *current-query-region* $\cap$ *current-quadrant*
10: *current-search-space* $\Leftarrow$ *current-quadrant*
11: **end if**
12: *next-match* $\Leftarrow$ *next-match* + ((the *derived-key* of the *current-quadrant*) $\ll$ (n(tree-height $-$ *current-tree-level*)))
{append the *derived-key* of the *current-quadrant* to the *next-match*}
13: *current-state* $\Leftarrow$ the *next-state* corresponding to the *derived-key* of the *current-quadrant* in the state diagram for the *current-state*
14: *current-tree-level* $\Leftarrow$ *current-tree-level* +1
15: **end while**
16: return TRUE

Algorithm 6.4.3 Binary Search of the *current-search-space* using State Diagrams

1: carry out each iteration of the binary search on the quadrants within the *current-search-space* as follows:
2: **if** the *current-query-region* intersects with quadrants in the lower half (ie quadrants whose *derived-keys* are lower than those of the upper half) **and** the maximum *derived-key* of any quadrant in the lower half is equal to or greater than H (ie the *page-key-point* lies in one of the quadrants of the lower half) **then**
3: **if** the *current-query-region* also intersects with quadrants in the upper half **then**
4: make a *'back-up'*, ie a record, of the current values of variables which may be restored later if back-tracking is required: these are *current-query-region*, *next-match*, *current-state*, *current-tree-level* and the *derived-keys* of the quadrants which define the bounds of the upper half of the quadrants of interest in the current iteration of the binary search
{Any back-up made in this manner replaces the previously made back-up, if it exists, whether it was made during the current iteration of the loop in Algorithm 6.4.1 or an earlier one. The search space will also be smaller than any previously stored}
5: **end if**
6: continue the binary search in the lower half
7: **else**
8: **if** the *current-query-region* intersects with the upper half **then**
9: continue the binary search in the upper half
{Note that H may or may not correspond to a quadrant in the upper half but this is of no concern at this point}
10: **else**
11: **if** no back-up exists **then**
12: return FALSE
{no *next-match* exists and the query process terminates}
13: **else**
14: restore the values of working variables to those recorded in the back-up
15: continue the binary search in the restored search space
16: **end if**
17: **end if**
18: **end if**

where *d_to_c* is a function which takes the *derived-key* of a quadrant as its parameter and returns its coordinates expressed as an *n-point* by looking up its value in the state diagram. The variable *partitioning_dimension* corresponds to the value labelled 'j' in Figure 6.7.

It now remains to be found whether the quadrants whose *derived-keys* are in the lower sub-range all have the value 0 or 1 in dimension i. This is done by testing the value of the expression

$$\text{d\_to\_c}\,(\textit{max-lower}) \wedge \textit{partitioning\_dimension} \tag{6.2}$$

If it evaluates to non-zero, then these quadrants all have the value 1 in dimension i, otherwise they have the value 0. This expression is referred to as '$a \wedge j$' in the examples shown in Figure 6.7 on page 118.

Finally, we recall that the *current-query-region* is always restricted to the intersection of the originally specified query and the *current-search-space*. Thus, for it to intersect with the quadrants whose *derived-keys* are in the lower sub-range, either or both of the lower and upper bounds of the *current-query-region* must have the same value in its coordinate for dimension i as these quadrants.

We determine whether the *current-query-region* intersects with the half of the sub-set of quadrants of current interest whose *derived-keys* are in the higher sub-range in a similar manner to that described above.

Once the binary search has been completed, the *derived-key* of a single quadrant, called the *current-quadrant*, is identified. This, at least tentatively, contains the *next-match* and so the *current-search-space* is restricted to it prior to the next iteration of the algorithm. This is described below in 'step 4'.

An alternative approach to performing a binary search as described above would be to determine the set of all of the quadrants of the *current-search-space* which intersect with the *current-query-region* and restrict our search to the one whose *derived-key* is equal to or minimally greater than that within which lies the *current-page-key-point*. In practice this would be significantly more computationally expensive, especially in higher-dimensional space in which a *current-query-region* may intersect with many thousands of quadrants.

Step 4: (Algorithm 6.4.1, Lines #14–17: Algorithm 6.4.2, Lines #8–11) Once the coordinates, expressed as an *n-point*, of a quadrant have been identified in which to pursue the search in the next iteration of the algorithm, restricting the *current-query-region* is achieved by comparing this *n-point* with the values of Q_{lower} and Q_{upper} found in step 1.

Coordinates of the *current-query-region's* lower bound are set to zero in dimensions corresponding to bits which are set to 1 following an EXCLUSIVE-OR operation between the quadrant's *n-point* and Q_{lower}. Bits in upper bounds coordinates are all set to to 1 following a similar EXCLUSIVE-OR operation between the *n-point* and Q_{upper}.

Adjusting the coordinates of the *current-query-region's* bounds in this simple manner *corrupts* bit values corresponding to higher levels than the *current-tree-level*. This is not important since their original values will have been processed in previous iterations of the algorithm.

Step 5: (Algorithm 6.4.1, Lines #18–21) In order to determine whether the *current-query-region* coincides with the *current-search-space*, we maintain two n-bit variables, one for each of the query bounds. Whenever a query coordinate is adjusted in step 4, a corresponding bit is set to 1 in one of these variables. When all of the bits in both of these variables have been set to 1, this signifies that the *current-query-region* coincides with the *current-search-space*. This enables us to curtail descent of the tree since the *current-page-key-point* must lie within the query region and so the *current-page-key* must be its own *next-match*.

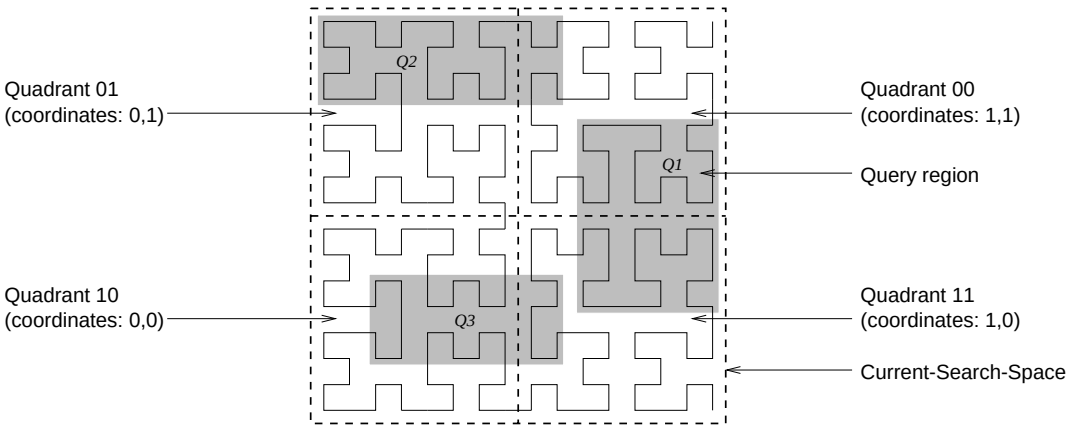

Quadrant coordinates of example Query regions

Query	Lower bound	Upper bound
Q1	1, 0	1, 1
Q2	0, 1	1, 1
Q3	0, 0	1, 0

Quadrants within the Current-Search-Space

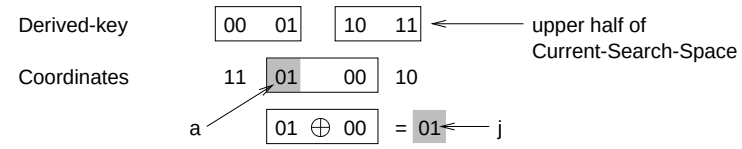

'j' contains one non-zero bit only, regardless of the number of dimensions in a space. It indicates that quadrants in lower half of Current-Search-Space all differ from quadrants in upper half in the Y-dimension, in this example.

The operation: a $\wedge$ j = 01 therefore indicates that quadrants in the lower half of the Current-Search-Space have coordinate values in the Y-dimension of 1 (thus quadrants in upper half have coordinate values in the Y-dimension of 0)

Q1: upper bound coordinates in Y-dimension = 1, therefore Query region intersects with quadrants in the lower half of the Curreent-Search-Space

Q2: lower AND upper bound coordinates in Y-dimension = 1, therefore Query region intersects with quadrants in the lower half of the Current-Search-Space

Q3: lower AND upper bound coordinates in Y-dimension = 0, therefore Query region does not intersect with quadrants in the lower half of the Current-Search-Space

Fig. 6.7: Examples: how to determine which sub-spaces intersect with a query region

Similarly, in lines 2–5 of Algorithm 6.4.2, coincidence of the *current-query-region* and the *current-search-space* enables us to avoid further searching of nodes in the tree since the *next-match* must be the lowest *derived-key* within the *current-search-space*. All unresolved lower bits within the *next-match* can immediately be set to zero.

6.4.2.1.3 Application Of The Algorithms In Higher Dimensions

The range query algorithm described in the previous section can be applied where mapping to the Hilbert curve is performed by calculation, for example, based on the technique proposed but Butz and developed in chapter 4. This enables the algorithm to be applied where the number of dimensions in space exceed the upper limit imposed by main memory requirements of state diagrams.

We recall that Butz' method of mapping from *derived-keys* to coordinates also entails an iterative descent of the tree representation of the Hilbert curve. In each iteration, n bits of the *derived-key* are taken and transformed into the coordinates of a quadrant or, at the leaf level, a point.

Three critical variables are required in this process. These variables are referred to as J, $\tilde{\tau}$ and ω in appendix B where Butz' mapping technique is reproduced. They encapsulate the characteristics of the current state and so enable the order of any quadrant within a node, or state, to be determined. On commencement of the *calculate_next_match* algorithm, these variables are all initialized to zero and they are updated during each iteration for use in the next iteration.

Several calculations are performed during each iteration of the *calculate_next_match* function which implements this algorithm and these are described below.

In 'step 3' of the commentary in section 6.4.2.1.2, we saw that the coordinates of two quadrants are required in each iteration of the binary search. The *derived-keys* of these quadrants were referred to as *max-lower* and *min-higher*. Their coordinates, expressed as *n-points* enable us to determine which dimension partitions a set of (ordered) quadrants, whose *derived-keys* only are known, into two halves. This was referred to as the *partitioning_dimension* in equation (6.1). In practice, however, we are able to find the *partitioning_dimension* without having to perform complete mappings to both of these *n-points*.

In accordance with Table B.8 in appendix B, it is first necessary to calculate σ values for each of the quadrants *max-lower* and *min-higher*. We refer to these as L_σ and H_σ and recall from chapter 5 that their calculation may be effected more simply than in the manner described by Butz [But71], as

$$L\_\sigma \Leftarrow \textit{max-lower} \oplus (\textit{max-lower}/2)$$

$$H\_\sigma \Leftarrow \textit{min-higher} \oplus (\textit{min-higher}/2)$$

From these two values, corresponding $\tilde{\sigma}$ values are found by performing right circular shifts to produce $L\_\tilde{\sigma}$ and $H\_\tilde{\sigma}$.

Instead of completing the mappings from *max-lower* and *min-higher* to their *n-points* (coordinates) and finding the *partitioning_dimension* in the combined operation:

$$(L\_\tilde{\sigma} \oplus \omega \oplus \tilde{\tau}) \oplus (H\_\tilde{\sigma} \oplus \omega \oplus \tilde{\tau})$$

we need only perform the calculation

$$L\_\tilde{\sigma} \oplus H\_\tilde{\sigma}$$

This simplification is possible since the EXCLUSIVE-OR operation is both commutative and associative and since $a \oplus a = 0$ and $a \oplus 0 = a$. Nevertheless, the coordinates of

max-lower need to be calculated in order to carry out the computation given previously in equation (6.2) on page 117.

Once the binary search has been completed, the *derived-key* of the *current-quadrant* is identified. The coordinates of this quadrant are required in order to restrict the *current-search-space* for the next iteration of the algorithm. There is a 50% probability that the *derived-key* of the *current-quadrant* is the same as *max-lower* from the final iteration of the binary search and so its coordinates will already have been calculated. At any rate, the σ and $\tilde{\sigma}$ of the *current-quadrant* will already have been calculated.

The three critical variables, J, $\tilde{\tau}$ and ω, must also be updated at the end of each iteration of the querying algorithm for use in the next. Their new values depend on the combination of their current values and the *derived-key* of the *current-quadrant* identified at the end of a binary search. The critical variables, once updated in the manner described by Butz in Table B.8, encapsulate the characteristics of the *next-state* corresponding to the *derived-key* of the *current-quadrant* in the current state.

6.4.2.2 Partial Match Queries

The algorithm described in section 6.4.2.1 can be applied to partial match queries where these are expressed as ranges. Alternatively, minor modifications can be made to suit partial match queries and they result in a small improvement in efficiency although no change to the overall complexity of the algorithm. In this section we summarize these modifications and note that they apply regardless of how mappings to the Hilbert curve are performed.

Steps 4 and 5 of Algorithm 6.4.1, described in section 6.4.2.1.2, can both be omitted, since they serve no useful purpose in the execution of partial match queries. In these steps, the *current-query-region* is restricted to the *current-search-space* and a possible coincidence of these 2 spaces is tested for.

The purpose of restricting the *current-query-region* to the *current-search-space* in range queries is to avoid the need, where possible, to search nodes in the tree representation of the curve as far as the leaf level. This can be achieved where these 2 spaces coincide. In the case of partial match queries, the *current-query-region* can never be restricted in dimensions where values are specified in the query, since lower and upper bound coordinate values are always identical. The query region could only ever be restricted in 'unspecified' dimensions. In contrast to some range queries, a partial match query always defines a space which contains no points which are internal, as distinct from lying of the surface of the query region. Thus the *current-query-region* coincides with the *current-search-space* only when these spaces contain a single point. This condition does not arise until descent of the tree has progressed to the leaf level.

In order to restrict the *current-query-region* to the *current-search-space*, the coordinates of the latter are required to be determined during execution of the algorithm. Where no restriction takes place, these coordinates are no longer needed. The saving in work carried out in omitting this operation is more significant where mapping to the Hilbert curve is performed by calculation rather than with the aid of a state diagram.

Whereas a range query is specified by two points, being the lower and upper bounds, a partial match query can be expressed more succinctly as a single point in which unspecified coordinates are assigned the value zero. This simplifies step 1 of the algorithm given in section 6.4.2.1.2. A supplementary n-bit variable is required in which bits corresponding to specified dimensions are set to 1. This is initialized at the outset of the execution of a query. These modifications require alterations in the detail of how it is determined whether the query region intersects with one half or the other of a set or sub-set of quadrants, but this is of no consequence.

6.5 The Z-order Curve

Certain characteristics of the Z-order curve, which are not present in the Hilbert curve, enable us to develop a radically different approach to implementing the *calculate_next_match* function for use with the Z-order curve. This relies on manipulating bit values within the *current-page-key* in order to transform it into its *next-match*, instead of successively partitioning space. Describing algorithms which achieve this for range queries and partial match queries is the main purpose of this section.

Our algorithms exploit the direct relationship, seen in chapter 3, between the values of the coordinates of a point and the values of bits within its Z-order *derived-key*. The result of this relationship is that the values of particular bits within a Z-order *derived-key* are independent of the values of higher bits. More specifically, we exploit the fact that a change in magnitude in a coordinate value in one direction always causes a change in its *derived-key* in the same direction. This does not apply to the Hilbert curve.

In addition to presenting new bit manipulation algorithms, we modify the algorithms described in the previous section to suit the Z-order curve specifically, since there is scope to simplify them for it. This enables a comparison of the tree descent and bit manipulation approaches for the Z-order curve but this is left as a topic for further work.

6.5.1 Bit Manipulation Querying Algorithms

6.5.1.1 Lowest and Highest Matches

The lowest, ie first, match to a Z-order range query is specifically the *derived-key* of the lower bound point, thus it can be found simply by using the function which maps points to *derived-keys*.

This observation is proven by showing that no point P within a query range can map to a *derived-key* which is less than that of the lower bound point L. Any such point P, if it exists, will contain a higher value than L in at least one coordinate. We consider the case where there is a difference in one coordinate j only; that is, where coordinate $P_j > L_j$. The highest bit B in which these values differ will therefore be set to 1 in P_j and 0 in L_j.

We saw in chapter 3, section 3.7.1, that the value of each bit in each coordinate of a point determines a particular bit in its *derived-key* and that higher bits in a coordinate determine higher bits in the *derived-key* than do lower bits in the same coordinate. It therefore follows that the *derived-key* of P will be higher than the *derived-key* of L since they will contain the same values in bits determined by bits higher than B in coordinate j and the bits determined by bit B will be set to 1 in the former *derived-key* and 0 in the latter.

In a similar manner, we can see that the maximum *derived-key* of any point within a query range is that of the upper bound point which defines it.

In the case of partial match queries, the lowest match is the *derived-key* of the point whose coordinates in unspecified dimensions are set to zero. Similarly, the highest match is the *derived-key* of the point whose coordinates in unspecified dimensions are set to the maximum possible coordinate value.

That a similar relationship between the *derived-keys* of the bounds to a range query and the lowest and highest matches does not apply to the Hilbert curve is immediately apparent from the example shown in Figure 6.4.

6.5.1.2 Range Queries

If the *current-page-key-point* lies outside of the query range then it follows that one or both of two possible conditions exists. These are that at least one of its coordinates is greater than the corresponding coordinate of the range upper bound, and that at least one

of its coordinates is less than the corresponding coordinate of the range lower bound. Our algorithm, given in Algorithm 6.5.1, therefore examines the values of the coordinates of the *current-page-key-point* and determines what changes must be made in order to bring it within the query range while *moving* it along the curve by a minimal amount.

A coordinate of a *current-page-key-point* which has a greater value than the corresponding coordinate in the query upper bound must be reduced in value. At the least, this implies that the highest non-zero valued bit in the point's coordinate which corresponds to a zero valued bit in the range upper bound's coordinate must be inverted to 0. We label the position occupied by this bit within a *derived-key* the *'Z-bit'*.

On its own, setting the *Z-bit* to 0 would clearly reduce the value of the *current-page-key* rather than increase it and so it is necessary to compensate, in part, by changing a higher bit corresponding to a different coordinate from 0 to 1. In order to minimally increment the *current-page-key*, however, we must change the lowest such bit possible.

A coordinate of a *current-page-key-point* which is less than the corresponding coordinate in the query lower bound can be dealt with more simply and must be increased in value. At the least, this implies that the highest zero valued bit in the point's coordinate which corresponds to a non-zero valued bit in the range lower bound's coordinate must be inverted to 1. We do not, however, need concern ourselves with the values of higher bits on account of this change.

Changing a bit within the *current-page-key* from 0 to 1 requires us, where possible, to reduce the value of that part of it which is defined by lower bits, again to ensure that the *next-match* is a minimum. We must, however, avoid producing a *derived-key* which corresponds to a point containing any coordinates whose values are less than those of corresponding coordinates within the query range lower bound.

In order to minimize the amount of work carried out, the algorithm begins by comparing all of the coordinates of the *current-page-key-point* with those of the lower and upper bounds of the query range in order to determine the *highest Z-bit*. The highest zero valued bit which must be inverted to 1 is then found, if this is not the highest *Z-bit* itself. Next the *current-page-key* is adjusted in accordance with the preceding discussion by setting all lower bits than the highest changed to zero. At this time, the coordinates which are reduced in value to less than the corresponding coordinates of the query range lower bound are identified. Finally, the bits in the *next-match* which correspond to these coordinates are increased to the lower bound coordinate values.

The Algorithm

The implementation of the algorithm as a function requires the following parameters: the coordinates of the *current-page-key-point* and the *current-page-key* itself, the coordinates and the *derived-key* of the query range lower bound and the coordinates of the query range upper bound.

The following terminology is used in our description of the algorithm:

- *key-P* is an abbreviation for *current-page-key-point*.
- *key-P*[*q*] is the coordinate value of *key-P* in dimension *q*.
- *Z-bit* – see description above.
- *Z-bit-dimension* is the dimension of the coordinate which corresponds to the *Z-bit*.
- *Z-bit-type* is a flag, taking the values *'lower'* or *'upper'*, which indicates whether the *Z-bit* corresponds to a coordinate of *key-P* which is less than the lower bound or greater than the upper bound.

- *L-Bound* is an abbreviation for the query range lower bound point.
- *U-Bound* is an abbreviation for the query range upper bound point.

The algorithm can now be expressed in more detail as Algorithm 6.5.1.

The algorithm finds the *next-match* to a *current-page-key* but will also determine, in step 2, if the *current-page-key* is its own *next-match* where the *current-page-key-point* lies within the range. It is not desirable or necessary to test for this latter case specifically, prior to deciding whether to invoke a call to the *calculate_next_match* function since, on the one hand, such a test would add to the cost of calculation where the *page-key* is not a match and, on the other, it can be accommodated without incurring extra work where the *page-key* point does lie within the query.

The algorithm as described does not identify situations where there is no higher match to the *current-page-key*. This can be checked prior to deciding whether to call the function by comparing the *current-page-key* with the highest possible match, ie the *derived-key* of the query upper bound. Alternatively, an additional step could be inserted between steps 2 and 3 of the algorithm. This would need only be executed when the *Z-bit* corresponds to a *current-page-key-point* coordinate which is greater than the upper bound, ie when the value of *Z-bit-type* equals *'upper'*. When this arises, no higher match exists if the *current-page-key* and the *derived-key* of the range upper bound share the same bit values above the *Z-bit*, since the former could only be increased to a higher value than the latter. If the value of *Z-bit-type* equals *'lower'* then it is guaranteed that a *next-match* will be found.

We discuss the complexities of our algorithms in a later section but, for the time being, note that it is preferable not to calculate the coordinates of the *page-key* point from the *page-key* as this would increase the overall complexity of the algorithm. The coordinates could be stored in the index along with the *page-key* but this would nearly double its size. Instead, a better option is to store them on the preceding logical page in the file store to the page for which the *page-key* is the index since this will always be the last page read into memory to be searched for matches to the query and so the coordinates of the *page-key* would be readily available.

For reasons of clarity, our description of the algorithm is a simplification of the implementation. A fuller appreciation of the use of logical bit-wise operations employed can be gained from the source code file 'zfuncs.c' included in appendix F. We provide an insight here, however, by illustrating how the *Z-bit* is determined in step 1, for a 2 dimensional curve of order 6.

Generally, if a coordinate of a *current-page-key-point* is greater than the upper bound, then the expression

$$key\text{-}P[q] \ \oplus \ (U\text{-}Bound[q] \ \wedge \ key\text{-}P[q])$$

yields a value containing non-zero bits where a bit value of 1 exists in the *current-page-key-point* and a 0 exists in the upper bound. Potentially, the highest non-zero bit in such a value determines the *Z-bit*. Similarly, if a coordinate of a *current-page-key-point* is less than the lower bound, then the expression

$$L\text{-}Bound[q] \ \oplus \ (key\text{-}P[q] \ \wedge \ L\text{-}Bound[q])$$

yields a value containing non-zero bits where a bit value of 0 exists in the *current-page-key-point* and a 1 exists in the upper bound.

Suppose for dimension numbers 0 and 1, values of 001001 and 001100 are calculated in the above manner and assigned to q_0 and q_1 respectively. Both of their highest non-zero bits are in the same bit position. We recall from chapter 3 that Z-order *derived-keys* are

Algorithm 6.5.1 Finding a Range Query *next-match* using the Z-order Curve (Part 1)

{STEP 1: Find the highest bit in the *current-page-key* which must change from 1 to 0 on account of a coordinate value exceeding the corresponding coordinate value in the range upper bound, or which must change from 0 to 1 on account of a coordinate value being less than the corresponding coordinate value in the range lower bound. It is necessary to cycle through the coordinate values in the order in which they contribute to bits in a Z-order *derived-key*; starting with the coordinate determining the top bit}

1: *Z-bit-dimension* $\Leftarrow -1$
2: *Z-bit* $\Leftarrow 0$
3: **for all** q such that $0 \leq q < n$ **do**
4: **if** (*key-P*$[q]$ > *U-Bound*$[q]$) **and** (the highest non-zero valued bit in *key-P*$[q]$ which corresponds to a zero-valued bit in *U-Bound*$[q]$ is higher than *Z-bit*) **then**
5: *Z-bit* $\Leftarrow$ this highest non-zero valued bit position
6: *Z-bit-dimension* $\Leftarrow q$
7: *Z-bit-type* $\Leftarrow$ *'upper'*
8: **else**
9: **if** (*key-P*$[q]$ < *L-Bound*$[q]$) **and** (the highest non-zero valued bit in *L-Bound*$[q]$ which corresponds to a zero valued bit in *key-P*$[q]$ is higher than *Z-bit*) **then**
10: *Z-bit* $\Leftarrow$ this highest non-zero valued bit position
11: *Z-bit-dimension* $\Leftarrow q$
12: *Z-bit-type* $\Leftarrow$ *'lower'*
13: **end if**
14: **end if**
15: **end for**

{STEP 2}

16: **if** *Z-bit-dimension* $= -1$ **then** {*current-page-key* is its own next match}
17: return TRUE
18: **end if**

{STEP 3: executed where the *Z-bit* is defined by a coordinate of the *current-page-key* which is greater than the corresponding coordinate of the range upper bound. It finds the lowest zero valued bit, which can be inverted to 1, in the *current-page-key* which is higher than the *Z-bit* such that, if lower bits are set to zero, no coordinate exceeds the corresponding coordinate of the range upper bound}

19: **if** *Z-bit-dimension* = *'upper'* **then**
20: *new-Z-bit* $\Leftarrow$ highest *derived-key* bit position + 1
21: **for all** q such that $0 \leq q < n$ **do**
22: **if** ($q \neq$ *Z-bit-dimension*) **and** (*key-P*$[q]$ < *U-Bound*$[q]$) **then**
23: *temp* $\Leftarrow$ *key-P*$[q]$ with 1 added to the lowest bit position which is higher than the *Z-bit* and lower bits than the *Z-bit* set to zero
24: **if** *temp* $\leq$ *U-Bound*$[q]$ **then**
25: **if** the highest non-zero valued bit in *temp* which corresponds to a zero valued bit in *key-[q]* is lower than *new-Z-bit* **then**
26: *new-Z-bit* $\Leftarrow$ this highest non-zero valued bit position
27: *new-Z-bit-dimension* $\Leftarrow q$
28: **end if**
29: **end if**
30: **end if**
31: **end for**
32: *Z-bit* $\Leftarrow$ *new-Z-bit*
33: *Z-bit-dimension* $\Leftarrow$ *new-Z-bit-dimension*
34: **end if**

Algorithm 6.5.1 Finding a Range Query *next-match* using the Z-order Curve (Part 2)

{STEP 4: Identify which coordinates in the *current-page-key-point* would have values which are less than those of the query range lower bound if lower bits than the *Z-bit* are set to zero. We store the result in an *n-point* variable, called *L-mask*, in which the top bit is set to 1 if the coordinate in dimension 0 is less than the lower bound, the bottom bit is set to 1 if the coordinate in dimension $n-1$ is less than the lower bound, and so on}

35: *L-mask* $\Leftarrow 0$
36: **for all** q such that $0 \leq q < n$ **do**
37: **if** $q \neq$ *Z-bit-dimension* **then**
38: *temp* $\Leftarrow$ *key-P*$[q]$ with lower bits than the *Z-bit* set to zero
39: **if** *temp* $<$ *L-Bound*$[q]$ **then**
40: *L-mask* $\Leftarrow$ *mask* $\vee (1 \ll (n-q-1))$
41: **end if**
42: **end if**
43: **end for**

{STEP 5}

44: *next-match* $\Leftarrow$ *current-page-key* with the *Z-bit* set to 1 and lower bits set to 0

{STEP 6: Increment bits in *next-match* which correspond to dimensions identified in the previous step as being less than the range lower bound to their corresponding values in the lowest match to the query. This is effected by passing *L-mask* along the *next-match* and lowest match in parallel, processing n bits in a number of steps equal to the order of the curve}

45: **for all** i such that $0 < i \leq$ *order of curve* **do**
46: *next-match* $\Leftarrow$ *next-match* $\vee$ (*L-mask* $\wedge$ *lowest match*)
47: *L-mask* $\Leftarrow$ *L-mask* $\ll n$ bits
48: **end for**
49: return TRUE

formed by interleaving bits taken from dimension 0 before dimension 1. Thus the highest non-zero bit of q_0 corresponds to a higher bit in the *current-page-key* than does the highest non-zero bit in q_1 and therefore q_0 qualifies as the *Z-bit-dimension*. We cannot determine this simply by comparing the values of q_0 and q_1 since, in this example, $q_0 < q_1$. Instead we confirm that there is no higher non-zero valued bit in q_1 than in q_0 by checking the truth of the expression $(q_0 \oplus (q_1 \wedge q_0)) \leq q_0$. Finally, we perform a binary search on q_0 in order to isolate the position of the highest non-zero bit; ie the *Z-bit*.

6.5.1.3 Bit Manipulation Partial Match Query Algorithm

In common with the Hilbert curve, the range query version of the Z-order curve *calculate_next_match* algorithm can be employed in the execution of partial match queries. It is also possible to improve the efficiency of its implementation for processing this type of query. In contrast to the Hilbert curve, however, we are able to adopt an alternative strategy altogether which yields an improvement in the order of complexity over the range query algorithm. This is described in this section.

We consider the case where the *current-page-key* is greater than the lowest match to the query and less than the highest match but is not a match itself. The *current-page-key* is not a match when one or more of its 'specified' bits are zero where they are non-zero in the query or when the inverse is the case or when a combination of these two conditions obtains.

We begin by finding the highest specified bit within the *current-page-key* which does not match the query. If this bit, again called the *Z-bit*, is zero then, in order to produce a *next-match*, it is set to 1 in the *current-page-key*, lower specified bits are set so they match the query and lower unspecified bits are all set to zero.

Alternatively, if this bit is non-zero then we must find the lowest zero valued unspecified bit within the *current-page-key* which occupies a higher bit position. In order to find this bit, we make use of the technique for finding the bits which are non-zero in one value where they are zero in another, as discussed at the end of the previous section. The lowest zero valued bit thus found becomes the *Z-bit* and the *current-page-key* is transformed into the *next-match* in the manner just described.

In contrast to the range query algorithm, the coordinates of points need not be known for the calculation to take place. The *current-page-key* and the lowest and highest matching *derived-keys* are required. In addition, a *derived-key* is required which contains bits set to 1 and 0 where they correspond to specified and unspecified coordinates respectively. This *derived-key* is called *Q-mask*. All of these *derived-keys* are calculated once only, at the inception of the query, regardless of the number of times that the *calculate_next_match* function is called, with the exception of the *current-page-key* which is read from the index prior to each call.

The querying algorithm is given in detail in Algorithm 6.5.2. An example showing the execution of the query is given in Figure 6.8 and Table 6.1.

This expression of the algorithm assumes that a *derived-key* can be accommodated in a single variable and so is a simplification of our implementation in which *derived-keys* are held in *arrays* of 32 bit words. For a curve of order 32, these arrays contain n elements.

The implementation processes elements of an array holding a *derived-key* iteratively, starting with that which contains the highest bits of the *derived-key*. Sometimes it is found that in one iteration, an element of the *current-page-key* matches the query but that a subsequently processed element is not a match and is greater in value than the corresponding element of the highest match. It then becomes necessary to return, ie backtrack, to the lowest but higher matching element and increase its value to that of a higher match to the query.

Algorithm 6.5.2 Finding a Partial Match Query *next-match* using the Z-order Curve

{A, B, C and D are temporary working variables, equal in size, ie number of bits, to *derived-keys*}

1: **if** (*current-page-key* $\wedge$ *Q-mask*) = *lowest-match* **then**
   {ie if *current-page-key* is a match to the query}
2: *next-match* $\Leftarrow$ *current-page-key*
3: return TRUE
4: **end if**
5: $A \Leftarrow$ *lowest-match* $\oplus$ (*current-page-key* $\wedge$ *lowest-match*)
   {A contains the specified non-zero valued bits in the query which are zero in the *current-page-key*}
6: $B \Leftarrow$ *current-page-key* $\oplus$ (*highest-match* $\wedge$ *current-page-key*)
   {B contains the specified zero valued bits in the query which are non-zero in the *current-page-key*}
   {NB the non-zero bits in A and B cannot occupy the same bit positions. This enables a simple comparison between A and B}
7: **if** $A < B$ **then**
   {The highest specified bit in which the *current-page-key* and the query differ is non-zero in the former: we must find the lowest unspecified zero valued bit in the *current-page-key* which is higher than this bit position}
8: $A \Leftarrow (\neg$*Q-mask*$) \oplus$ (*current-page-key* $\wedge$ ($\neg$*Q-mask*))
   {A now contains the unspecified zero valued bits in the *current-page-key*}
9: $C \Leftarrow A - B$
   {C differs from A in that the lowest non-zero bit in A which is higher than the highest non-zero bit in B is inverted to zero. (The values of one or more lower bits are also different but we are not concerned with these). This bit is also the highest bit in which A and C differ}
10: $D \Leftarrow A \oplus (C \wedge A)$
   {The highest non-zero bit in D is the highest bit in which A and C differ. This bit position corresponds to the lowest zero valued unspecified bit in the *current-page-key* which is higher than the highest non-zero in the query which corresponds to a zero bit in the *current-page-key*. It corresponds to the *Z-bit*}
11: $A \Leftarrow D$
12: **end if**
13: perform a binary search on A to identify the position of the *Z-bit*, ie the highest non-zero bit in A
14: $A \Leftarrow 1 \ll$ *Z-bit*
   {A contains zeros except in the *Z-bit* bit position}
15: *next-match* $\Leftarrow$ *current-page-key* $\vee A$
   {Invert the zero valued *Z-bit* in the *current-page-key*}
16: *next-match* $\Leftarrow$ *next-match* $\wedge$ ($\neg(A-1)$)
   {Set lower bits than the *Z-bit* in the *next-match* all to zero}
17: *next-match* $\Leftarrow$ *next-match* $\vee$ *lowest-match*
   {Set specified bits lower than the *Z-bit* in the *next-match* equal to the query}
18: return TRUE

Query:	$\langle$? ? ? ?, 1 0 1 0 $\rangle$
current-page-key	1 1 0 1 0 0 1 1

Parameter	**Initial value**
Q-mask	0 1 0 1 0 1 0 1
lowest-match	0 1 0 0 0 1 0 0
highest-match	1 1 1 0 1 1 1 0
current-page-key	1 1 0 1 0 0 1 1

Execution of the Algorithm

Variable		**Value**								line #
lowest-match		0	1	0	0	0	1	0	0	
current-page-key		1	1	0	1	0	0	1	1	$\oplus$
		1	0	0	1	0	1	1	1	
lowest-match		0	1	0	0	0	1	0	0	$\wedge$
A	$\Leftarrow$	0	0	0	0	0	1	0	0	5
current-page-key		1	1	0	1	0	0	1	1	
highest-match		1	1	1	0	1	1	1	0	$\oplus$
		0	0	1	1	1	1	0	1	
current-page-key		1	1	0	1	0	0	1	1	$\wedge$
B	$\Leftarrow$	0	0	0	1	0	0	0	1	6
$\neg$*Q-mask*		1	0	1	0	1	0	1	0	
current-page-key		1	1	0	1	0	0	1	1	$\oplus$
		0	1	1	1	1	0	0	1	
$\neg$*Q-mask*		1	0	1	0	1	0	1	0	$\wedge$
A	$\Leftarrow$	0	0	1	0	1	0	0	0	8
A		0	0	1	0	1	0	0	0	
B		0	0	0	1	0	0	0	1	$-$
C	$\Leftarrow$	0	0	0	1	0	1	1	1	9
A		0	0	1	0	1	0	0	0	
C		0	0	0	1	0	1	1	1	$\oplus$
		0	0	1	1	1	1	1	1	
A		0	0	1	0	1	0	0	0	$\wedge$
D	$\Leftarrow$	0	0	1	0	1	0	0	0	10
A	$\Leftarrow$	0	0	1	0	0	0	0	0	14
current-page-key		1	1	0	1	0	0	1	1	
A		0	0	1	0	0	0	0	0	$\vee$
next-match	$\Leftarrow$	1	1	1	1	0	0	1	1	15
next-match		1	1	1	1	0	0	1	1	
$\neg(A-1)$		1	1	1	0	0	0	0	0	$\wedge$
next-match	$\Leftarrow$	1	1	1	0	0	0	0	0	16
next-match		1	1	1	0	0	0	0	0	
lowest-match		0	1	0	0	0	1	0	0	$\vee$
next-match	$\Leftarrow$	1	1	1	0	0	1	0	0	17

Line numbers relate to Algorithm 6.5.2
Refer to comments in the Algorithm for the semantics of the operations
Refer to Figure 6.8 for an illustration of the query

Tab. 6.1: Example Z-order Partial Match Query Calculation in 2 Dimensions

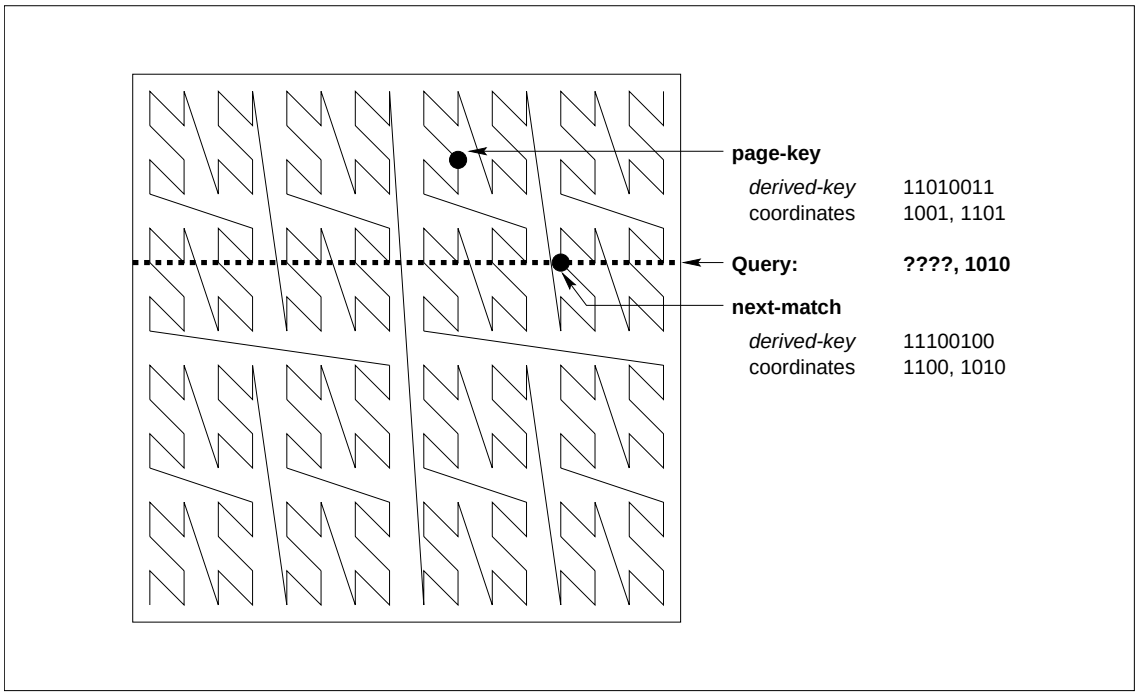

Fig. 6.8: Example Z-order Partial Match Query in 2 Dimensions

At each iteration, therefore, a matching element which, if incremented remains lower or equal to the highest match, is *marked* as an element to which back-tracking may return. As with the mechanism for back-tracking described in the range query algorithm for the Hilbert curve, any element so identified replaces any previously *marked* element, corresponding to higher bits in the *derived-key*. Similarly, back-tracking is required at most once and after taking place the calculation process may terminate swiftly. A requirement to back-track in the absence of an element previously marked signifies that the *current-page-key* is greater than the highest match.

6.5.2 Tree-descent Range Query Algorithm

In this section we briefly describe the modifications which are required to be made to the Hilbert curve range query algorithm, described in section 6.4.2.1.2, in order to adapt it for application to the Z-order curve. We also describe optimizations which can be introduced as a result of using the Z-order curve, but which cannot be exploited where the Hilbert curve is used instead.

The most important of these is a significant simplification of the second loop within the algorithm. This loop is given in Algorithm 6.4.2 on page 115. We recall from section 6.4.2.1.2 that when it is entered all that remains to be done is to set unresolved lower bits of the *next-match* equal to the corresponding bit values of the *derived-key* of the point within the *current-query-region* mapping to the lowest *derived-key*. We recall from section 6.5.1.1 that this point will always be the lower bound of the *current-query-region*; a point whose coordinates are known.

It therefore follows that we need not concern ourselves with whether the *current-query-region* coincides with the *current-search-space* and do not need to carry out binary searches of quadrants within nodes within the tree. This is in contrast to the application of the algorithm to the Hilbert curve.

We also note that the process of bit-interleaving results in the identity function defining a Z-order mapping between *derived-keys* of quadrants within a *current-search-space* and

the coordinates of those quadrants, expressed as *n-points*.

This obviates the need to perform mappings from *derived-keys* to *n-points* in the binary searching of quadrants carried out in 'step 3' described in section 6.4.2.1.2 and relating to Algorithm 6.4.3. This is particularly beneficial in higher-dimensional space where state diagrams cannot be used for the Hilbert curve. In this binary search operation, we recall that we must find the *n-points* corresponding to the maximum *derived-key* of the lower half of a sub-range of quadrants and the minimum *derived-key* of the upper sub-range in order to determine the dimension which divides them.

This simplification is partially but trivially offset by measures required to accommodate the fact that adjacent Z-order *derived-keys* do not necessarily correspond to points which are adjacent in space, ie consecutive points may differ in more than one coordinate value. Where the *derived-keys* and *n-points* of the quadrants are in the range

$$[\ lowest, \ldots,\ max\text{-}lower,\ min\text{-}higher, \ldots,\ highest\ ]$$

the *n-point* which contains a single non-zero bit corresponding to the dimension which divides this range into two is evaluated as

$$(lowest \wedge max\text{-}lower) \oplus (min\text{-}higher \wedge highest).$$

In step 4, the *n-point* of the quadrant in which we restrict the *current-search-space* in the next iteration of the algorithm is required so that we may also restrict the *current-query-region*. Again this is available without the need to perform a mapping calculation.

Finally, since the Z-order curve is encapsulated by a state diagram containing a single state defined by the identity function, it is unnecessary to store the state in memory and the *current-state* variable is not required.

6.6 Complexity of the Algorithms

In this section, we consider the complexity of the algorithms described in this chapter. The algorithms fall into 2 categories; the tree-descent approach which is suited to all curves and the bit manipulation algorithms which appertain specifically to the Z-order curve. In the case of tree-descent algorithms, we do not distinguish between algorithms tailored to partial match queries and those which are more generally applicable to range queries since they do not differ in their complexity.

6.6.1 Tree Descent Algorithms

The complexity of the tree-descent algorithms is, in part, determined by the height of the tree, which we have already seen in chapter 3 is dependent on the order of the curve, k, or, equivalently, by the number of bits required to hold any coordinate value. This is reflected in the total number of iterations of the two loops which comprise the algorithm given in section 6.4.2.1.2.

In the case of the Hilbert curve or any curve where a state diagram is utilized, a node or state is *visited* during each iteration and it is necessary to extract 1 bit from each coordinate of the range lower and upper bounds or from a partial match query specification. The complexity of this is determined by the number, n, of coordinates or dimensions which define a point. Furthermore, we perform a binary search on the values which comprise a node or state and this too results in a complexity of n. Modifying the query region, in the case of range queries only, also takes up to n steps. Once a node has been processed, an additional n bits of the *next-match* are known but these are placed in the *next-match* variable in a single step.

Of the operations performed during each iteration, none has a complexity which exceeds $O(n)$. Thus the overall complexity of the algorithms can be stated as $O(kn)$.

Where Hilbert curve mapping is performed by calculation rather than with the aid of a state diagram, more work is required but the overall complexity is not increased. The mappings from *derived-keys* to *n-points* which take place during binary searches are performed in a fixed number of steps, regardless of the number of dimensions. Determining the characteristics of the next state for the next iteration is effected with operations performed with a complexity of $O(n)$.

Whereas the algorithms can be optimized during implementation for the Z-order curve, the complexity is unchanged.

In the worst case, it is necessary to perform k iterations of the first loop for both the Hilbert and Z-order curves, followed by a back-tracking to the root which is effected in a single step. Thereafter, the second loop is iterated $k - 1$ times. Its execution is considerably simpler than that of the first and considerably simpler for the Z-order curve still but, nevertheless, the complexity of each iteration remains $O(n)$. Thus in the worst case, the height of the tree is effectively doubled.

In the best case, the first loop is iterated once only, and back-tracking occurs within it. Subsequently, the *current-query-region* is found to be coincident with the *current-search-space* prior to executing the second iteration, whereupon the $n(k-1)$ unresolved lower bits of the *next-match* are instantly all set to zero and the *calculate_next_match* function terminates. In this case, the complexity of the search for a *next-match* is reduced to $O(n)$ for both the Hilbert and Z-order curves. A best case situation, however, will only be encountered where query regions are larger than a quadrant of the whole search space. This is unlikely ever to be the case except, perhaps, in high-dimensional space.

6.6.2 Z-order Bit Manipulation Algorithms

The Z-order curve bit manipulation algorithms described in section 6.5 offer an improvement in terms of the order of complexity over the tree-descent approach.

In the case of the range query algorithm given in section 6.5.1.2, it can readily be seen that steps 1, 3 and 4 entail operations of complexity $O(n)$ and that step 5 entails an operation of complexity $O(k)$ and so the overall complexity is $O(n + k)$.

The complexity of the partial match query algorithm given in section 6.5.1.3 is determined by the binary search to find the *Z-bit*. This is determined by the number of bits in a *derived-key*, which is $(n * k)$ and so is an operation of complexity $O(log(n * k))$.

Chapter 7

FILE IMPLEMENTATION

We describe in chapters 3 to 5 how n-dimensional points are placed in order along a one-dimensional interval using a space-filling curve and how the curve is divided into contiguous sections corresponding to 'pages' of storage. In chapter 6, we describe how to identify which of these pages intersect with the sections of curve passing through a hyper-rectangular query region. In this chapter, we describe our practical implementation in software of a multi-dimensional data storage and retrieval system which utilizes these techniques and enables data to be held persistently in secondary storage and accessed with the aid of an index which is compact, flexible and simple to maintain.

The first 3 sections of this chapter provide an outline of the implementation and summarize the variations of the concept of mapping data to space-filling curves which have been accommodated. These variations principally relate to the choices of curves used in the mappings and the methods of performing the mappings. In section 7.4, we focus on details of the format and order in which data is stored on pages. In particular, for update and query operations, we examine the implications arising from the choices we make. We examine the reasons why certain choices were made, explain how various problems were overcome and consider how the application of space-filling curves impact on these issues.

In the concluding section, we discuss possible variations to our implementation which may be pursued as topics for further research. These variations relate to the manner in which data is partitioned and how pages are referenced in the index.

Our implementation is carried out using the ANSI version of the 'C' programming language except that UNIX system calls are used for file handling. The replacement of UNIX system calls by ANSI C equivalents would be a trivial exercise. The implementation currently runs over the standard UNIX file management software which would probably be replaced, were the implementation developed into a commercial product.

7.1 Design Summary

7.1.1 Curves used in the Mappings

Our implementation can be customized to make use of one of a number of space-filling curves in mappings between one dimension and n dimensions.

These curves are the Hilbert curve, the two variations of the Z-order curve described in section 3.7.1, the three variations of the Gray-code curve described in section 3.7.2 of chapter 3 and our variation of Moore's curve introduced in section 4.3.5.2 of chapter 4.

The choice of curve is made at the time of compiling the source code and cannot be changed subsequently.

7.1.2 Number of Dimensions

Where mappings to Hilbert and Z-order curves are performed by calculation, our implementation currently accommodates spaces of up to 16 dimensions but it is not restricted to this number. We leave an extension of the implementation into higher-dimensional space as an area for further work.

Where mappings are performed with the aid of state diagrams, however, the number of dimensions which can be accommodated is restricted by the memory requirements of the diagrams. A summary of memory requirements is provided in Table 4.4 on page 77. Thus our implementation functions in up to 8 dimensions using the Hilbert curve, 9 dimensions using our variation of Moore's curve and 10 dimensions using the Gray-code^F curve. In the case of the Gray-code^A and Gray-code^B curves, an upper limit of approximately 20 dimensions applies but we currently accommodate only 16 dimensions in the implementation.

7.1.3 Order of Curve

All of our program versions utilize curves of order 32. Thus the cardinality of any attribute domain is 2^{32} and any attribute value can readily be accommodated on a computer supporting 32 bit words. This is considered sufficient for most applications. The implementation could easily be adapted to suit attribute domains of different cardinalities by making use of variables supported by a compiler of other than 32 bits in size, such as 8, 16, 64 and 128 bits. Since the complexity of our algorithms is in part determined by the order of a curve, it is clearly advantageous to make use of variables of a size which is the minimum required.

Our implementation assumes that the cardinality of every attribute domain is the same. This is equivalent to working in a space which is hyper-cubic in shape. To deviate from this approach would not be unduely troublesome where the Z-order curve is used in a mapping but it is less feasible in the case of other curves. Where the cardinality of one dimension is significantly less than that of another, we have found it advantageous to map its values to the whole domain which can be accommodated in the variable type used for the dimension which has the greatest cardinality.

7.1.4 Storage of Data During the Execution of Computer Programs

In our computer programs, the coordinates of a point are held in an array of variables with each element storing the value of a different coordinate. Since the total number of bits required to represent the *derived-key* of a point is the same as the total number of bits required to represent all of a point's coordinates, it is convenient also to hold the *derived-key* in an array of the same type and size. This imposes a small overhead in that bitwise manipulation of a set of n bits within a *derived-key* may require processing of some most significant bits of one array element together with some least significant bits of the next *higher* array element but for the most part this is unavoidable. An exception would, for example, be where we are using a 4-dimensional curve of order 16 where a *derived-key* could be held in a single 64 bit word.

Because of the extensive use of bit manipulation employed in our algorithms, we exclusively use variables of the *unsigned integer* type. As a result of this, any attribute domain which comprises values of a different type, such as signed integers or real numbers, must be mapped to unsigned integers. This can be facilitated by the application of a *lexical token convertor*, as noted below in section 7.3.

7.1.5 The Data File

A data file comprises a set of fixed length pages of data. The capacity of a page is predetermined at compile-time and cannot be altered subsequently. Each page represents a section of curve and holds all of the *datum-points* lying on that section. The lowest *derived-key* corresponding to a *datum-point* which is placed on a page becomes the page's index entry, called the *page-key*, together with the page number. If the point is subsequently deleted, it is not necessary to alter the index entry for the page. The page corresponding to the first section of the curve is indexed with the *derived-key* of zero, regardless of whether it corresponds to a *datum-point*.

Page numbers are assigned in the sequence in which pages are created and there is no relationship between the ordering of page numbers and the ordering of contiguous sections of curve. If a page is deleted, its page number is placed in a list of page numbers which are available for re-use. The physical page is not deleted from the file but instead it is effectively *marked* as being deleted since the index will contain no entry for it. If no free pages are available then any new page is assigned a number which is one greater than the last new page number which was generated previously.

A page of data comprises a set of coordinates of *datum-points*, rather than their *derived-keys*. The coordinates of a point are ordered according to the ordering or numbering of the dimensions in a space. In our application, we order data on a page in a consistent manner. For example, if the dimensions are numbered $1, 2, \ldots, n$ then we order points first by coordinate values in dimension 1. *Datum-points* with the same values in dimension 1 are ordered by values in dimension 2 and so on. The reasons for ordering data and the alternatives to it are also discussed in more detail in section 7.4.

The mapping techniques employed ensure that data in a file is, in effect, fully and flexibly indexed on any combination of coordinate values. In addition to the data held as coordinate values, a page of data may optionally contain non-indexed data associated with each point. Whether such data is to be stored and the amount of such data must be determined at compile-time and it cannot be altered subsequently.

7.1.6 The Index

The purpose of mapping data to one dimension is to be able to index it using concepts which are suitable for one-dimensional data. Any one-dimensional indexing method is suitable and we choose to use the B^+-Tree.

In our implementation, the index is held in a separate file. The entire index is read into memory on opening of the data store and it is written back to the file when the data store is closed, if it has been updated. The implementation could easily be extended so that not all of the index needs to reside in memory should its size dictate.

7.1.7 Main Memory Buffer

Data is held persistently in a file which is maintained in secondary storage. On opening the file, an area of primary storage is allocated as a buffer. This buffer has a predetermined capacity to hold a fixed number of pages of data from the file. The buffer capacity may be varied for a particular file but changes to it require recompilation of the program executable.

A B^+-Tree index, separate to that used for indexing the data file, is maintained in memory to record which pages reside in the buffer at any particular time. If a page is required to be accessed and it is not currently contained in the buffer then the least recently used page which is in the buffer is swapped out. This may entail updating the file store if the contents of the page have been changed since it was last read from the

file. A flag indicates whether the page has been updated and a variable associated with each page in the buffer keeps track of the sequence in which pages are read from the file. Alternative strategies to the *least recently used* one could be implemented.

An additional flag is stored for each page in the buffer to indicate whether it is currently in use, ie is being searched, as part of the execution of a query. This flag is intended to avoid pages being swapped out of memory or being merged with other pages if they are being searched.

7.1.8 Ancillary Files

Associated with each data file and its index file are two additional files. The first of these contains a list of free pages within the data file, if any. The second file contains meta-data such as the number of free pages, the highest page number which has been assigned to date and information on page size, curve type and the number of dimensions relating to the data file. Some of this information is used to verify the compatibility between the data file and the executable program file which opens it for data processing.

7.1.9 Query Execution Strategy

We adopt a similar strategy for the management of the processing of queries to that used by Derakhshan in his Grid File implementation [Der89] which enables a number of queries to be executed concurrently. An upper limit on how many queries may be processed concurrently is, however, specified at compile-time but this may be changed during the lifetime of a data store, simply by changing a parameter and re-compiling the source code.

An array of numbered blocks of memory, called *retrieval-sets*, is allocated to hold information on all queries which are active at any particular time. When a query is invoked, the array is searched in order to find a block which is not already in use by another query. If no such block is found then the query cannot proceed. When an unused block is found, it is reserved for use by the query for the duration of its execution. The query is assigned a retrieval-set identity number which is the array element number of the memory block.

Information stored about a query in its retrieval-set block includes the specification of the query, the location of the page in the buffer which is currently being searched for matches to the query and the location on the page of the next record to be examined. Additional information which aids the detail of the implementation is also stored, such as a count of the number of unspecified coordinates in a partial match query.

7.2 The Application Interface

The implementation of our work comprises low level software which is intended to provide facilities, in the form of a set of functions, for use by higher level applications. No user interface exists and the responsibility for providing one, if required, lies with the higher level applications.

In this section we summarize the functions which are provided and which enable an application to create, update and query a data store. Function names are given and parameters passed to them are in parenthesis.

db_create (database-name) This creates a new database, including all of its ancillary files. An empty page with a *page-key* of zero is placed in the data file and an entry for it is made in the index. The free page list is initially empty. Once created, the database is closed.

db_open (database-name) Opens a database for updating and querying. The index is read into memory from file and main memory is reserved for use as a buffer.

db_close (database-name) Causes the database to be closed. The buffer is scanned to check whether any modifications have been made to any page but not yet written to the file store. The index is rewritten to file and the free page list data is also written to file.

db_data_insert (*datum-point*) Inserts a *datum-point* into the database. A return value of zero indicates that the *datum-point* is already present, otherwise a non-zero return value signifies successful insertion. A non-zero return value also represents the page occupancy following an insertion and may trigger a page split, but this is transparent to the application which calls the function.

db_data_delete (*datum-point*) Deletes a *datum-point* from the database. A return value of zero indicates that the *datum-point* was absent to begin with, otherwise a non-zero return value signifies successful deletion. A non-zero return value also represents the page occupancy following a deletion and may trigger action to resolve underpopulation, again transparently to the application which calls the function.

db_open_set (partial-match-query, set-number) This identifies a free retrieval-set element if one exists and initializes it in accordance with the partial match query specification. The set number is placed in the second parameter. The function's return value indicates whether a free retrieval-set was found.

db_fetch_another (set-number, *datum-point*) This lazily searches the database for, at most, a single match to the partial match query, the details of which are stored in the retrieval set element with number 'set-number'. The return value indicates whether a match was found, in which case the results are placed in the *datum-point* parameter, or whether no further matches are to be found. The function is called once for every *datum-point* retrieved and once when it signifies no further matches are to be found. A single call to the function may result in the searching of more than one page of data.

db_close_set (set-number) This releases a retrieval-set block of memory for use by another query.

db_range_open_set (range-query, set-number) This is similar to db_open_set but applies to range queries.

db_range_fetch_another (set-number, *datum-point*) This is similar to db_open_set but applies to range queries.

7.3 Use and Compatibility with other TriStarp Group Software

The research described in this thesis has been carried out within the Triple Store Applications Research Project (TriStarp) of the Department of Computer Science at Birkbeck College. Previous work carried out within this Project includes the development of a number of functional programming languages for use with functional databases [Ayr95, Mer99, Pou89, Sut95]. Data storage facilities are currently provided by Derakhshan's [Der89] implementation of the Grid File [NHS84].

The data storage application developed and implemented in this thesis may be used as an alternative to the existing Grid File. The functionality of the interface to our implementation is similar to that of the existing Grid File, but it differs in detail, principally in our use of unsigned integers rather than signed integers.

In order to use and test our software under higher level TriStarp applications, we have created a set of 'wrapper' functions which have names, parameters and return value types which are identical to those provided by Derakhshan. These functions call functions provided within our implementation and act as an interface between the latter and higher level software.

Provision of this interface results in a number of benefits. We are able to demonstrate empirically the correct functioning of our application which can be tested with a variety of data sets used in the research and teaching activities of the TriStarp Group. The use of TriStarp Group languages over our application entails subjecting it to a realistic variety of updates, both insertion and deletion. Our application is only tested in 3 and 4 dimensions, however, when used by higher level TriStarp Group software.

In practical data storage applications, not all of the attributes of records of data are necessarily integers; for example they may be real numbers or strings of characters. Thus where a data storage implementation holds all values as integers, a facility is required which maps non-integer values to integers. Derakhshan achieves this by utilizing a *lexical token convertor* [LW84] and this approach is equally suitable for our implementation and, indeed, other methods such as the original Grid file and the BANG file [Fre87].

Since the existing TriStarp Grid File utilizes a lexical token convertor, we have incorporated its implementation in software into our own implementation where the latter is used under existing higher level TriStarp applications. Thus our implementation may be used transparently with the high level software.

7.4 Implementation Details

In carrying out an implementation, various issues of detail need to be resolved. In some cases they conflict and, certainly, they influence each other. An obvious example is that any file organization design must accommodate the requirement to update a data store whilst also providing an optimum environment for facilitating the selective retrieval of data.

In section 7.1, we provide a summary of the implementation of our design and in this section we explore the implications of some of the decisions and consider some of the alternative options which were rejected. We also elaborate on the detail of how some operations, such as page splitting and merging, are performed and how the use of space-filling curves impact on these operations.

The choice of the format in which data is stored and the order in which it is stored are intimately related and they impact both on the manner in which page searching is performed and how an efficient page utilization is maintained. This is true for any method of file organization but where space-filling curves are used it appears that there is a greater choice of combinations of format and order.

If data is not maintained in some order on a page then the cost of searching a page which may contain data which matches some query specification is expensive since every data value on it must always be examined to determine whether it is a match. Furthermore, insertions require a serial search of the whole of a page to ensure a data value is not already present before it is appended. Similarly, deletions will on average require a serial search of half of a page to locate any record to be removed, provided it exists. On the other hand, maintenance of data in some order also imposes an overhead in terms of work required.

In common with all file organization methods, it is desirable to ensure that all pages

of data contain a minimum of free space otherwise the ratio of the volume of data to the size of the data file degenerates and the index size increases unnecessarily. To maintain a high page occupancy there must exist satisfactory mechanisms to divide a page into two pages when its data occupancy has reached its 'capacity', to merge two adjacent pages into a single page when their combined occupancy falls below the capacity of a single page and to move data to an underpopulated page from a neighbouring page when the two adjacent pages hold more data than can be stored on a single page. At the same time it is desirable to set thresholds in such a way that redistribution of data is delayed to some extent otherwise periods of high activity in terms of both insertion and deletion can give rise to unnecessary page splitting and merging.

The term *underpopulated* relates to a page whose occupancy has fallen below some arbitrary threshold, typically about 50% of potential capacity. A higher threshold could be set in an attempt to maximise storage utilization but clearly as soon as a page is divided into two, its replacements would be *underpopulated* and some mechanism would be required to prevent an immediate redistribution of records between neighbouring pages.

In exploring the implications of the details of an implementation we first consider the case where data is stored in *derived-key* format, and then consider the case where data is stored as sets of coordinates of *datum-points*.

7.4.1 Storing Data as *derived-keys*

In this section, we first consider the implications of storing *derived-keys* sorted in order on pages, and then the implications of not maintaining any order.

7.4.1.1 Ordered Data

When data is stored as a sorted list of *derived-keys*, in searching a page during query execution, it is possible to perform a binary search of the page to determine the point at which the page search begins. This is irrespective of whether the query type is a range query or a partial match query and, in the latter case, regardless of which coordinates are specified. This is an efficient way of finding the *next-match* on any page, if it corresponds to a *datum-point*.

In order to find subsequent matches, two alternative approaches are available. The first is to search the page serially, beginning from the position where the search for the lowest *derived-key* terminated, whether or not this search resulted in finding a match. Each *derived-key* is mapped to its corresponding n-dimensional set of coordinates, and these are compared with the query specification to see if the *datum-point* lies within the query region. This entails an operation of complexity $O(kn)$ to perform each mapping followed by an operation of complexity $O(n)$ to determine if a match is found.

The second approach is to execute the *calculate_next_match* function, described in chapter 6, to calculate the value of the *next-match* which might exist and then perform a binary search on the rest of the page to find whether it is present and then repeat this process until it is found that no higher match can possibly exist on the page.

We have seen that finding the *next-match* is an operation with a complexity of $O(kn)$. How many times this function would need to be called and followed by a binary search of the remaining records on the page, depends on the distribution of data on the page and this is not predictable. Only when a *next-match* is found to exist on a page would a mapping calculation be required in order to return its corresponding *datum-point*. In a worst case situation, it would be necessary to call the *next-match* function and perform a binary search for every record on the page following the position of the first possible match.

When required as a result of performing updates on a data store, moving data from one page to another would be trivial where data is stored as *derived-keys*. Where a page must be split into two, we simply move the bottom half of a full page to the head of a newly created page. Merging two pages entails appending the contents of one to the other. Similarly, moving records from a page to an underpopulated neighbour entails the transfer of a contiguous block of records from the former to the beginning or the end of the latter. Records may need to be moved to make room for additions to a page and any gaps created would need to be closed up, depending on whether records moved to a preceding or succeeding page.

Data updating would require moving contiguous blocks of records to make room for a new record inserted or to close up a gap after a deletion.

7.4.1.2 Unordered Data

Where data is unordered, the only operation which can be carried out in a relatively simple manner is the merging of two adjacent underpopulated pages. Page merging entails the moving of a block of *derived-keys* from one page to the end of another.

A newly inserted *derived-key* is simply placed at the end of a page but before doing so, it is necessary to examine each of the existing *derived-keys* on a page to ensure that the *derived-key* to be inserted is not already present. Deletion of a *derived-key* entails a serial search of the page to locate it. Gaps created by deletion can be filled simply by the last record on a page.

Each search to find matches to a query requires a serial pass through the whole of a page, mapping each *derived-key* to its corresponding *datum-point* encountered.

Splitting an overpopulated page requires finding the median value on the page and then extracting *derived-keys* greater in value and moving them to the new page, closing up gaps on the original page as required. More is said in a later section in this chapter about finding the median *derived-key* on a page. Moving data from a page to an underpopulated page poses similar problems.

7.4.2 Storing Data in Coordinate Format

In this section we consider the case where we store data as sets of coordinates. Unless stated otherwise, we assume that the coordinates are stored in the same order as is used to specify queries. We also assume in the case of the Z-order curve, that the coordinates are stored in the same order in which bits are taken from coordinates and interleaved in order to generate Z-order *derived-keys*.

7.4.2.1 Ordered Data

Where data is ordered by coordinate value, page searching proceeds in the same way for applications implemented over space-filling curves as it does for some other methods such as the existing Grid File implementation currently used by the TriStarp Group.

The specification of a range query allows, for any page intersecting with the query, a binary search to be performed to locate the position where the first possible match will be stored on the page, if it is a *datum-point*. The same is true of partial match queries but only where at least the 'first' coordinate is specified, otherwise a serial search of the whole page is necessary.

Following a binary search, the page is then searched serially until a *datum-point* is found which is not a match to the query. Subsequently, the next matching *datum-point*, if it exists, is found either by performing another binary search (if possible) or by continuing with a serial search.

Page searching can sometimes be terminated before the end of the page is reached. As soon as a *datum-point* is found whose 'first' coordinate is greater than the 'first' coordinate of the query range upper bound, then no further matches can exist on the page. Where a mapping to the Z-order curve is used, this condition arising also signifies completion of the query process, but in the case of other curves further matches may still be present on other pages. Similarly, if the first i, $i < n$, coordinates of a *datum-point* are all equal to the corresponding range upper bound coordinates but coordinate $i + 1$ is greater in value, then no further matches exist on the page. Terminating the search in this way is not possible where data is ordered by *derived-key* value, except where a search is made of the last page which may contain matches to the query.

Reorganizing data by moving it from one page to another is, however, more problematic where space-filling curves are employed and where data is stored, in order, as sets of coordinates rather than as *derived-keys*. The simplest case is where pages are merged but the *datum-points* do need to be interleaved on a new combined page to maintain them in order and we are unable simply to copy a block in a contiguous manner.

Where a page is to be split, its *datum-points* need to be partitioned into two halves such that the *derived-keys* of those in one half are lower than those of the other. However, there is not generally any correlation between the position of a *datum-point* on a page and the value of its *derived-key*. We address this problem by determining the *approximate median derived-key* of the *datum-points* about which the latter are partitioned. This is discussed further in section 7.4.3 below. Moving data to an underpopulated page from an adjacent page presents a similar problem to that faced when splitting pages. Problems of a different nature exist for other existing file organization methods and we discuss some of these further in chapter 8.

As with *datum-points* stored as *derived-keys* and in sort order, existing *datum-points* must be moved to accommodate an insertion and gaps must be closed following a deletion. Locations for insertion and deletion are determined by binary searching and so determining whether a *datum-point* to be inserted is already present is trivial.

7.4.2.2 Unordered Data

Where data is stored as sets of coordinates but not stored in order on a page, we suffer almost all of the disadvantages encountered above with the most notable exception being that page merging is as simple as described in section 7.4.1.2.

Serial searching of the whole page is always required during querying and before insertion can take place although new data is simply placed at the end of a page. Identifying which records to move from one page to another during page splitting or data redistribution entails resolving similar problems to those encountered in section 7.4.2.1.

7.4.3 Redistribution of Data Stored in Coordinate Format and in Sort Order

In this section we describe our technique for redistributing some data from one page to another, where the data is stored in coordinate format and maintained in sorted order. The need for this occurs in two situations; firstly, where a page must be split into two because its data occupancy has reached its capacity and, secondly, where data must be moved from one page to a neighbouring page which has become underpopulated. We discuss the two situations separately although they are related. We do not discuss the merging of two pages into one as this is a relatively trivial operation.

7.4.3.1 Page Splitting

When *datum-points* are stored on a page in attribute order they are sorted according to their *derived-keys* under a mapping to the 'Scan' curve, described in section 3.7.3 of chapter 3. Clearly, where any other curve is used, they are not stored in *derived-key* order.

In order to divide a page into two, we must therefore calculate the *derived-keys* corresponding to all of the *datum-points* and then determine the median of these values. *Datum-points* which map to *derived-keys* which are less than the median remain on the original page and all others are placed on the new page. Once the page has been split, *datum-points* on both the original and new pages must be ordered according to their attribute values.

In our implementation, the *derived-keys*, once calculated, are initially placed on a temporary page of storage. An obvious way of determining the median would be to sort the *derived-keys* but this operation would be computationally expensive, especially given that a page of data may contain thousands of *datum-points*.

As an alternative to sorting *derived-keys*, we explored the option of finding the approximate median by using a *median-of-medians* algorithm. This is an iterative technique and begins by dividing a set of i values into j sub-sets each containing m values, where $j = i/m$ and m is a small odd integer, typically 3, 5 or 7. Each of the sub-sets is then sorted, at little cost, and a set of j median values are found, one taken from each sub-set. In the next iteration, we repeat the process but begin with a smaller set of values where $i = j$ and the members of the set are the medians found in the previous iteration. The process continues until the set of values under consideration contains only m members and its median is the approximate median of the original set of values. The number of iterations required equals $\log_m i$.

We carried out experiments populating data stores with randomly generated data and setting m variously to 3, 5 and 7. In some experiments *datum-points* were stored in coordinate value order and in others they were stored in no order. We noted that where *datum-points* were stored in a random or arbitrary order, the median-of-medians technique generally found medians which were closer to the true medians. As a result, the data stores created generally contained fewer pages since, when pages were split, they were divided more evenly. It appears that when *datum-points* are ordered by coordinate value a partial ordering by *derived-keys* results, and to some extent this frustrates the process of calculating an approximate median.

In order to improve the balance of page splitting where *datum-points* are sorted by coordinate value, we place the calculated *derived-keys* in randomly chosen positions on the temporary page referred to above. This simulates a random ordering of *datum-points* on the original page. This strategy enables us to achieve similar results in terms of final file size for sorted data as we had achieved with unsorted data.

As a final refinement, once the median-of-medians process has reduced its set of working data to between 30 and 50 median values, then rather than continue we simply sort these values and take their median as the approximate median. In experiments, this approach was also found to result in identifying approximate medians which are closer to true medians of a set of *derived-keys*.

7.4.3.2 Moving Data to Underpopulated Pages

Determining which *datum-points* to move from one page to an underpopulated neighbour proceeds in a similar manner to that described in the previous section except that we need to find the approximate median *derived-key* of all of the *datum-points* on both pages. In describing the technique, we assume that the underpopulated page is the successor of the page from which *datum-points* will be moved, although the reverse situation is equally

possible and handled in a similar manner.

Initially, it would appear that finding the approximate median of two pages of data entails twice as much work as finding the median of a single page. Nevertheless, when we move data to an underpopulated page, the combined occupancy of the two pages participating in the process will never exceed the sum of the capacity of one page plus the minimum allowed occupancy of a page. Furthermore, we know that the median cannot lie on the underpopulated page. Where the latter is the successor page, we also know that all of the *datum-points* on it must map to *derived-keys* which are greater than the median and thus we are able to disregard their actual values and assume instead that they are arbitrarily high. It is therefore unnecessary to perform any median calculations relating to *datum-points* on the underpopulated page, thus simplifying the procedure. Having found the approximate median, which will be on the larger page, we transfer *datum-points* which map to this *derived-key* and higher *derived-keys* to the underpopulated page in a manner such that records on both pages are maintained in coordinate value order.

7.4.3.3 General Procedure for Dealing with Underpopulated Pages

The techniques described in the previous section leads us to adopt the procedure given in Algorithm 7.4.1 when dealing with pages which have become underpopulated following record deletion. It can be seen that this is no different from that which is applied to one-dimensional data.

Algorithm 7.4.1 Procedure for Dealing with Underpopulated Pages

```
1:  if the page is underpopulated then
2:    if the page has a predecessor then
3:      retrieve the predecessor page
4:      if the combined capacity of the underpopulated page and its predecessor is less
        that that of a single page then
5:        merge the underpopulated page and its predecessor
6:        delete the underpopulated page from the index
7:      else
8:        move some records from the predecessor to the underpopulated page
9:        update the index entry for the underpopulated page
10:     end if
11:   else
12:     retrieve the successor page
13:     if the combined capacity of the underpopulated page and its successor is less that
        that of a single page then
14:       merge the underpopulated page and its successor
15:       delete the successor page from the index
16:     else
17:       move some records from the successor to the underpopulated page
18:       update the index entry for the successor page
19:     end if
20:   end if
21: end if
```

An advantage of our approach to indexing of multi-dimensional data is that it is possible to experiment and implement a variety of alternatives to this strategy. One example would be to always attempt to perform a page merge as a first priority. We conjecture, however, that the opportunity to merge two adjacent pages would occur relatively rarely.

This strategy would, therefore, probably almost always entail retrieving both the predecessor and the successor of an underpopulated page and ultimately result in moving data from one of an underpopulated page's neighbours anyway. Thus the overhead of possibly reading an additional page into memory, if it is not already present, would not be worthwhile. Our strategy, therefore, gives priority to merging an underpopulated page with its predecessor or moving data from the latter.

7.5 Potential Variations to the Indexing Implementation

The particular querying experiments carried out, using random data, and reported on later in chapter 10 found fewer pages required to be searched where data is held in the Grid File, rather than in our storage application.

Although the number of pages searched is not the only factor of importance in comparing the two file organization approaches, we are motivated to investigate whether strategies exist for improving the performance of our implementation which are not available to the Grid File. We therefore consider two variations for determining what *derived-key* values are stored in an index, which we investigated at a preliminary level. We also briefly consider the application of B*-Tree concepts to page splitting and reorganization in our implementation.

We believe these variations to be worth considering as part of a programme for future work. They entail the carrying out of more work during updating operations but they are intended to facilitate querying. We see in chapter 10 that there is a case to be made for improving the efficiency of querying at the expense of updating since the former is the more costly operation.

7.5.1 Indexing Intervals

The indexing method we have hitherto described envisages partitioning a space-filling curve into contiguous but variable length sections, on each of which lies a set of *datum-points* of roughly the same size which is stored on a distinct page in a data file. We have seen that the *derived-key* of the first *datum-point* which is placed on a page determines its *page-key*, even if the *datum-point* is subsequently deleted.

In any database, the *datum-points* are likely to be a very sparse sub-set of all of the points which lie on a space-filling curve and so it follows that there will be many sections of curve on which no *datum-points* lie at all and that many of these may be 'long'. It is also probable that there will often be many points which will map to *derived-key* values which lie between the highest *derived-key* of a *datum-point* on a page and the *page-key* of the succeeding page.

These observations lead us to an alternative approach in which we consider a page of data as being a section of curve bounded at both ends by the *derived-keys* of actual *datum-points* rather than being bounded at the start by a *page-key* and bounded at the end by a value equal to the succeeding page's *page-key* minus one.

This alternative approach, therefore, envisages that an index entry for a page comprises of a pair of *page-keys* rather than a single one. It enables us to infer from the index some of the sections of curve on which no *datum-points* lie and so this may allow us to reduce the number of pages which must be searched in the execution of a query.

Once a page has been searched, we calculate the *next-match* which is greater than or equal to the first *page-key* of its succeeding page. We then look in the index to see whether the *next-match* lies between the pair of *page-keys* for a page and if it does, we retrieve and search the page in the normal manner. If, on the other hand, the *next-match* lies between the second *page-key* of a page and the first *page-key* of its succeeding page then we do

not need to retrieve any page at this stage and, instead, we perform a further *next-match* calculation on the first *page-key* of the succeeding page. We continue in this way until we either find a *next-match* which lies between a page's *page-keys* or until we find there is no higher match to the query.

The penalties which are associated with this approach relate to index maintenance. The most obvious implication is that the index size is almost double that of the method described previously, since a page requires two *page-keys* instead of one.

If a *datum-point* is inserted into the data store and its *derived-key* does not lie between a page's *page-keys*, then we must decide which of two possible pages to place it on and update one of that page's *page-keys* in the index to suit.

If a *datum-point* is deleted, we must check to see if its *derived-key* is a *page-key* for the page it is stored on and, if so, examine the other *datum-points* on the page, calculating their *derived-keys* in the process, in order update the appropriate *page-key* for the page. This task would clearly be simple if data is stored in *derived-key* order but not if data is stored in coordinate order unless an index is held on a page to map *datum-point* locations to their *derived-key* order. Nevertheless, such an index would be relatively compact, occupying one or two bytes times the number of *datum-points* which can be stored on a page. The relative cost of such an index, as a proportion of the size of a data file, decreases as the number of dimensions in space increases.

A further complication which we may choose to address is that a page may overlap longer sections of curve on which lie no *datum-points* than exist between pages. This invites consideration of the potential for maximising the lengths of curve sections which lie between pages by judiciously moving *datum-points* from a page to one of its neighbours.

We performed some limited experiments with randomly generated data on a variation of our software which implements the concept of indexing pages with pairs of *page-keys* which are updated as records are inserted and deleted but did not find the results to be very promising. On reflection, this is perhaps not surprising where random data is used since the length of a curve section which lies between two pages is typically no longer than a curve section which lies between any pair of *datum-points*. This leads us to speculate that the concept is more likely to prove beneficial in an application where data is highly and multiply clustered.

7.5.2 Adjusting Page-key Values to Influence Page Shape

We note that partitioning space by dividing a space-filling curve into sections can result in sub-spaces with lower volume to surface area ratios than sub-spaces created by the Grid File and having similar minimum lower bound and maximum upper bound coordinate values. These sub-spaces can have convoluted boundaries which, in turn, can result in hyper-rectangular query regions intersecting with more pages than where sub-spaces are themselves also hyper-rectangular. This is illustrated by example in Figure 7.1.(a).

By moving certain *datum-points* from one page to an adjacent page the 'shapes' of the pages are changed and it is sometimes possible to coerce them into forms which are more hyper-rectangular. This can reduce the number of pages which intersect with a query region and is illustrated in Figure 7.1.(b) in which one *datum-point* has been moved from page number j to page number $j-1$ for $1 < j \leq 4$.

We note that if all of the *page-keys* in an index had values of zero in their bottom i bit positions, where i is an arbitrary number, then the partitioning would in effect result in a set of hyper-cubes. Such a partitioning is likely only to be achieved in practice where data is randomly distributed and where a page size is chosen fortuitously.

Nevertheless, it would be possible to attempt to index pages with *page-keys* which contain as many zeros as possible in lower bit positions. Such *page-keys* would, in general,

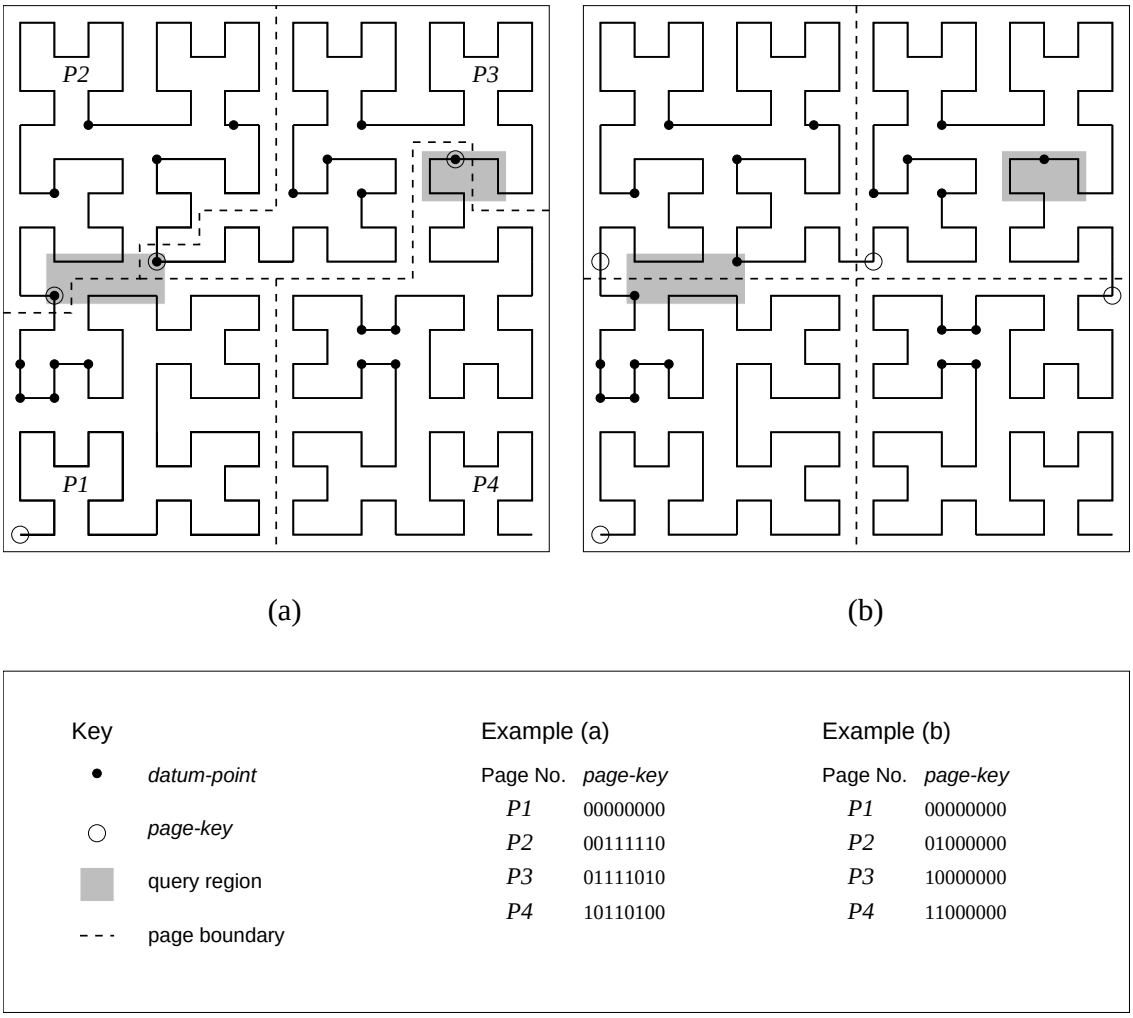

Fig. 7.1: Example showing how the choice of page-key affects page shape

not correspond to *datum-points* placed on pages. In order to determine these *page-keys*, the only information required in addition to that which is available in our standard implementation would be the highest *derived-key* of any *datum-point* on a page. A page's *page-key* would then be a value which lies between the lowest *derived-key* of any *datum-point* on it and the highest *derived-key* of any *datum-point* on the preceding page. As in the previous section, it would be necessary to keep track of the highest *derived-key* of a *datum-point* on a page during updating but the index size would remain the same as in our standard implementation.

7.5.3 The Application of B*-Tree Concepts

Our data store design utilizes a B^+-Tree index to organize pages of data but such a distinction between index and data is arbitrary and the data pages may be considered simply as leaf nodes of a B^+-Tree.

This notion encourages us to consider the application of characteristics of variations to the B-Tree, other than those of the B^+-Tree, in managing page splitting and merging on the insertion and deletion of data. For example, the B*-Tree, attributed to Knuth [Knu73] and discussed by Comer [Com79], is of particular interest since it guarantees a minimum node occupancy of 66%, compared with 50% for the B^+-Tree. This is achieved by delaying page splitting. When a page is fully occupied, instead of it being split into 2 pages, data

is transferred to a sibling node. When both siblings are full, they are divided into 3 pages, each with an average data occupancy of 66%. This strategy could be readily applied to page splitting (and page merging) within our implementation and thus potentially result in more compact data stores (and indexes) requiring fewer pages to be searched in the execution of queries.

7.6 Concluding Remarks

In this chapter we have described our implementation of the concept of using a mapping to a space-filling curve in an application for the storage and retrieval of multi-dimensional data. This implementation comprises a number of component parts addressing different requirements of the application. To varying degrees these parts influence each other or they are independent of each other.

Particularly where they are independent of each other, scope exists to vary the implementation and such variations may impact on its performance. During the course of our research it has been necessary to make considered choices but we cannot be certain that these have, in all cases, been optimum choices. Determining this is an area for further research and the observations we make in section 7.5 suggest a number of directions this research might take.

Chapter 8

COMPARISON WITH OTHER FILE ORGANIZATION METHODS

In chapter 2 we summarize previous work relating, inter alia, to the organization of multi-dimensional data. In this chapter we return to this subject, having described our approach and its implementation, in order to compare it in some detail with two other well known approaches; the Grid File and the BANG File. In particular we focus on some of the implications of the design strategies for issues such as index growth, page occupancy, what is stored on a page and how updates are managed.

8.1 The Grid File

The Grid File is a method for partitioning multi-dimensional space proposed by Nievergelt et al [NHS84] which has been the subject of considerable interest and which we found to be the most frequently cited in research literature on the subject. It forms the basis for the existing Triple Store implementation utilized by the TriStarp Group.

8.1.1 The Index

We noted in chapter 2 that a drawback of the Grid File is the exponential growth rate of its index size and a need for periodic substantial index reorganization. Ameliorating this was the principal contribution of the research carried out by Derakhshan [Der89] but, in our view, problems remain and these contribute to the motivation for our research. They relate to the amount of reorganization that is required to the index when a data store is updated, the growth in size of the index as data is added, the conflicts which arise in determining the way pages are divided and the manner in which pages are identified for searching in the execution of a query.

We recall that in the Grid File design, a page of storage corresponds to a hyper-rectangular sub-space of the key-data domain and that a hyper-rectangle is defined by n sub-intervals, one for each dimension. A sub-interval in dimension d is delimited by a lower bound and an upper bound value in dimension d.

Derakhshan's system for indexing these sub-spaces comprises 3 principal components called *E-Scales*, *S-Modules* and *R-Modules*. A simple 2-dimensional example is shown in Figure 8.1.

An *E-Scale* exists for each dimension and comprises a list of the sub-intervals into which a dimension has been divided. A division exists in an *E-Scale* for dimension d if at least one page has been divided on dimension d. If all sub-spaces span the whole domain in some dimension d then the *E-Scale* for that dimension is not divided and contains a single entry.

For each entry or sub-interval which exists in an *E-Scale* for dimension d, the *S-Module* contains an *S-List* which is a list of the identifiers of all of the pages or sub-spaces which intersect with the sub-interval in dimension d. If a page spans more than one sub-interval

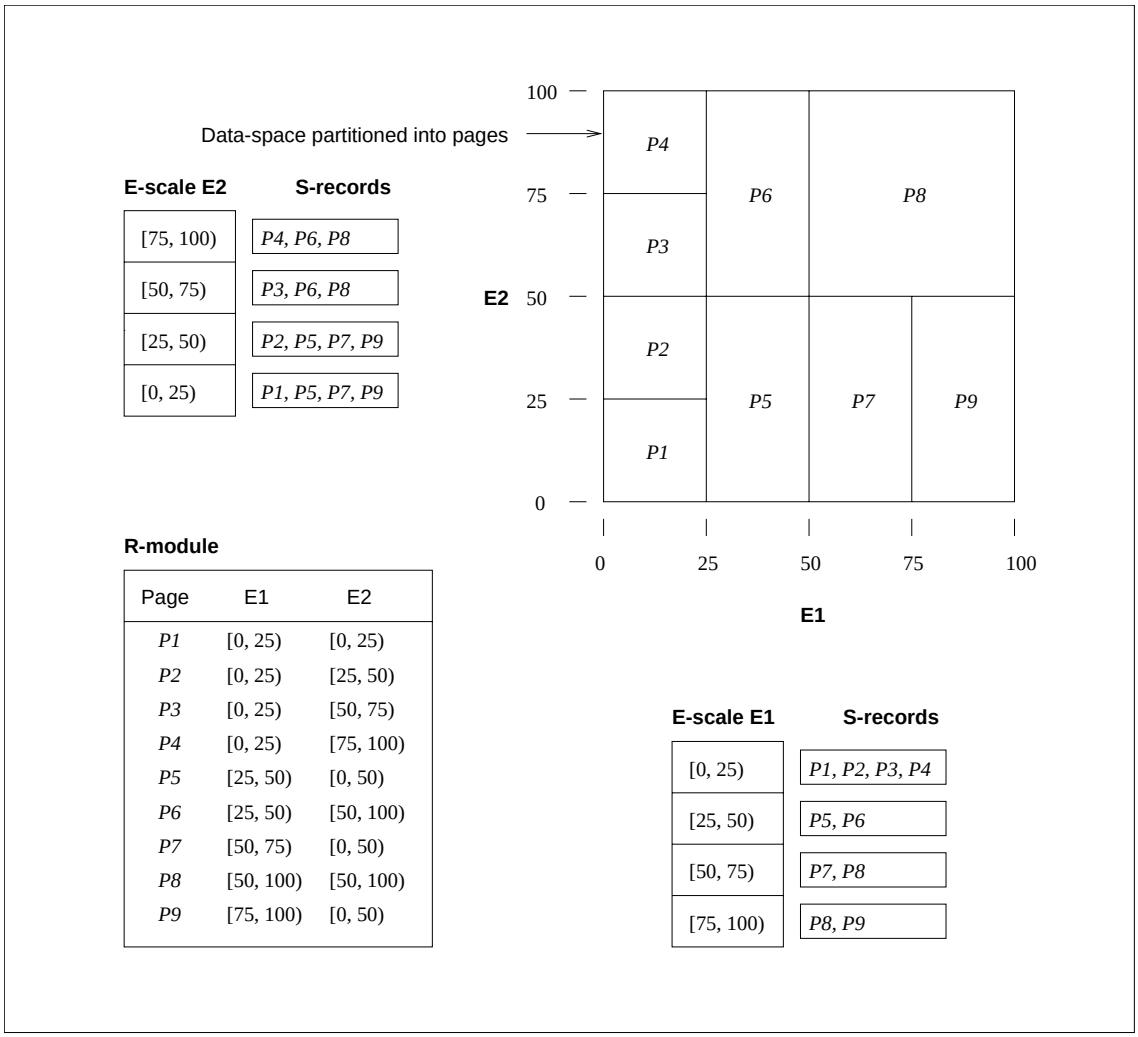

Fig. 8.1: Example of Derakhshan's Grid File Index

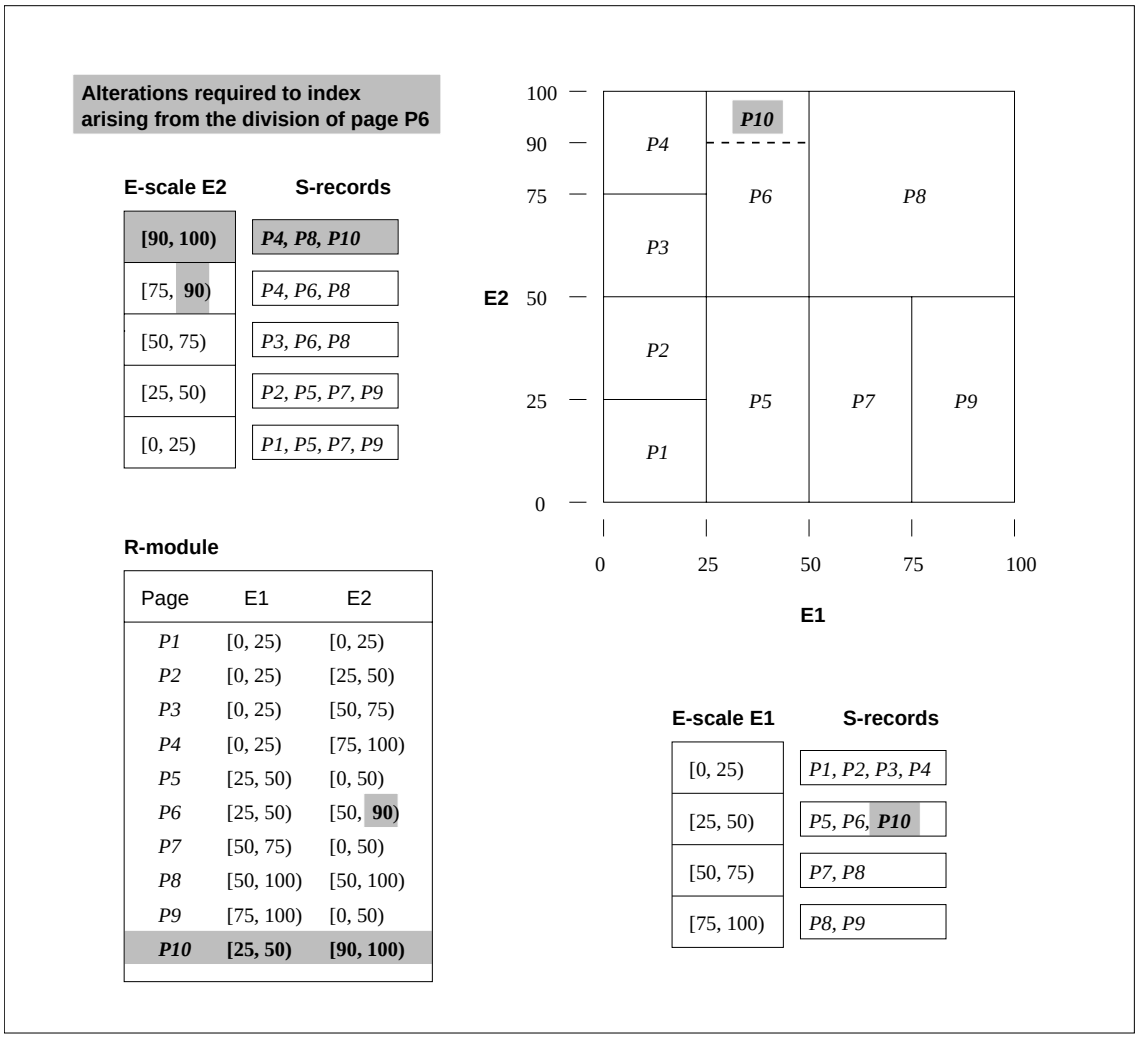

Fig. 8.2: Example showing the implications of a page-split in the Grid File

into which a dimension has been divided then its identifier appears in more than one *S-List*.

The *R-Module* is a list of page identifiers and their corresponding pairs of lower and upper bound coordinate values in each dimension.

In Figure 8.2 we show an example of updates required to the components of the index if an existing page, $P6$, is divided into two disjoint sub-spaces, with page identifiers $P6$ and $P10$, along a boundary in a dimension which requires the division into two of an existing sub-interval in an *E-Scale*.

Changes required to the index are as follows:

1. A new entry is added to the *E-Scale* for dimension y.
2. The interval for the original entry is redefined.
3. A new *S-List* is created for the new entry which is identical to the original except it contains the identifier for page $P10$ instead of $P6$.
4. One *S-List* for all other dimensions, just one in our 2 dimensional example, is updated to include the new page.
5. The entry for $P6$ in the *R-Module* is updated and an entry for $P10$ is added.

Had the boundary between pages $P6$ and $P10$ in dimension y coincided with that between pages $P3$ and $P4$ then less work would have been required: steps 1-3 would have been replaced by simply updating the *S-List* for the sub-interval in the dimension y *E-Scale* which contains $P3$ so that $P10$ replaces $P6$.

It can be seen from this example that a significant amount of growth in and modification to the index can be required on the creation of a new data page. This can be ameliorated by preferentially dividing an overpopulated page along a hyper-plane which has previously been used to divide some other page. A conflict therefore arises in dividing a page, between choosing a dividing hyper-plane leading to minimal index modification and one which evenly distributes *datum-points* between the two resulting pages. This problem is not unique to any particular implementation of the Grid File and also arises in other file organization methods which partition the space containing the key-data rather than partitioning the data itself.

8.1.2 Management of the Storage of Data

The natural choice of format for storing data in a Grid File is the same as that chosen in our space-filling curve application. Data is stored as sets of coordinates of points and ordered by coordinate value and so the insertion and deletion of records and page searching is carried out in the same way as described in chapter 7.

8.1.2.1 Page Splitting

When a page becomes overpopulated it is necessary to determine along which dimension and on which value in the chosen dimension to perform a division. The dimension may be chosen in a cyclical manner or, alternatively, certain dimensions may be chosen in preference over others by the database administrator, if prior knowledge exists relating to the distribution of data and the nature of the queries which will be performed.

Comparative calculations are performed to determine the implications of various different options and these influence the final decision. A balance needs to be arrived at between a number of factors including facilitating the administrator's 'splitting policy', if any, and the amount of index reorganization and growth which would result from divisions along particular values in the different dimensions. The data distribution on a page clearly influences the value in a particular dimension along which a division may occur and, indeed, there may be more than one suitable value to choose from. Furthermore, it is desirable from the point of view of maintaining a balanced page occupancy if the final choice results in dividing a page into two which contain roughly the same numbers of *datum-points*.

Conceivably, an implementation could perform a considerable amount of calculation to determine an ideal combination of value and dimension on which to perform a division. The task becomes more formidable as the number of dimensions in a space increases and also as the size of a data file increases. In practice it is necessary to compromise in order to make the task manageable and preference is given to performing divisions along values in dimensions which coincides with divisions made previously in other pages in order to minimize the impact on the index.

In order to identify where to perform a division of a page in a particular dimension, a binary search is performed on the interval which defines the page or sub-space in that dimension until a value is found such that at least one *datum-point* exists on the page which has a coordinate value in that dimension which is less than or equal to the value and at least one *datum-point* exists on the page which has a coordinate value in that dimension which is greater than it.

Identifying a suitable value is straightforward in the case of the dimension which corresponds to the first coordinate on which *datum-points* are ordered on a page but identifying values in other dimensions results in at least a partial serial search of the page. If a value is required such that a division would result in two sets of *datum-points* which are approximately equal in size, then the process becomes more problematic for dimensions other than the one in which *datum-points* are primarily ordered. One option would be to find the approximate medians in all dimensions in a similar manner to that adopted in our space-filling curve implementation.

The compromise which is therefore adopted in the Grid File implementation is that emphasis is placed on the division of sub-spaces into two sub-spaces which are as similar in size as possible but with no regard to the division of *datum-points* save that no new page is created which would be empty. It is conceivable that an overpopulated page may be divided so that only one *datum-point* is placed on the new page or remains on the original page. It follows that in a pathologically worst case scenario, a data store may contain just one *datum-point* on all but one page.

8.1.2.2 Underpopulated Pages

As with dividing overpopulated pages, the merging of an underpopulated with another or the redistribution of data to an underpopulated page from a neighbouring page in the Grid File system is less straightforward than in an application underpinned by space-filling curves.

The Grid File requires that all sub-spaces corresponding to pages are hyper-rectangular in form. Thus an underpopulated page can only be merged with a neighbouring page if both pages correspond to hyper-rectangles defined, in part, by hyper-planes which are of the same size and unit distance apart in one dimension. Where this requirement is not met by a hyper-rectangle and any of its neighbours, the well known problem of *deadlock* arises. An example of this in 2 dimensions is illustrated in Figure 8.3, where a page shares a boundary of the same length with none of its neighbours. Deadlock can be difficult to resolve and entail redistributing *datum-points* from an underpopulated page to several of its neighbours. The hyper-rectangles which define the recipient pages will inevitably change in one or more dimensions and this needs to be reflected in their index entries. Identifying candidate pages with which to merge can entail a significant amount of analysis of the index and in some situations there may be a variety to choose from.

As an alternative to merging an underpopulated page with one or more others, it may be possible to *import* data from a neighbour and this will require adjusting their boundary positions and updating the index accordingly. In order to maintain the hyper-rectangular form of all pages, it may be necessary to import data from more than one page to an underpopulated page.

Adjusting the position of a boundary between two pages is not necessarily difficult where it is orthogonal to the dimension in which *datum-points* are primarily ordered on a page but this is not the case in other dimensions. Moving a boundary results in zero or more records being moved from one page to its neighbour. It is necessary to serially scan the whole of the page which will become smaller in order to determine exactly how many records will move from it. If the result is too many or not enough records, then an alternative new boundary position must be chosen and the process of counting the number of records affected must be repeated.

8.1.3 Query Execution

A characteristic of Derakhshan's Grid File which arises from its index design is that in order to identify which pages overlap with a query region, it is necessary to perform an intersection of all of the page lists which overlap with all of the sub-intervals in all

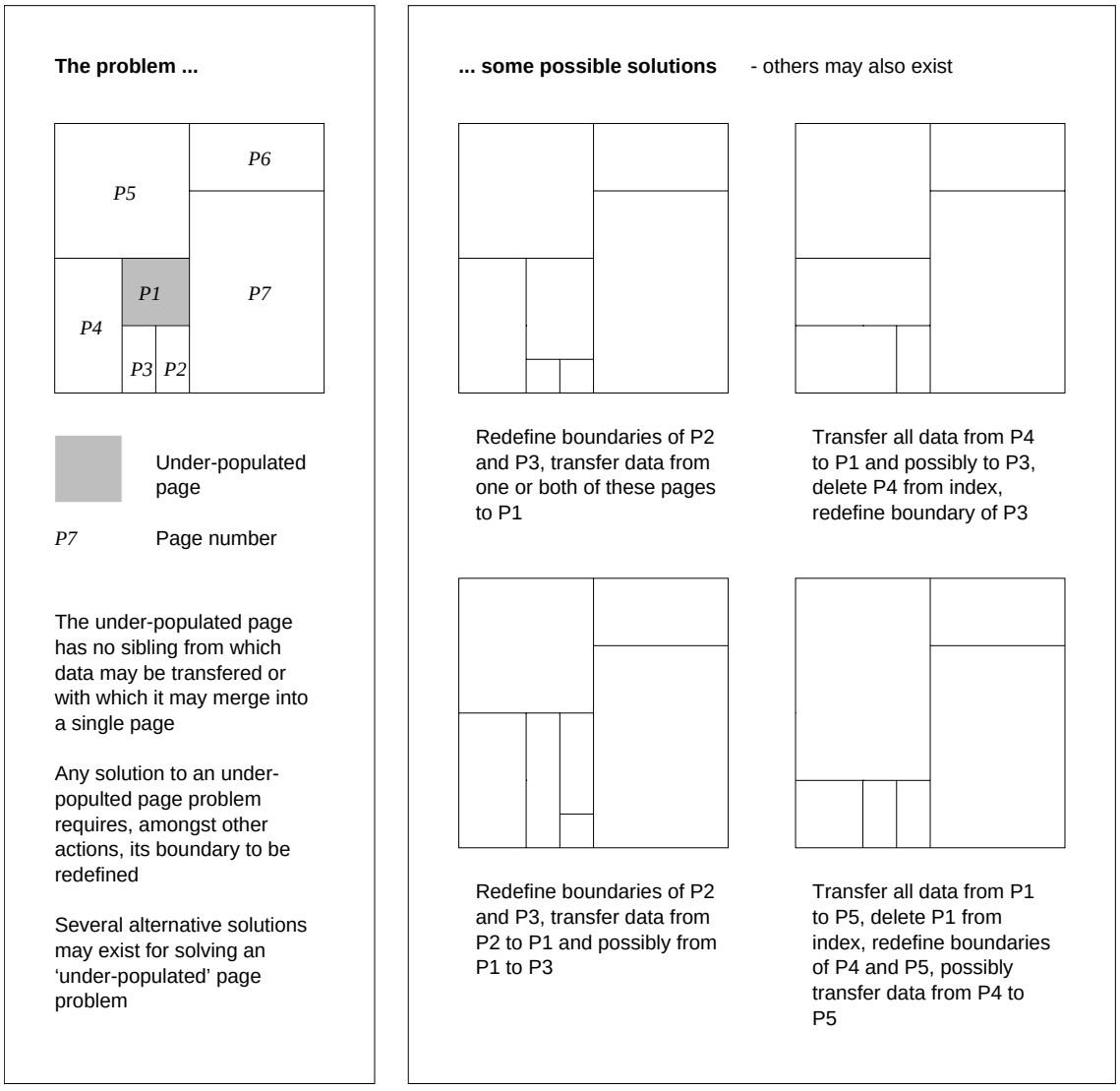

Fig. 8.3: Example showing *deadlock* in a Grid File

dimensions which define a query. If the *E-Scales* are divided into relatively few sub-intervals by ensuring wherever possible that page boundaries coincide, then *S-Lists* are likely to be long in consequence. On the other hand, if there are many divisions of *E-Scales*, then a query region is more likely to overlap in any dimension with more sub-intervals. This means that more intersections of *S-Lists* relating to the same *E-Scale* will be required prior to performing of merged *S-Lists* relating to different *E-Scales*.

The scale of this problem increases with the number of dimensions in space and we illustrate this with a simple example. Suppose we have a data-store in 16 dimensions in which *datum-points* are randomly distributed on 65,536 pages, then if the dimensions are divided in a cyclical manner, then each dimension will have been divided once. Even if a query region does not cross any divide, identifying which pages to search will entail initially intersecting two *S-Module* lists of $65,536/2$ pages, followed by 15 intersections of the result of the previous operation with lists of $65,536/2$ pages.

A further disadvantage encountered by the Grid File is that although records can be returned in a lazy fashion to the user, a list of all of the pages which overlap a query region must be constructed in an eager fashion regardless of how many records are actually required. Applications such as the TriStarp Group's functional programming language

FDL, which utilizes a Triple Store, frequently execute queries where a list of values is returned but only the head of the list is required.

Eager evaluation of pages which overlap a query region imposes restrictions or at least obstacles in terms of concurrent querying and updating. If a page is added or deleted or even if data is redistributed from one page to another then lists of pages which are required by on-going queries must be re-evaluated.

8.2 The BANG File

Like the Grid File, the BANG File of Freeston [Fre87] is prominent in the literature. This method of indexing multi-dimensional data also approaches the problem by partitioning data space rather than *datum-points* but it overcomes some of the problems encountered in the Grid File. In common with our application of space-filling curves, the BANG File utilizes a tree structure for its index but instead of indexing points or their *derived-keys*, it indexes sub-spaces, drawing on concepts of Z-ordering in doing so.

A major characteristic which differentiates the BANG File from other file organization methods is that it allows a partitioning in which sub-spaces can be nested within others. This offers a number of advantages, including a greater flexibility and ease with which space can be partitioned. This facilitates maintaining a more optimum storage utilization (a minimum of 33%) and avoids the deadlock problem of the Grid File. It also permits the implementation of an index structure which has a worst case growth rate which is proportional to the amount of data which is stored.

A sub-space is identified by the prefix which is common to all of the Z-order *derived-keys* of points lying within it. If the identifier of one sub-space is a prefix of that of another then the latter is 'nested' within the former. A prefix may contain an odd number of bits in which case the corresponding sub-space is twice as long in one or more dimensions than it is in at least one other. Smaller sub-spaces are identified by longer prefixes. A simple 2-dimensional example, based on an example which appears in [Fre95a], is given in Figure 8.4(a).

We note that *datum-points* which are not in close proximity to each other, for example points A and B in the Figure, may be placed on the same page of storage and that *datum-points* lying between them may be clustered together on separate pages.

8.2.1 The Index

The original paper describing the BANG File [Fre87] concentrates on the method of partitioning a data space and the bulk of the subsequent work [Fre89a, Fre89b, Fre92, Fre93, Fre95a, Fre95b, Fre97] addresses the index design. Dividing sets of overlapping sub-spaces into nodes in the index structure appears to have been particularly problematic.

Freeston's BANG File index, called the BV-Tree [Fre93], is not height balanced but aims to achieve a level of performance which is equivalent to that of the B-Tree, in part by allowing variable node sizes in the tree. The index to the partitioning example given in Figure 8.4(a) is given in Figure 8.4(b) and illustrates the characteristics of the BV-Tree. Sub-space identifiers are placed in order of decreasing size from left to right within a node; thus a sub-space is placed to the left of those which it encloses, if any. If the superscript of a sub-space's label is lower in value than those of any to the right then the former encloses (but does not coincide with) the latter and it is called a 'guard'. In a worst case situation, approximately half of the entries in an index may be guards.

We note from the existence of guards that a space cannot always be partitioned in a manner which allows a page containing a particular point to be identified by a direct and simple index traversal from the root of the tree to a leaf. For example, in locating the

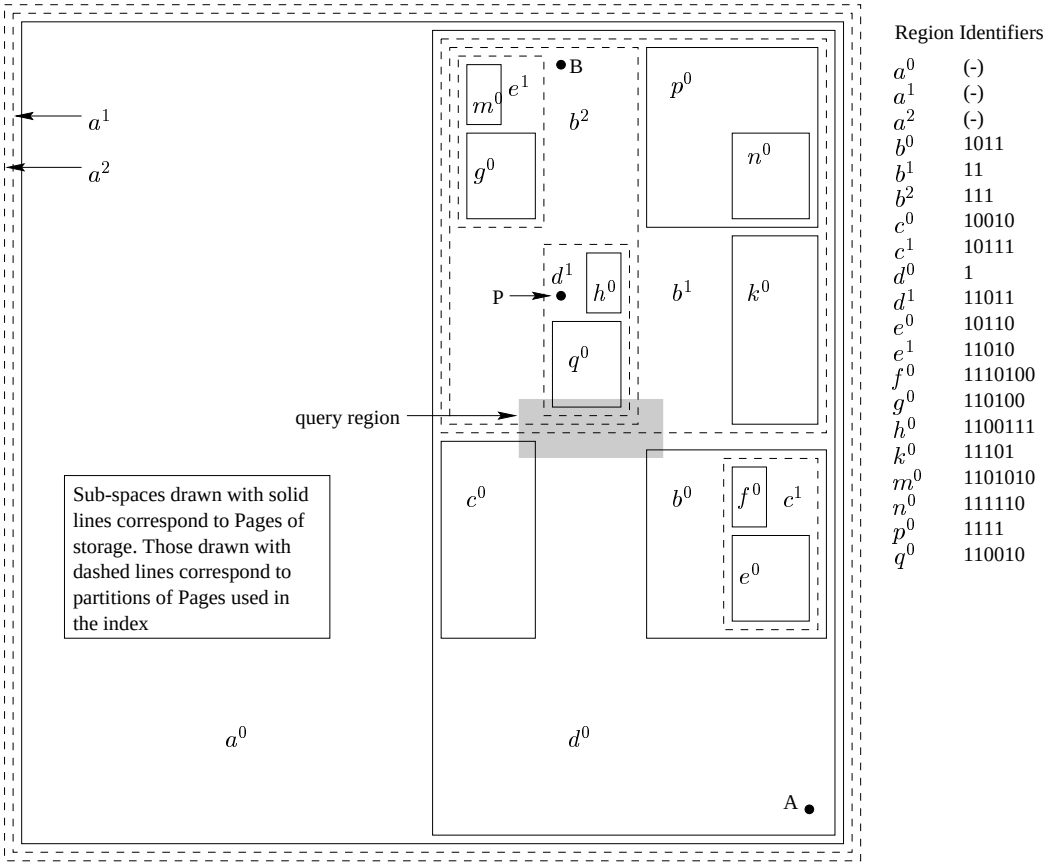

(a) Example of a Partitioning of Space into Pages

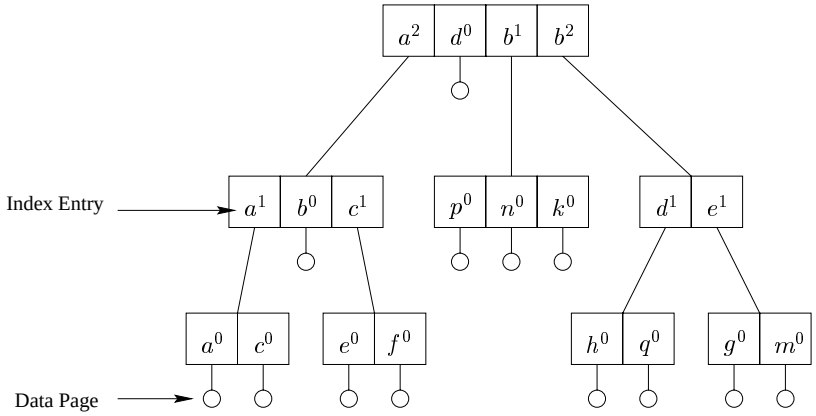

(b) BV-Tree Index for Example

Fig. 8.4: Example Partitioning of Space in the BANG File and Associated Index

page enclosing point P in Figure 8.4(a), the root is initially visited and found to contain three sub-spaces, d^0, b^1 and b^2, enclosing the point. These are examined in turn, starting with the smallest; b^2. Within the child node pointed to by b^2, sub-space d^1 is found to enclose P and so the node containing sub-spaces g^0 and m^0 is searched, but found not to enclose P. The process conceptually back-tracks to b^1 and searches its child node, which does not contain a sub-space enclosing P, before 'back-tracking' again to find that d^0 is the matching page.

8.2.2 Management of the Storage of Data

It is not clear from [Fre97] in what format or order data is stored in the BANG File although, as with our system, this is an issue which is, to some degree, independent of the file organization method design. It does appear, however, that an optimum solution which simultaneously serves the interests of updates and queries is more difficult to arrive at in the BANG File.

8.2.2.1 Overpopulated Pages

An overpopulated page is divided into two by separating out from the original a sub-set of *datum-points*, all of the members of which map to Z-order *derived-keys* sharing a common prefix. Freeston shows that in a worst case it is possible to achieve a $1/3 : 2/3$ ratio of the sizes of sub-sets when a page is divided into two.

In some cases it may be necessary to choose between a number of alternative possible partitioning options and this is most simply illustrated by example in Figure 8.5. The relative implications of different options for the complexity of index reorganization required during the course of significant amounts of updating is not known. A complex decision process can be avoided by adopting an arbitrary strategy. Two options are to create sub-spaces of equal size where possible and to create nested sub-spaces which are as small as possible.

In order to identify a sub-set of *datum-points* lying on a page and sharing a common Z-order *derived-key* prefix, it is necessary to view the *datum-points* as a list of totally ordered Z-order *derived-keys*. If the *datum-points* are not stored in this form then it is first necessary to calculate the *derived-key* of each one and then to sort them. As noted in chapter 7, our application of space-filling curves allows pages to be divided about an approximate median *derived-key*. Finding an approximate medium of a set of values is significantly less computationally expensive than sorting it.

8.2.2.2 Underpopulated Pages

When a page of data becomes underpopulated, there may be several candidates with which it may be merged or from which records can be transferred onto it. As with processing overpopulated pages, the BANG File strategy for maintaining a minimum page occupancy on deletion of data is not known.

Where two pages are merged into a new single page, the impact on the index may entail the removal of an entry or, possibly, the removal of two entries and the insertion of a third, where two adjacent but not nested sub-spaces are combined.

Where data is transferred onto an underpopulated page, at least one page's identifier is deleted from the index and a new one is added if one is nested within the other. If, instead, data is transferred onto a page from an adjacent page corresponding to the same sized sub-space, ie a sibling, then two entries are deleted from the index and one is added.

Modifications to the index arising from the insertions and deletions noted here appear to be more complex than those required in our index design, particularly since entries in

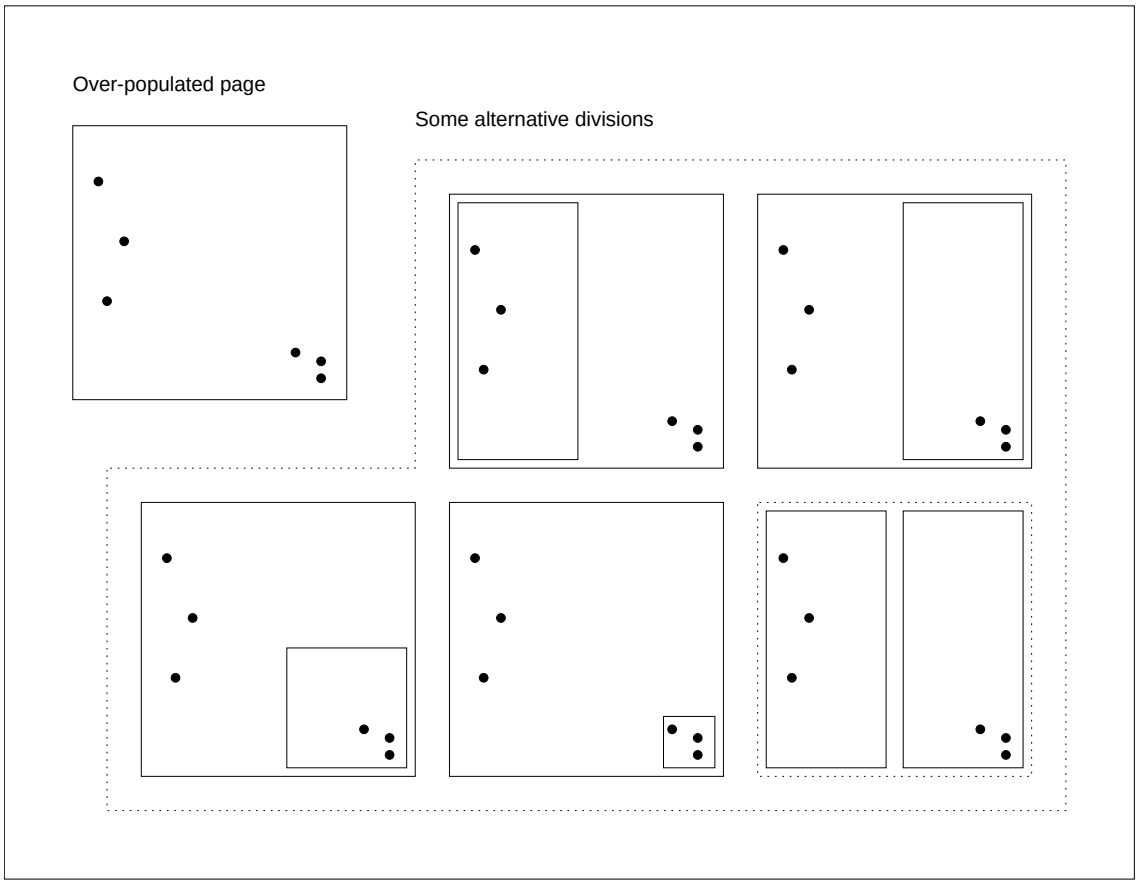

Fig. 8.5: Example showing Options for Page-splitting in the BANG File

BV-Tree nodes must under certain circumstances migrate from one tree level to another.

8.2.3 Query Execution

The manner in which a range query is executed is not given by Freeston in the literature but it appears to be a potentially complex operation. We note that the relatively small range illustrated in Figure 8.4(a) entails a search of all but two nodes in the index; ie those containing pointers to pages e^0, f^0, g^0 and m^0.

We note above in section 8.2.2.1 that storage of data on pages as ordered Z-order *derived-keys* would facilitate page splitting operations but also note, in chapter 7, that this may impede an efficient within-page search process.

Chapter 9

INDEXING OF SPATIAL DATA USING SPACE-FILLING CURVES

9.1 Introduction

Much of the previous work discussed in chapter 2 relates to file organization methods oriented towards the storage and retrieval of spatial data, as distinct from multi-dimensional point data. A point, however, is simply a particular type of spatial object and so these file organization methods may be specialized to accommodate point data, although they are not necessarily optimized for point data.

In this chapter we consider data from the opposite perspective and briefly explore the *generalization* of our point data application to the storage and retrieval of spatial data. This generalization is effected by mapping hyper-rectangular spatial objects in n-dimensional space to points in $2n$-dimensional space. For the most part, adapting our implementation to spatial data simply impacts on our querying strategy.

We do not discuss the indexing of spatial data in great detail in this thesis but we explore the potential for the application of space-filling curves with a view to carrying out further work in the future. At the present stage we are interested in the viability of the application of space-filling curves and how the approach compares with others in terms of performance. We have carried out some very limited performance testing and this has produced particularly encouraging results, as reported on in chapter 10.

Mapping to higher-dimensional space is limited to some extent in that only hyper-rectangular shaped objects can be accommodated in an application. Nevertheless, this is also a restriction which obtains in some well known systems, such as the R-tree, which are specifically designed to manage spatial data.

Hyper-rectangles are commonly used as 'minimum bounding boxes' (MBBs) which enclose and so approximate objects of a more complex spatial form. When a query such as *find the objects which overlap a particular query region* is posed, the data store is searched for all objects whose MBBs overlap the query region. If an MBB lies wholly within the region then its contents will certainly overlap it. If an MBB only partially overlaps the region then it is left to higher level software to examine the object which it contains and compare it with the region.

In this chapter we focus on 2-dimensional data but the concepts may be extended into higher-dimensional space without modification.

9.2 The Representation of Spatial Data

We use the term *base dimensions* to refer to the dimensions of a space in which a spatial object exists and the term *virtual dimensions* to refer to the dimensions of a space in which it is mapped as a point. Thus a 2-dimensional rectangle exists in 2 base dimensions and is represented as a point in 4 virtual dimensions.

A rectangle in 2 *base dimensions* is defined in the same way as a range query for point data; by the coordinates of the lower and upper bound points. Thus if a rectangle is defined in 2 dimensions as follows;

$$\text{lower bound: } \langle L_x, L_y \rangle$$

$$\text{upper bound: } \langle U_x, U_y \rangle$$

then in mapping 2-dimensional space to 4 virtual dimensions, we store the rectangle as a 4-dimensional point with the coordinates;

$$\langle L_x, L_y, U_x, U_y \rangle$$

9.3 Querying Spatial Data

Two of the most important forms of querying spatial data are *'find all objects which overlap a given query region'* and *'find all objects which are contained within a given query region'*.

When n-dimensional spatial data is mapped to $2n$ dimensions, such queries can be expressed as range queries on $2n$-dimensional points. We are able, therefore, to apply our strategy for querying point data and our *calculate_next_match* functions, described in chapter 6, without modification. It is simply necessary to express the query ranges in appropriate ways and these are described in the remainder of this section.

9.3.1 Overlap Queries

We can express the query, defined in 2 base dimensions, *'find all boxes which overlap the range with lower bound coordinates of* $\langle qL_x, qL_y \rangle$ *and upper bound coordinates of* $\langle qU_x, qU_y \rangle$*'*, by converting the query range into a 4-dimensional range query on 4-dimensional points.

We note that for an overlap to occur, then in all base dimensions the upper bound coordinates of a matching MBB must be greater than or equal to the corresponding coordinate of the query lower bound. Additionally, in all base dimensions the lower bound coordinates of a matching MBB must be less than or equal to the corresponding coordinate of the query upper bound.

We specify the query range as follows;

$$\text{lower bound: } \langle MIN, MIN, qL_x, qL_y \rangle$$

$$\text{upper bound: } \langle qU_x, qU_y, MAX, MAX \rangle$$

where *'MIN'* and *'MAX'* are the minimum and maximum coordinate domain values. In our implementation, these are zero and $2^k - 1$ respectively, where k is the order of the curve. A query of this form will retrieve all MBBs, with lower bounds of $\langle L_x, L_y \rangle$ and upper bounds of $\langle U_x, U_y \rangle$, which simultaneously satisfy all of the following requirements:

$$\text{MIN} \leq L_x \leq qU_x$$

$$\text{MIN} \leq L_y \leq qU_y$$

$$qL_x \leq U_x \leq \text{MAX}$$

$$qL_y \leq U_y \leq \text{MAX}$$

9.3.2 Containment Queries

Distinct from *overlap* queries, *containment* queries retrieve all MBBs which are totally enclosed within a query range. For containment to occur, then in all base dimensions both the lower and upper bound coordinates of a matching MBB must be greater than or equal to the corresponding coordinates of the query lower bound and less than or equal to the corresponding coordinates of the query upper bound.

We specify the query range as follows;

$$\text{lower bound: } \langle\, qL_x,\, qL_y,\, qL_x,\, qL_y \,\rangle$$

$$\text{upper bound: } \langle\, qU_x,\, qU_y,\, qU_x,\, qU_y \,\rangle$$

A query of this form will retrieve all MBBs, again with lower bounds of $\langle\, L_x,\, L_y \,\rangle$ and upper bounds of $\langle\, U_x,\, U_y \,\rangle$, which simultaneously satisfy all of the following requirements:

$$qL_x \leq L_x \leq qU_x$$

$$qL_y \leq L_y \leq qU_y$$

$$qL_x \leq U_x \leq qU_x$$

$$qL_y \leq U_y \leq qU_y$$

9.4 Implementation and Testing

The concepts described in this chapter are implemented simply and enable us to carry out preliminary experimentation which is documented in chapter 10.

We noted above that the concept of mapping n-dimensional hyper-rectangles to $2n$-dimensional space can be applied to any point data file organization method. Thus we are able to repeat the our experiments on Derakhshan's [Der89] Grid File implementation for comparative purposes.

Furthermore, we have been able to obtain a copy of the source code [Gut95] for Guttman's [Gut84] R-Tree on which we are also able to repeat our experiments for comparative purposes.

Chapter 10

RESULTS OF SOME PRELIMINARY TESTING

In the preceding chapters we describe our development of the concept of organizing data by mapping multi-dimensional points to points on a line, and the implementation of the concept to produce a working persistent data store. The implementation is sufficiently developed to enable it to be applied to practical application domains, in up to sixteen dimensions. Little modification is required to enable the implementation to be applied in higher dimensional space.

Our implementation enables the concept of the application of space-filling curves to the organization of multi-dimensional data to be tested in a more realistic manner than already reported on in the literature. In contrast, we noted in section 2.2.1 of chapter 2 that previous work has been confined to theoretical analysis and simulation experimentation to explore the clustering properties of space-filling curves. Furthermore, previous work has generally been restricted to 2 and 3-dimensional spaces containing a limited number of points only.

Considerable scope exists for carrying out performance tests on our application. In this chapter, we provide an outline of possible tests and the principal parameters which should be taken into consideration. More importantly, we report on the results of tests which we were able to undertake during our research. These tests are, however, necessarily preliminary in nature due to the limitations of the time available in which to carry them out. Time constraints also restricted us to using randomly generated data, which is not ideally suited to the purpose. We conclude this chapter by also reporting on preliminary tests carried out on spatial data.

Much of our testing focuses on comparing the characteristics of different space-filling curves. In addition, we have repeated the tests executed over our implementation on the TriStarp Group's existing Grid File implementation of Derakhshan, again for comparative purposes. This entailed implementing some improvements to the Grid File software, where scope for this was identified following experience gained in producing our own implementation.

10.1 Test Parameters

In this section we summarize parameters to be measured and comparisons to be made during the course of our practical experiments carried out using our implementation and described below in section 10.2.

Parameters to be measured

- Storage Utilization: the ratio of the volume of data which is held within a file to the size of the file.
- Index size: the ratio of the size of the data store to the data structure(s) used to index it.

- Time taken to update a data file.
- Time taken to execute partial match and range queries on a data file.
- The number of pages 'touched', ie searched, in the course of query execution.

Storage utilization is largely influenced by how evenly the data on a fully occupied page of storage is divided between two replacement pages, which initially have an average 50% storage utilization. Utilization is subsequently improved as more data is added to these pages but can degrade if pages do not merge when their occupancies fall below some predetermined threshold when data is deleted. If page merging is a complex process, then a file organization method may delay the operation at the expense of maintaining a high storage utilization. Ideally, a high level of storage utilization should also be maintained throughout the 'life' of a data store, rather than it be allowed to fluctuate during the course of updating.

Running times taken in the execution of updates and queries are clearly of practical importance but they are difficult to assess accurately, particularly in multi-tasking environments commonly used. Nevertheless, we record the running times of our experiments since they provide a useful measure for comparison between different space-filling curves and file organization methods.

In the case of updates, running times are mainly determined by the algorithm for identifying which page may accommodate a data value. The algorithm is in turn influenced by the index design.

In the case of query execution, running time depends in part on the detail of the specification of a query. We note in section 6.2 of chapter 6 that queries of the forms we address specify hyper-rectangular regions within a data space. The number of pages in a file intersected by a query is influenced by the volume of the query region and by the ratio of the surface area to the volume. It is also influenced by the manner in which a file organization method partitions space and by the density of *datum-points* in the vicinity of the query. The complexity of the algorithm used to identify which pages must be searched is also significant in determining the running time of query execution.

The number of pages searched, or 'touched', by a query is important, not just because searching a page takes time but also because a requirement to search a page may result in reading data from secondary storage into main memory. Furthermore, a page which is already in memory may need to be written back to secondary storage in order to free memory for another page to be read. Reading and writing can be a particulary time consuming operations.

Comparisons to be made

During the course of experiments, comparisons of the following nature are of particular interest:

- The impact of the choice of space-filling curve used in the mapping.
- A comparison of mapping techniques for the Hilbert curve in less than 9 dimensions. Mappings may be carried out either with the aid of state diagrams or by calculation.
- Comparisons of performance as the number of dimensions in space increase.
- A comparison of applications underpinned by space-filling curves and the Grid File.

10.2 Tests Carried Out and their Results

In this section we describe the detail of practical experiments, carried out using our data storage implementation, and report on the results of the experiments. The experiments were repeated using a variety of space-filling curves passing through spaces of varying numbers of dimensions, and were also repeated using the TriStarp Group's existing Grid File, for comparative purposes.

As a result of the limited time available for carrying out tests, randomly generated data has been used to populate data stores and queries have also been randomly generated.

The experiments were oriented to observing the characteristics of our implementation in relation to the insertion and querying of data. No experiments entailing deletion of data or mixed updating (alternating insertion and deletion) were carried out and these are left as a topic for further research. Nevertheless, in using our implementation under the higher level TriStarp Group software, we were able to ascertain that it functions correctly with respect to those aspects of updating other than simple insertion.

We carried out tests using the following space-filling curves: the Hilbert curve, our variation of Moore's curve, the Z^A-order and Z^B-order variations of the Z-order curve, and the Gray-code^A, Gray-code^B, and Gray-code^F variations of the Gray-code curve.

Tests were carried out using randomly generated data in 3, 4, 6, 8, 10, 12 and 16-dimensional spaces. As noted in chapter 7, our implementation is easily extended into higher-dimensional space. Experimentation in higher-dimensional space is left as a topic for further research.

Mappings for the Hilbert curve were facilitated both by calculation and by using state diagrams, although tests were limited to a maximum of 8 dimensions where the latter method was used. State diagrams only were used for mappings for the Gray-code curves and for our variation of Moore's curve. Tests were limited to a maximum of 8 dimensions for the Gray-code^F curve and Moore's curve. Since Gray-code^A and Gray-code^B curve state diagrams are relatively compact, containing 2 states for all values of n, we were able to carry out experiments in spaces of all of the chosen numbers of dimensions. Z-order mappings were carried out using calculation.

Memory buffer sizes were chosen to be sufficiently large to enable data files to be accommodated wholly within main memory.

Pages sizes were varied in the experiments such that page capacity, in terms of the number of records, remained a constant regardless of the number of dimensions in space. The page size for experiments carried out in $2n$ dimensions was twice as large as that used in n dimensions. Thus, in practice, our data stores all contained approximately the same number of pages of data, typically 8450 +/- 150 pages.

10.2.1 Data File Creation

All data stores created for use in the experiments were populated with 3 million randomly generated *datum-points*. All coordinate values of *datum-points* were integers in the range $[0 \ldots 2^{32} - 1]$.

As we see below, storage utilization for the Grid File can fluctuate significantly as data is inserted. The number of 3 million records inserted was chosen following preliminary experiments in which this number (amongst others) was found to result in Grid File data stores whose storage utilizations were average, for the page sizes used.

	3	4	6	8	10	12	16
Hilbert (sd)	6:54	7:31	9:32	11:52			
Hilbert (calc)	12:42	11:23	19:18	17:55	25:37	26:21	28:14
Moore	5:58	6:19	7:51	11:14			
Gray-code^A	4:45	6:29	8:32	9:31	13:18	15:44	19:43
Gray-code^B	6:00	6:11	7:50	9:59	13:24	19:24	20:03
Gray-code^F	4:46	6:19	7:48	10:26			
Z^A-order	2:58	3:33	5:54	7:47	8:06	13:29	12:21
Z^B-order	2:23	3:07	5:02	7:16	8:10	13:19	12:36
Grid File	12:18	27:15	1:12:45	2:05:28	3:04:38	4:27:54	7:19:33

Notes
1. (sd) = mappings use state diagram
2. (calc) = mappings all calculated
3. Times are 'mins : secs' or 'hours : mins : secs'

Tab. 10.1: Point Data: Time taken to insert 3 million *datum-points*

The following parameters were measured during each experiment:

- How the data store grew in size as *datum-points* were inserted. The number of pages in the store was recorded at intervals of 50,000 insertions.
- The amount of time which elapsed as the *datum-points* were placed in the store.
- The size of the index relative to the number of *datum-points* placed in the store.

A summary of the times taken to insert the data into the files is given in Table 10.1.

The most striking outcome of the experiments is that all of the space-filling curve implementations required considerably less time for data insertion than did the Grid File. The performance difference between the approaches increases significantly as the number of dimensions increases.

The storage utilization of all data stores was found to be approximately 70%. Where space-filling curves are used, storage utilization was maintained at this level throughout the data insertion process. In the case of the Gid File, however, storage utilization fluctuated between approximately 55% and 85% as alternating periods of rapid growth and no growth occurred. We conjecture that this arises from the implementation failing to split pages into halves containing roughly equal numbers of *datum-points*

The simplicity of the Z-order mapping process appears to have resulted in lower running times for experiments using Z-order curves compared with other curves. Where state diagrams are used for Hilbert, Gray-code and Moore curves, running times for the Hilbert curve are generally longer, probably since its state diagrams are larger.

As expected, where Hilbert curve mappings are carried out using state diagrams, running times are less than where calculation is used. It appears, however, that the benefit of state diagrams diminishes as the number of dimensions in space increases. The difference between the running times of programs using calculated Hilbert mappings and Gray-code mappings using state diagrams also diminishes as the number of dimensions increases.

The rate at which the time required to carry out the updates increases with the number of dimensions suggests that the application of space-filling curves in the indexing of data in higher-dimensional space is viable but that the same is not true of the Grid File.

10.2.2 Query Execution

All data stores were subjected to batches of 20,000 partial match queries and batches of 200,000 range queries, generated randomly.

	3	4	6	8	10	12	16
Hilbert (sd)	15:32	25:13	32:53	36:39			
Hilbert (calc)	27:08	28:39	1:03:43	42:10	1:12:15	1:08:40	33:41
Moore	14:57	24:47	32:25	37:45			
Gray-code^A	17:34	26:22	34:19	38:07	33:53	32:16	31:22
Gray-code^B	17:23	26:33	35:19	38:37	35:03	46:22	1:12:57
Gray-code^F	17:31	25:34	34:24	38:44			
Z^A-order	15:40	24:51	30:40	33:23	28:31	32:50	1:10:37
Z^B-order	14:24	22:18	28:28	28:04	24:56	30:24	23:20
Grid File	9:07	15:55	23:07	22:02	18:45	21:00	20:27

Notes
1. (sd) = mappings use state diagram
2. (calc) = mappings all calculated
3. Times are 'mins : secs' or 'hours : mins : secs'

Tab. 10.2: Point Data: Time taken to execute 20,000 partial match queries

	3	4	6	8	10	12	16
Hilbert	5297	7012	7433	6904	6035	5008	4401
Moore	5354	7026	7432	6962			
Gray-code^A	5405	7167	7550	6855	5988	5133	4485
Gray-code^B	5775	7415	7927	7177	6207	5276	4714
Gray-code^F	5393	7171	7559	6865			
Z^A-order	6138	8106	8397	7721	6587	5645	4973
Z^B-order	6115	8023	8395	7643	6714	5627	5008
Grid File	4856	6869	7886	6467	5280	4374	3894

Tab. 10.3: Point Data: Number of pages (1000's) searched during 20,000 partial match queries

In the case of partial match queries, different queries with all possible combinations of specified and unspecified coordinate values have been used in the tests. In the case of range queries, ranges of varying size and orientation have been specified by randomly choosing lower bound coordinate values and setting upper bound coordinates to values 10% greater than the former or to the domain upper bounds, whichever is the smaller.

The following parameters were measured during each experiment:

- The amount of time which elapsed during query execution.
- The number of pages touched during each batch of queries.

A summary of the results of the experiments are given in Tables 10.2 and 10.3 for partial match queries[1] and in Tables 10.4 and 10.5 for range queries.

Random data is not ideally suited for the exploration of the clustering properties of a file organization design. Nevertheless, the experiments, in general, appear to show a correlation between the amount of discontinuity in a space-filling curve and its clustering properties in terms of the number of pages touched during query execution. Comparing the space-filling curves with each other, queries executed over data mapped to the Z-order curves result in the highest number of pages being touched, followed by the Gray-code curves. The least number of pages are touched where the Hilbert curve is used in mapping

[1] NB there are 2^n possible different forms of partial match query and so where $n = 16$, 65536 partial match queries were executed. The results have been multiplied by $\frac{20000}{65536}$ for comparison with lower values of n.

	3	4	6	8	10	12	16
Hilbert (sd)	7:32	3:14	3:18	5:58			
Hilbert (calc)	10:49	4:08	7:37	6:15	7:02	8:15	7:52
Moore	6:17	2:30	3:12	4:48			
Gray-code^A	6:52	3:55	3:52	4:18	3:31	6:07	8:02
Gray-code^B	6:52	2:58	3:32	4:02	2:28	11:35	5:52
Gray-code^F	5:48	2:53	3:31	5:15			
Z^A-order	7:01	2:52	3:25	4:27	1:35	8:21	4:57
Z^B-order	6:22	2:06	2:48	5:15	1:18	4:46	5:19
Grid File	13:00	14:01	27:53	43:36	1:00:44	1:40:19	2:09:37

Notes
1. (sd) = mappings use state diagram
2. (calc) = mappings all calculated
3. Times are 'mins : secs' or 'hours : mins : secs'

Tab. 10.4: Point Data: Time taken to execute 200,000 range queries

	3	4	6	8	10	12	16
Hilbert	1875	1070	650	544	498	457	418
Moore	1909	1074	659	541			
Gray-code^A	2021	1119	668	542	490	453	420
Gray-code^B	2079	1142	680	551	497	458	425
Gray-code^F	2106	1131	663	539			
Z^A-order	2096	1169	694	563	507	466	429
Z^B-order	2108	1164	694	564	510	465	428
Grid File	1614	878	492	411	398	403	403

Tab. 10.5: Point Data: Number of pages (1000's) searched during 200,000 range queries

data. The distinction is more pronounced in the case of partial match queries than range queries.

A comparison of the space-filling curve applications shows that queries were processed most rapidly where the Z-order curve is used and that little difference emerges between curves where mappings are performed using state diagrams. It appears that the relative complexities of the search algorithms and sizes of state diagrams has, in these experiments, offset the variations in the numbers of pages touched where different curves are used.

The main distinction between the Z^A-order and Z^B-order curves lies in the time taken to execute range queries. Less time is required for the Z^B-order curve although similar numbers of pages are searched for both variations. Since both curves rely on the same querying algorithms, it appears that the difference is accounted for in the way pages are searched.

As expected, when Hilbert curve mappings are effected by calculation rather than with the aid of a state diagram, more time is taken to execute queries and, in particular, to perform updates.

In comparing the space-filling curves as the number of dimensions in space increases, we note that the times taken to execute the queries increase but, in general, such increases are linear.

In the experiments, the retrieval of data held in Grid Files requires fewer pages to be touched[2] than the retrieval of data mapped to space-filling curves.

The running times for executing partial match queries on data held in the Grid File are approximately half those for data mapped to the Z-order curve (and less than half those for data mapped to other curves). Running times appear to increase at a linear rate with the increase in the number of dimensions for all data stores tested. In contrast, running times for range query execution on data held in Grid Files appears to increase exponentially with an increase in the number of dimensions.

10.3 Discussion and Conclusions

It is apparent from the experiments that the choice of space-filling curve has implications in a practical data storage application and this justifies the exploration into them and motivates further work. In particular we note that, in general, fewer pages are touched where data is mapped to the Hilbert curve but that queries are executed in less time where data is mapped to the Z-order curve. Nevertheless, we recall that the experiments were carried out in main memory. Thus we expect that, where pages must be swapped into memory from secondary storage, implementations using the Hilbert curve should in general outperform those using the Z-order curve.

As expected, the use of state diagrams for performing mappings enable programs to be executed in less time than where mappings are calculated. Nevertheless, where calculation is used, running times do not appear to be prohibitive.

There appears to be little difference between the 3 variations of the Gray-code curve from the point of view of clustering. Whether this observation would continue to apply where data is less evenly distributed remains to be investigated. Except that state diagrams can be used in mappings for the Gray-code curve in a higher number of dimensions than for the Hilbert curve, it is not immediately obvious why use of the former should be chosen over use of the latter.

We noted that fewer pages are touched by queries executed over data held in the Grid File than where the data is mapped to space-filling curves. We conjecture that this arises from a partitioning of space within the Grid File into hyper-rectangular sub-spaces which

[2] This applies where data stores have comparable storage utilizations. Where data volumes result in Grid Files with low storage utilizations, the numbers of pages touched during query execution increases.

	Hilbert	Z-order	Grid File	R-Tree
No. of Pages Created	4201	4214	5183	5172
Elapsed Time (mins:secs)	4:28	2:33	9:47	16:07

Tab. 10.6: Spatial Data: Data Store Generation

	Hilbert	Z-order	Grid File	R-Tree
Pages Searched (1000s)	5208	5973	6630	515700
Elapsed Time (hours:mins)	1:11	0:29	5:38	16:25

Tab. 10.7: Spatial Data: Range Queries

manifest lower surface area to volume ratios than partitions defined by lengths of space-filling curve. We see in pages $P6$ and $P7$ in Figure 3.22 on page 50, for example, that sections of space-filling curve can correspond to n-dimensional spaces having relatively high surface area to volume ratios.

We believe, however, that the variations to the design of our implementation discussed in section 7.5 of chapter 7 should reduce the numbers of pages required to be searched during query execution where mapping data to a space-filling curve is exploited.

In contrast to our file organization design, the Grid File appears to encounter some problems which appear to grow exponentially as the number of dimensions increases. These relate to identifying which pages intersect with a range query and identifying which page may contain a particular data value; this latter operation being performed prior to inserting (or deleting) a *datum-point*.

10.4 Spatial Data

In this section we report on preliminary tests in which we apply our implementation to the storage of spatial data, in the manner described in chapter 9. We restrict ourselves to 2-dimensional rectangles which are stored as 4-dimensional points and execute range queries in which we retrieve all rectangles which overlap with specified rectangles.

As with tests carried out for point data, we randomly generated spatial data and query rectangles. Data stores were populated with 1.5 million rectangles placed on pages of 8192 bytes, and subjected to batches of 100,000 queries.

Tests were carried out using the Hilbert and Z-order space-filling curves and repeated for the Grid File. In addition, we were able to obtain the source code for Guttman's R-Tree, which is a file organization method which was specifically designed with spatial data in mind. This source code is made available on the internet by Guttman [Gut95].

A summary of the results of the tests are given in Tables 10.6 and 10.7.

The differences in the performances of the implementations were more distinct than was the case with point data experiments. Perhaps most surprising is the poor performance of the R-Tree, particularly in the number of pages requiring searching, and consequently the time required to search them. We also note that the Grid File performance was inferior to that of space-filling curve applications in all respects.

Chapter 11

CONCLUSIONS

The work described in this thesis addresses the problem of the indexing and retrieval of multi-dimensional point data which, although well-known, has no generally agreed optimum solution.

The main achievement and contribution of our work has been to explore and develop the application of space-filling curves in solving this problem. This approach has been suggested in the literature but little work, other than mostly of a theoretical nature, has previously been carried out in its pursuit. Furthermore, previous work has generally been restricted to only 2 or 3 dimensions. The approach regards multi-dimensional data as points lying on a space-filling curve passing through every point. Each point lies a unique distance along the curve from its origin and can, therefore, be mapped to a one-dimensional value, and stored in a simple one-dimensional storage structure.

Our work has entailed the design and practical implementation of an application for the storage and retrieval of data, which supports but is not limited to handling data in up to 16 dimensions and in any quantity.

The implementation makes use of one of a number of alternative space-filling curves used in mappings between one and n dimensions and thereby enables comparisons to be made of their characteristics and relative suitability for the purpose.

Our attention is focussed in particular on the Hilbert curve but also on variations of the Z-order curve and the Gray-code curve, as alternatives. The Hilbert curve is distinct from the others considered, since it is 'continuous' and so is of particular interest since it offers the prospect of superior data clustering properties.

The development of our implementation required us to address and resolve two important subsidiary problems:

- How to perform mappings between one and n dimensions.
- How to execute queries on data mapped to a space-filling curve.

Z-order and Gray-code mappings are relatively straightforward but only a limited amount of previous work relates to the Hilbert curve in higher than 2 dimensions. During our literature search we identified a rule-based procedure for constructing state diagrams for defining space-filling curves but this is general-purpose and does not relate to the Hilbert curve specifically. The rules were found to be too ambiguous to allow the automatic construction of state diagrams, while their application manually becomes increasingly impracticable as the number of dimensions in a space increases.

We extended and specialized the state diagram generation rules to enable state diagrams for the Hilbert curve specifically to be generated automatically. This proves to be practicable in up to 8 or 9 dimensions, but in higher-dimensional space, state diagram memory requirements become prohibitive.

We also adapted the state diagram generation technique for discontinuous variations of the Hilbert curve and the Gray-code curve. Apart from enabling mappings to be

performed efficiently and in a higher number of dimensions, the use of state diagrams for these curves enables the same algorithms and even computer software to be used with different curves. The state diagram is simply a parameter which is passed to the program. Although memory requirements limit the number of dimensions in which state diagrams can be used, whatever the curve represented, this tool is useful in the exploration of nuances between curves.

The development of the state diagram approach for performing mappings was useful for a number of reasons. Most importantly, the simplicity of the technique enabled us to focus on the development of querying algorithms. It also provided us with insights which enabled us to improve Butz' existing calculation-based technique for the Hilbert curve.

Given the limited number of dimensions in which state diagrams can be applied for the Hilbert curve, however, it appears that future research efforts would be most effective if focussed on applications using calculation rather than state diagrams, for any number of dimensions. This view is encouraged by noting, from the experiments reported in chapter 10, a convergence in the times taken by implementations employing the two alternative mapping methods as the number of dimensions increases. We conjecture that this arises from an increasing processing overhead in manipulating data within state diagrams as they increase in size.

The existence of mapping techniques is of little value in the absence of an effective means of querying multi-dimensional data mapped to one dimension. The lack of reports of the practical application of space-filling curves in the literature led us to speculate that the concept was flawed because no algorithms could be discovered to execute queries effectively. Dispelling this notion was thus the preoccupation of the early part of our research.

Having developed an understanding of space-filling curves by representing them as trees, we developed 'tree-descent' algorithms for querying the Hilbert curve. A broadly similar approach has been adopted previously but only for the Z-order curve by Orenstein [OM84] for spatial data and by Tropf and Herzog [TH81]. The algorithm developed by the latter exploits the notion that the lowest and highest matching *derived-keys* to a query correspond to the coordinates of the upper and lower bounds. However, this cannot be applied to the Hilbert curve.

We found no algorithms in the literature relating to the Hilbert curve and developing tree-descent querying algorithms for it is therefore an important contribution of this thesis. Utilization of state diagrams assisted in the development of these algorithms in that they enabled them to be expressed in a simplified manner. The querying algorithms were then extended for use in higher-dimensional space where mappings must be performed by calculation.

In the case of the Z-order curve, we adopted a radically different approach to querying which relies on manipulating bits within coordinates and *derived-keys*. This approach proves to be more computationally efficient than the tree-descent approach but it cannot be applied to other curves.

In developing a fully-functioning data storage implementation a number of peripheral, though important, matters of detail were addressed, particularly in relation to what is stored on a page and in what order. These matters were also discussed in relation to prominent alternatives to our design.

Further Work

Probably the most important area for further work is the testing of our implementation using data collected from 'real-world' applications, rather than with randomly generated data. Random data cannot be expected to fully reveal the clustering characteristics of space-filling curves and the differences between them, although some preliminary indica-

tion is provided by those tests carried out.

We note from the particular tests reported on in chapter 10 that more pages were searched during query execution when data was mapped to a space-filling curve than when it was held in the Grid File. A number of possible enhancements to our implementation are described in chapter 7 which we believe should reduce the average number of pages searched and so are worth pursuing. These are:

- To regard 'adjacent' pages as sections of curve which are not necessarily contiguous. We recall that a page corresponds to a section of curve and, in the current implementation, the union of all of the pages corresponds to the whole curve. An index entry for a page denotes the start of a curve section and its end is implied by the index entry of the next page. By explicitly storing in the index the highest *derived-key* corresponding to a *datum-point* on a page (in addition to the first), the index implies some sections of curve containing no *datum-points*; ie sections lying between the *datum-points* with the highest *derived-key* on one page and the lowest *derived-key* on the next page. This strategy enables us to avoid searching some parts of the data-space known not to contain data.

- To select *page-keys* for pages which maximize the volume to surface area ratios of the spaces through which the curve sections corresponding to the pages pass. To implement this concept, it is necessary to be aware of the least and greatest *derived-keys* of *datum-points* on a page. Optimum solutions in terms of locating page boundaries are likely to require moving data between pages.

- To implement a page splitting and merging strategy similar to equivalent operations on nodes in the B*-Tree. The objective of this option is to increase average page occupancy, thereby reducing the number of pages held within the data file. It would be possible to apply B*-Tree concepts to page splitting (and merging) only or additionally apply them to the index implementation.

Of the measures listed above, the last is likely to be the simplest to implement.

We noted when concluding section 3.8.2 of chapter 3 that coordinates of points and their *derived-keys* may be expressed in a radix of 4 (or another power of 2) rather than in binary. Since the number of points on a first order curve equals r^n, a greater variety of curve 'designs' may be produced and explored when the radix is increased. We also note that where a radix of, for example, 4 is used, a tree representing a curve passing through i points has a height which is half that arising where a radix of 2 is used, thus mappings may be performed more efficiently. Little or no improvement in efficiency of query execution is expected, however, since node (or state) sizes increase exponentially with an increase in radix, thus adding correspondingly to the cost of performing binary searches as described in chapter 6.

We have studied the application of space-filling curves to the storage and retrieval of spatial objects of the form of hyper-rectangles in chapter 9 but only at a preliminary level. We compared the performance of our implementation with that of the R-Tree in section 10.4 of chapter 10. The results were very encouraging, particularly since the R-Tree is designed specifically to accommodate hyper-rectangular data. They motivate us to pursue further the application of our implementation to spatial data in general and in the area of Geographical Information Systems in particular.

We noted in chapter 2 that most analysis of the clustering properties of space-filling curves has been theoretical and confined to data-spaces of limited size and in 2 or 3 dimensions. Our implementation provides the opportunity to carry out further work of an analytical nature, and in a higher number of dimensions.

It is clear from the way in which the Hilbert curve is constructed that coordinate domains of points in all dimensions are of the same cardinality. As a result, more storage may be used than is required to store the values of attributes whose domains are smaller than the largest. For example, where a mapping to a curve of order 32 is used, then each of a record's attributes are stored as 32 bit integers even if one or more of the attributes can be accommodated in 8 bit integers. Thus scope exists to find ways of avoiding unnecessary use of storage. One option to be explored is the use of a single coordinate of a *datum-point* to hold the values of more than one attribute of a record.

In chapter 4, populating column X_2, in particular, of state diagram generator tables followed the identification of patterns in sequences of numbers. Once implemented, these patterns produced correct results but formulation of proofs of correctness is outstanding.

Since our software is experimental and intended to explore the suitability of mapping multi-dimensional data to one dimension, features such as concurrency control and recovery have not been included in the implementation. Nevertheless, there appears to be no reason to believe that these issues need be dealt with in a novel manner as a result of the application of space-filling curves.

In chapter 7 we discussed issues relating to the format and order in which data is stored on a page within the data store. These are independent of the indexing and querying strategies explored in this thesis. Nevertheless the application of space-filling curves has implications which can be explored. For example, the storage of *derived-keys* in addition to the 'coordinates' of *datum-points* may be beneficial in certain application domains.

The procedure for the calculation of a *next-match* in the execution of a query takes only the *page-key* of the successor page to the one most recently searched and the query specification as input. However, the index contains some information about the distribution of data in the data store. It may therefore be beneficial to explore whether reference to this information can accelerate the calculation process.

Concluding Remarks

We do not yet claim that the application of space-filling curves provides the optimum solution to the problem of storage and retrieval of multi-dimensional data. Instead, our aim has been to ascertain the feasibility of the concept and this requires suitable methods of performing mappings and executing queries. We believe we have achieved this aim. Additionally, we have carried out some preliminary experimentation which has produced some encouraging results which indicate that the concept merits further study and development.

BIBLIOGRAPHY

[AN98] Jochen Alber and Rolf Niedermeier. On multi-dimensional hilbert indexings. In Wen-Lian Hsu and Ming-Yang Kao, editors, *Proceedings of Computing and Combinatorics, 4th Annual International Conference, COCOON '98*, volume 1449 of *Lecture Notes in Computer Science*, pages 329–338. Springer-Verlag, 1998.

[ARR+95] Tetsuo Asano, Desh Ranjan, Thomas Roos, Emo Welzl, and Peter Widmayer. Space filling curves and their use in the design of geometric data structures. In Ricardo A. Baeza-Yates, Eric Goles Ch., and Patricio V. Poblete, editors, *LATIN '95: Theoretical Informatics, Second Latin American Symposium*, volume 911 of *Lecture Notes in Computer Science*, pages 36–48. Springer-Verlag, 1995.

[Ayr95] Robert Ayres. *Enhancing the Secmantic Power of Functional Database Languages*. PhD thesis, Birkbeck College, University of London, 1995.

[BBK98] Stefan Berchtold, Christian Böhm, and Hans-Peter Kriegel. The Pyramid-Tree: Breaking the curse of dimensionality. In Laura M. Haas and Ashutosh Tiwary, editors, *SIGMOD 1998, Proceedings ACM SIGMOD International Conference on Management of Data, June 2-4, 1998, Seattle, Washington, USA*, pages 142–153. ACM Press, 1998.

[Ben75] J.L. Bentley. Multidimensional binary search trees used for associative searching. *Communications of the ACM*, 18(9):509–517, 1975.

[Bia67] Theodore Bially. *A Class of Dimension Changing Mappings and its Application to Bandwidth Compression*. PhD thesis, Polytechnic Institute of Brooklyn, 1967.

[Bia69] Theodore Bially. Space-filling curves: Their generation and their application to bandwidth reduction. *IEEE Transactions on Information Theory*, IT-15(6):658–664, Nov 1969.

[BKK96] Stefan Berchtold, Daniel A. Keim, and Hans-Peter Kriegel. The X-Tree : An index structure for high-dimensional data. In T. M. Vijayaraman, Alejandro P. Buchmann, C. Mohan, and Nandlal L. Sarda, editors, *VLDB'96, Proceedings of 22th International Conference on Very Large Data Bases, September 3-6, 1996, Mumbai (Bombay), India*, pages 28–39. Morgan Kaufmann, 1996.

[BKSS90] Norbert Beckmann, Hans-Peter Kriegel, Ralf Schneider, and Bernhard Seeger. The R*-Tree: An efficient and robust access method for points and rectangles. In Hector Garcia-Molina and H. V. Jagadish, editors, *Proceedings of the 1990 ACM SIGMOD International Conference on Management of Data, Atlantic City, NJ, May 23-25, 1990*, pages 322–331. ACM Press, 1990.

[BM72] R. Bayer and C. McCreight. Organization and maintenance of large ordered indexes. *Acta Informatica*, 1(3):172–189, 1972.

[But68] Arthur R. Butz. Space filling curves and mathematical programming. *Information and Control*, 12:314–330, 1968.

[But69] Arthur R. Butz. Convergence with hilbert's space filling curve. *Journal of Computer and System Science*, 3:128–146, 1969.

[But71] Arthur R. Butz. Alternative algorithm for hilbert's space-filling curve. *IEEE Transactions on Computers*, 20:424–426, April 1971.

[Cod70] E.F. Codd. A relational model for large shared data banks. *Communications of the ACM*, 13(6):377–387, 1970.

[Col83] A. J. Cole. A note on space filling curves. *Software – Practice and Experience*, 13(12):1181–1189, December 1983.

[Col86] A.J. Cole. Direct transformations between sets of integers and hilbert polygons. *International Journal of Computer Mathematics*, 20:115–122, 1986.

[Col87] A.J. Cole. Compaction techniques for raster scan graphics using space-filling curves. *The Computer Journal*, 30(1):87–92, 1987.

[Com79] Douglas Comer. The ubiquitous B-Tree. *ACM Computing Surveys*, 11(2):121–137, 1979.

[Der89] Mir Derakhshan. *A Development of the Grid File for the Storage of Binary Relations.* PhD thesis, Birkbeck College, University of London, 1989.

[Fal86] Christos Faloutsos. Multiattribute hashing using gray codes. In Carlo Zaniolo, editor, *Proceedings of the 1986 ACM SIGMOD International Conference on Management of Data, Washington, D.C., May 28-30, 1986*, pages 227–238. ACM Press, 1986.

[Fal88] Christos Faloutsos. Gray codes for partial match and range queries. *IEEE Transactions on Software Engineering*, 14(10):1381–1393, Oct 1988.

[Fis86] A. J. Fisher. A new algorithm for generating Hilbert curves. *Software – Practice and Experience*, 16(1):5–12, January 1986.

[FR89a] Christos Faloutsos and Shari Roseman. Fractals for secondary key retrieval. In *Proceedings of the Eighth ACM SIGACT-SIGMOD-SIGART Symposium on Principles of Database Systems, March 29-31, 1989, Philadelphia, Pennsylvania*, pages 247–252. ACM Press, 1989.

[FR89b] Christos Faloutsos and Shari Roseman. Fractals for secondary key retrieval (an extended version of [FR89a]). Technical Report UMIACS-TR-89-47, University of Maryland, 1989. http://www.cs.cmu.edu/ christos/cpub.html.

[FR91] Christos Faloutsos and Yi Rong. Dot: A spatial access method using fractals. In *Proceedings of the Seventh International Conference on Data Engineering, April 8-12, 1991, Kobe, Japan*, pages 152–159. IEEE Computer Society, 1991.

[Fre87] M. Freeston. The BANG file: A new kind of grid file. In Umeshwar Dayal and Irving L. Traiger, editors, *Proceedings of the Association for Computing Machinery Special Interest Group on Management of Data 1987 Annual Conference, San Francisco, California, May 27-29, 1987*, pages 260–269. ACM Press, 1987.

[Fre89a] M. Freeston. Advances in the design of the BANG file. In *Foundations of Data Organization and Algorithms: Proceedings of the 3rd International Conference (FODO '89)*, volume 367 of *Lecture Notes in Computer Science*, pages 322–338. Springer-Verlag, 1989.

[Fre89b] M. Freeston. A well-behaved file structure for the storage of spatial objects. In Alejandro P. Buchmann, Oliver Günther, Terence R. Smith, and Y.-F. Wang, editors, *Design and Implementation of Large Spatial Databases: Proceedings of the 1st Symposium (SSD '89)*, volume 409 of *Lecture Notes in Computer Science*, pages 287–300. Springer-Verlag, July 1989.

[Fre92] M. Freeston. The comparative performance of bang indexing for spatial objects. In *Proceedings of the 5th International Symposium on Spatial Data Handling*, pages 190–199, 1992.

[Fre93] M. Freeston. Begriffsverzeichnis: A concept index. In Michael F. Worboys and A. F. Grundy, editors, *Advances in Databases: Proceedings of the 11th British National Conference on Databases (BNCOD11)*, volume 696 of *Lecture Notes in Computer Science*, pages 1–22. Springer-Verlag, July 1993.

[Fre95a] M. Freeston. The application of multi-dimensional indexing methods to constraints. In Gabriel M. Kuper and Mark Wallace, editors, *Constraint Databases and Applications: Proceedings of the ESPRIT WG CONTESSA Workshop*, volume 1034 of *Lecture Notes in Computer Science*, pages 102–119. Springer-Verlag, Sept 1995.

[Fre95b] M. Freeston. A general solution of the n-dimensional B-Tree problem. In Michael J. Carey and Donovan A. Schneider, editors, *Proceedings of the 1995 ACM SIGMOD International Conference on Management of Data, San Jose, California, May 22-25, 1995*, pages 80–91. ACM Press, 1995.

[Fre97] M. Freeston. *Data Structures for Knowledge Bases.* PhD thesis, University of Southampton, 1997.

[GG98] Volker Gaede and Oliver Günther. Multidimensional access methods. *ACM Computing Surveys*, 30(2):170–231, June 1998.

[Gol81] Leslie M. Goldschlager. Short algorithms for space-filling curves. *Software – Practice and Experience*, 11(1):99, January 1981. Short Communication.

[Gra53] F. Gray. Pulse code communications. U.S Patent 2 632 058, March 1953.

[Gri85] J.G. Griffiths. Table-driven algorithms for generating space-filling curves. *Computer Aided Design*, 17(1):37–41, Jan/Feb 1985.

[Gri86] J.G. Griffiths. An algorithm for displaying a class of space-filling curves. *Software Practice and Experience*, 16(5):403–411, May 1986.

[Gut84] Antonin Guttman. R-Trees: A dynamic index structure for spatial seaching. In *SIGMOD '84: Proceedings of the Annual Meeting*, volume 14(2) of *SIGMOD Record*, pages 47–57. ACM, 1984.

[Gut95] Antonin Guttman. Source code for the R-Tree. Technical report, University of California, 1995.

[Hil91] David Hilbert. Ueber stetige abbildung einer linie auf ein flachenstuck. *Mathematische Annalen*, 38:459–460, 1891.

[Hin85] Klaus Hinrichs. Implementation of the grid file: Design concepts and experience. *BIT*, 25:569–592, 1985.

[HSW88] Andreas Hutflesz, Hans-Werner Six, and Peter Widmayer. The twin grid file: A nearly space optimal index structure. In *Proceedings of the International Conference on Extending Database Technology (EDBT '88)*, volume 303 of *Lecture Notes in Computer Science*, pages 352–363. Springer-Verlag, 1988.

[Jag90] H. V. Jagadish. Linear clustering of objects with multiple atributes. In Hector Garcia-Molina and H. V. Jagadish, editors, *Proceedings of the 1990 ACM SIGMOD International Conference on Management of Data, Atlantic City, NJ, May 23-25, 1990*, volume 19, pages 332–342. ACM Press, 1990.

[Jag97] H.V. Jagadish. Analysis of the hilbert curve for representing two-dimensional space. *Information Processing Letters*, 62(1):17–22, April 1997.

[Jan95] J. Jannink. Implementing deletion in B^+-Trees. *SIGMOD Record*, 24(1):33–38, April 1995.

[KDPS90] Peter King, Mir Derakhshan, Alexandra Poulovassilis, and Carol Small. TriStarp - an investigation into the implementation and exploitation of binary relational storage structures. In Alan W. Brown and Peter Hitchcock, editors, *BNCOD-8 Proceedings of the 8th Bristish National Conference on Databases*, pages 64–84. Pitman Publishing, 1990.

[Ken73] Hubert C. Kennedy. *Selected Works of Giuseppe Peano*, chapter 10, pages 143–149. George Allen and Unwin, 1973.

[KF94] Ibrahim Kamel and Christos Faloutsos. Hilbert R-Tree: An improved R-Tree using fractals. In Jorge B. Bocca, Matthias Jarke, and Carlo Zaniolo, editors, *VLDB'94, Proceedings of 20th International Conference on Very Large Data Bases, September 12-15, 1994, Santiago de Chile, Chile*, pages 500–509. Morgan Kaufmann, 1994.

[KKN95] S. Kamata, E. Kawaguchi, and M. Niimi. An interactive analysis method for multi-dimensional images using a hilbert curve. *Systems and Computers in Japan*, 26(3):83–92, 1995.

[Knu73] D. Knuth. *The Art of Computer Programming*, volume 3, Searching and Sorting. Addison-Wesley, 1973.

[KP88] P. J. H. King and A. Poulovassilis. FDL: A language which integrates database and functional programming. In *Congres INFORSID 1988, La Rochelle, France*, 1988.

[KS97] Norio Katayama and Shin'ichi Satoh. The SR-Tree: An index structure for high-dimensional nearest neighbor queries. In Joan Peckham, editor, *SIGMOD 1997, Proceedings ACM SIGMOD International Conference on Management of Data, May 13-15, 1997, Tucson, Arizona, USA*, pages 369–380. ACM Press, 1997.

[Kum94] Akhil Kumar. A study of spatial clustering techniques. In Dimitris Karagiannis, editor, *Proceedings of the 5th International Conference on Database and Expert Systems Applications (DEXA '94)*, volume 856 of *Lecture Notes in Computer Science*, pages 57–71. Springer-Verlag, Sept 1994.

[LS96] Xian Liu and Günther Schrack. Encoding and decoding the Hilbert order. *Software – Practice and Experience*, 26(12):1335–1346, December 1996.

[LW84] S. Lavington and C. Wang. A lexical token convertor for the IFS. Technical Report IFS/5/84, University of Manchester, 1984.

[Man82] B. B. Mandelbrot. *The Fractal Geometry of Nature*. W. H. Freeman and Co., 1982.

[Mer99] Paul Meredith. *A Functional Programming Language which integrates queries and updates for managing an Entity-Function Database*. PhD thesis, Birkbeck College, University of London, 1999.

[MJFS99] Bongki Moon, H.V. Jagadish, Christos Faloutsos, and Joel H. Saltz. Analysis of the clustering properties of the hilbert space-filling curve. Technical Report 99-10, University of Arizona, 1999.

[Moo00] Eliakim Hastings Moore. On certain crinkly curves. *Transactions of the American Mathematical Society*, 1:72–90, Jan 1900.

[Mor66] G.M. Morton. A computer oriented geodetic data base and a new technique in file sequencing. Technical report, IBM, Ottawa, Canada, 1966.

[NHS84] Jürg Nievergelt, Hans Hinterberger, and Kenneth C. Sevcik. The grid file: An adaptable, symmetric multikey file structure. *ACM Transactions on Database Systems (TODS)*, 9(1):38–71, 1984.

[OM84] Jack A. Orenstein and T. H. Merrett. A class of data structures for associative searching. In *Proceedings of the Third ACM SIGACT-SIGMOD Symposium on Principles of Database Systems, April 2-4, 1984, Waterloo, Ontario, Canada*, pages 181–190. ACM, 1984.

[OM88] Jack A. Orenstein and F.A. Manola. Probe: Spatial data modeling and query processing in an image database application. *IEEE Transactions on Software Engineering*, 14(5):611–629, 1988.

[OM91] M. Aris Ouksel and Otto Mayer. The nested interpolation based grid file. In *Proceedings of the 3rd Symposium on Mathematical Fundamentals of Database and Knowledge Base Systems (MFDBS '91)*, volume 495 of *Lecture Notes in Computer Science*, pages 173–187. Springer-Verlag, 1991.

[OM92] M. Aris Ouksel and Otto Mayer. A robust and efficient spatial data structure: The nested interpolation based grid file. *Acta Informatica*, 29:335–373, 1992.

[Ooi90] B.C. Ooi. *Efficient Query Processing in Geographic Information Systems*, volume 471 of *Lecture Notes in Computer Science*. Springer-Verlag, 1990.

[Ora97] Oracle. Oracle8 spatial cartridge: Advances in relational database technology for spatial data management. Technical report, Oracle Corporation, 1997.

[Ore86] Jack A. Orenstein. Spatial query processing in an object-oriented database system. In Carlo Zaniolo, editor, *Proceedings of the 1986 ACM SIGMOD International Conference on Management of Data, Washington, D.C., May 28-30, 1986*, pages 326–336. ACM Press, 1986.

[Ore89a] Jack A. Orenstein. Redundancy in spatial databases. In James Clifford, Bruce G. Lindsay, and David Maier, editors, *Proceedings of the 1989 ACM SIGMOD International Conference on Management of Data, Portland, Oregon, May 31 - June 2, 1989*, pages 294–305. ACM Press, 1989.

[Ore89b] Jack A. Orenstein. Strategies for optimizing the use of redundancy in spatial databases. In Alejandro P. Buchmann, Oliver Günther, Terence R. Smith, and Y.-F. Wang, editors, *Design and Implementaion of Large Spatial Databases: Proceedings of the 1st Symposium (SSD '89)*, volume 409 of *Lecture Notes in Computer Science*, pages 115–134. Springer-Verlag, July 1989.

[Ore90] Jack A. Orenstein. A comparison of spatial query processing techniques for native and parameter spaces. In Hector Garcia-Molina and H. V. Jagadish, editors, *Proceedings of the 1990 ACM SIGMOD International Conference on Management of Data, Atlantic City, NJ, May 23-25, 1990*, pages 343–352. ACM Press, 1990.

[Ore91] Jack A. Orenstein. An algorithm for computing the overlay of k-dimensional spaces. In Hans-Jörg Schek Oliver Günther, editor, *Advances in Spatial Databases: Proceedings of the 2nd International Symposium (SSD '91)*, volume 525 of *Lecture Notes in Computer Science*, pages 381–400. Springer-Verlag, August 1991.

[Pea90] Giuseppe Peano. Sur une courbe, qui remplit toute une aire plane (on a curve which completely fills a planar region). *Mathematische Annalen*, 36:157–160, 1890. Translated in [Ken73].

[PJS92] Heinz-Otto Peitgen, Hartmut Jurgens, and Dietmar Saupe. *Chaos and Fractals: New Frontiers of Science*. Springer-Verlag, 1992.

[Pou89] Alex Poulovassilis. *The Design and Implementation of FDL - a Functional Database Language*. PhD thesis, Birkbeck College, University of London, 1989.

[QB81] Joël Quinqueton and Marc Berthod. A locally adaptive peano scanning algorithm. *IEEE Transactions on Pattern Analysis and Machine Intelligence*, PAMI-3(4):403–412, July 1981.

[RND77] E.M. Reingold, J. Nievergelt, and N. Deo. *Combinatorial Algorithms: Theory and Practice*. Prentice Hall, 1977.

[Rob81] John T. Robinson. The K-D-B-Tree: A search structure for large multidimensional dynamic indexes. In Y. Edmund Lien, editor, *Proceedings of the 1981 ACM SIGMOD International Conference on Management of Data, Ann Arbor, Michigan, April 29 - May 1, 1981*, pages 10–18. ACM Press, 1981.

[Sag94] Hans Sagan. *Space-Filling Curves*. Springer-Verlag, 1994.

[Sam90a] Hanan Samet. *Applications of Spatial Data Structures*. Addison-Wesley, 1990.

[Sam90b] Hanan Samet. *The Design and Analysis of Spatial Data Structures*. Addison-Wesley, 1990.

[SRF87] Timos K. Sellis, Nick Roussopoulos, and Christos Faloutsos. The R^+-Tree: A dynamic index for multi-dimensional objects. In Peter M. Stocker, William Kent, and Peter Hammersley, editors, *VLDB'87, Proceedings of 13th International Conference on Very Large Data Bases, September 1-4, 1987, Brighton, England*, pages 507–518. Morgan Kaufmann, 1987.

[Sut95] David Sutton. *A Functional Database Language with Certainty and Possibility Operators*. PhD thesis, Birkbeck College, University of London, 1995.

[TH81] H. Tropf and H. Herzog. Multi-dimensional range search in dynamically balanced trees. *Angewandte Informatik*, 23(2):71–77, 1981.

[Wir76] N. Wirth. *Algorithms + data structures = programs*. Prentice Hall, 1976.

[WJ96] David A. White and Ramesh Jain. Similarity indexing with the SS-Tree. In Stanley Y. W. Su, editor, *Proceedings of the Twelfth International Conference on Data Engineering, February 26 - March 1, 1996, New Orleans, Louisiana*, pages 516–523. IEEE Computer Society, 1996.

[WW83] Ian H. Witten and Brian Wyvill. On the generation and use of space-filling curves. *Software – Practice and Experience*, 13(6):519–525, June 1983.

Appendix A

SYMBOLS

Symbol	Description
$\vee$	bitwise inclusive OR operator
$\oplus$	bitwise exclusive OR operator
$\wedge$	bitwise AND operator
$\neg$	bitwise NOT operator
$\ll$	bitwise left-shift operator
$\gg$	bitwise right-shift operator
$\%$	modulus operator
$\Leftarrow$	assignment operator
$=$	equality operator
$\neq$	not equal to
$<$	less than
$>$	greater than
$\leq$	less than or equal to
$\geq$	greater than or equal to
$\cap$	set intersection

Tab. A.1: Table of Symbols

Appendix B

THE HILBERT CURVE

This appendix is concerned with mapping to the Hilbert curve. Section B.1 contains examples relating to the state diagram approach and section B.2 relates to the method of calculation of Hilbert curve mappings given by Butz in [But71].

B.1 The State Diagram Approach – Some Examples

Examples of state diagram generator tables for 2 – 4 dimensions appear in chapter 4. The corresponding table for 5 dimensions is given here in Table B.1 and was produced in accordance with the algorithms given in section 4.3.3 in chapter 4.

This is followed by examples of state diagrams, in tabular form, which have been derived from generator tables.

Tables B.2 and B.3 are state diagrams for the Hilbert curve in 2 dimensions. The first is used for mapping from one dimension to 2 dimensions and the second is used for the inverse mapping, from 2 dimensions to one dimension. They represent the state diagram given later in this appendix in Figure B.1 and are derived from the state diagram generator table given in Table 4.1 in chapter 4.

Table B.2 contains a pair of rows defining each state, or first order curve, and a column for each *derived-key*, or sequence number of a point on a first order curve. The first of a pair of rows for any state, S, contains the *n-points*, or coordinates of points on a first order curve concatenated into single values, one for each *derived-key*. The second of a pair of rows contains the 'next-state' for each *n-point* lying on state S. The values of *derived-keys* and *n-points* are in binary format, while state numbers are in decimal format.

Table B.3 is derived from Table B.2. The former differs from the latter in that *derived-key* : *n-point* pairs are sorted by *n-point* values. Thus each column corresponds to an *n-point* value and the first of a pair of rows for any state contains *derived-key* values.

Tables B.4 and B.5 are state diagrams for the Hilbert curve in 3 dimensions and correspond to the generator table given in Table 4.2 and the state diagram illustrated in Figure B.2.

Tables B.6 and B.7 are state diagrams for the Hilbert curve in 4 dimensions and correspond to the generator table given in Table 4.3. All values are given in decimal format, however, in order for the table to be presented compactly.

Examples of state diagrams represented graphically for 2 and 3 dimensions are given in Figures B.1 and B.2. They are expressed in the same format as examples given in Bially's paper [Bia69]. They are constructed from the generator tables given in Tables 4.1 and 4.2 and are graphical representations of the state diagrams given in Tables B.2, B.3, B.4, and B.5.

Y	X_1	X_2	δY	$\overline{T(Y)}$
00000	00000	00000	00001	0 0 0 0 1
		00001		1 0 0 0 0
				0 1 0 0 0
				0 0 1 0 0
				0 0 0 1 0
00001	00001	00000	00010	0 0 0 1 0
		00010		0 0 0 0 1
				1 0 0 0 0
				0 1 0 0 0
				0 0 1 0 0
00010	00011	00000	00010	0 0 0 1 0
		00010		0 0 0 0 1
				1 0 0 0 0
				0 1 0 0 0
				0 0 1 0 0
00011	00010	00011	00100	0 0 1 0 0
		00111		0 0 0 -1 0
				0 0 0 0 -1
				1 0 0 0 0
				0 1 0 0 0
00100	00110	00011	00100	0 0 1 0 0
		00111		0 0 0 -1 0
				0 0 0 0 -1
				1 0 0 0 0
				0 1 0 0 0
00101	00111	00110	00010	0 0 0 -1 0
		00100		0 0 0 0 1
				1 0 0 0 0
				0 1 0 0 0
				0 0 -1 0 0
00110	00101	00110	00010	0 0 0 -1 0
		00100		0 0 0 0 1
				1 0 0 0 0
				0 1 0 0 0
				0 0 -1 0 0
00111	00100	00101	01000	0 1 0 0 0
		01101		0 0 -1 0 0
				0 0 0 1 0
				0 0 0 0 -1
				1 0 0 0 0
01000	01100	00101	01000	0 1 0 0 0
		01101		0 0 -1 0 0
				0 0 0 1 0
				0 0 0 0 -1
				1 0 0 0 0
01001	01101	01100	00010	0 0 0 1 0
		01110		0 0 0 0 1
				1 0 0 0 0
				0 -1 0 0 0
				0 0 -1 0 0
01010	01111	01100	00010	0 0 0 1 0
		01110		0 0 0 0 1
				1 0 0 0 0
				0 -1 0 0 0
				0 0 -1 0 0
01011	01110	01111	00100	0 0 -1 0 0
		01011		0 0 0 -1 0
				0 0 0 0 -1
				1 0 0 0 0
				0 -1 0 0 0
01100	01010	01111	00100	0 0 -1 0 0
		01011		0 0 0 -1 0
				0 0 0 0 -1
				1 0 0 0 0
				0 -1 0 0 0
01101	01011	01010	00010	0 0 0 -1 0
		01000		0 0 0 0 1
				1 0 0 0 0
				0 -1 0 0 0
				0 0 1 0 0
01110	01001	01010	00010	0 0 0 -1 0
		01000		0 0 0 0 1
				1 0 0 0 0
				0 -1 0 0 0
				0 0 1 0 0
01111	01000	01001	10000	1 0 0 0 0
		11001		0 -1 0 0 0
				0 0 1 0 0
				0 0 0 1 0
				0 0 0 0 -1

Top half of table

Y	X_1	X_2	δY	$\overline{T(Y)}$
10000	11000	01001	10000	1 0 0 0 0
		11001		0 -1 0 0 0
				0 0 1 0 0
				0 0 0 1 0
				0 0 0 0 -1
10001	11001	11000	00010	0 0 0 1 0
		11010		0 0 0 0 1
				-1 0 0 0 0
				0 -1 0 0 0
				0 0 1 0 0
10010	11011	11000	00010	0 0 0 1 0
		11010		0 0 0 0 1
				-1 0 0 0 0
				0 -1 0 0 0
				0 0 1 0 0
10011	11010	11011	00100	0 0 1 0 0
		11111		0 0 0 -1 0
				0 0 0 0 -1
				-1 0 0 0 0
				0 -1 0 0 0
10100	11110	11011	00100	0 0 1 0 0
		11111		0 0 0 -1 0
				0 0 0 0 -1
				-1 0 0 0 0
				0 -1 0 0 0
10101	11111	11110	00010	0 0 0 -1 0
		11100		0 0 0 0 1
				-1 0 0 0 0
				0 -1 0 0 0
				0 0 -1 0 0
10110	11101	11110	00010	0 0 0 -1 0
		11100		0 0 0 0 1
				-1 0 0 0 0
				0 -1 0 0 0
				0 0 -1 0 0
10111	11100	11101	01000	0 -1 0 0 0
		10101		0 0 -1 0 0
				0 0 0 1 0
				0 0 0 0 -1
				-1 0 0 0 0
11000	10100	11101	01000	0 -1 0 0 0
		10101		0 0 -1 0 0
				0 0 0 1 0
				0 0 0 0 -1
				-1 0 0 0 0
11001	10101	10100	00010	0 0 0 1 0
		10110		0 0 0 0 1
				-1 0 0 0 0
				0 1 0 0 0
				0 0 -1 0 0
11010	10111	10100	00010	0 0 0 1 0
		10110		0 0 0 0 1
				-1 0 0 0 0
				0 1 0 0 0
				0 0 -1 0 0
11011	10110	10111	00100	0 0 -1 0 0
		10011		0 0 0 -1 0
				0 0 0 0 -1
				-1 0 0 0 0
				0 1 0 0 0
11100	10010	10111	00100	0 0 -1 0 0
		10011		0 0 0 -1 0
				0 0 0 0 -1
				-1 0 0 0 0
				0 1 0 0 0
11101	10011	10010	00010	0 0 0 -1 0
		10000		0 0 0 0 1
				-1 0 0 0 0
				0 1 0 0 0
				0 0 1 0 0
11110	10001	10010	00010	0 0 0 -1 0
		10000		0 0 0 0 1
				-1 0 0 0 0
				0 1 0 0 0
				0 0 1 0 0
11111	10000	10001	00001	0 0 0 0 -1
		10000		-1 0 0 0 0
				0 1 0 0 0
				0 0 1 0 0
				0 0 0 1 0

Bottom half of table

Tab. B.1: State Diagram Generator Table the Hilbert Curve in 5 Dimensions

state no.	*derived-key* 00	01	10	11
0	00	01	11	10
	1	0	0	2
1	00	10	11	01
	0	1	1	3
2	11	01	00	10
	3	2	2	0
3	11	10	00	01
	2	3	3	1

Tab. B.2: Hilbert Curve State Diagram: for Mapping from One Dimension (*derived-keys*) to 2-dimensional Points

state no.	*n-point* 00	01	10	11
0	00	01	11	10
	1	0	2	0
1	00	11	01	10
	0	3	1	1
2	10	01	11	00
	2	2	0	3
3	10	11	01	00
	3	1	3	2

Tab. B.3: Hilbert Curve State Diagram: for Mapping from 2-dimensional Points to One Dimension (*derived-keys*)

state no.	*derived-key* 000	001	010	011	100	101	110	111
0	000 1	001 2	011 2	010 3	110 3	111 5	101 5	100 4
1	000 2	010 0	110 0	100 8	101 8	111 7	011 7	001 6
2	000 0	100 1	101 1	001 9	011 9	111 11	110 11	010 10
3	011 11	010 6	000 6	001 0	101 0	100 9	110 9	111 8
4	101 9	111 7	011 7	001 11	000 11	010 0	110 0	100 5
5	110 10	010 8	011 8	111 6	101 6	001 4	000 4	100 0
6	011 3	111 11	110 11	010 5	000 5	100 1	101 1	001 7
7	101 4	100 9	110 9	111 10	011 10	010 6	000 6	001 1
8	110 5	100 10	000 10	010 1	011 1	001 3	101 3	111 9
9	101 7	001 4	000 4	100 2	110 2	010 8	011 8	111 3
10	110 8	111 5	101 5	100 7	000 7	001 2	011 2	010 11
11	011 6	001 3	101 3	111 4	110 4	100 10	000 10	010 2

Tab. B.4: Hilbert Curve State Diagram: for Mapping from One Dimension (*derived-keys*) to 3-dimensional Points

state no.	*n-point* 000	001	010	011	100	101	110	111
0	000 1	001 2	011 3	010 2	111 4	110 5	100 3	101 5
1	000 2	111 6	001 0	110 7	011 8	100 8	010 0	101 7
2	000 0	011 9	111 10	100 9	001 1	010 1	110 11	101 11
3	010 6	011 0	001 6	000 11	101 9	100 0	110 9	111 8
4	100 11	011 11	101 0	010 7	111 5	000 9	110 0	001 7
5	110 4	101 4	001 8	010 8	111 0	100 6	000 10	011 6
6	100 5	111 7	011 5	000 3	101 1	110 1	010 11	001 11
7	110 6	111 1	101 6	100 10	001 9	000 4	010 9	011 10
8	010 10	101 3	011 1	100 1	001 10	110 3	000 5	111 9
9	010 4	001 4	101 8	110 8	011 2	000 7	100 2	111 3
10	100 7	101 2	111 11	110 2	011 7	010 5	000 8	001 5
11	110 10	001 3	111 2	000 6	101 10	010 3	100 4	011 4

Tab. B.5: Hilbert Curve State Diagram: for Mapping from 3-dimensional Points to One Dimension (*derived-keys*)

state no.	*derived-key*															
	0	1	2	3	4	5	6	7	8	9	10	11	12	13	14	15
0	0	1	3	2	6	7	5	4	12	13	15	14	10	11	9	8
	1	2	2	3	3	5	5	4	4	9	9	8	8	7	7	6
1	0	2	6	4	12	14	10	8	9	11	15	13	5	7	3	1
	2	11	11	13	13	16	16	15	15	17	17	14	14	12	12	10
2	0	4	12	8	9	13	5	1	3	7	15	11	10	14	6	2
	11	0	0	23	23	20	20	18	18	22	22	24	24	21	21	19
3	3	11	10	2	0	8	9	1	5	13	12	4	6	14	15	7
	22	25	25	7	7	1	1	17	17	26	26	9	9	27	27	14
4	5	4	6	7	3	2	0	1	9	8	10	11	15	14	12	13
	26	18	18	19	19	10	10	0	0	28	28	29	29	30	30	23
5	6	2	10	14	15	11	3	7	5	1	9	13	12	8	0	4
	19	13	13	15	15	14	14	10	10	4	4	6	6	31	31	11
6	9	11	15	13	5	7	3	1	0	2	6	4	12	14	10	8
	28	17	17	14	14	12	12	25	25	11	11	13	13	16	16	7
7	10	14	6	2	3	7	15	11	9	13	5	1	0	4	12	8
	29	21	21	27	27	22	22	30	30	20	20	26	26	0	0	16
8	15	7	6	14	12	4	5	13	9	1	0	8	10	2	3	11
	14	24	24	5	5	23	23	12	12	6	6	2	2	15	15	22
9	12	8	0	4	5	1	9	13	15	11	3	7	6	2	10	14
	16	31	31	1	1	4	4	28	28	14	14	25	25	13	13	29
10	3	7	15	11	10	14	6	2	0	4	12	8	9	13	5	1
	3	22	22	24	24	21	21	5	5	0	0	23	23	20	20	12
11	0	8	9	1	3	11	10	2	6	14	15	7	5	13	12	4
	0	1	1	28	28	25	25	29	29	27	27	30	30	26	26	31
12	5	13	12	4	6	14	15	7	3	11	10	2	0	8	9	1
	4	26	26	9	9	27	27	8	8	25	25	7	7	1	1	20
13	6	7	5	4	0	1	3	2	10	11	9	8	12	13	15	14
	27	5	5	12	12	2	2	22	22	7	7	17	17	9	9	24
14	15	14	12	13	9	8	10	11	3	2	0	1	5	4	6	7
	24	30	30	16	16	28	28	21	21	10	10	11	11	18	18	27
15	10	8	12	14	6	4	0	2	3	1	5	7	15	13	9	11
	7	29	29	31	31	19	19	1	1	3	3	4	4	8	8	28
16	12	4	5	13	15	7	6	14	10	2	3	11	9	1	0	8
	31	23	23	18	18	24	24	19	19	15	15	10	10	6	6	0
17	9	1	0	8	10	2	3	11	15	7	6	14	12	4	5	13
	20	6	6	2	2	15	15	3	3	24	24	5	5	23	23	4
18	5	1	9	13	12	8	0	4	6	2	10	14	15	11	3	7
	12	4	4	6	6	31	31	2	2	13	13	15	15	14	14	3
19	6	14	15	7	5	13	12	4	0	8	9	1	3	11	10	2
	13	27	27	30	30	26	26	16	16	1	1	28	28	25	25	21
20	9	8	10	11	15	14	12	13	5	4	6	7	3	2	0	1
	6	28	28	29	29	30	30	31	31	18	18	19	19	10	10	1
21	10	11	9	8	12	13	15	14	6	7	5	4	0	1	3	2
	15	7	7	17	17	9	9	14	14	5	5	12	12	2	2	25
22	3	2	0	1	5	4	6	7	15	14	12	13	9	8	10	11
	25	10	10	11	11	18	18	13	13	30	30	16	16	28	28	15
23	12	14	10	8	0	2	6	4	5	7	3	1	9	11	15	13
	9	16	16	21	21	11	11	27	27	12	12	22	22	17	17	30
24	15	13	9	11	3	1	5	7	6	4	0	2	10	8	12	14
	30	8	8	20	20	3	3	26	26	19	19	0	0	29	29	9
25	3	1	5	7	15	13	9	11	10	8	12	14	6	4	0	2
	10	3	3	4	4	8	8	6	6	29	29	31	31	19	19	2
26	5	7	3	1	9	11	15	13	12	14	10	8	0	2	6	4
	18	12	12	22	22	17	17	24	24	16	16	21	21	11	11	5
27	6	4	0	2	10	8	12	14	15	13	9	11	3	1	5	7
	5	19	19	0	0	29	29	23	23	8	8	20	20	3	3	18
28	9	13	5	1	0	4	12	8	10	14	6	2	3	7	15	11
	17	20	20	26	26	0	0	9	9	21	21	27	27	22	22	8
29	10	2	3	11	9	1	0	8	12	4	5	13	15	7	6	14
	21	15	15	10	10	6	6	11	11	23	23	18	18	24	24	13
30	15	11	3	7	6	2	10	14	12	8	0	4	5	1	9	13
	8	14	14	25	25	13	13	7	7	31	31	1	1	4	4	17
31	12	13	15	14	10	11	9	8	0	1	3	2	6	7	5	4
	23	9	9	8	8	7	7	20	20	2	2	3	3	5	5	26

Tab. B.6: Hilbert Curve State Diagram: for Mapping from One Dimension (*derived-keys*) to 4-dimensional Points

state no.	*n-point* 0	1	2	3	4	5	6	7	8	9	10	11	12	13	14	15
0	0	1	3	2	7	6	4	5	15	14	12	13	8	9	11	10
	1	2	3	2	4	5	3	5	6	7	8	7	4	9	8	9
1	0	15	1	14	3	12	2	13	7	8	6	9	4	11	5	10
	2	10	11	12	13	14	11	12	15	15	16	17	13	14	16	17
2	0	7	15	8	1	6	14	9	3	4	12	11	2	5	13	10
	11	18	19	18	0	20	21	22	23	23	24	24	0	20	21	22
3	4	7	3	0	11	8	12	15	5	6	2	1	10	9	13	14
	7	17	7	22	9	17	9	14	1	1	25	25	26	26	27	27
4	6	7	5	4	1	0	2	3	9	8	10	11	14	15	13	12
	10	0	10	19	18	26	18	19	28	0	28	29	30	23	30	29
5	14	9	1	6	15	8	0	7	13	10	2	5	12	11	3	4
	31	4	13	14	11	10	19	10	31	4	13	14	6	6	15	15
6	8	7	9	6	11	4	10	5	15	0	14	1	12	3	13	2
	25	25	11	12	13	14	11	12	7	28	16	17	13	14	16	17
7	12	11	3	4	13	10	2	5	15	8	0	7	14	9	1	6
	26	26	27	27	0	20	21	22	16	30	29	30	0	20	21	22
8	10	9	13	14	5	6	2	1	11	8	12	15	4	7	3	0
	6	6	15	15	23	23	24	24	2	12	2	22	5	12	5	14
9	2	5	13	10	3	4	12	11	1	6	14	9	0	7	15	8
	31	4	13	14	1	1	25	25	31	4	13	14	16	28	29	28
10	8	15	7	0	9	14	6	1	11	12	4	3	10	13	5	2
	5	12	5	3	0	20	21	22	23	23	24	24	0	20	21	22
11	0	3	7	4	15	12	8	11	1	2	6	5	14	13	9	10
	0	28	29	28	31	30	29	30	1	1	25	25	26	26	27	27
12	12	15	11	8	3	0	4	7	13	14	10	9	2	1	5	6
	7	20	7	8	9	4	9	8	1	1	25	25	26	26	27	27
13	4	5	7	6	3	2	0	1	11	10	8	9	12	13	15	14
	12	2	22	2	12	5	27	5	17	7	22	7	17	9	24	9
14	10	11	9	8	13	12	14	15	5	4	6	7	2	3	1	0
	10	11	10	21	18	11	18	27	28	16	28	21	30	16	30	24
15	6	9	7	8	5	10	4	11	1	14	0	15	2	13	3	12
	19	3	1	1	19	3	31	4	29	8	7	28	29	8	31	4
16	14	13	9	10	1	2	6	5	15	12	8	11	0	3	7	4
	6	6	15	15	23	23	24	24	0	10	19	10	31	18	19	18
17	2	1	5	6	13	14	10	9	3	0	4	7	12	15	11	8
	6	6	15	15	23	23	24	24	2	20	2	3	5	4	5	3
18	6	1	9	14	7	0	8	15	5	2	10	13	4	3	11	12
	31	4	13	14	2	12	2	3	31	4	13	14	6	6	15	15
19	8	11	15	12	7	4	0	3	9	10	14	13	6	5	1	2
	16	28	21	28	16	30	13	30	1	1	25	25	26	26	27	27
20	14	15	13	12	9	8	10	11	1	0	2	3	6	7	5	4
	10	1	10	19	18	31	18	19	28	6	28	29	30	31	30	29
21	12	13	15	14	11	10	8	9	3	2	0	1	4	5	7	6
	12	2	25	2	12	5	14	5	17	7	15	7	17	9	14	9
22	2	3	1	0	5	4	6	7	13	12	14	15	10	11	9	8
	10	11	10	25	18	11	18	13	28	16	28	15	30	16	30	13
23	4	11	5	10	7	8	6	9	3	12	2	13	0	15	1	14
	21	22	11	12	27	27	11	12	21	22	16	17	9	30	16	17
24	10	5	11	4	9	6	8	7	13	2	12	3	14	1	15	0
	19	3	0	20	19	3	26	26	29	8	0	20	29	8	9	30
25	14	1	15	0	13	2	12	3	9	6	8	7	10	5	11	4
	19	3	2	10	19	3	31	4	29	8	6	6	29	8	31	4
26	12	3	13	2	15	0	14	1	11	4	10	5	8	7	9	6
	21	22	11	12	5	18	11	12	21	22	16	17	24	24	16	17
27	2	13	3	12	1	14	0	15	5	10	4	11	6	9	7	8
	19	3	0	20	19	3	5	18	29	8	0	20	29	8	23	23
28	4	3	11	12	5	2	10	13	7	0	8	15	6	1	9	14
	26	26	27	27	0	20	21	22	9	17	9	8	0	20	21	22
29	6	5	1	2	9	10	14	13	7	4	0	3	8	11	15	12
	6	6	15	15	23	23	24	24	11	10	21	10	11	18	13	18
30	10	13	5	2	11	12	4	3	9	14	6	1	8	15	7	0
	31	4	13	14	1	1	25	25	31	4	13	14	7	17	7	8
31	8	9	11	10	15	14	12	13	7	6	4	5	0	1	3	2
	20	2	3	2	26	5	3	5	20	7	8	7	23	9	8	9

Tab. B.7: Hilbert Curve State Diagram: for Mapping from 4-dimensional Points to One Dimension (*derived-keys*)

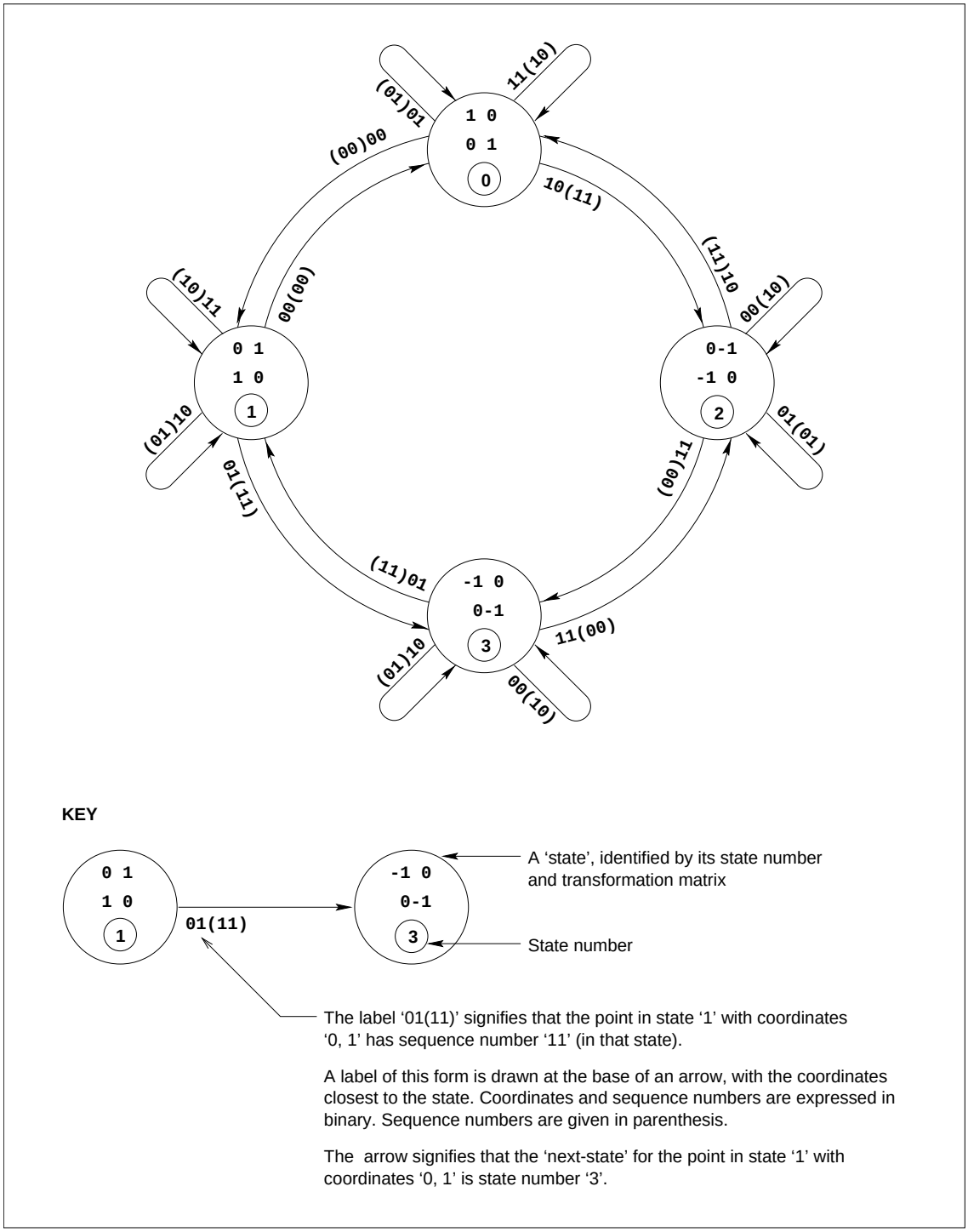

Fig. B.1: A State Diagram for the Hilbert Curve in 2 Dimensions

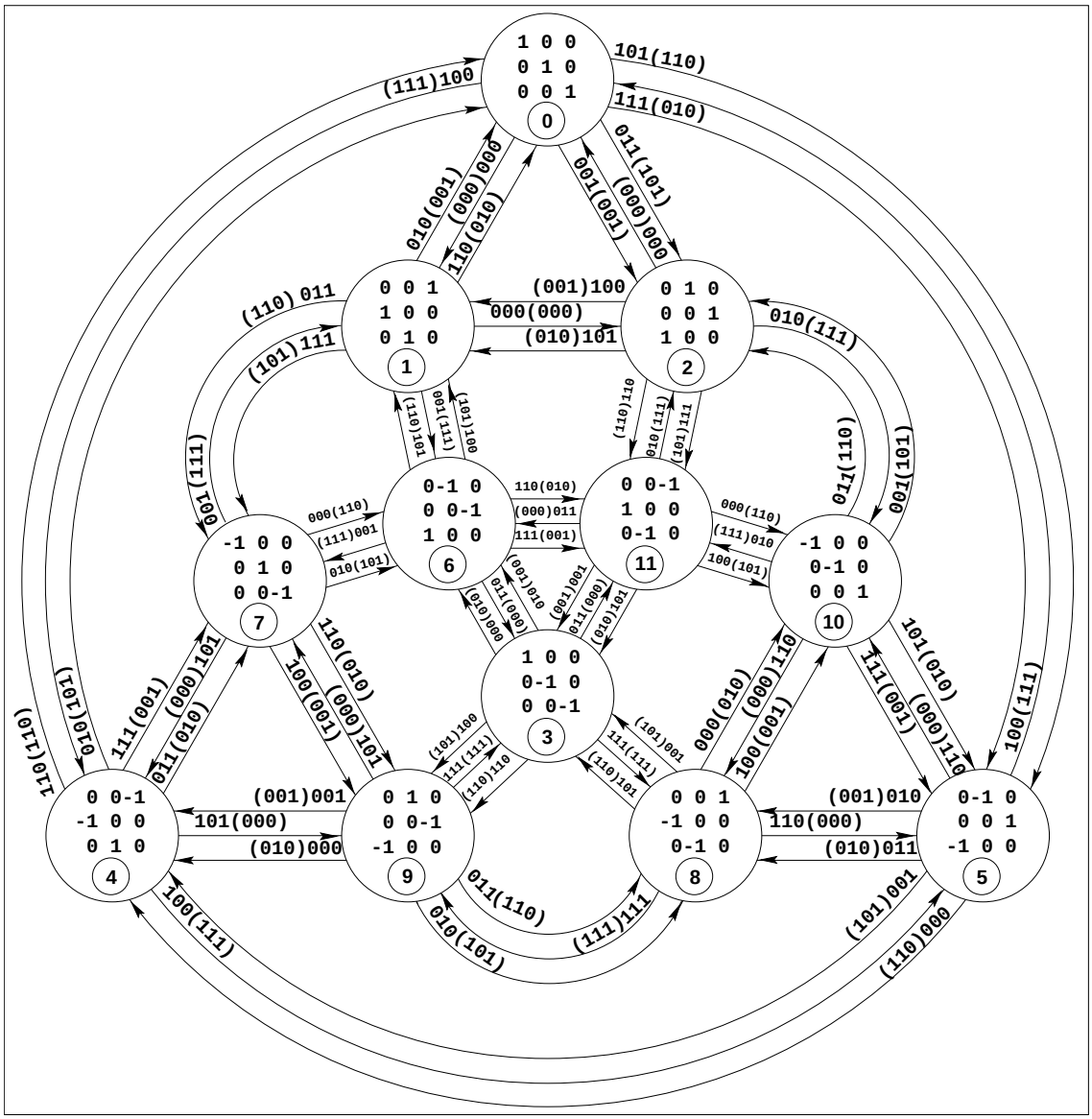

from state	(Y)	X_1	to state
0	011	010	3
	100	110	
1	011	100	8
	100	101	
2	011	001	9
	100	011	
3	011	001	0
	100	101	
4	011	001	11
	100	000	
5	011	111	6
	100	101	
6	011	010	5
	100	000	
7	011	111	10
	100	011	
8	011	010	1
	100	011	
9	011	100	2
	100	110	
10	011	100	7
	100	000	
11	011	111	4
	100	110	

Fig. B.2: A State Diagram for the Hilbert Curve in 3 Dimensions with supplementary table listing links not shown (for clarity) in the illustration

B.2 Calculated Hilbert Curve Mappings

In this section, we reproduce the algorithm for mapping from a Hilbert *derived-key* to the coordinates of a point, given by Butz in [But71].

Butz' algorithm is iterative, requiring a number of iterations equal to the order of the curve. Butz explains the algorithm using two tables. The first, Table B.8, lists working variables and specifies how they are assigned values. These variables are ordered in the sequence in which their values are calculated, and new values are assigned within each iteration of the algorithm. With the exception of the variable α^i, information is not provided on their semantics in [But71]. The second, Table B.9, provides an example of the calculation process.

Butz does not give the inverse algorithm, for mapping from the coordinates of a point to its Hilbert *derived-key* in his paper. We therefore give the algorithm in Table B.10, presented in the same format as used by Butz. The values of variables J_i, τ^i and ω^i are calculated in the same way as described in Table B.8. All other variables are calculated differently.

The tables make use of the following variables and terms defined in or inferred from Butz' paper:

***n*:** the number of dimensions in a space.

***m*:** the order of the curve passing through a space.

***N*:** the number of bits in a *derived-key*, ie nm.

***i*:** the number of the iteration of the algorithm, in the range $[1, \ldots, m]$.

***r*:** an N-bit binary Hilbert *derived-key*, expressed as a real number in the range $[0, 1)$.

byte: a word containing n bits.

ρ^i_j: a binary digit in r, such that $r = 0.\rho^1_1\rho^1_2 \cdots \rho^1_n\rho^2_1\rho^2_2 \cdots \rho^2_n\rho^3_1\rho^3_2 \cdots \rho^m_n$. Thus ρ^i represents the ith byte in r, such that $\rho^i = \rho^i_1\rho^i_2 \cdots \rho^i_n$.

a_j: a coordinate in dimension j of the point, $\langle a_1, a_2, \cdots, a_n \rangle$ whose *derived-key* is r. A coordinate is also expressed as a real number in the range $[0, 1)$.

α^i_j: a binary digit in a coordinate a_j, such that $a_j = \alpha^1_j\alpha^2_j \cdots \alpha^m_j$. Thus in Table B.8, $\alpha^i = \alpha^i_1\alpha^i_2 \cdots \alpha^i_n$ is an *n-point* formed from the ith bits of all of the coordinates in the point $\langle a_1, a_2, \cdots, a_n \rangle$.

principal position: the last, or least significant, bit position, j, in ρ^i such that $\rho^i_j \neq \rho^i_n$. If all bits in ρ^i are equal, the principal position is the nth, or least significant. The most significant bit position is considered to occupy poistion 1.

parity: the number of bits in a byte which are set to 1.

In section 5.3 of chapter 5 we noted that Butz' σ^i values appear to correspond to ρ^i values in the same way that column X_1 values correspond to column Y values within Bially's state diagram generator table. Similarly, the term τ^i appears to be equivalent to the first of pairs of entries in column X_2.

Equivalences between other terms used by Butz and terms used by Bially also appear to exist and we make the following conjectures:

***J_i*:** encapsulates the generator table column δY value corresponding to a ρ^i (Butz) or column Y (Bially) value, where $\delta Y = 2^{n-J_i}$.

$(J_1 - 1) + (J_2 - 1) + \cdots + (J_{i-1} - 1)$: encapsulates the current state permuation matrix following successive matrix multiplication operations. If we divide this sum by n and assign the remainder to t then the n-bit binary number 2^{n-t-1} corresponds to the first row of the current state's matrix, where a bit in the number corresponds to a column in the matrix. We saw in chapter 4 that, given the first row of a matrix, the other rows can be inferred.

ω^i: as an n-bit binary number, encapsulates the signs of the non-zero elements of the current state's transformation matrix in the same way that the first column X_2 entry in a row in the generator table encapsulates the signs of the non-zero elements in column $\overline{T(Y)}$. Takem together, t and ω^i completely define the current state transformation matrix.

TABLE I

ENTITIES USED IN SPACE-FILLING CURVE ALGORITHM

J_i: An integer between 1 and n equal to the subscript of the principal position of ρ^i. In the following four examples of ρ^i for the case $n = 5$, the values of J_i are 5, 2, 4 and 5, respectively (the principal positions are circled):

$$\begin{array}{ccccc} 1 & 1 & 1 & 1 & \textcircled{1} \\ 1 & \textcircled{0} & 1 & 1 & 1 \\ 0 & 0 & 1 & \textcircled{1} & 0 \\ 0 & 0 & 0 & 0 & \textcircled{0} \end{array}$$

σ^i: A byte of n bits, such that $\sigma^i_1 = \rho^i_1$, $\sigma^i_2 = \rho^i_2 \oplus \rho^i_1$, $\sigma^i_3 = \rho^i_3 \oplus \rho^i_2, \cdots, \sigma^i_n = \rho^i_n \oplus \rho^i_{n-1}$, where $\oplus$ stands for the EXCLUSIVE-OR operation.

τ^i: A byte of n bits obtained by complementing σ^i in the nth position and then, if and only if the resulting byte is of odd parity, complementing in the principal position. Hence, τ^i is always of even parity. Note that the parity of σ^i is given by the bit ρ^i_n and that a mask for performing the second complementation may be set up in the same process which calculates J_i.

$\tilde{\sigma}^i$: A byte of n bits obtained by shifting σ^i right circular a number of positions equal to

$$(J_1 - 1) + (J_2 - 1) + \cdots + (J_{i-1} - 1)$$

There is no shift in σ^1.

$\tilde{\tau}^i$: A byte of n bits obtained by shifting τ^i in exactly the same way.

ω^i: A byte of n bits where

$$\omega^i = \omega^{i-1} \oplus \tilde{\tau}^{i-1}, \qquad \omega^1 = 0\ 0 \cdots 0\ 0$$

and where $\oplus$ indicates the EXCLUSIVE-OR operation on corresponding bits.

α^i: A byte of n bits where $\alpha^i = \omega^i \oplus \tilde{\sigma}^i$.

Tab. B.8: 'TABLE I' from [But71]

TABLE II

EXAMPLE OF CALCULATION OF a FROM r

$n = 5 \qquad m = 4 \qquad N = 20$

$r = 0.10011000100010111000$

i	1	2	3	4	5
ρ^i	1 0 0 1 1	0 0 0 1 0	0 0 1 0 1	1 1 0 0 0	0 0 0 0 0
J_i	3	4	4	2	5
σ^i	1 1 0 1 0	0 0 0 1 1	0 0 1 1 1	1 0 1 0 0	0 0 0 0 0
τ^i	1 1 0 1 1	0 0 0 0 0	0 0 1 1 0	1 1 1 0 1	0 0 0 0 0
$\tilde{\sigma}^i$	1 1 0 1 0	1 1 0 0 0	0 0 1 1 1	1 0 0 1 0	0 0 0 0 0
$\tilde{\tau}^i$	1 1 0 1 1	0 0 0 0 0	0 0 1 1 0	1 0 1 1 1	0 0 0 0 0
ω^i	0 0 0 0 0	1 1 0 1 1	1 1 0 1 1	1 1 1 0 1	0 1 0 1 0
α^i	1 1 0 1 0	0 0 0 1 1	1 1 1 0 0	0 1 1 1 1	0 1 0 1 0

$a_1 = 0.1010$
$a_2 = 0.1011$
$a_3 = 0.0011$
$a_4 = 0.1101$
$a_5 = 0.0101$

Tab. B.9: 'TABLE II' from [But71]

α^i: A byte of n bits, such that $\alpha^i_1 = a^i_1,\ \alpha^i_2 = a^i_2, \cdots, \alpha^i_n = a^i_n$.

ω^i: A byte of n bits where

$$\omega^i = \omega^{i-1} \ \oplus \ \tilde{\tau}^{i-1}, \qquad \omega^1 = 0\ 0 \cdots 0\ 0$$

and where $\oplus$ indicates the EXCLUSIVE-OR operation on corresponding bits.

$\tilde{\sigma}^i$: A byte of n bits where

$$\tilde{\sigma}^i = \alpha^i \ \oplus \ \omega^i, \qquad \tilde{\sigma}^1 = \alpha^1$$

σ^i: A byte of n bits obtained by shifting $\tilde{\sigma}^i$ left circular a number of positions equal to

$$(J_1 - 1) + (J_2 - 1) + \cdots + (J_{i-1} - 1)$$

There is no shift in σ^1.

ρ^i: A byte of n bits, such that $\rho^i \oplus \ (\rho^i/2) = \sigma^i$, where $\oplus$ stands for the EXCLUSIVE-OR operation.

J_i: An integer between 1 and n equal to the subscript of the principal position of ρ^i.

τ^i: A byte of n bits obtained by complementing σ^i in the nth position and then, if and only if the resulting byte is of odd parity, complementing in the principal position. Hence, τ^i is always of even parity. Note that the parity of σ^i is given by the bit ρ^i_n and that a mask for performing the second complementation may be set up in the same process which calculates J_i.

$\tilde{\tau}^i$: A byte of n bits derived from τ^i in a similar way that σ^i is derived from $\tilde{\sigma}^i$, except that the direction of shifting is right circular instead of left circular.

Tab. B.10: Entities used in the algorithm for mapping from the coordinates of a point to a Hilbert *derived-key*

Appendix C

MOORE'S CURVE: OUR VARIATION

This appendix contains examples of state diagram generator tables for our variation of Moore's curve in 2 to 4 dimensions. These were produced in accordance with the algorithms given in section 4.3.5.2 in chapter 4.

Y	X_1	X_2	δY	$\overline{T(Y)}$	
00	00	10	01	0	1
		11		-1	0
01	01	10	01	0	1
		11		-1	0
10	11	01	01	0	-1
		00		1	0
11	10	01	01	0	-1
		00		1	0

Tab. C.1: State Diagram Generator Table for our Variation to Moore's Curve in 2 Dimensions

Y	X_1	X_2	δY	$\overline{T(Y)}$
000	000	110	001	0 0 1
		111		0 -1 0
				-1 0 0
001	001	110	001	0 0 1
		111		0 -1 0
				-1 0 0
010	011	101	001	0 0 -1
		100		0 1 0
				-1 0 0
011	010	101	001	0 0 -1
		100		0 1 0
				-1 0 0
100	110	000	001	0 0 1
		001		0 1 0
				1 0 0
101	111	000	001	0 0 1
		001		0 1 0
				1 0 0
110	101	011	001	0 0 -1
		010		0 -1 0
				1 0 0
111	100	011	001	0 0 -1
		010		0 -1 0
				1 0 0

Tab. C.2: State Diagram Generator Table for our Variation to Moore's Curve in 3 Dimensions

Y	X_1	X_2	δY	$\overline{T(Y)}$
0000	0000	1110	0001	0 0 0 1
		1111		0 -1 0 0
				0 0 -1 0
				-1 0 0 0
0001	0001	1110	0001	0 0 0 1
		1111		0 -1 0 0
				0 0 -1 0
				-1 0 0 0
0010	0011	1101	0001	0 0 0 -1
		1100		0 -1 0 0
				0 0 1 0
				-1 0 0 0
0011	0010	1101	0001	0 0 0 -1
		1100		0 -1 0 0
				0 0 1 0
				-1 0 0 0
0100	0110	1000	0001	0 0 0 1
		1001		0 1 0 0
				0 0 1 0
				-1 0 0 0
0101	0111	1000	0001	0 0 0 1
		1001		0 1 0 0
				0 0 1 0
				-1 0 0 0
0110	0101	1011	0001	0 0 0 -1
		1010		0 1 0 0
				0 0 -1 0
				-1 0 0 0
0111	0100	1011	0001	0 0 0 -1
		1010		0 1 0 0
				0 0 -1 0
				-1 0 0 0
Top half of table				

Y	X_1	X_2	δY	$\overline{T(Y)}$
1000	1100	0010	0001	0 0 0 1
		0011		0 1 0 0
				0 0 -1 0
				1 0 0 0
1001	1101	0010	0001	0 0 0 1
		0011		0 1 0 0
				0 0 -1 0
				1 0 0 0
1010	1111	0001	0001	0 0 0 -1
		0000		0 1 0 0
				0 0 1 0
				1 0 0 0
1011	1110	0001	0001	0 0 0 -1
		0000		0 1 0 0
				0 0 1 0
				1 0 0 0
1100	1010	0100	0001	0 0 0 1
		0101		0 -1 0 0
				0 0 1 0
				1 0 0 0
1101	1011	0100	0001	0 0 0 1
		0101		0 -1 0 0
				0 0 1 0
				1 0 0 0
1110	1001	0111	0001	0 0 0 -1
		0110		0 -1 0 0
				0 0 -1 0
				1 0 0 0
1111	1000	0111	0001	0 0 0 -1
		0110		0 -1 0 0
				0 0 -1 0
				1 0 0 0
Bottom half of table				

Tab. C.3: State Diagram Generator Table for our Variation to Moore's Curve in 4 Dimensions

Appendix D

THE GRAY-CODE CURVE

This appendix relates to mapping to the Gray-code curves we define in chapter 3. In section D.1, we show how Bially's [Bia69] state diagram generator table approach, described in chapter 4, can be adapted to these curves enabling them to be represented by state diagrams. This is followed in section D.2 with a number of examples of state diagram generator tables.

D.1 Creation of State Diagram Generator Tables

We identify three of a number of possible curves which use Gray-codes in section 3.7.2 of chapter 3 and they are referred to as Gray-code^F, Gray-code^A and Gray-code^B.

Means of calculating mappings between Gray-codes and their sequence numbers, or *derived-keys*, are relatively simple and are described in chapter 5. In this section, we apply Bially's state diagram approach to performing mappings to the various Gray-code curves as an alternative to calculation.

The principal advantage of this lies in the ability to utilize not just the same algorithms for querying but also the same computer programs, with little or no modification, for the Gray-code curve as are used for the Hilbert curve. Once constructed, it is a simple matter to substitute a state diagram for the Hilbert curve with one for the Gray-code curve. This readily enables the characteristics of the two curves to be explored during experimentation.

In applying Bially's state diagram generation technique to the Gray-code curves, it is necessary to deviate from the 'rules' in populating column X_2 of the generator table and also in populating column X_1 in the case of the Gray-code^B curve.

Graphical representations of 2-dimensional Gray-code^F, Gray-code^A and Gray-code^B curves are shown in chapter 3 in Figures 3.14, 3.16 and 3.18 respectively. Equivalent second order representations in 3 dimensions are shown in Figures 3.15, 3.17 and 3.19. From these, generator tables are constructed manually. They are given below in this appendix. These generator tables provide insights which enable us to develop rules for constructing other tables for the Gray-code curves in higher-dimensional space, automatically.

Column Y

State diagram generator tables for all three interpretations of the Gray-code curve are populated in column Y in the same way as the Hilbert curve.

Column X_1

Column X_1 values follow from the definitions of the mappings given in section 3.7.2 of chapter 3. Thus for the Gray-code^F and Gray-code^A curves they are the Gray-codes of their corresponding column Y values and for the Gray-code^B curve they are the Gray-code *derived-keys* of their corresponding column Y values. Column X_1 values define 'continuous' Gray-code^F and Gray-code^A first order curves but in the case of the Gray-code^B curve a

discontinuity exists between each group of 4 consecutive rows in the table, regardless of the number of dimensions.

Column X_2

We note from the 2 and 3-dimensional examples that in column X_2 the number of different pairs of entries equals half the number of rows in the table in the case of the Gray-code^F curve. In the case of the Gray-code^A and Gray-code^B curves, the number of different pairs of entries equals 2.

Algorithms for populating column X_2 values in n dimensions are formulated by extending the sequences which are present in the tables for 2 and 3 dimensions. They are different for the three interpretations of the Gray-code curve.

Gray-code^F

As with the Hilbert curve and our variation of Moore's curve, we provide examples for the sequences of orders[1] 1–3.
Order 1: [0, 1, 0, 1]
Order 2: [00, 10, 11, 01, 11, 01, 00, 10]
Order 3: [000, 100, 101, 001, 011, 111, 110, 010, 110, 010, 011, 111, 101, 001, 000, 100]

Our rules which generate the sequences for order n are given as follows:

1. Append a reflection of the sequence for order $n-1$ to the sequence for order $n-1$, thus doubling its size.
2. Divide the members of the enlarged sequence into groups each containing 4 members.
3. For groups in the first half of the enlarged sequence:
   (a) Prefix individual members with a bit taken successively from the sequence [0, 1, 1, 0].
   (b) If the most significant bit of a member is non-zero then invert the value of the next lower bit; from 1 to 0 or from 0 to 1.
4. For groups in the second half of the enlarged sequence:
   (a) Prefix individual members with a bit taken successively from the sequence [1, 0, 0, 1].
   (b) If the most significant bit of a member is zero then invert the value of the next lower bit; from 1 to 0 or from 0 to 1.

The sequence of order n is then used to populate the column in the generator table for n dimensions.

Gray-code^A

In all even numbered rows in the generator table, the first column X_2 entry equals the first column X_1 entry and the second column X_2 entry equals the last column X_1 entry. In all odd numbered rows, the same values are used in column X_2 except that the last column X_1 entry is used in place of the first column X_1 entry and vice versa.

[1] NB: usage of the term *order* here is distinct from usage in the context of *order of curve*

Gray-code^B

In the first of the two formats of pairs of column X_2 entries, the first value of the pair equals the first entry in column X_1 and the second value equals the last entry in column X_1. In the second format, the entries are bitwise complements of the first format. We label the formats A and B.

For generator tables in n dimensions, we express the way in which it is determined whether column X_2 in a row should contain a pair of entries of format A or B using the following rules:

1. For $n = 1$, initialize column X_2 with a pair of entries of format A followed by a pair of entries of format B.
2. For $n > 1$:
   (a) Copy the sequence of format types in column X_2 from the table for $n - 1$ dimensions into both the first and second halves of the column for n dimensions.
   (b) In the second half of the table, exchange format A entries for format B and vice versa.

Column δY

The column X_2 entries cause all of the column δY entries to equal the last entry in column X_1.

Column $\overline{T(Y)}$

Column δY entries result in the matrices in column $\overline{T(Y)}$ being initialized as identity matrices. The signs of their non-zero elements are adjusted in the way specified by Bially.

D.2 Some Examples of State Diagram Generator Tables

Tables D.1 to D.3 are for the Gray-code^F curve in 2 to 4 dimensions and were produced in accordance with the algorithms given in section 4.3.5.3 in chapter 4.

Tables D.4 to D.6 are for the Gray-code^A curve in 2 to 4 dimensions and were produced in accordance with the algorithms given in section 4.3.5.3 in chapter 4.

Tables D.7 to D.9 are for the Gray-code^B curve in 2 to 4 dimensions and were produced in accordance with the algorithms given in section 4.3.5.3 in chapter 4.

Y	X_1	X_2	δY	$\overline{T(Y)}$
00	00	00	10	1 0
		10		0 1
01	01	11	10	-1 0
		01		0 -1
10	11	11	10	-1 0
		01		0 -1
11	10	00	10	1 0
		10		0 1

Tab. D.1: State Diagram Generator Table for the Gray-code^F Curve in 2 Dimensions

Y	X_1	X_2	δY	$\overline{T(Y)}$
000	000	000	100	1 0 0
		100		0 1 0
				0 0 1
001	001	101	100	-1 0 0
		001		0 1 0
				0 0 -1
010	011	011	100	1 0 0
		111		0 -1 0
				0 0 -1
011	010	110	100	-1 0 0
		010		0 -1 0
				0 0 1
100	110	110	100	-1 0 0
		010		0 -1 0
				0 0 1
101	111	011	100	1 0 0
		111		0 -1 0
				0 0 -1
110	101	101	100	-1 0 0
		001		0 1 0
				0 0 -1
111	100	000	100	1 0 0
		100		0 1 0
				0 0 1

Tab. D.2: State Diagram Generator Table for the Gray-code^F Curve in 3 Dimensions

Y	X_1	X_2	δY	$\overline{T(Y)}$
0000	0000	0000	1000	1 0 0 0
		1000		0 1 0 0
				0 0 1 0
				0 0 0 1
0001	0001	1001	1000	-1 0 0 0
		0001		0 1 0 0
				0 0 1 0
				0 0 0 -1
0010	0011	0011	1000	1 0 0 0
		1011		0 1 0 0
				0 0 -1 0
				0 0 0 -1
0011	0010	1010	1000	-1 0 0 0
		0010		0 1 0 0
				0 0 -1 0
				0 0 0 1
0100	0110	0110	1000	1 0 0 0
		1110		0 -1 0 0
				0 0 -1 0
				0 0 0 1
0101	0111	1111	1000	-1 0 0 0
		0111		0 -1 0 0
				0 0 -1 0
				0 0 0 -1
0110	0101	0101	1000	1 0 0 0
		1101		0 -1 0 0
				0 0 1 0
				0 0 0 -1
0111	0100	1100	1000	-1 0 0 0
		0100		0 -1 0 0
				0 0 1 0
				0 0 0 1
Top half of table				

Y	X_1	X_2	δY	$\overline{T(Y)}$
1000	1100	1100	1000	-1 0 0 0
		0100		0 -1 0 0
				0 0 1 0
				0 0 0 1
1001	1101	0101	1000	1 0 0 0
		1101		0 -1 0 0
				0 0 1 0
				0 0 0 -1
1010	1111	1111	1000	-1 0 0 0
		0111		0 -1 0 0
				0 0 -1 0
				0 0 0 -1
1011	1110	0110	1000	1 0 0 0
		1110		0 -1 0 0
				0 0 -1 0
				0 0 0 1
1100	1010	1010	1000	-1 0 0 0
		0010		0 1 0 0
				0 0 -1 0
				0 0 0 1
1101	1011	0011	1000	1 0 0 0
		1011		0 1 0 0
				0 0 -1 0
				0 0 0 -1
1110	1001	1001	1000	-1 0 0 0
		0001		0 1 0 0
				0 0 1 0
				0 0 0 -1
1111	1000	0000	1000	1 0 0 0
		1000		0 1 0 0
				0 0 1 0
				0 0 0 1
Bottom half of table				

Tab. D.3: State Diagram Generator Table for the Gray-code^F Curve in 4 Dimensions

Y	X_1	X_2	δY	$\overline{T(Y)}$
00	00	00	10	1 0
		10		0 1
01	01	10	10	-1 0
		00		0 1
10	11	00	10	1 0
		10		0 1
11	10	10	10	-1 0
		00		0 1

Tab. D.4: State Diagram Generator Table for the Gray-code^A Curve in 2 Dimensions

Y	X_1	X_2	δY	$\overline{T(Y)}$
000	000	000	100	1 0 0
		100		0 1 0
				0 0 1
001	001	100	100	-1 0 0
		000		0 1 0
				0 0 1
010	011	000	100	1 0 0
		100		0 1 0
				0 0 1
011	010	100	100	-1 0 0
		000		0 1 0
				0 0 1
100	110	000	100	1 0 0
		100		0 1 0
				0 0 1
101	111	100	100	-1 0 0
		000		0 1 0
				0 0 1
110	101	000	100	1 0 0
		100		0 1 0
				0 0 1
111	100	100	100	-1 0 0
		000		0 1 0
				0 0 1

Tab. D.5: State Diagram Generator Table for the Gray-code^A Curve in 3 Dimensions

Y	X_1	X_2	δY	$\overline{T(Y)}$
0000	0000	0000	1000	1 0 0 0
		1000		0 1 0 0
				0 0 1 0
				0 0 0 1
0001	0001	1000	1000	-1 0 0 0
		0000		0 1 0 0
				0 0 1 0
				0 0 0 1
0010	0011	0000	1000	1 0 0 0
		1000		0 1 0 0
				0 0 1 0
				0 0 0 1
0011	0010	1000	1000	-1 0 0 0
		0000		0 1 0 0
				0 0 1 0
				0 0 0 1
0100	0110	0000	1000	1 0 0 0
		1000		0 1 0 0
				0 0 1 0
				0 0 0 1
0101	0111	1000	1000	-1 0 0 0
		0000		0 1 0 0
				0 0 1 0
				0 0 0 1
0110	0101	0000	1000	1 0 0 0
		1000		0 1 0 0
				0 0 1 0
				0 0 0 1
0111	0100	1000	1000	-1 0 0 0
		0000		0 1 0 0
				0 0 1 0
				0 0 0 1
Top half of table				

Y	X_1	X_2	δY	$\overline{T(Y)}$
1000	1100	0000	1000	1 0 0 0
		1000		0 1 0 0
				0 0 1 0
				0 0 0 1
1001	1101	1000	1000	-1 0 0 0
		0000		0 1 0 0
				0 0 1 0
				0 0 0 1
1010	1111	0000	1000	1 0 0 0
		1000		0 1 0 0
				0 0 1 0
				0 0 0 1
1011	1110	1000	1000	-1 0 0 0
		0000		0 1 0 0
				0 0 1 0
				0 0 0 1
1100	1010	0000	1000	1 0 0 0
		1000		0 1 0 0
				0 0 1 0
				0 0 0 1
1101	1011	1000	1000	-1 0 0 0
		0000		0 1 0 0
				0 0 1 0
				0 0 0 1
1110	1001	0000	1000	1 0 0 0
		1000		0 1 0 0
				0 0 1 0
				0 0 0 1
1111	1000	1000	1000	-1 0 0 0
		0000		0 1 0 0
				0 0 1 0
				0 0 0 1
Bottom half of table				

Tab. D.6: State Diagram Generator Table for the Gray-code^A Curve in 4 Dimensions

Y	X_1	X_2	δY	$\overline{T(Y)}$
00	00	00	10	1 0
		10		0 1
01	01	11	10	-1 0
		01		0 -1
10	11	11	10	-1 0
		01		0 -1
11	10	00	10	1 0
		10		0 1

Tab. D.7: State Diagram Generator Table for the Gray-code^B Curve in 2 Dimensions

Y	X_1	X_2	δY	$\overline{T(Y)}$
000	000	000	101	1 0 0
		101		0 1 0
				0 0 1
001	001	111	101	-1 0 0
		010		0 -1 0
				0 0 -1
010	011	111	101	-1 0 0
		010		0 -1 0
				0 0 -1
011	010	000	101	1 0 0
		101		0 1 0
				0 0 1
100	111	111	101	-1 0 0
		010		0 -1 0
				0 0 -1
101	110	000	101	1 0 0
		101		0 1 0
				0 0 1
110	100	000	101	1 0 0
		101		0 1 0
				0 0 1
111	101	111	101	-1 0 0
		010		0 -1 0
				0 0 -1

Tab. D.8: State Diagram Generator Table for the Gray-code^B Curve in 3 Dimensions

Y	X_1	X_2	δY	$\overline{T(Y)}$
0000	0000	0000	1010	1 0 0 0
		1010		0 1 0 0
				0 0 1 0
				0 0 0 1
0001	0001	1111	1010	-1 0 0 0
		0101		0 -1 0 0
				0 0 -1 0
				0 0 0 -1
0010	0011	1111	1010	-1 0 0 0
		0101		0 -1 0 0
				0 0 -1 0
				0 0 0 -1
0011	0010	0000	1010	1 0 0 0
		1010		0 1 0 0
				0 0 1 0
				0 0 0 1
0100	0111	1111	1010	-1 0 0 0
		0101		0 -1 0 0
				0 0 -1 0
				0 0 0 -1
0101	0110	0000	1010	1 0 0 0
		1010		0 1 0 0
				0 0 1 0
				0 0 0 1
0110	0100	0000	1010	1 0 0 0
		1010		0 1 0 0
				0 0 1 0
				0 0 0 1
0111	0101	1111	1010	-1 0 0 0
		0101		0 -1 0 0
				0 0 -1 0
				0 0 0 -1
Top half of table				

Y	X_1	X_2	δY	$\overline{T(Y)}$
1000	1111	1111	1010	-1 0 0 0
		0101		0 -1 0 0
				0 0 -1 0
				0 0 0 -1
1001	1110	0000	1010	1 0 0 0
		1010		0 1 0 0
				0 0 1 0
				0 0 0 1
1010	1100	0000	1010	1 0 0 0
		1010		0 1 0 0
				0 0 1 0
				0 0 0 1
1011	1101	1111	1010	-1 0 0 0
		0101		0 -1 0 0
				0 0 -1 0
				0 0 0 -1
1100	1000	0000	1010	1 0 0 0
		1010		0 1 0 0
				0 0 1 0
				0 0 0 1
1101	1001	1111	1010	-1 0 0 0
		0101		0 -1 0 0
				0 0 -1 0
				0 0 0 -1
1110	1011	1111	1010	-1 0 0 0
		0101		0 -1 0 0
				0 0 -1 0
				0 0 0 -1
1111	1010	0000	1010	1 0 0 0
		1010		0 1 0 0
				0 0 1 0
				0 0 0 1
Bottom half of table				

Tab. D.9: State Diagram Generator Table for the Gray-code^B Curve in 4 Dimensions

Appendix E

SOURCE CODE FOR GENERATION OF STATE DIAGRAMS

The source code required for constructing state diagram generator tables for the Hilbert curve, our variation of Moore's curve and the Gray-code^F, Gray-code^A and Gray-code^B curves has been omitted from this version of the thesis.

Appendix F

SOURCE CODE FOR DATA MANAGEMENT IMPLEMENTATION

The source code for the current implementation of our application for the storage, indexing and retrieval of multi-dimensional data has been omitted from this version of the thesis.

Index of definitions